

# Synthesis and Characterization of Copolymers from Lignin

A Dissertation

Presented in Partial Fulfillment of the Requirements for the

Degree of Doctorate of Philosophy

with a

Major in Natural Resources

in the

College of Graduate Studies

University of Idaho

by

Hui Li

June 2014

Major Professor: Armando G. McDonald, Ph.D.

## Authorization to Submit Dissertation

This dissertation of Hui Li, submitted for the degree of Doctorate of Philosophy with a major in Natural Resources and titled "Synthesis and Characterization of Copolymers from Lignin" has been reviewed in final form. Permission, as indicated by the signatures and dates given below, is now granted to submit final copies to the College of Graduate Studies for approval.

Major Professor: \_\_\_\_\_ Date \_\_\_\_\_

Armando G. McDonald, Ph.D.

Committee

Members: \_\_\_\_\_ Date \_\_\_\_\_

Thomas M. Gorman, Ph.D.

\_\_\_\_\_ Date \_\_\_\_\_

D. Eric Aston, Ph.D.

\_\_\_\_\_ Date \_\_\_\_\_

Mark F. Roll, Ph.D.

Department

Administrator: \_\_\_\_\_ Date \_\_\_\_\_

Anthony S. Davis, Ph.D.

Discipline's

College Dean: \_\_\_\_\_ Date \_\_\_\_\_

Kurt S. Pregitzer, Ph.D.

Final Approval and Acceptance

Dean of the College

of Graduate Studies: \_\_\_\_\_ Date \_\_\_\_\_

Jie Chen, Ph.D.

## Abstract

Development of bio-based materials, especially from agricultural and forestry industrial byproduct streams, is urgent and necessary under the circumstances of sustainability and the environment. Industrial lignin is an underutilized biopolymer byproduct from both the pulping and cellulosic ethanol biorefinery industries with tremendous availability, showing potential as a substrate for producing biobased polyester materials because of its structure and abundance of hydroxyl functional groups.

In this study, lignin based copolymeric elastomers were synthesized by simple one pot two step polycondensation of methanol soluble (MS) fractions of industrial lignins and a series hyperbranched prepolymers (HBP) with different branching and core structures using various multifunctional monomers. Specifically, three industrial lignins (Indulin AT Kraft softwood (IN), Protobind 1000 (PB), and corn stover (CS)) were first subjected to methanol fractionation and then to a detailed chemical and thermal characterization. Fractionation and characterization of three industrial lignins were carried out to provide a hard (or netpoint) segment substrate for the copolymer synthesis. Correlations between chemical and thermal properties were observed in terms of condensation index, hydroxyl group, and molar mass versus the glass transition temperature ( $T_g$ ).

A series of lignin-copolymers were prepared using the three different lignins and a HBP composed of triethanolamine (TEA, trifunctional) and adipic acid (AA, difunctional),  $A_2B_3$  to evaluate the effects of lignin types and lignin contents. Tensile properties were dominated by HBP <45% lignin content while lignin dominated at 45% content. The copolymers  $T_g$  increased with lignin content, while lignin type did not play a significant role. Thermally-stimulated dual shape memory effects ( $T_s$ -SME) of the copolymers were obtained and quantified by cyclic thermomechanical tests. All copolymers had shape fixity rate >95% and shape recovery >90% for all copolymers. The copolymer shape memory transition temperature ( $T_{trans}$ ) increased with lignin content and  $T_{trans}$  was 20 °C higher than  $T_g$ .

To obtain different HBP structure, a prepolymer was synthesized composing of long alkyl ( $C_{12}$ ) chain diacid (DDDA), TEA, and tris(hydroxymethyl)aminomethane (THAM, tetrafunctional),  $B_3-A_2-CB_3^1$ ). The  $C_{12}$  diacid contributed to a partially crystalline structure, while THAM contributed to more branching as well as forming stiff amide linkages in the prepolymer. Lignin-copolymers were synthesized with these prepolymers and PB lignin. Tensile properties were dominated by HBP <25% lignin content while lignin dominated >25% content. The  $T_g$ s of copolymers increased with lignin content. The lignin-copolymer with 30% lignin content demonstrated optimal mechanical properties (tensile strength 5.3 MPa, Young's modulus 8.9 MPa, strain at break 301%, and toughness 1.03 GPa). Good  $T_g$ -SME was obtained and could be tailored by lignin content and activation temperatures ranged between ambient and body temperature.

Finally, in order to pursue higher biobased content in the lignin-copolymers, HBP were prepared from AA, Glycerol (Gly, trifunctional), and enhanced by additions of diisopropanolamine (DIPA, trifunctional), or THAM,  $B^2B^3_2-A_2$ ,  $B^2B^3_2-DB^4_2-A_2$ , and  $B^2B^3_2-CB^1_3-A_2$ ) to form branched to hyper branched structures. The higher branching crosslinkers, DIPA and THAM, were shown to influence the chemical and thermal properties of the prepolymers. The highly biobased lignin-copolymers demonstrated good shape memory and elastic properties.  $T_{trans}$  could be tuned by variations of Gly, DIPA and THAM proportions for applications under different temperature circumstances.

Different branching and core structures of prepolymers (soft segment) were shown to influence the properties of prepolymers and corresponding lignin-copolymers. All the lignin-copolymers were shown to be elastomeric and possess great  $T_g$ -SME. The results demonstrated that properties of lignin-copolymers could be tuned through lignin type, lignin content, prepolymer structure, and monomer variations. This study demonstrated that lignin, a renewable byproduct, can be promisingly valorized to apply as a netpoint segment in biobased polymer systems with SME behavior.

## Acknowledgements

I would like to sincerely thank my advisor and mentor Dr. Armando G. McDonald for his insightful instruction throughout my Ph.D. research. His great dedication to the research guides and inspires me to further scientific career. I also want to thank my other committee members Dr. Tom Gorman, Dr. Eric Aston, and Dr. Mark Roll for their valuable advice, participation, and support on my dissertation research.

I also thank the College of Graduate Study, the College of Natural Resources, Department of Forest Resources, Rangeland and Fire Sciences, and Renewable Materials Program for providing wonderful and diverse academic and experimental atmosphere. Special thanks go to Dr. Noridah Osman for her experimental instruction of lignin characterization and Dr. Gopakumar Sivasankarapillai for his help and instruction of lignin-copolymer synthesis and characterization. Also would like to thank my fellow research group members for their assistance, cooperation and supports. Also thank Dr. Alexander Blumenfeld for his technical help with NMR, and Binying Ye for providing access to a DMA.

I would like to thank all faculty, staff and graduate students in Department of Forest Resources, Rangeland and Fire Sciences for their friendly help and great support.

Thanks also go to all my friends met in Palouse area during the past four years.

This dissertation dedicates to my loved parents for their understanding and love to make all these achievements possible.

I appreciate the financial support from USDA-NIFA Wood Utilization Research grant number 2010-34158-20938.

## Table of Contents

Authorization to Submit Dissertation .....	ii
Abstract .....	iii
Acknowledgements.....	v
Table of Contents .....	vi
Table of Figures .....	xii
Table of Tables .....	xvii
Table of Abbreviations .....	xix
1 Introduction and Literature Review .....	1
1.1 Introduction.....	1
1.1.1 Petroleum-based polymers and situation .....	1
1.1.2 The necessity of developing bio-based renewable materials.....	2
1.1.3 Types of natural renewable bio-based polymers .....	2
1.2 Literature review .....	4
1.2.1 Chemistry of lignocellulosic biomass .....	4
1.2.1.1 Cellulose.....	5
1.2.1.2 Hemicelluloses .....	6
1.2.1.3 Extractives.....	7
1.2.2 Lignin structure and biosynthesis .....	7
1.2.2.1 Lignin structure .....	7
1.2.2.2 Lignin biosynthesis.....	8
1.2.3 Industrial lignin and isolation processes .....	10
1.2.3.1 Sulfur lignin .....	11
1.2.3.1.1 Lignosulfonate lignin .....	11
1.2.3.1.2 Kraft lignin.....	12
1.2.3.2 Sulfur free lignin.....	14
1.2.3.2.1 Organosolv lignin .....	14
1.2.3.2.2 Soda lignin .....	15
1.2.3.2.3 Pyrolytic lignin .....	15

1.2.3.2.4	Bio-ethanol lignin.....	16
1.2.3.3	Research isolated lignin .....	17
1.2.4	Utilization of industrial lignin for use in polymers and resins .....	17
1.2.4.1	Macromolecular properties of industrial lignins .....	17
1.2.4.1.1	Chemical properties.....	17
1.2.4.1.2	Thermal properties .....	18
1.2.4.2	Material applications of industrial lignin .....	20
1.2.4.2.1	Lignin polymer blends .....	20
1.2.4.2.2	Lignin chemical modification.....	20
1.2.4.2.2.1	Alkylation .....	20
1.2.4.2.2.2	Esterification to obtain lignin polyesters .....	21
1.2.4.2.2.3	Lignin-based polyurethane .....	25
1.2.4.2.3	Lignin-based adhesives.....	26
1.2.5	General polymer (Peacock and Calhoun, 2006; Rodriguez et al., 2003) .....	28
1.2.5.1	Chain-growth and step-growth polymers .....	28
1.2.5.2	Homopolymer and copolymer .....	28
1.2.5.3	Linear and branched polymers .....	29
1.2.5.4	Thermoplastics and thermosets .....	29
1.2.6	Shape memory polymers .....	30
1.2.7	Hyperbranched polymers.....	32
1.3	Research objectives.....	33
1.4	References .....	35
2	Fractionation and Characterization of Industrial Lignin .....	48
2.1	Abstract .....	48
2.2	Introduction.....	48
2.3	Materials and methods .....	50
2.3.1	Lignin preparation and fractionation.....	50
2.3.2	Chemical analysis .....	50
2.3.3	Thermal analysis.....	52

2.4	Results and Discussion .....	53	
2.4.1	Chemical analysis .....	53	
2.4.1.1	FTIR results.....	53	
2.4.1.2	Py-GC-MS results .....	56	
2.4.1.3	DFRC results .....	59	
2.4.1.4	S/G determination by FTIR, py-GC-MS and DFRC.....	59	
2.4.2	Thermal analysis.....	60	
2.4.2.1	T <sub>g</sub> determination .....	60	
2.4.2.2	Thermal Degradation .....	65	
2.4.3	Correlations of lignin chemical structure and thermal properties .....	68	
2.5	Conclusions.....	70	
2.6	References .....	70	
3 Lignin Valorization by Forming Toughened Thermally-stimulated Shape Memory			
Copolymeric Elastomers: Evaluation of Different Industrial Lignins .....			79
3.1	Abstract .....	79	
3.2	Introduction.....	79	
3.3	Materials and methods .....	82	
3.3.1	Materials .....	82	
3.3.2	Methods .....	83	
3.3.2.1	Synthesis of HB prepoly(ester-amine) (E1).....	83	
3.3.2.2	Synthesis of lignin-copoly(ester-amine) .....	83	
3.3.3	Characterization techniques .....	84	
3.3.3.1	FTIR and NMR .....	84	
3.3.3.2	Electrospray Ionization – MS .....	85	
3.3.3.3	Thermal and Mechanical analysis.....	85	
3.4	Results and Discussion .....	86	
3.4.1	Preparation and analyses of lignin and HBP samples .....	86	
3.4.2	Synthesis of lignin-copoly(ester-amine) elastomers.....	89	
3.4.3	Mechanical properties .....	91	



3.4.4	Thermal properties .....	93
3.4.5	Thermal stability of the lignin-copoly(ester-amine)s.....	95
3.4.6	Thermally-stimulated dual shape memory effect ( $T_s$ -SME).....	97
3.5	Conclusions.....	101
3.6	References.....	101
4 Lignin Valorization by Forming Thermally-stimulated Shape Memory Copolymeric		
Elastomers - Partially Crystalline Hyperbranched Polymer as Crosslinks.....		
4.1	Abstract .....	109
4.2	Introduction.....	109
4.3	Materials and Methods .....	111
4.3.1	Materials .....	111
4.3.2	Methods.....	111
4.3.2.1	Synthesis of hyperbranched prepoly(ester-amine-amide) (D1).....	111
4.3.2.2	Synthesis of lignin-copoly(ester-amine-amide) (lignin-D1-copolymer) ...	112
4.3.3	Characterization techniques .....	113
4.3.3.1	FTIR and NMR .....	113
4.3.3.2	Electrospray Ionization – MS .....	113
4.3.3.3	Thermal and Mechanical analysis.....	114
4.3.3.4	Morphological analysis .....	115
4.4	Results and Discussion .....	115
4.4.1	Preparation of D1 prepolymer and lignin-D1-copolymers .....	115
4.4.2	Mechanical properties .....	117
4.4.3	Thermal properties .....	118
4.4.4	Cross-link properties .....	120
4.4.5	Thermal stability.....	121
4.4.6	Thermal-stimulated shape memory effect ( $T_s$ -SME) .....	122
4.4.7	Morphological properties .....	126
4.5	Conclusions.....	126
4.6	References.....	127

5 Lignin Valorization by Forming Thermally-stimulated Shape Memory Copolymeric Elastomers: High Biobased Copolymer as Mixing Phase .....	133
5.1 Abstract .....	133
5.2 Introduction.....	133
5.3 Materials and Methods .....	136
5.3.1 Materials .....	136
5.3.2 Methods.....	136
5.3.2.1 Synthesis of hyperbranched prepolymers G1 and G2 .....	136
5.3.2.2 Synthesis of hyperbranched prepoly(ester-amide)s (D1-D4).....	137
5.3.2.3 Synthesis of hyperbranched prepoly(ester-amide)s (T1 - T4) .....	138
5.3.2.4 Synthesis of lignin-copolyesters and -copoly(ester-amide)s.....	139
5.3.3 Characterization techniques .....	141
5.3.3.1 FTIR and NMR .....	141
5.3.3.2 Electrospray Ionization – MS .....	141
5.3.3.3 Rheology analysis.....	141
5.3.3.4 Thermal analysis .....	141
5.4 Results and Discussion .....	143
5.4.1 Monomer selections .....	143
5.4.2 Preparation of Gly based prepolymers .....	144
5.4.3 Characterization of Gly-based prepolymers .....	144
5.4.4 Characterization of lignin-copolymers (LG1, LG2, LD1-LD4, and LT1-LT4) .....	150
5.4.4.1 FTIR results.....	150
5.4.4.2 Mechanical properties .....	153
5.4.4.3 Thermal properties .....	154
5.4.4.4 Thermal-stimulated shape memory effect ( $T_s$ -SME) .....	157
5.5 Conclusions.....	160
5.6 References.....	161
6 Summary and Future Work.....	168
6.1 Summary of dissertation .....	168

6.2 Recommendation for the future work ..... 172

## Table of Figures

Figure 1.1 (a), three-dimensional structure of the plant secondary cell wall of a tracheid (xylem cell) (Plomion et al., 2001); and (b), chemical structure of cell wall (Doherty et al., 2011). .....	5
Figure 1.2 Molecular structure of cellulose (Klemm et al., 2005) .....	6
Figure 1.3 Structures of (a) hardwood 4-O-methylglucurono-xylan, (b) softwood arabino-(4-O-methylglucurono)-xylan, and (c) arabinoxylan (Ebringerova and Heinze, 2000). .....	6
Figure 1.4 Monomers structure of lignin macromolecules .....	7
Figure 1.5 Resonance stabilized phenoxy radical of coniferyl alcohol (Sjostrom, 1993) .....	9
Figure 1.6 Softwood lignin model structure as well as linkages (Alder, 1977) .....	9
Figure 1.7 Extraction processes to separate lignin from lignocellulosic biomass and the corresponding productions of industrial lignin and less-alternative lignin (Holladay et al., 2007; Laurichesse and Avérus, 2013). .....	11
Figure 1.8 (a), Reaction mechanism of lignosulfonate lignin during acid sulfite pulping (Gellerstedt, 1976); (b), Model structure of lignosulfonate lignin (Gargulak and Lebo, 2000) .....	12
Figure 1.9 Reaction scheme for the cleavage of phenolic $\beta$ -O-4 structures and competing reactions in lignin during kraft pulping. L denotes a lignin residue (Gellerstedt, 2009). ..	13
Figure 1.10 Model structure of pine kraft lignin proposed by Marton (Marton, 1971).....	14
Figure 1.11 A proposed reaction scheme, (a) depolymerization and (b) repolymerization reactions in lignin under acidic conditions with a carbocation intermediate (Sannigrahi et al., 2010).....	15
Figure 1.12 The cleavage of lignin non-phenolic $\beta$ -O-4 structures in soda pulping. ....	15
Figure 1.13 A proposed hexamer structure of pyrolytic lignin (Bayerbach and Meier, 2009)	16
Figure 1.14 Lignin derivatives from acetate, propionate, or butyrate, etc. ....	22
Figure 1.15 Lignin based polyester from sebacoyl or dodecandioyl dichlorides.....	22
Figure 1.16 Lignin based polyester from reacting with $\epsilon$ -caprolactone .....	23
Figure 1.17 Lignin-polybutadiene ester .....	24

Figure 1.18 DMA thermogram of F-Lignin-PBD(COOH) <sub>2</sub> with varied F-Lignin content (Saito et al., 2012).....	24
Figure 1.19 Lignin based copoly(ester-amide)s from hyperbranched prepolymers (Sivasankarapillai and McDonald, 2011).....	25
Figure 1.20 Oxypropylation process to obtain a lignin polyol .....	25
Figure 1.21 Possible reactions during condensation of lignosulfonates by thermal treatments (Nimz, 1983).....	27
Figure 1.22 Homopolymer and copolymer structure .....	29
Figure 1.23 Structures of linear and branched polymers .....	29
Figure 1.24 Schematic illustration of dual-shape memory cycle (Xie, 2011).....	31
Figure 1.25 Schematic representation of the molecular mechanism of the thermally induced shape-memory effect for a polymer network with $T_{trans}=T_g$ . If the increase in temperature is higher than $T_{trans}$ of the switching segments, these segments are flexible (shown in red) and the polymer can be deformed elastically. The temporary shape is fixed by cooling down below $T_{trans}$ (shown in blue). If the polymer is heated up again, the permanent shape is recovered. (Lendlein and Kelch, 2002) .....	31
Figure 1.26 Structural morphological demonstration of sub-classes in the dendritic family (Carlmark et al., 2009).....	33
Figure 1.27 Structural scheme of lignin-hyperbranched elastomeric polymer, black circles (lignin) will act as netpoint segment and red part (hyper branched prepolymer) will be switching segment. ....	34
Figure 2.1 FTIR spectra of all the lignin samples.....	54
Figure 2.2 DSC thermograms of IN-MS lignin: (a) conventional DSC without annealing, (b), conventional DSC with annealing, (c) reversible heat flow from MTDSC. Note: arrows pointed to $T_g$ .....	61
Figure 2.3 TMA thermograms of lignin samples: (a) IN, IN-MS, and IN-MI; (b) PB, PB-MS and PB-MI; and (c) CS, CS-MS and CS-MI. Note: arrows pointed to $T_g$ .....	64
Figure 2.4 Dynamic rheological thermograms of various lignin samples.....	65

Figure 2.5 TGA thermograms of the various lignin samples: (a), IN, IN-MS and IN-MI; (b), PB, PB-MS and PB-MI; and (c), CS, CS-MS and CS-MI. ....	66
Figure 2.6 Correlations between lignin $T_g$ (by MTDSC and TMA) with (a), aromatic/aliphatic OH; (b), condensation index (CI); and (c), $M_w$ .....	69
Figure 3.1 Synthetic route for lignin-copoly(ester-amine) elastomer .....	84
Figure 3.2 Branching structures in E1 prepolymer; Dendritic (D), linear (L) and terminal (T). 88	88
Figure 3.3 Positive ion distribution of E1 prepolymer from ESI-MS .....	88
Figure 3.4 Possible cyclic structures in E1 prepolymer.....	89
Figure 3.5 FTIR spectra of (a), PB; (b), acetylated PB; (c), E1-0 polymer; and (d), PBE1-40 copolymer .....	90
Figure 3.6 FTIR spectra of the carbonyl region of (a), PBE1-20 to 45 copolymer; (b), INE1-30 to 45 copolymer; and (c), CSE1-30 to 45 copolymer. Note: arrows mean increase in lignin content.....	91
Figure 3.7 Tensile stress-strain curves of PBE1-45, INE1-45 and CSE1-45 copolymers.....	93
Figure 3.8 DSC (a) and DMA (b) thermograms of PBE1-40 copolymer.....	94
Figure 3.9 $T_g$ of IN, PB and CS lignin-copolymers as a function of lignin content: a, obtained from DMA $E''$ ; and b, from DSC.....	94
Figure 3.10 Thermograms showing tensile loss moduli ( $E''$ ) for all PBE1-20 to 45 copolymers and E1-0 polymer .....	95
Figure 3.11 TGA thermograms of lignin based copolymers: (a), PB based copolymer; (b), IN based copolymer; (c), CS based copolymer; and d, starting materials PB, IN, CS, and E1. 97	97
Figure 3.12 Molecular mechanism of Ts-SME of lignin-co-poly(ester-amine) elastomer. ....	99
Figure 3.13 Tensile stress-temperature-strain ( $\sigma$ -T- $\epsilon$ ) curve of PBE1-20 copolymer. ....	99
Figure 3.14 (a), $R_f$ ; (b), $R_f$ ; and (c), $T_{trans}$ results of IN, PB and CS lignin-copoly(ester-amine)s as a function of lignin content.....	100
Figure 4.1 Synthesis approach for producing the lignin-D1-copolymer .....	113
Figure 4.2 FTIR spectra of lignin, D1 polymer and lignin-D1-copolymers .....	117
Figure 4.3 Tensile properties of lignin-D1-copolymers.....	118

Figure 4.4 (a), MTDSC thermograms of lignin-D1 copolymers showing the reversible heat flow; and (b), $T_g$ values of lignin-D1-copolymers from $E''$ of DMA and MTDSC. ....	119
Figure 4.5 Bulk density ( $\rho$ ) (a), cross-link density ( $\eta$ ) and molecular weight between crosslinks ( $M_c$ ); and (b), correlation between $\eta$ and $T_g$ (c) of lignin-D1-copolymers .....	120
Figure 4.6 TGA (a) and DTG (b) thermograms of lignin, D1 polymer and lignin-D1 copolymers .....	122
Figure 4.7 (a), Shape recovery ( $R_r$ ), shape fixity ( $R_f$ ) and $T_{trans}$ of Ts-SME lignin-D1-copolymers determined by cyclic thermomechanical testing; and (b), Elasticity recovery ( $R_{r,e}$ ) determined at 30 °C .....	124
Figure 4.8 Cyclic thermomechanical testing of lignin-D1-copolymer (15% lignin content) showing (a), Ts-SME behavior (Four steps: 1, Stretching at $T_{high}$ , 2, keep load at $T_{low}$ , 3, unload at $T_{low}$ , and 4, recovery at $T_{high}$ ); and (b), elasticity recovery behavior at 30 °C (Two steps: 1, stretching at 30 °C, and 2, unload and recovery at 30 °C) .....	125
Figure 4.9 SEM micrographs of cut cross-sections of the lignin-D1-copolymers with increasing lignin content ( $\times 1000$ ). .....	126
Figure 5.1 Synthesis of glycerol-based prepolymers and corresponding lignin based copolymers. ....	140
Figure 5.2 Carboxylic acid dimer .....	145
Figure 5.3 $^1H$ NMR spectra of G1, D4 and T4 Gly based prepolymers.....	147
Figure 5.4 $^{13}C$ and DEPT 135 NMR spectra of G1, D4 and T4 Gly based prepolymers. ....	148
Figure 5.5 Apparent viscosity of Gly based prepolymers: (a), G1 and G2; (b), D1 to D4; and (c), T1 to T4. ....	149
Figure 5.6 FTIR spectra of lignin-copolymers.....	151
Figure 5.7 Expanded FTIR spectral region (1540-1800 $cm^{-1}$ ) of lignin-copolymers: (a) LG1 and LG2, (b) LD1 to LD4, and (c) LT1 to LT4. ....	152
Figure 5.8 Oxazolinium-carboxylic ion formation in the D series prepolymer .....	152
Figure 5.9 Tensile properties results of the lignin-copolymers. ....	154
Figure 5.10 $T_g$ of lignin-copolymers from DSC and $E''$ DMA. ....	155
Figure 5.11 TGA results of lignin-copolymers .....	157

Figure 5.12 Photographs showing the SME of LD1 copolymer: (1) Curled at room temperature (25 °C); (2) Subjected into ice (0 °C), curled shape was maintained in ice even after 180s; (3) taken back to room temperature; and (4) gradually recovered the original shape in 150s.....	159
Figure 5.13 Cyclic thermomechanical testing of LD1 copolymer showing $T_s$ -SME behavior (Four steps: (1) Stretching at $T_{high}$ (21 °C); (2) keep load at $T_{low}$ (-19 °C); (3) unload at $T_{low}$ (-19 °C); and (4) recovery at $T_{high}$ (21 °C)) for 3 cycles .....	160
Figure 6.1 Summary of research conducted in the dissertation.....	169
Figure 6.2 Summary of synthetic approaches of lignin based copolymers .....	171



## Table of Tables

Table 1.1 Common commercial plastics and market sales of 2013 in U.S. (Council, 2014b) ....	1
Table 1.2 Common bio-based polymers .....	3
Table 1.3 Constituents of lignocellulosic biomass (Sjostrom, 1993) .....	5
Table 1.4 Composition of lignin monomers in different plants (Henriksson, 2009) .....	9
Table 1.5 Calculated monomer formula and molecular weight of various lignins (Marton, 1971; Zakzeski et al., 2010) .....	18
Table 1.6 Functional groups and weight average molar mass ( $M_w$ ) of some industrial lignins (Doherty et al., 2011) .....	18
Table 1.7 Glass transition temperature of various lignins (Glasser, 2000; Goring, 1971; Hatakeyama and Hatakeyama, 2010) .....	19
Table 2.1 Lignin contents based on Klason lignin and acid soluble lignin .....	53
Table 2.2 Assignments of FTIR bands of lignin (Faix, 1991a) .....	55
Table 2.3 Lignin aromatic/aliphatic OH group ratios on acetylated samples and lignin condensation indices (CI) determined by FTIR spectroscopy .....	56
Table 2.4 Compound identification and intensities of the various lignins by py-GC-MS .....	57
Table 2.5 DFRC results of aryl ether linkage levels for the various lignin samples.....	59
Table 2.6 Syringyl to guaiacyl ratios (S/G) of the various lignin samples by FTIR, py-GC-MS and DFRC .....	60
Table 2.7 Comparison of $T_g$ s of the various lignin samples determined by DSC, MTDSC, TMA and rheometry. ....	62
Table 2.8 Thermogravimetric analysis results of the various lignin samples .....	67
Table 2.9 Thermal decomposition activation energies ( $E_a$ ) determined by TGA for IN, IN-MS and IN-MI samples. ....	68
Table 3.1 Hydroxyl group determination from acetylated lignin by FTIR and $^1\text{H}$ NMR.....	87
Table 3.2 Molar mass determination of different fractionated industrial lignins and E1 prepolymer.....	87
Table 3.3 ESI-MS ion assignments of E1 oligomeric structures .....	89

Table 3.4 Tensile properties of different industrial lignin based copolymers at room temperature .....	92
Table 3.5 Thermal decomposition of different lignin based copolymers from TGA data .....	96
Table 4.1 Thermal decomposition of lignin based long chain elastomers .....	121
Table 5.1 Analysis of bio-based components in Gly based prepolymers and lignin-copolymers .....	144
Table 5.2 Reaction conditions for preparing Gly based prepolymers and properties.....	146
Table 5.3 Thermal decomposition of the lignin-copolymers .....	156
Table 5.4 Shape memory effect parameters ( $R_r$ , $R_f$ , and $T_{trans}$ ) and elasticity recovery $R_{r,e}$ of the lignin-copolymers .....	159

## Table of Abbreviations

AA	Adipic acid
ATR	Attenuated total reflectance
<sup>13</sup> C NMR	Carbon 13 nuclear magnetic resonance
CEL	Cellulosic enzymes lignin
CI	Condensation Indices
COSY	Proton-proton correlation spectroscopy
CS	Corn stover lignin
CS-MI	Corn stover lignin methanol insoluble fraction
CS-MS	Corn stover lignin methanol soluble fraction
DB	Degree of branching
DDDA	Dodecanedioic acid
DFRC	Derivatization followed by reductive cleavage
DIPA	Diisopropanolamine
DMA	Dynamic mechanical analyzer
DSC	Differential scanning calorimeter
DTG	Differential thermogravimetric
ESI-MS	Electrospray ion – mass spectroscopy
ESR	Electron spin resonance
FTIR	Fourier transform infrared spectroscopy
G	Guaiacyl unit
Gly	Glycerol
GPC	Gel permeation chromatography
<sup>1</sup> H NMR	Proton nuclear magnetic resonance
H-bonding	Hydrogen bonding
HBP	Hyperbranched polymer
HDPE	High density polyethylene
HSQC	Heteronuclear single quantum coherence spectroscopy
IR	Infrared spectroscopy
IN	Indulin AT softwood lignin
IN-MI	Indulin AT softwood lignin methanol insoluble fraction
IN-MS	Indulin AT softwood lignin methanol soluble fraction
LDPE	Low density polyethylene
LLDPE	Linear low density polyethylene
$M_n$	Number-average molar mass
$M_w$	Weight-average molar mass
MTDSC	Modulated-temperature differential scanning calorimetry
MWL	Milled wood lignin
P	<i>p</i> -Hydroxy phenyl unit
PB	Protobind 1000 lignin
PB-MI	Protobind 1000 lignin methanol insoluble fraction
PB-MS	Protobind 1000 lignin methanol soluble fraction

PDI	Polydispersity index
PE	Polyethylene
PHAs	Polyhydroxyalkanoates
PLA	Poly(lactic acid)
PP	Polypropylene
PS	Polystyrene
PVC	Polyvinylchloride
Py-GC-MS	Pyrolysis-gas chromatography-mass spectrum
$R_f$	Shape fixity rate
$R_r$	Shape recovery rate
$R_{r,e}$	Elastic recovery rate
S	Syringyl unit
S/G	Syringyl to guaiacyl ratio
SEC	Size exclusion chromatography
SEM	Scanning electron microscopy
SME	Shape memory effect
SMP	Shape memory polymer
TEA	1,1,1-triethanolamine
TGA	Thermogravimetric analyzer
THAM	Tris(hydroxymethyl)aminomethane
THF	Tetrahydrofuran
$T_g$	Glass transition temperature
TMA	Thermomechanical analyzer
$T_s$	Softening temperature
$T_s$ -SME	Thermal-stimulated shape memory effect
$T_{trans}$	Shape transition temperature

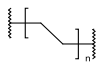
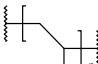
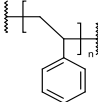
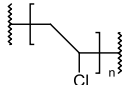
## 1 Introduction and Literature Review

### 1.1 Introduction

#### 1.1.1 Petroleum-based polymers and situation

Petroleum-based polymers have become a very important part of modern society. U.S. produced 48.8 billion kg but sold 49.3 billion kg in 2013, and merely 0.46 billion kg plastic films and wraps were recycled according to the American Chemistry Council (ACC) Plastics Industry Producers' Statistics (PIPS) Group (Council, 2014a, b). Of all the petroleum-based polymers, polyethylene (PE), polypropylene (PP), polystyrene (PS), and polyvinylchloride (PVC) accounted for dominant plastics in films, packaging, pipes, consumer products, etc (Table 1.1). However, petroleum-based polymers have some negative issues: solid pollution to farmland and deep sea due to difficult to degrade polymer wastes, limited petroleum resource and supply, and global warming due to production and incineration of the polymers. Polymers do have merits, for instance, can be processed into many different products, durability, plasticity, low cost, mechanical flexibility, abundant variety, and lightness (Teramoto, 2011). Under these circumstances, it is necessary to develop sustainable and renewable based bioplastic materials.

Table 1.1 Common commercial plastics and market sales of 2013 in U.S. (Council, 2014b)

Synthetic polymers	Structure	Sales in 2013 (billion kg)	
Polyethylene (PE)		HDPE	8.1
		LDPE	3.1
		LLDPE	6.3
Polypropylene (PP)		7.4	
Polystyrene (PS)		2.0	
Polyvinylchloride (PVC)		7.0	

### **1.1.2 The necessity of developing bio-based renewable materials**

Sustainability and renewability are two global thematic topics, where sustainability refers to “the ability to meet current needs without putting in jeopardy the ability of future generations to meet their own needs” (Dube and Salehpour, 2014); and renewability relates to natural resources, such as solar energy, water, or biomass, that is never used up or that can be replaced by new growth in a realistic time scale. The term “bio-based product,” under the sustainable and renewable category, is “a commercial or industrial product (other than food or feed) that is composed, in whole or in significant part, of biological products or renewable domestic agricultural materials (including plant, animal, and marine material) or forestry material” (Economist and Uses, 2008). The US Department of Agriculture (USDA) has reported that the total polymer market for 2005 was \$250 billion with bio-based polymer merely accounting for \$0.3 billion. Furthermore, the USDA has estimated that the total polymers market will grow to \$452 billion and the bio-based polymers will also grow to \$45-90 billion by 2025 (Economist and Uses, 2008).

### **1.1.3 Types of natural renewable bio-based polymers**

To date, numerous bio-based monomers and polymers have been made from renewable resources including poly(lactic acid) (PLA), polyhydroxyalkanoates (including poly(hydroxybutyrate) (PHAs), poly(hydroxybutyrate-co-hydroxyvalerate) (PHBV)), vegetable-oil based polymers, cellulose derivatives, thermoplastic starch, protein, and lignin to name a few. Basically, they could be divided into three categories (Chen, 2010): the 1<sup>st</sup> category consists of polymers totally obtained from renewable feedstock (PLA and PHAs); the 2<sup>nd</sup> category contains polymers partially derived from renewable feedstock (vegetable oil based polymer); the 3<sup>rd</sup> category is naturally occurred polymers directly or with modification for polymers (polyisoprene, cellulose derivatives, thermoplastic starch, protein, and lignin).

Table 1.2 Common bio-based polymers

Polymers	Structures	General descriptions
Poly(lactic acid) (PLA)		Industrial scale; Resulting from the condensation polymerization of lactic acid or from ring-opening polymerization of lactide.
Polyhydroxyalkanoates (PHAs)		Not industrial scale; Bacteria produced; The carbon chain length of the repeating units in PHAs varies depending on the bacteria.
Vegetable-oil based polymers		Involving triglyceride modification, especially double bonds. Foams and thermoplastics were obtained.
Polyisoprene		Natural rubber, widely used.
Cellulose derivatives		Oldest applied before modern polymers. Commercially like cellulose nitrate.
Protein		Vegetable proteins such as soy, corn, etc. were applied as polymer materials.

Several recent reviews have covered the development of the bio-based polymers as well as green chemistry concept related to bio-based polymers. Quirino, et al. (2014) reviewed the progress over the last decade in the development of a select group of bio-based matrices for biocomposites applications. Yao and Tang (2013) critically reviewed from the perspective on preparing renewable polymers from monomeric building blocks. This includes oxygen-rich monomers, hydrocarbon-rich monomers, hydrocarbon monomers, and non-hydrocarbon monomers (e.g. CO<sub>2</sub>) plus using a variety of emerging synthetic tools such as controlled polymerization and click chemistry. Miller (2013) had discussed the design of sustainable polymers, specifically addressing opportunities for monomer development and polymer

degradation. This study developed several concepts, which include water degradability instead of biodegradability, incorporation of novel main-chain functionality (acetals), utilization of lignin-based aromatics, and direct polymerization of biogenic C1 feed-stocks. Dube and Salehpour (2014) reviewed 12 principles of green chemistry and subsequently applied them to polymer production. All of these scientific and government efforts seek to utilize and develop bio-based polymers in a wide range of applications, which guarantee the possibility of developing the sustainable polymers.

Although considerable efforts have been devoted to the utilization of bio-based polymers (such as cellulose) in biomaterial or bioplastic (such as cellulose acetate) applications, under developed naturally occurring polymers, such as lignin, still exist. Therefore, with the purpose of contributing to new bio-based polymer use, especially lignin based polymers, this literature review will first overview lignocellulosic biomass, then systematically introduce about lignin structure, properties and application, then lignin polymer systems.

## **1.2 Literature review**

### **1.2.1 Chemistry of lignocellulosic biomass**

Lignocellulosic biomass is a complex of natural polymer substances: cellulose, hemicelluloses, lignin (Saka, 2000). These substances are located in the plant cell wall as illustrated in Figure 1.1a. The cell wall is divided into different layers (primary, secondary and middle lamella), each layer having its own particular arrangement of cellulose microfibrils (MF), determining the mechanical and physical properties of wood. These MFs may be aligned irregularly (as in the primary cell wall), or aligned in a particular angle to the cell axis (as in layer S1, S2, and S3). The middle lamella is the region between adjacent cells and composed primarily of lignin (Plomion et al., 2001). Three major components in cell wall function differently in lignocellulosic biomass (Figure 1.1b). Cellulose acts as the structural framework in the form of cellulose MFs, while hemicellulose is the matrix substance present between these MFs and lignin. Lignin is the encapsulating substance binding adjacent wood cells together and giving rigidity to the cell wall (Saka, 2000).



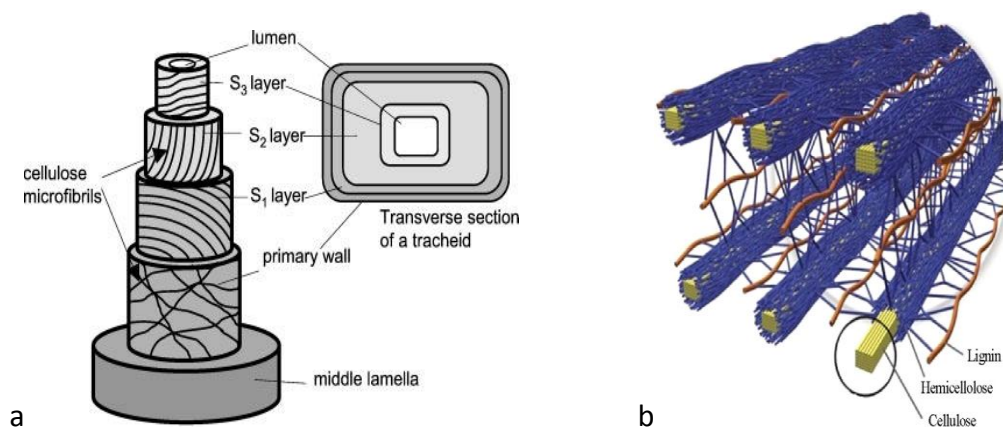


Figure 1.1 (a), three-dimensional structure of the plant secondary cell wall of a tracheid (xylem cell) (Plomion et al., 2001); and (b), chemical structure of cell wall (Doherty et al., 2011).

Table 1.3 Constituents of lignocellulosic biomass (Sjostrom, 1993)

Constituent	Scots Pine ( <i>Pinus sylvestris</i> )	Spruce ( <i>Picea glauca</i> )	Eucalyptus ( <i>Eucalyptus camaldulensis</i> )	Silver Birch ( <i>Betula verrucosa</i> )
Cellulose (%)	40	39.5	45.0	41.0
Hemicelluloses				
-Glucomanan (%)	16.0	17.2	3.1	2.3
-Glucuronoxylan (%)	8.9	10.4	14.1	27.5
-Other polysaccharides (%)	3.6	3.0	2.0	2.6
Lignin (%)	27.7	27.5	31.3	22.0
Extractives (%)	3.5	2.1	2.8	3.0

### 1.2.1.1 Cellulose

Cellulose represents the most abundant biomacromolecules on earth (Brown, 2004), with  $1.5 \times 10^{15}$  kg of the total annual biomass production (Klemm et al., 2005). Molecular structure (Figure 1.2) of cellulose as a carbohydrate polymer generated from repeating  $\beta$ -(1-4)-D-glucopyranosyl units with a degree of polymerization ranging from 10000 in native wood to 1000 in bleached kraft pulps (Klemm et al., 2005). As a result, cellulose is an extensive, linear-chain polymer with a large number of hydroxyl groups which ensure the highly crystallinity, hydrophilicity, chirality, degradability, and broad chemical variability due to their high donor reactivity. The cellulose products involve tremendous varieties, for example, paper industry, cotton, fabrics, and some derivatives as discussed aforementioned.

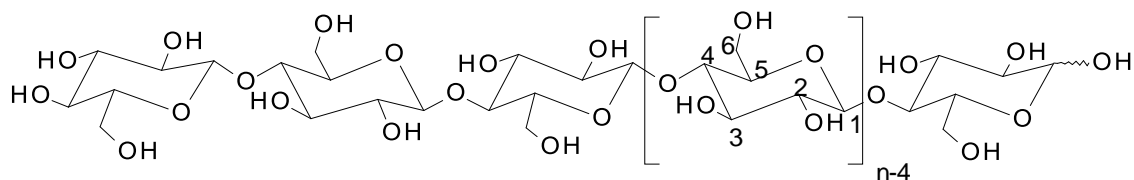


Figure 1.2 Molecular structure of cellulose (Klemm et al., 2005)

### 1.2.1.2 Hemicelluloses

Hemicelluloses are the second most polysaccharides in nature, owning about 20–35% of lignocellulosic biomass (Saha, 2003). Hemicelluloses are heterogeneous polymers of pentoses (xylose, arabinose), hexoses (mannose, glucose, galactose), and sugar acids with lower degree of polymerization comparing to cellulose. Unlike cellulose, hemicelluloses are not chemically homogeneous (Table 1.3). Hardwood hemicelluloses contain mostly xylans, whereas softwood hemicelluloses contain mostly glucomannans (Brownell and Saddler, 1984).

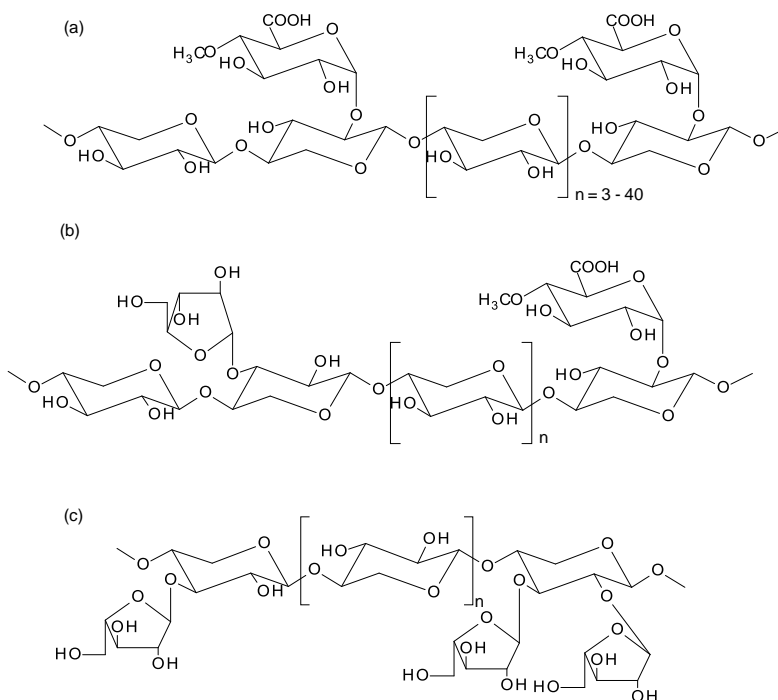


Figure 1.3 Structures of (a) hardwood 4-O-methylglucurono-xylan, (b) softwood arabino-(4-O-methylglucurono)-xylan, and (c) arabinoxylan (Ebringerova and Heinze, 2000).

### 1.2.1.3 Extractives

Extractives are constituents of lignocellulosic biomass with low content and low molar mass (Table 1.3) extracted with neutral solvents (Umezawa, 2000). Extractives are the predominant contributors to wood color, fragrance, and durability. These organic components of extractive content of lignocellulosic biomass comprise of tannins and other polyphenolics, coloring matter, essential oils, fats, resins, waxes, gum starch, and simple metabolic intermediates, which could be applied in various areas (Fabiya, 2007).

## 1.2.2 Lignin structure and biosynthesis

### 1.2.2.1 Lignin structure

The term “lignin” is derived from the Latin word “lignum” for wood (Sarkanen and Ludwig, 1971). Lignin, a phenolic polymer resulting from the oxidative combinatorial coupling of 4-hydroxyphenylpropanoids (*p*-coumaryl alcohol, coniferyl alcohol, and synapyl alcohol) as shown in Figure 1.4, is widely present in plant kingdom, especially in tracheophytes (Vanholme et al., 2010; Weng and Chapple, 2010). Lignin is second in abundance to cellulose (Lewis and Lantzy, 1989). Lignin’s occurrence is in plant material such as lignocellulosic biomass, fruit, bark, root, bast, pith, and cork cells (Pearl, 1967), and even seaweed (Martone et al., 2009). In wood, lignin content varies depending on species with typically 20-30% for hardwoods and 25-35% for softwoods (Dimmel, 2010). Detailed composition information of various biomass could be found in (Vassilev et al., 2010).

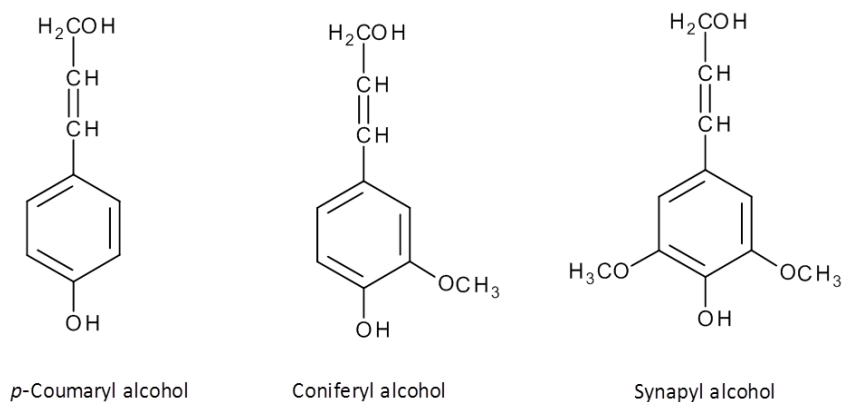


Figure 1.4 Monomers structure of lignin macromolecules

### 1.2.2.2 Lignin biosynthesis

Research on lignin biosynthesis has been advanced by need to develop lignocellulosic biomass crops with low lignin contents or modified structure for pulping and cellulosic ethanol applications (Boerjan et al., 2003; Grabber et al., 2004; Ralph, 1999; Ralph, 2010; Ralph et al., 2007; Ralph et al., 2004; Simmons et al., 2010; Vanholme et al., 2010; Vanholme et al., 2008; Wagner et al., 2012).

During the cell growth process, lignification is the last event before programmed cell death, involving development of the secondary cell wall by deposition of cellulose elementary fibrils together with hemicelluloses. Once the polysaccharide skeletal framework is formed lignin is deposited and forms a matrix to bond the macromolecular system together as shown in Figure 1.4. Lignin provides stiffness to the cell wall plus bonds adjacent cells together in the middle lamella region. The middle lamella contains the highest concentration of lignin in the xylem (Sjostrom, 1993).

Lignification involves several steps: biosynthesis of monolignols (Figure 1.4), diffusion of the monolignols into the secondary cell wall and middle lamella, generation of free radicals via peroxidase/laccase action (Figure 1.5), and free radical coupling of the free radical monolignols (only during initiation reactions), and/or more typically cross-coupling reactions with the growing lignin polymer/oligomer, to build up a three-dimensional phenylpropanoid polymer architecture (Figure 1.3) (Ralph et al., 2007). Lignin is non-optically active unlike polysaccharides (Henriksson, 2009; Ralph et al., 1999). Lignin structure is highly species dependent as shown in Table 1.4 (Henriksson, 2009). Lignin is comprised of several inter-unit linkages to connect monomeric units, such as  $\beta$ -aryl ether (or  $\beta$ -O-4), phenylcoumaran (or  $\beta$ -5), resinol (or  $\beta$ - $\beta$ ), biphenyl (or 5-5), diphenyl ether (or 4-O-5), and other common linkages are shown in Figure 1.6. The  $\beta$ -O-4 linkage is the dominant inter-lignin unit linkage accounting for 50% in softwood lignin and 60% in hardwood lignin (Sjostrom, 1993). Moreover, new linkages have been recently found, such as the dibenzodioxocins, with aid of new spectroscopic NMR techniques and methods (Ralph, 1999).

Table 1.4 Composition of lignin monomers in different plants (Henriksson, 2009)

Plant	<i>p</i> -Coumaryl alcohol (%)	Coniferyl alcohol (%)	Sinapyl alcohol (%)
Coniferous softwood	<5	>95	None or trace
Eudicotyledonous hardwood	0-8	25-50	46-75
Monocotyledonous grass	5-33	33-80	20-54

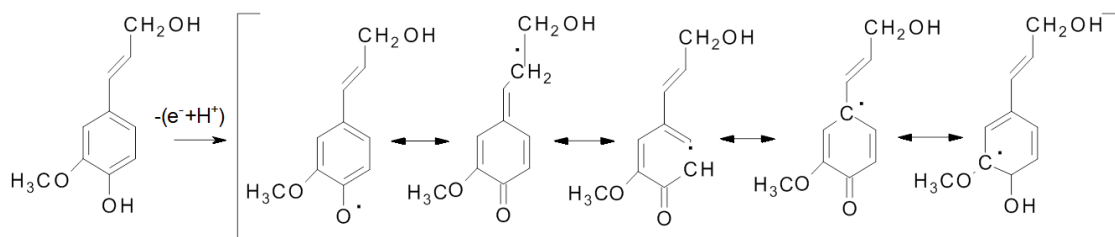


Figure 1.5 Resonance stabilized phenoxy radical of coniferyl alcohol (Sjostrom, 1993)

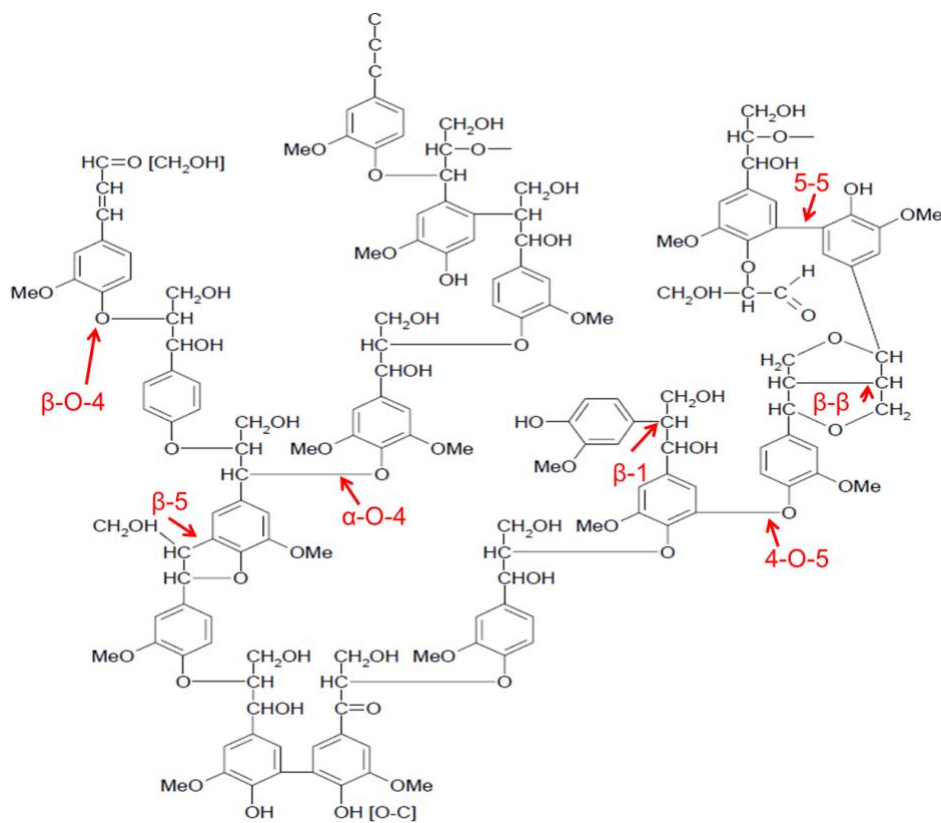


Figure 1.6 Softwood lignin model structure as well as linkages (Alder, 1977)

### 1.2.3 Industrial lignin and isolation processes

Lignin is isolated as by-product of the wood pulping industry and it is estimated that 95% of lignin generated is used as fuel to drive the energy recovery system in a pulp mill (Feldman, 2002). The remaining 5% of this lignin is isolated from the pulp liquor, called industrial lignin or technical lignin in order to differentiate it from native lignin or protolignin. Lignin structure is species, process, and isolation method dependent. As a by-product of wood pulping and cellulosic ethanol operations, the types of process determine lignin's properties and structure. Industrial lignin can be categorized into sulfur lignin (kraft lignin and lignosulfonate lignin) and sulfur free lignin (soda lignin, organosolv lignin, pyrolytic lignin, and bio-ethanol lignin) in terms of processing techniques (Laurichesse and Avérous, 2013; Lora, 2008; Lora and Glasser, 2002; Meister, 2002; Zakzeski et al., 2010). Besides industrial processes, analytical methods to isolate lignin have also been developed, such as cellulosic enzymes lignin (CEL), and ball milled wood lignin (MWL) primarily for research purposes (Sjostrom, 1993). Figure 1.7 illustrated the corresponding processes to extract lignin from lignocellulosic biomass. Lignin isolation methods always involve some depolymerization and reforming of new linkages in the final product and therefore native and isolated lignin are different.

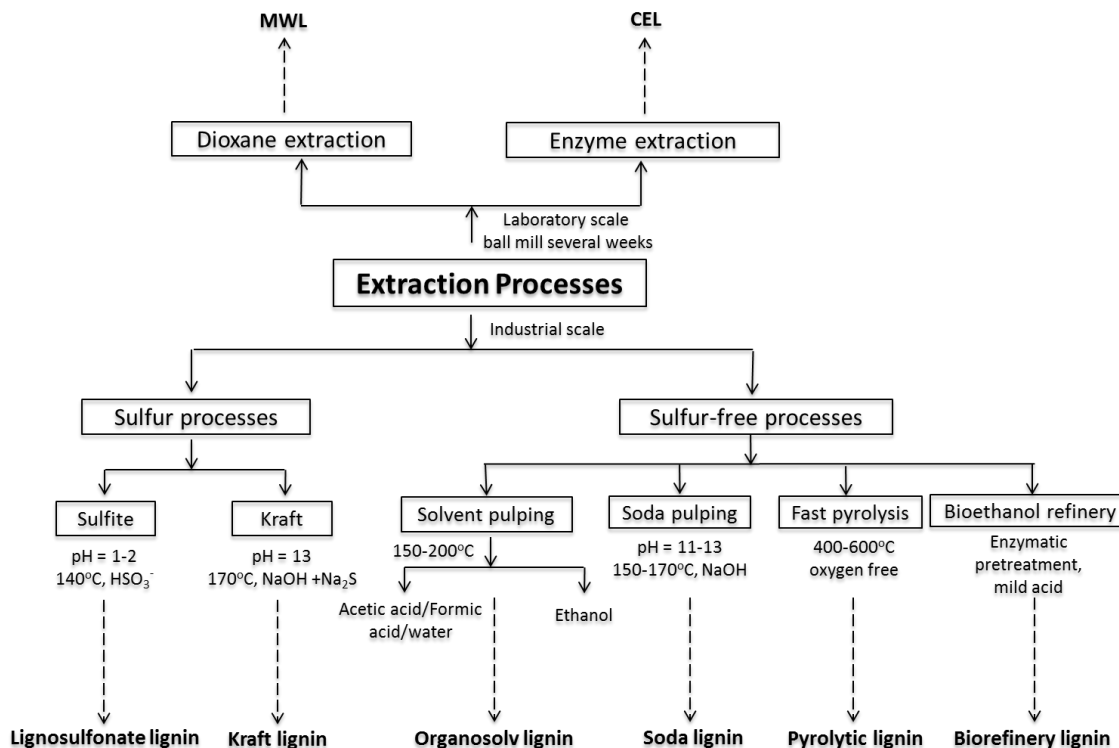


Figure 1.7 Extraction processes to separate lignin from lignocellulosic biomass and the corresponding productions of industrial lignin and less-alternative lignin (Holladay et al., 2007; Laurichesse and Avérous, 2013).

### 1.2.3.1 Sulfur lignin

#### 1.2.3.1.1 Lignosulfonate lignin

The sulfite process for separating lignin from lignocellulosic biomass produces a class of lignin derivatives named lignosulfonates by attacking the biomass with an aqueous solution of sulfite or bisulfite salt of sodium, ammonium, magnesium or calcium at 140-170°C under neutral to acidic conditions (Lora, 2008; Meister, 2002). The reaction mechanism and model structure are shown in Figure 1.8a and b. Wood reacts with sulfur dioxide and hydrogen sulfite and consequently sulfonic acid groups are attached to the lignin backbone, thereby making lignin water soluble. The lignin reactions are controlled through regulating pH value of reaction solution ranging from neutral to acidic conditions (Fox, 2006). The sulfur content of lignosulfonate lignin is reported as 6.5% and molar mass of 10,000-40,000 g/mol (Meister, 2002). The application of lignosulfonate lignin includes binders, dispersing agent, surfactant,

adhesives and cement additives (Gargulak and Lebo, 2000). However, environmental restrictions limit the development of this lignin.

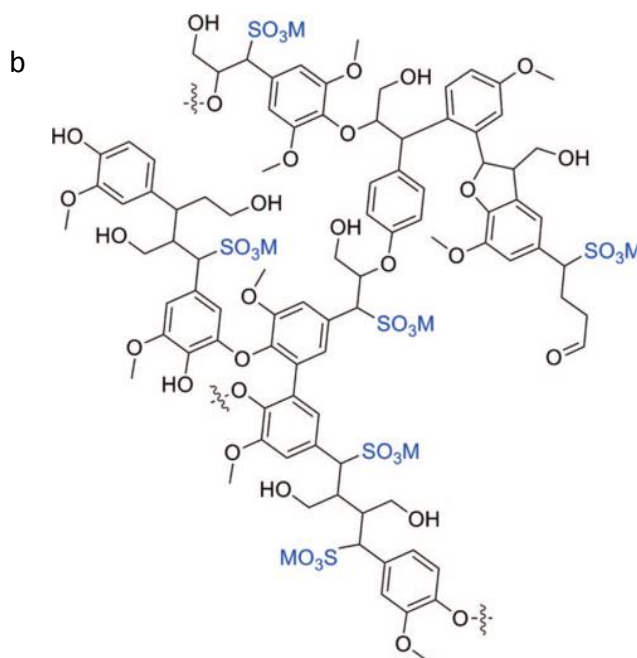
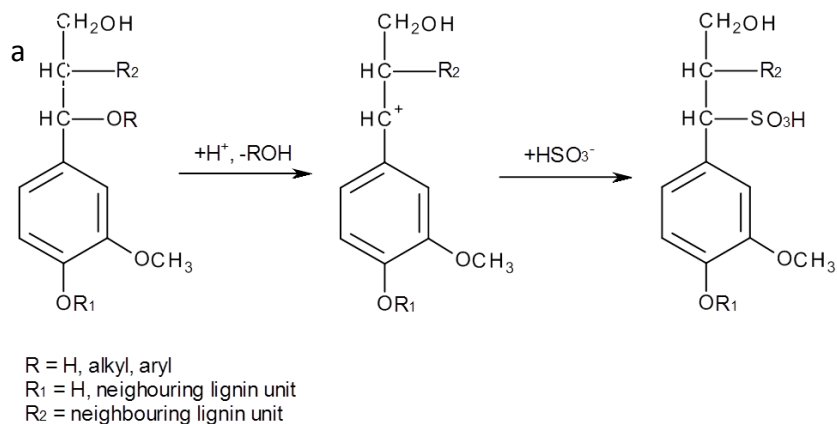


Figure 1.8 (a), Reaction mechanism of lignosulfonate lignin during acid sulfite pulping (Gellerstedt, 1976); (b), Model structure of lignosulfonate lignin (Gargulak and Lebo, 2000)

#### 1.2.3.1.2 Kraft lignin

The Kraft pulping process is the most dominant chemical pulping technique, which employs high pH (13) and appreciable amounts of aqueous NaOH and Na<sub>2</sub>S at temperatures 170 °C for 2 h to degrade and solubilize lignin in a stepwise process (Holladay et al., 2007). The ether groups ( $\beta$ -O-4) of native lignin are attacked to form quinone methide intermediate and



consequently lignin molecules are fragmented into smaller units and the number of phenolic hydroxyl groups increases which impart the solubility under alkaline conditions. The reaction scheme of lignin ( $\beta$ -O-4) inter-unit cleavage is proposed in Figure 1.9. A model structure of Kraft lignin is illustrated in Figure 1.10. Kraft lignin contains a small amount of aliphatic thiol groups causing the final product to have a distinct odor. The sulfur content of kraft lignin is 1-2%. Only a small amount of kraft pulping liquors are used to produce kraft lignin in the United States and Europe (Gargulak and Lebo, 2000), while the majority of the black liquor is directly burnt as fuel for the energy compensate for boiler (Lora and Glasser, 2002).

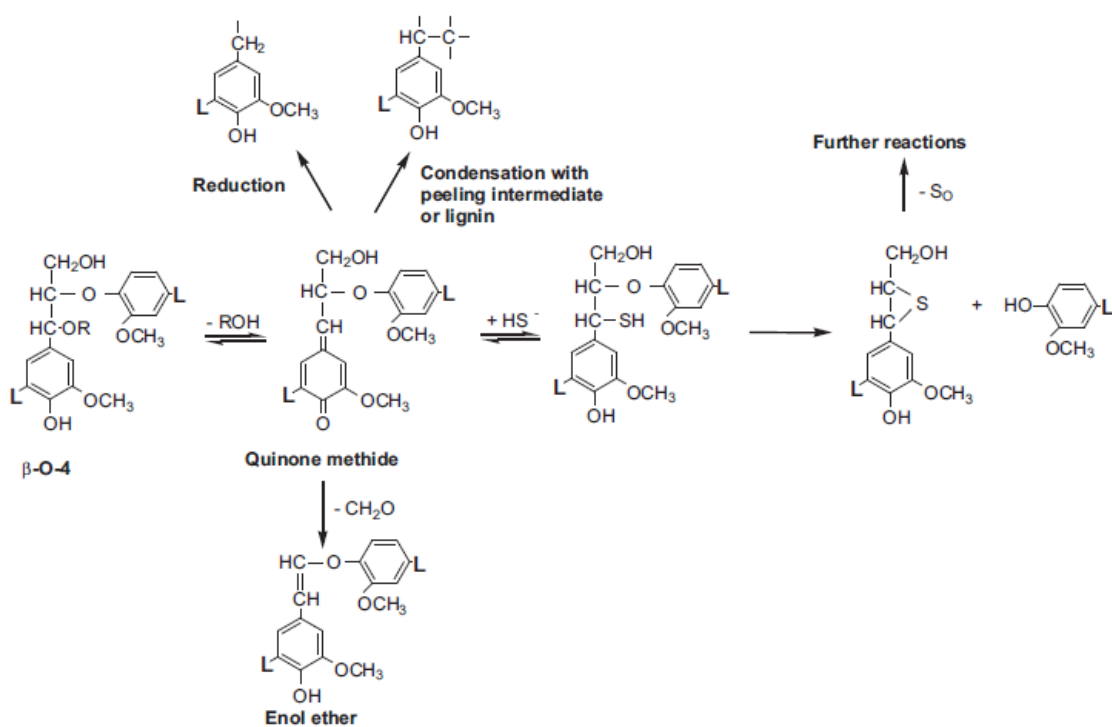


Figure 1.9 Reaction scheme for the cleavage of phenolic  $\beta$ -O-4 structures and competing reactions in lignin during kraft pulping. L denotes a lignin residue (Gellerstedt, 2009).

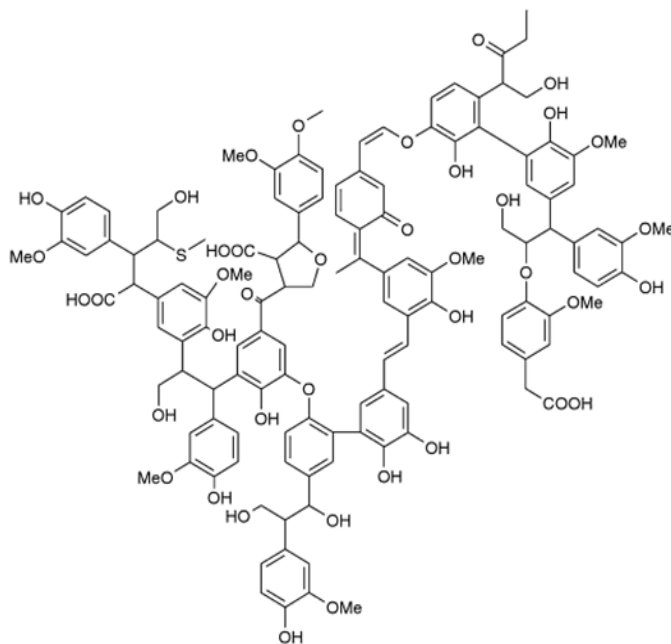


Figure 1.10 Model structure of pine kraft lignin proposed by Marton (Marton, 1971)

### 1.2.3.2 Sulfur free lignin

#### 1.2.3.2.1 Organosolv lignin

Organosolv lignin is obtained by treatment of lignocellulosic biomass with various organic solvents (ethanol, methanol, formic acid, and acetic acid) in the presence of an acid or base catalyst (Kim and Pan, 2010; Pan et al., 2006; Pan et al., 2007; Stockburger, 1993). The pulping reaction involves the cleavage of ether linkages as in other pulping processes. The  $\alpha$ -O-4 bonds are very labile and the  $\beta$ -aryl-ether bonds can also be cleaved under certain conditions as shown in Figure 1.11 (Sannigrahi et al., 2010). Organosolv lignin is usually of high-purity, low number average molar mass ( $M_n < 1000$  g/mol) with a polydispersity index (PDI) of 2.4-6.4. Solvent pulping is an alternative to traditional kraft and sulfite pulping in terms of being an environmentally-friendly process (Holladay et al., 2007). Organosolv lignin has a high solubility in organic solvents but limited solubility in water (Lora and Glasser, 2002).

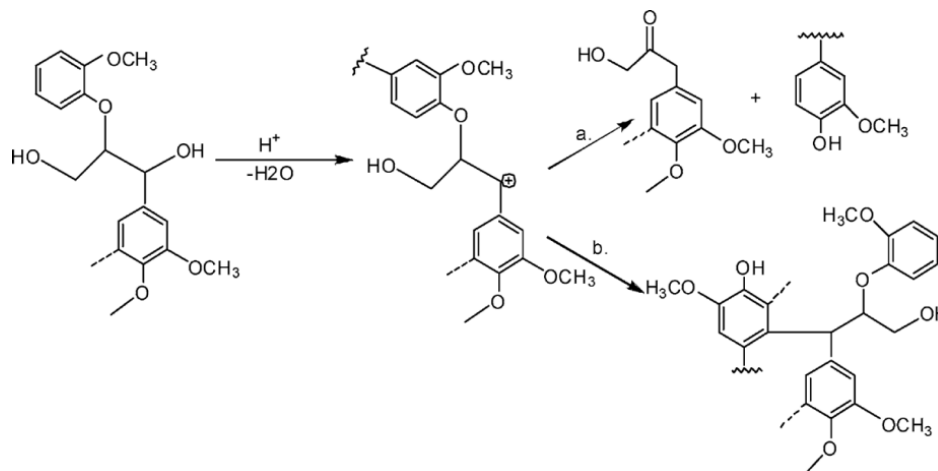


Figure 1.11 A proposed reaction scheme, (a) depolymerization and (b) repolymerization reactions in lignin under acidic conditions with a carbocation intermediate (Sannigrahi et al., 2010)

#### 1.2.3.2.2 Soda lignin

The soda process is the oldest pulping technique and is generally used for pulping non-woody biomass, including bagasse, sisal, kenaf, hemp, and wheat straw (Chung and Washburn, 2013). The process is similar to kraft pulping but without  $\text{Na}_2\text{S}$  and in turn the lignin is sulfur free and a suitable raw materials of various applications (Lora, 2002). The mechanism for  $\beta$ -O-4 cleavage in soda pulping is shown in Figure 1.12.

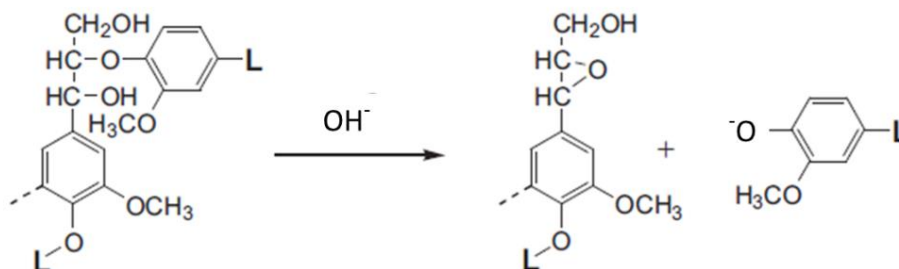


Figure 1.12 The cleavage of lignin non-phenolic  $\beta$ -O-4 structures in soda pulping.

#### 1.2.3.2.3 Pyrolytic lignin

Fast pyrolysis is the thermal decomposition of materials in the absence of oxygen at 400-600°C with short hot vapor residence times ( $\sim 1$  s) (Bridgwater, 2012; Bridgwater et al., 1999;

Mohan et al., 2006). The final product contains 13%, 75% and 12 % of gas, liquid (bio-oil), and solid (bio-char) fractions, respectively. Pyrolytic lignin is extracted from bio-oil with an organic solvent (Sahaf et al., 2013) or precipitated by the addition iced water with high-speed stirring (Zhou et al., 2013a; Zhou et al., 2013b; Zhou et al., 2013c) to give a yield of about 20% (Qin and Kadla, 2012). The major difference between pyrolytic lignin and industrial lignin is its low molar mass (weight average molar mass ( $M_w$ ) = 600-1300 g/mol and  $M_n$  = 300-600 g/mol) (Bayerbach and Meier, 2009; Bayerbach et al., 2006; Scholze et al., 2001; Scholze and Meier, 2001). The low molar mass of pyrolytic lignin results from a high degree of depolymerization during pyrolysis and are oligomeric in nature, while industrial lignins have a high molar mass due to highly condensed (cross-linked) structures. Furthermore, the flow characteristic of pyrolytic lignin was likely due its low molar mass (Scholze et al., 2001; Uraki et al., 2012). A proposed pyrolytic lignin hexamer is shown in Figure 1.13.

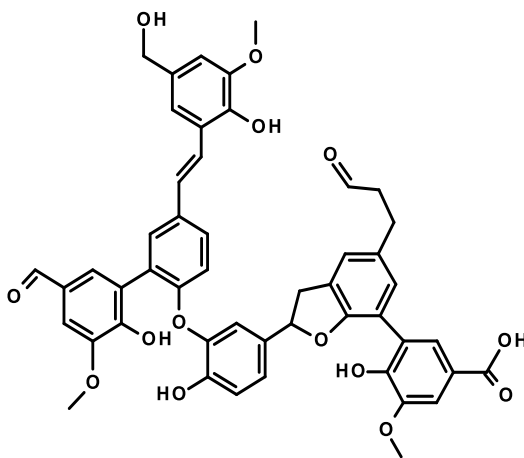


Figure 1.13 A proposed hexamer structure of pyrolytic lignin (Bayerbach and Meier, 2009)

#### 1.2.3.2.4 Bio-ethanol lignin

In producing cellulosic ethanol, lignin is an insoluble byproduct after generating sugars from cellulose and hemicellulose. In order to obtain sugars from lignocellulosic materials, it require a pretreatment step, usually a mild hydrothermal process, in order to make the carbohydrate accessible for enzymatic hydrolysis to sugars (Kumar et al., 2009). The

obtained lignin fraction is relatively unaltered as compared to pulping processes, however, residual sugars may contaminate this lignin rich material (Holladay et al., 2007).

### **1.2.3.3 Research isolated lignin**

Milled wood lignin (MWL) is the general method to obtain lignin for research purposes. This involves ball milling the lignocellulosic biomass to obtain very small particles (<25  $\mu\text{m}$ ) for subsequent solvent extraction to obtain yields of 10% based on original lignin content (Meister, 2002). In the production of MWL the composition may be slightly different than native lignin due to selective extraction (only 10%) or slight alteration during ball milling (Sjostrom, 1993). Cellulosic enzyme lignin (CEL) is a more efficient approach to obtain a "lignin" samples and again involves ball milling wood to a fine powder and then treating this with a cellulase enzyme to remove cellulose and hemicellulose leaving behind a lignin rich CEL fraction which is more representative of native lignin (Glasser et al., 1983). Therefore, these two lignin isolation methods are extensively used in lignin characterization studies. Other approaches to isolate lignin have involved hot water extraction, ammonia fiber explosion (AFEX) process, and steam explosion (Holladay et al., 2007).

## **1.2.4 Utilization of industrial lignin for use in polymers and resins**

### **1.2.4.1 Macromolecular properties of industrial lignins**

#### **1.2.4.1.1 Chemical properties**

The chemical properties of an industrial lignin will govern its use in polymeric materials and properties of several technical lignins are given in Tables 1.5 and 1.6. Table 1.5 gives the monomer formula of isolated lignins. Functional groups (methoxyl content, hydroxyl content and carboxylic acid content) and molar mass of some industrial lignins are given in Table 1.6.

Table 1.5 Calculated monomer formula and molecular weight of various lignins (Marton, 1971; Zakzeski et al., 2010)

Lignin	Monomer molecular formula
MWL (spruce)	$C_9H_{8.8}O_{2.37}(OCH_3)_{0.96}$
MWL (birch)	$C_9H_{8.24}O_{2.95}(OCH_3)_{1.38}$
Kraft lignin	$C_9H_{8.5}O_{2.1}S_{0.1}(OCH_3)_{0.8}(CO_2H)_{0.2}$
Technical kraft lignin	$C_9H_{7.98}O_{2.28}S_{0.08}(OCH_3)_{0.77}$
Unreacted kraft lignin	$C_9H_{8.97}O_{2.65}S_{0.08}(OCH_3)_{0.89}$
Lignosulfonate lignin (softwood)	$C_9H_{8.5}O_{2.5}(OCH_3)_{0.85}(SO_3H)_{0.4}$
Lignosulfonate lignin (hardwood)	$C_9H_{7.5}O_{2.5}(OCH_3)_{0.39}(SO_3H)_{0.6}$
Organosolv lignin	$C_9H_{8.53}O_{2.45}(OCH_3)_{1.04}$
Pyrolytic lignin	$C_8H_{6.3-7.3}O_{0.6-1.4}(OCH_3)_{0.3-0.8}(OH)_{1-1.2}$
Steam explosion lignin	$C_9H_{8.53}O_{2.45}(OCH_3)_{1.04}$
Dilute acid lignin	$C_9H_{8.53}O_{2.45}(OCH_3)_{1.04}$
Alkaline oxidation lignin	$C_9H_{8.53}O_{2.45}(OCH_3)_{1.04}$
Beech lignin	$C_9H_{8.83}O_{2.37}(OCH_3)_{0.96}$

Table 1.6 Functional groups and weight average molar mass ( $M_w$ ) of some industrial lignins (Doherty et al., 2011)

Lignin	$M_w$ (g/mol)	COOH (%)	OH phenolic (%)	Methoxy (%)
Soda (bagasse)	2160	13.6	5.1	10.0
Organosolv (bagasse)	2000	7.7	3.4	15.1
Soda (wheat straw)	1700	7.2	2.6	16
Organosolv (hardwood)	800	3.6	3.7	19
Kraft (softwood)	3000	4.1	2.6	14

#### 1.2.4.1.2 Thermal properties

Lignin is generally a brittle glassy polymer with a high glass transition temperature ( $T_g$ ). The  $T_g$  of a polymer reflects the ability of an entire molecule, or of sections of the molecule, to undergo transitional motion from a glassy state to a rubbery state (Glasser, 2000). Several factors affect  $T_g$ , such as free volume between polymer chains; molar mass; the existence and abundance of attractive forces between molecules (related to solubility); the freedom of molecular side groups, degree of branching, and segments to rotate around inter-monomer

bonds; chain stiffness and length. As discussed, lignin is a three-dimensional phenyl-propyl polymer containing polar functional groups (Table 1.6). Therefore, the  $T_g$  of lignin is appreciably higher than that of synthetic polymer which contributes to lignin's brittle nature (Yoshida et al., 1987). Table 1.7 lists the  $T_g$ s of several lignin samples as determined by various measuring techniques. Lignin  $T_g$  has a wide range due to differences between species and isolation protocols. Softwood lignin has generally a higher  $T_g$  than hardwood lignin because it has a more condensed structures and inter- or intra-molecular H-bonds. To use lignin in polymeric applications, the  $T_g$  of lignin will need to be reduced to make it less brittle and more processable.

Table 1.7 Glass transition temperature of various lignins (Glasser, 2000; Goring, 1971; Hatakeyama and Hatakeyama, 2010)

Lignin		$T_g$ ( $^{\circ}$ C)	Measuring Techniques
Lignin <i>in situ</i>	Hardwood	65-85	DMA <sup>a</sup>
	Softwood	90-105	DMA
MWL	Hardwood	110-130	DSC <sup>b</sup> , IR <sup>c</sup> , ESR <sup>d</sup>
	Softwood	138-160	TMA <sup>e</sup> , DSC, Powder collapse <sup>f</sup>
Periodate lignin		193	Powder collapse
Kraft lignin		124-174	DSC, TMA
Organosolv lignin		91-97	DSC
Steam explosion lignin		113-139	DSC
Dioxane Lignin		120-150	DSC, X-ray <sup>g</sup> , b-NMR <sup>h</sup>
Soda Lignin (Wheat straw)		160-185	Not mentioned

<sup>a</sup> DMA is dynamic mechanical analyzer,  $T_g$  is defined at onset of storage modulus, peak of loss modulus, or peak of damping factor;

<sup>b</sup> DSC is differential scanning calorimeter,  $T_g$  is defined at onset, midpoint or inflection point of heat flow change;

<sup>c</sup> IR is infrared spectroscopy,  $T_g$  is defined at a temperature where the relative optical baseline density of IR absorption band at  $1500-1510\text{cm}^{-1}$  decreased steeply;

<sup>d</sup> ESR is electron spin resonance,  $T_g$  is defined at a temperature where the number of radicals decreased sharply;

<sup>e</sup> TMA is thermomechanical analyzer,  $T_g$  is defined at a temperature where position or volume change abruptly;

<sup>f</sup> powder collapse defines  $T_g$  at a temperature where sharp maximum in the plunger velocity curve occurs;

<sup>g</sup> X-ray defines  $T_g$  at a temperature where inter-molecular distance increases when halo pattern of lignin was measured as a function of temperature;

<sup>h</sup> b-NMR is broad line NMR,  $T_g$  is defined at a temperature where the second moment decreased steeply.

## **1.2.4.2 Material applications of industrial lignin**

### **1.2.4.2.1 Lignin polymer blends**

Polymer blends involves the physical mixing of two or more polymers in appropriate proportions to give a final product with more desirable properties or low cost than those of the components (Feldman, 2002). With blending with other synthetic or natural polymers, tunable mechanical and thermal properties could be obtained. Lignin polymer blends between protein-lignin blends, starch-lignin blends, polyolefin–lignin blends, lignin blends with vinyl polymers, lignin–polyester blends, and synthetic rubber–lignin blends were extensively reviewed (Calvo-Flores and Dobado, 2010; Doherty et al., 2011; Feldman, 2002; Gandini and Belgacem, 2008). Some lignin-polymer blends have been used as precursors for making low grade carbon fiber.

### **1.2.4.2.2 Lignin chemical modification**

Chemical modification offers a viable solution to improve lignin properties. Lignin has a variety of functional groups, such as hydroxyl, carbonyl and carboxyl groups, which provide sites for chemical modification, such as alkylation/dealkylation, oxyalkylation, amination, carboxylation, acylation, halogenation, nitration, hydrogenolysis, methylation, oxidation and reduction, sulfomethylation, sulfonation, silylation, phosphorylation, and nitroxide formation (Calvo-Flores and Dobado, 2010; Laurichesse and Avérous, 2013; Meister, 2002). Modification of lignin can reduce H-bonding and therefore reduce the  $T_g$  of the modified lignin for use as resins or thermoplastics. The OH group is the easiest group to modify, by substitution, such as alkylation, esterification, and oxypropylation for polyurethane and this will be discussed in detail below.

#### **1.2.4.2.2.1 Alkylation**

Alkylation of hydroxyl groups is a relatively easy procedure and has been explored for lignin modification (Meister, 2002). Li and Sarkanen (2000) successfully alkylated kraft lignin which showed mechanical properties comparable to polystyrene (Young's modulus of 1.9 GPa and tensile strength of 37 MPa). Furthermore, the properties were enhanced by blending with



polyesters (Li and Sarkanen, 2002; Li and Sarkanen, 2005). Cui et al. (2013) methylated kraft lignin and improved the thermal stability and reduced the  $T_g$  from 153°C to 128°C. McDonald and Ma (2012) benzylated kraft lignin to produce a thermoplastic material which was easily molded. In addition, the thermal and mechanical properties could be tuned by the degree of substitution (DS) of the benzyl group. For example,  $T_g$  could be reduced from 183°C to 48°C as DS increased from 0.45 to 2.5. The use of halogenated reagents (e.g. chloromethane or benzylchloride) may limit the use of this approach to produce lignin derivatives.

#### **1.2.4.2.2 Esterification to obtain lignin polyesters**

Esterification is a viable approach to substitute hydroxyl groups generally with acid anhydrides (e.g. acetic anhydride) and to a lesser extent acid chlorides, or acid itself. Lignin acetates (Figure 1.14) are considered useful derivatives due to their solubility in organic solvent, thermoplastic behavior, and widely used in characterizing lignin chemical properties (Glasser and Jain, 1993). The chain length of the acid (e.g.  $C_4$  for butyrate) can also dramatically influence thermal and mechanical properties (Fox and McDonald, 2010). Glasser and Jain (1993) esterified series of lignin esters with different chain lengths ( $C_2$  to  $C_4$ ). The higher the ester group chain length the lower the  $T_g$  (organosolv lignin acetate ( $C_2$ ) 126°C, propionate ( $C_3$ ) 116°C and butyrate ( $C_4$ ) 93°C). The authors compared with Lewis and Brauns's results (from ( $C_2$  -  $C_{16}$ )). Fox and McDonald (2010) conducted similar research on three industrial lignin samples. They also found the same trends about reducing  $T_g$ . Thielemans and Wool (2004; 2005) developed a butyrate lignin and applied it as a compatibilizer for natural fiber composites with acrylated epoxidized soybean oil and styrene. The solubility model of these polymer systems was achieved with alkylated lignins.

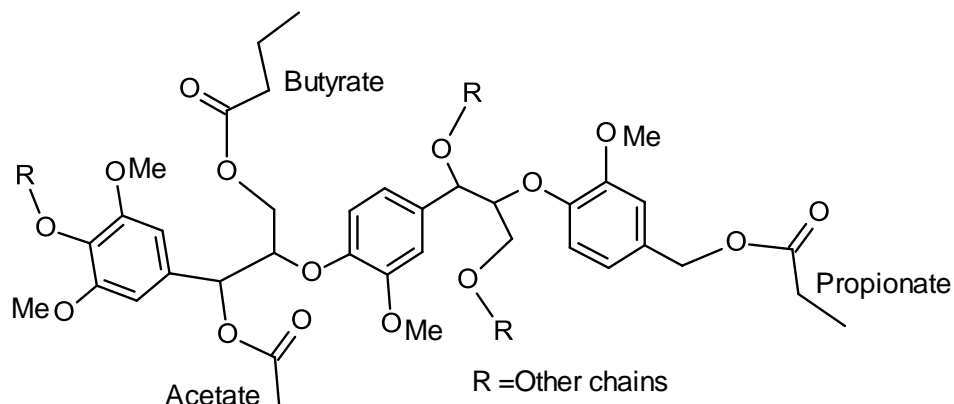


Figure 1.14 Lignin derivatives from acetate, propionate, or butyrate, etc.

Lignin esterification studies focused on producing lignin derivatives to improve their thermal and solubility properties. In addition, diacid or diacid chlorides were carried to produce lignin polyesters (Figure 1.15). Guo et al. (1991; 1992) produced kraft lignin-sebacoyl and terephthaloyl polyester hydrogels. Binh et al. (2009) also polymerized a kraft lignin based copolyester with sebacoyl chloride in the presence of triethylamine in dimethylacetamide. Kang et al. (2014) produced a thermoplastic film composed of lignin-sebacic acid and poly(ethylene glycol) with good thermal properties and toughness (tensile strength of 1.27 MPa, breaking elongation of 62.8% and Young's modulus of 10.79 MPa). Bonini et al. (2005) also synthesized lignin based polyesters with dodecandioyl dichloride. Fang et al. (2011) prepared a lignin-diacid graft copolymer which reduced the rigidity of lignin.

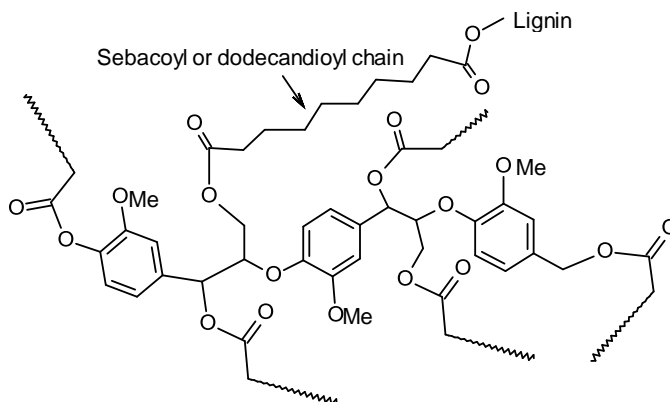


Figure 1.15 Lignin based polyester from sebacoyl or dodecandioyl dichlorides

Further development of lignin polyester involved introducing more complicated macromolecule structures. de Oliveira and Glasser (1994) developed polyesters from hydroxypropyl lignin (HPL) with  $\epsilon$ -caprolactone (Figure 1.16). Different thermal properties were obtained with tuning the extent of the hydroxypropyl chain via anionic polymerization. The melt temperature ( $T_m$ ) increased with chain length as the degree of polymerization (DP) of the  $\epsilon$ -caprolactone rose to 50. Crystallinity was established for all copolymers, even those with a DP of 10 caprolactone units. A similar study by Matsushita et al. (2011) carried out polyester synthesis by a hydrothermal sulfuric acid lignin (treated with hydrothermal under alkali conditions) and  $\epsilon$ -caprolactone.

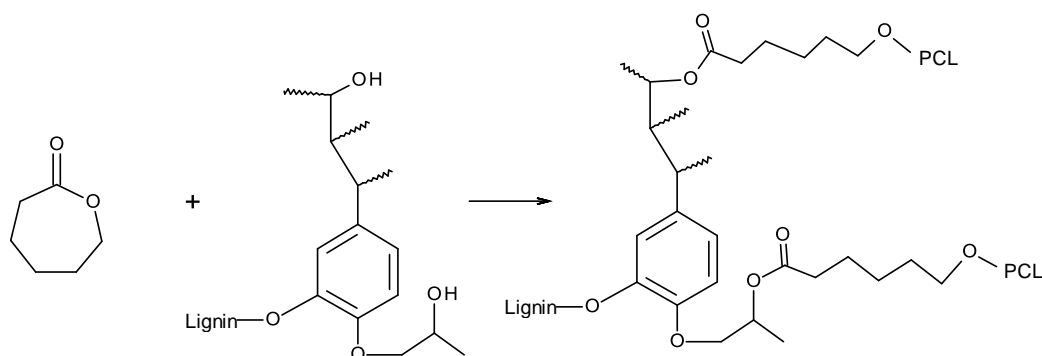


Figure 1.16 Lignin based polyester from reacting with  $\epsilon$ -caprolactone

Saito et al. (2012) developed a lignin thermoplastic material by reacting with formaldehyde (F-lignin) and subsequently reacted with dicarboxy-terminated polybutadiene (PBD-(COOH)<sub>2</sub>) as shown in Figure 1.17. The lignin-based thermoplastic showed two distinct phase transitions by dynamic mechanical analysis (DMA) (Figure 1.18). The polymer showed an increase in storage modulus ( $E'$ , 25 to 82 MPa) as lignin content increased (12 to 38 %). Chung et al. (2013) synthesized a lignin-lactide copolymer catalyzed by an organocatalyst via ring-opening polymerization. The PLA chain was controlled by varying the lignin/lactide ratio. The lignin based copolymers displayed a  $T_g$  between 45 to 85°C.

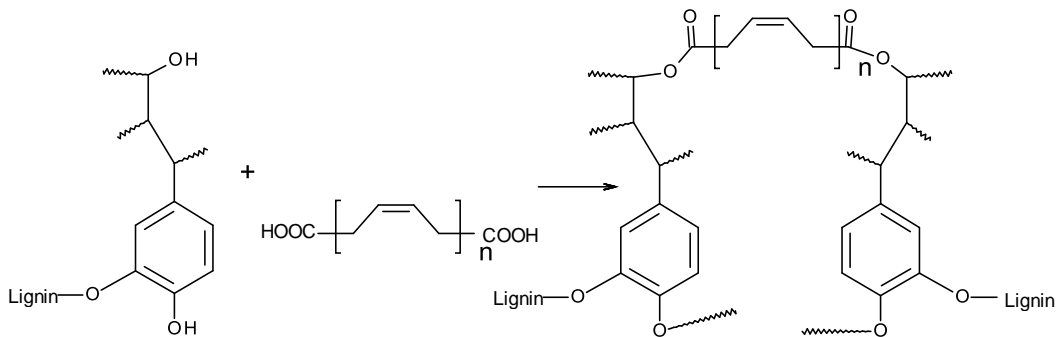
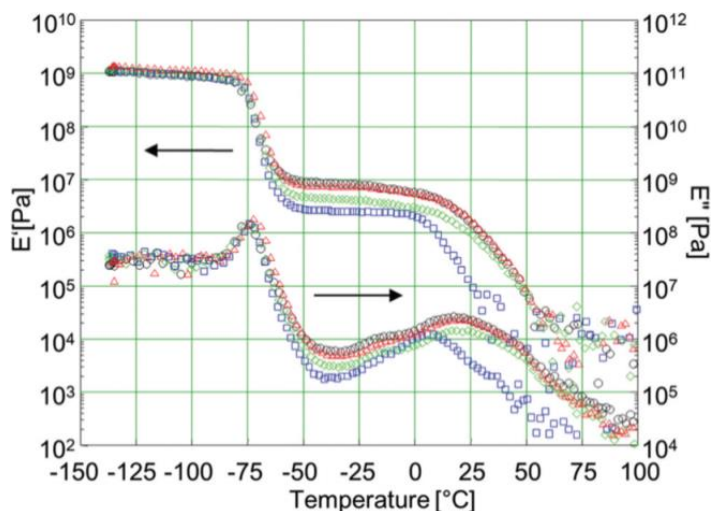


Figure 1.17 Lignin-polybutadiene ester

Figure 1.18 DMA thermogram of F-Lignin-PBD(COOH)<sub>2</sub> with varied F-Lignin content (Saito et al., 2012)

More sophisticated procedures were conducted by incorporation of hyperbranched prepolymers into lignin backbone (Figure 1.19). Under this concept, lignin based polymers would own elastomeric properties. Sivasankarapillai and McDonald (2011) developed soda lignin based elastomers by reacting with a branched poly(ester-amine) prepolymer via polycondensation. The obtained elastomers were flexible and tough material ( $T_g$  of 7.7°C and  $E'$  of 3.5 GPa at 40% lignin content). A subsequent study (Sivasankarapillai et al., 2012) produced a series of highly branched poly(ester-amine-amide) prepolymers which were polycondensed with lignin to form elastomers with good properties (tensile strength of 12 MPa, Young's modulus of 33 MPa and 149% elongation at 50 % lignin content).

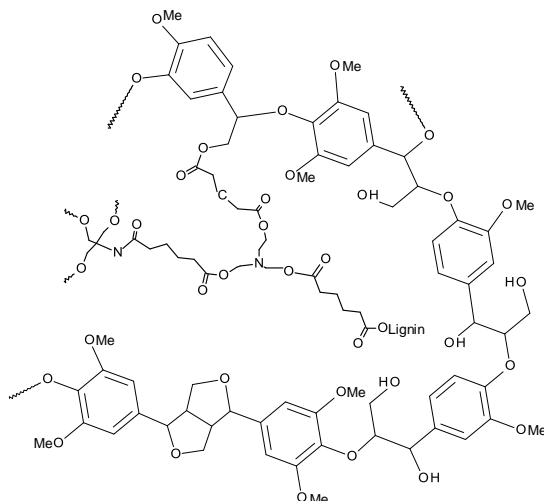


Figure 1.19 Lignin based copoly(ester-amide)s from hyperbranched prepolymers (Sivasankarapillai and McDonald, 2011)

#### 1.2.4.2.2.3 Lignin-based polyurethane

Lignin-based polyurethanes has been studies extensively due to the polyol nature of lignin (Chung and Washburn, 2013). Lignin often needs to be modified prior to fabricating polyurethane. Oxypropylation has been the feasible pathway to obtain lignin polyols (Figure 1.20). Glasser's group developed series of polyurethanes back to the 1980s but has not been commercialized (Glasser et al., 1984; Kelley et al., 1988; Rials and Glasser, 1984a, b, 1986; Saraf and Glasser, 1984; Saraf et al., 1985a, b; Wu and Glasser, 1984). Lignin based polyurethanes are still been developed with tunable properties and composed of different polyurethane segments (Li and Ragauskas, 2012a, b; Pohjanlehto et al., 2014; Saito et al., 2013).

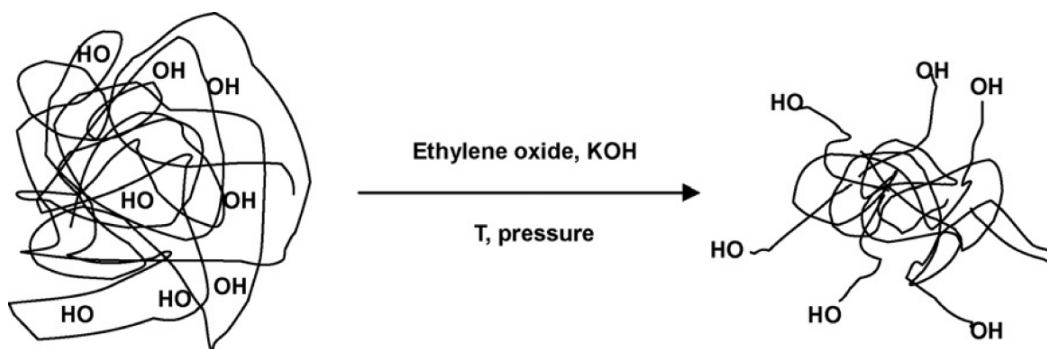


Figure 1.20 Oxypropylation process to obtain a lignin polyol

#### 1.2.4.2.3 Lignin-based adhesives

The main parameters used in judging adhesives whether or not can be applied in wood industry commercially are based on costs, reactivity, performance (resin level, type of bond), homogeneity of chemical composition, and environmental problems (Roffael and Dix, 1991). Since lignin is a low cost feedstock and readily available, it seems a great candidate for use as the main component in an adhesive. However, some disadvantages exist such as low reactivity, high  $T_g$ , performance and inhomogeneity and work has focused on overcoming these issues. Spent sulfur liquor (SSL) and lignosulfonates have been used to form adhesives. There are two methods for the producing SSL-based adhesives, that is, by a condensation reaction or by free-radical polymerization (Lewis, 1987). Figure 1.21 shows the possible condensation reactions of lignosulfonates. However, In his book *Advanced Wood Adhesive Technology*, Pizzi elaborated that condensation reactions in lignin by heat or mineral acids cannot be as effective as in synthetic phenol formaldehyde (PF) resins, due to the lower reactivity of free positions in the aromatic nuclei of lignin and their considerably lower reactivity than in PF resins. First, there is only 0.5 free *O*-positions (ortho to the phenolic groups) per  $C_9$  unit; the 6- and 2- positions are less reactive. Second, there is less than one benzyl alcohol or ether group per  $C_9$  unit in lignin, while in synthetic PF resins up to three methylol groups can be introduced into one phenolic ring. Finally, the aromatic nuclei in lignin are considerably less reactive than phenol toward hydroxybenzyl alcohol groups, due to the presence of methoxy or methoxy-equivalent groups rather than hydroxy groups on the lignin aromatic rings (Pizzi, 1994). These lignin based resins were shown to have poor performance and long pressing cycles (Roffael and Dix, 1991).

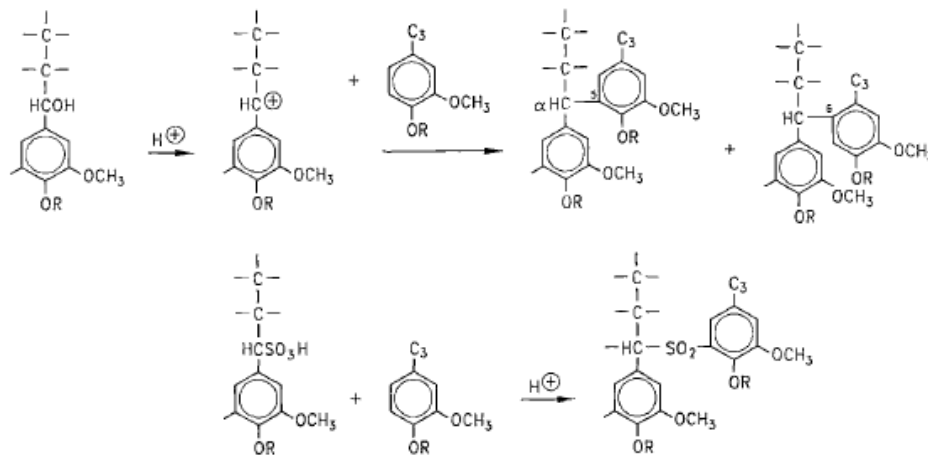


Figure 1.21 Possible reactions during condensation of lignosulfonates by thermal treatments (Nimz, 1983)

To improve poor bonding the pressed particleboard was autoclaved at 200°C for two-hours to develop the full bond properties of the SSL. The rate of condensation herein depends on the types of lignosulfonates. NH<sub>4</sub>-lignosulfonates condenses at a higher rate than Ca-lignosulfonates, the condensation rates of Mg- and Na-lignosulfonates lie between these extremes (Roffael and Dix, 1991). The industry discarded this autoclaving-step method due to high energy consumption of the autoclaving step and environmental problems associated with the emission of sulfur dioxide during the autoclaving treatment although comparable moisture resistant properties to PF resin were obtained.

Lignin has been incorporated into PF resins and lignin acts as a filler and coreactant (Feldman, 2002). Sellers et al. (2004) reviewed lignin-modified PF resin development for fiberboard. Pizzi et al. (1989) studied soda bagasse lignin adhesives applied for particleboard. Lignin was hydroxymethylated and used in blends with 33% PF as a thermosetting adhesive. Lignin content in the PF resin was shown to increase the rate of cure and heat of reaction. Piccolo et al. (1997) showed that lignin reacts chemically with the phenol growing chain and acts as a chain extender. Olivares et al. (1988) had examined methylation, demethylation and ultrafiltration separation of lignin from *Pinus radiata* black liquor as a copolymer in PF resin. The best performing resin was composed of 18.8% ultra-filtrated high molar mass lignin, 22.9% phenol and 58.3% formaldehyde.

Lignin also has been applied in other adhesives, such as epoxy resin (Feldman, 2002). Shiraishi (1989) phenolated lignin with bisphenol-A to obtain an epoxy-kraft lignin adhesives. The resins were found to be completely soluble in certain organic solvent including acetone. The obtained epoxy-lignin resin was tested as adhesive for plywood with hot-pressing at 140°C with good waterproof performance (Shiraishi, 1989). Epoxy-kraft lignin adhesives were assessed for bonding steel, aluminum, concrete and other materials (Feldman and Banu, 1988; Feldman et al., 1991; Wang et al., 1992).

### **1.2.5 General polymer (Peacock and Calhoun, 2006; Rodriguez et al., 2003)**

At the basic level, a polymer molecule consists of hundreds, thousands, or even millions of chemical building block units to form a chain with an extended length at least an order of magnitude greater than its thickness. Polymers can be classified to various categories based on different purposes, for example, Chain-growth and step-growth polymers, homopolymer and copolymer, linear and branched polymers, thermoplastics and thermosets.

#### **1.2.5.1 Chain-growth and step-growth polymers**

From reaction kinetic point of view, polymer can be divided into chain growth and step-growth polymers. In a typical chain growth polymer, each polymer is formed in a comparatively short time and then is “dead” and remains unchanged by reaction with any remaining monomer. Growing chains can add a monomer unit, but neither monomer itself nor “dead” polymer can add a monomer. The monomer, growing polymer, and “dead” polymer are quite different from one another in reactivity. Furthermore, the reaction needs to be initiated. In contrast, for step growth polymer, each polymer strand formed can react further with a monomer or other polymers. No initiators are needed.

#### **1.2.5.2 Homopolymer and copolymer**

Homopolymer and copolymers were classified based on monomer types (Figure 1.22). Polymers only containing one monomer are called homopolymers, such as polyethylene, while polymers with two or more monomers called copolymers, such as nylon 6,6. Copolymers can be subdivided into either a random copolymer, block copolymer or graft



copolymer. Relatively small changes in comonomer content can lead to significant changes in physical or chemical properties of polymers.

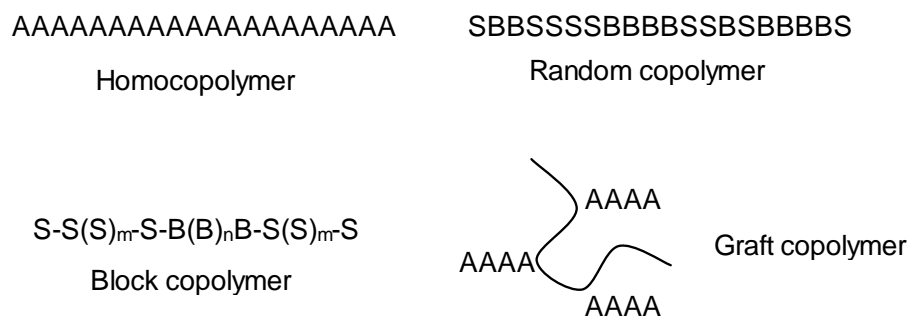


Figure 1.22 Homopolymer and copolymer structure

### 1.2.5.3 Linear and branched polymers

Based on differences of monomer functionalities, polymers can be made to linear and branched molecularly (Figure 1.23). Monomers with only two functionalities can form linear polymers, while with more than two functionalities for at least monomer can form branched polymers. PE, PP, and PS are generally normal linear polymers, while PF thermoset resin is a cross-linked polymer.

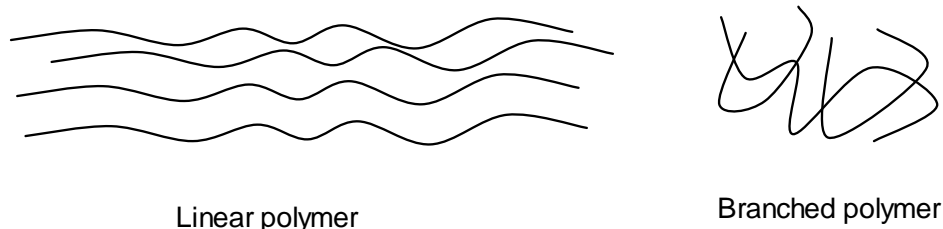


Figure 1.23 Structures of linear and branched polymers

### 1.2.5.4 Thermoplastics and thermosets

Polymers can also be classified as a thermoplastic or a thermoset. Thermoplastics consist of linear or lightly branched chains that can slide past one another under the influence of temperature and pressure, flowing at high temperature and thus allowing processing (e.g. extrusion or molding) to form a particular product. PE, PP, PS as described aforementioned are thermoplastics. However, thermosets consist of a network of interconnected chains whose positions are relatively fixed to their neighbors. They do not flow when heated,

instead, will degrade to char when exposed to high temperature. Examples of thermosets are epoxy or PF resins which are chemically reacted to form a vitrified polymer. Therefore, thermosets are always first synthesized as prepolymer (low polymerizations) forms.

Therefore, polymer structures are essential to determine morphology, process, as well as functions of the polymer.

### 1.2.6 Shape memory polymers

Polymers that have capability to memorize different shapes and can be recovered in a predefined way upon exertion of suitable stimulus such as heat, magnetism, electricity, moisture, or light, are designated as shape memory polymers (SMPs) (Behl and Lendlein, 2007; Beloshenko et al., 2005; Lendlein and Kelch, 2002; Lendlein and Langer, 2002; Liu et al., 2007; Xie, 2010, 2011; Yakacki, 2013). If a SMP owns two shapes change, it is called a dual SMP, and if three shapes change, then called triple, etc. Since SMPs were first introduced in 1984 (Dietsch and Tong, 2007), they have attracted increasingly attention both in academic and industrial fields and extensively been employed in smart fabrics, heat shrinkable tubes for electronics or films for packaging, self-deployable sun sails in spacecraft, self-disassembling mobile phones, intelligent medical devices, or implants for minimally invasive surgery (Behl and Lendlein, 2007) which covers numerous areas. Temperature caused shape change is named as thermally stimulated shape memory effect ( $T_s$ -SME) and for polymers a  $T_s$ -SMP (Lendlein and Kelch, 2002).

The principle of  $T_s$ -SMP is illustrated in Figure 1.24. The  $T_s$ -SMP is first heated to a deformation temperature ( $T_d$ ), which leads to the material softening (storage modulus drop). A deformation force is subsequently applied (i.e. loading, strain controlled or stress controlled (Wagermaier et al., 2010)). The SMP is then cooled down to lower temperature with load. The deformed shape is then fixed before removal of load. The programming is the procedure of the shape fixing. When the deformed SMP under temporary shape is re-heated to a higher temperature without stress exertion, the permanent shape is recovered. Typically both deformation temperature and so-called recovery temperature are above the reversible thermal transition temperature ( $T_g$  or melting point  $T_m$ ) of the SMP, which is thus

called shape memory transition ( $T_{trans}$ ) (Xie, 2011). Liu, et. al. (2007) comprehensively reviewed four classes of SMPs in molecular based mechanism, ie., chemically cross-linked glassy thermosets; chemically cross-linked semi-crystalline rubbers; physically cross-linked thermoplastics; and physically cross-linked block copolymers; respectively. The first mechanism (chemically cross-linked glassy thermosets) seems to be simplest type to manipulate SME as illustrated in Figure 1.25 where  $T_{trans}$  is controlled by  $T_g$ .

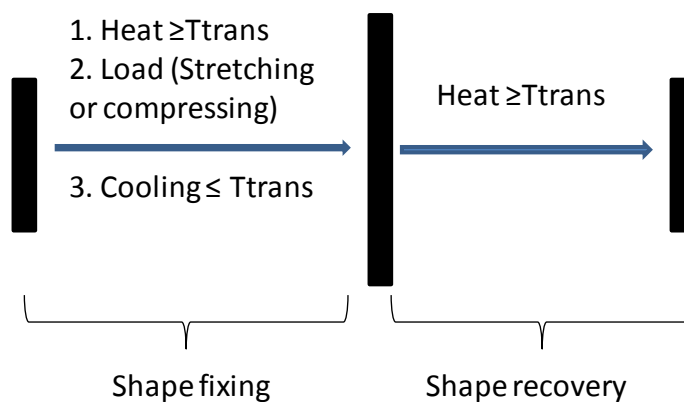


Figure 1.24 Schematic illustration of dual-shape memory cycle (Xie, 2011)

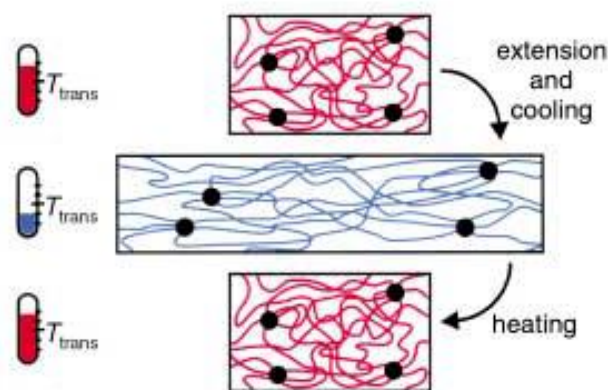


Figure 1.25 Schematic representation of the molecular mechanism of the thermally induced shape-memory effect for a polymer network with  $T_{trans}=T_g$ . If the increase in temperature is higher than  $T_{trans}$  of the switching segments, these segments are flexible (shown in red) and the polymer can be deformed elastically. The temporary shape is fixed by cooling down below  $T_{trans}$  (shown in blue). If the polymer is heated up again, the permanent shape is recovered. (Lendlein and Kelch, 2002)

As illustrated above, SMP formation, principle as well as mechanisms, is important to demonstrate the compositions of the polymer system. SME could not be simply obtained via

a single polymer type, but a combination of different polymer structures and morphologies, where two segments are responsible for the SME. That is the netpoint segment for controlling permanent shape and sometimes also called hard segment, while the switching segment is for controlling temporary shape and also called the soft segment.

From a thermodynamic point of view, entropy is the major controlling force for the SME (also called entropy elasticity (Lendlein and Kelch, 2002)). In permanent macroscopic shape, the molecular chains of a SMP contain chain conformations with the highest entropy, where the molecular chains are in a thermodynamically stable state. After heating to  $T_{\text{high}}$  (above the  $T_{\text{trans}}$ ), the chain mobility of the SMP is significantly activated. When an external deformation load (such as stretching force) is applied, the chain conformations are changed, leading to a lower entropy state and macroscopic shape change (stretched state as illustrated in Figure 1.24). When the SMP is cooled to  $T_{\text{low}}$  (below  $T_{\text{trans}}$  shown in Figure 1.25), this lower entropy state (or the temporary shape) is kinetically trapped because of the freezing of the molecular chain segments, resulting in the macroscopic shape fixation. After reheating to the  $T_{\text{high}}$  under a stress free condition, the molecular mobility is reactivated, which allows the chains to bounce back to their highest entropy state (i.e. permanent shape recovery) (Xie, 2011).

### 1.2.7 Hyperbranched polymers

Hyperbranched polymer (HBP) defines as a special type of dendritic polymers and has a high branching density with the potential of branching in each repeating unit (Voit and Lederer, 2009). Flory has proposed that monomers with different functionalities, where each one should have at least 2 functionalities, could be synthesized to cross-linking polymer with various branches and morphologies (Flory, 1953).

As illustrated in Figure 1.26, dendrimers own perfect molecular structure and a monodispersable distribution while HBPs show heterogeneous molar mass distribution and branching. Although not as perfect structure as dendrimers, HBP can be synthesized under easy and affordable ways, using a one-pot synthesis route, which guarantees a rapid development both in industrial and academic applications. Applications include coatings and

resins, polymer additives in linear polymers for improving rheological properties and for surface modifications. The polycondensation reaction is normally a classical method to produce HBP through various monomers with and without core moieties, such as using different functionally symmetric diacid ( $A_2$ ) and trihydroxy ( $B_3$ ) monomers. Direct melt polycondensation was proved to be a cost effective and environmentally beneficial approach for making HBPs (Sivasankarapillai, et. al., 2012). Moreover, different core structures, degree of branching would be achieved via varying monomer functionalities. Due to their highly branched property, the HBPs show interestingly thermal property, ie., low  $T_g$ , which would act as an flexible and excellent switching segment for  $T_s$ -SMPs synthesis.

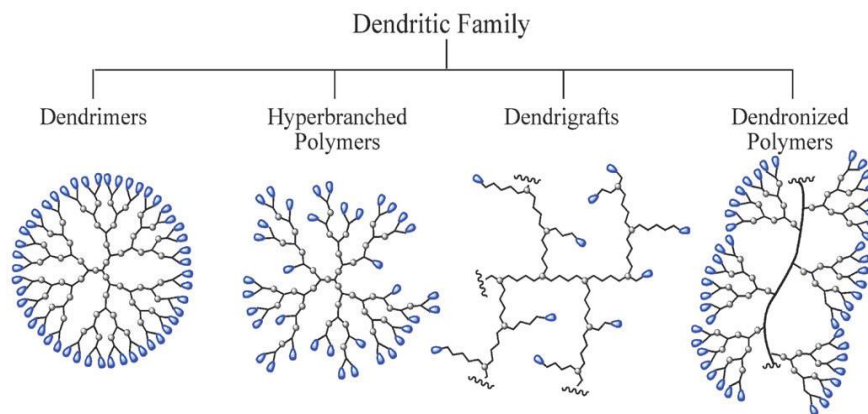


Figure 1.26 Structural morphological demonstration of sub-classes in the dendritic family (Carlmark et al., 2009)

### 1.3 Research objectives

This dissertation builds on work by (Sivasankarapillai and McDonald, 2011) to form lignin based copolymers that were derived from synthesizing with a soda lignin and a highly branched prepoly(ester-amine) subsequent work to form hyperbranched lignin-poly(ester-amine-amide)s (Sivasankarapillai et al., 2012). It is believed that the lignin copolymer system would possess SME in which lignin might be a good candidate as the netpoint segment and flexible hyperbranched prepolymer be as switching segment (Figure 1.27).

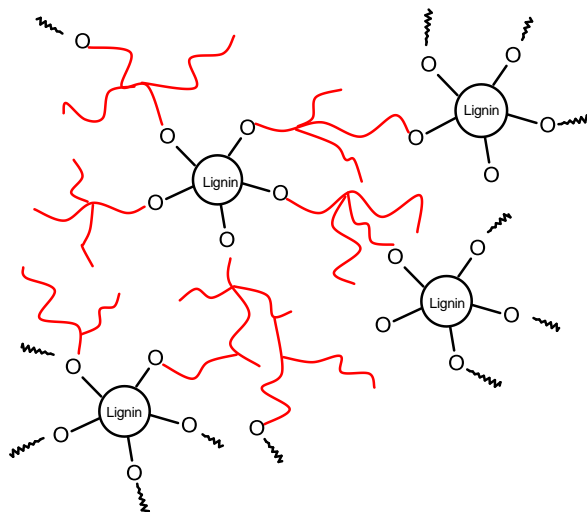


Figure 1.27 Structural scheme of lignin-hyperbranched elastomeric polymer, black circles (lignin) will act as netpoint segment and red part (hyperbranched prepolymer) will be swithcing segment.

Therefore, as an extension of these earlier studies, the pursuit of producing bio-based polymer systems with SME forms the base of this dissertation based on the following objectives:

- Fractionate different lignin sources with different  $T_g$ s;
- Tailor HBP structure based on branching structure;
- Synthesize copolymers and evaluate properties

which were addressed and organized as separate chapters and manuscripts:

1. Methanol fractionation and characterization of different industrial lignins (Chapter 2);
2. Synthesis and characterization of lignin-based thermal-stimulated copolymeric elastomers—effect of different industrial lignins (Chapter 3);
3. Synthesis and characterization of lignin-based thermal-stimulated copolymeric elastomers—effect of chain length of prepolymer (Chapter 4);
4. Synthesis and characterization of lignin-based thermal-stimulated copolymeric elastomers—application of glycerol based prepolymers (Chapter 5).

Chapter 6 will conclude the research and recommendation for future work.

#### 1.4 References

- Alder, E. **1977**. Lignin chemistry-Past, present and future. *Wood Science and Technology*, *11*, 169-218.
- Bayerbach, R., Meier, D. **2009**. Characterization of the water-insoluble fraction from fast pyrolysis liquids (pyrolytic lignin). Part IV: Structure elucidation of oligomeric molecules. *Journal of Analytical and Applied Pyrolysis*, *85*, 98-107.
- Bayerbach, R., Nguyen, V.D., Schurr, U., Meier, D. **2006**. Characterization of the water-insoluble fraction from fast pyrolysis liquids (pyrolytic lignin) - Part III. Molar mass characteristics by SEC, MALDI-TOF-MS, LDI-TOF-MS, and Py-FIMS. *Journal of Analytical and Applied Pyrolysis*, *77*, 95-101.
- Behl, M., Lendlein, A. **2007**. Shape-memory polymers. *Materials Today*, *10*, 20-28.
- Beloshenko, V.A., Varyukhin, V.N., Voznyak, Y.V. **2005**. The shape memory effect in polymers. *Uspekhi Khimii*, *74*, 285-306.
- Binh, N.T.T., Luong, N.D., Kim, D.O., Lee, S.H., Kim, B.J., Lee, Y.S., Nam, J.D. **2009**. Synthesis of Lignin-Based Thermoplastic Copolyester Using Kraft Lignin as a Macromonomer. *Composite Interfaces*, *16*, 923-935.
- Boerjan, W., Ralph, J., Baucher, M. **2003**. Lignin biosynthesis. *Annu Rev Plant Biol*, *54*, 519-546.
- Bonini, C., D'Auria, M., Ernanuele, L., Ferri, R., Pucciariello, R., Sabia, A.R. **2005**. Polyurethanes and polyesters from lignin. *Journal of Applied Polymer Science*, *98*, 1451-1456.
- Bridgwater, A.V. **2012**. Review of fast pyrolysis of biomass and product upgrading. *Biomass & Bioenergy*, *38*, 68-94.
- Bridgwater, A.V., Meier, D., Radlein, D. **1999**. An overview of fast pyrolysis of biomass. *Organic Geochemistry*, *30*, 1479-1493.
- Brown, R.M. **2004**. Cellulose structure and biosynthesis: What is in store for the 21st century? *Journal of Polymer Science Part a-Polymer Chemistry*, *42*, 487-495.

Brownell, H.H., Saddler, J.N. **1984**. Steam-Explosion Pretreatment for Enzymatic-Hydrolysis. *Biotechnology and Bioengineering*, 55-68.

Calvo-Flores, F.G., Dobado, J.A. **2010**. Lignin as renewable raw material. *ChemSusChem*, 3, 1227-1235.

Carlmark, A., Hawker, C.J., Hult, A., Malkoch, M. **2009**. New methodologies in the construction of dendritic materials. *Chemical Society Reviews*, 38, 352-362.

Chen, F. **2010**. Investigation of soy protein blends prepared by simultaneous plasticization and mixing, Material science program. Washington State University, Pullman, WA.

Chung, H., Washburn, N.R. **2013**. Chemistry of lignin-based materials. *Green Materials*, 1, 137-160.

Chung, Y.L., Olsson, J.V., Li, R.J., Frank, C.W., Waymouth, R.M., Billington, S.L., Sattely, E.S. **2013**. A Renewable Lignin-Lactide Copolymer and Application in Biobased Composites. *ACS Sustainable Chemistry & Engineering*, 1, 1231-1238.

Council, A.C. **2014a**. 2012 National Postconsumer Plastic Bag & Film Recycling Report.

Council, A.C. **2014b**. U.S. Resin Production, Sales & Captive Use.

Cui, C., Sadeghifar, H., Sen, S., Argyropoulos, D.S. **2013**. Toward thermoplastic lignin polymers; part II: Thermal & polymer characteristics of Kraft lignin & derivatives. *BioResources*, 8, 864-886.

de oliveira, W., Glasser, W.G. **1994**. Multiphase Materials with Lignin .11. Starlike Copolymers with Caprolactone. *Macromolecules*, 27, 5-11.

Dietsch, B., Tong, T. **2007**. A review - Features and benefits of shape memory polymers. *Journal of Advanced Materials*, 39, 3-12.

Dimmel, D. **2010**. Overview, in: Heitner, C., Dimmel, D. (Eds.), *Lignin and lignans: Advances in chemistry*. CRC press, Boca Raton, FL, pp. 1-10.

Doherty, W.O.S., Mousavioun, P., Fellows, C.M. **2011**. Value-adding to cellulosic ethanol: Lignin polymers. *Industrial Crops and Products*, 33, 259-276.



Dube, M.A., Salehpour, S. **2014**. Applying the Principles of Green Chemistry to Polymer Production Technology. *Macromolecular Reaction Engineering*, 8, 7-28.

Ebringerova, A., Heinze, T. **2000**. Xylan and xylan derivatives - biopolymers with valuable properties, 1 - Naturally occurring xyans structures, procedures and properties. *Macromolecular Rapid Communications*, 21, 542-556.

Economist, O.o.t.C., Uses, O.o.E.P.a.N. **2008**. U.S. Biobased Products: Market Potential and Projections Through 2025, in: *Agriculture*, U.S.D.o. (Ed.).

Fabiyi, J. **2007**. *Chemistry of Wood Plastic Composite Weathering, Forest Products*. University of Idaho, Moscow, ID.

Fang, R., Cheng, X.S., Lin, W.S. **2011**. Preparation and Application of Dimer Acid/Lignin Graft Copolymer. *BioResources*, 6, 2874-2884.

Feldman, D. **2002**. Lignin and its polyblends -- a review, in: Hu, T.Q. (Ed.), *Chemical modification, properties, and usage of lignin*. Kluwer Academic/Plenum, New York, pp. 81-99.

Feldman, D., Banu, D. **1988**. Kinetic Data on the Curing of an Epoxy Polymer in the Presence of Lignin. *Journal of Polymer Science Part a-Polymer Chemistry*, 26, 973-983.

Feldman, D., Banu, D., Luchian, C., Wang, J. **1991**. Epoxy Lignin Polyblends - Correlation between Polymer Interaction and Curing Temperature. *Journal of Applied Polymer Science*, 42, 1307-1318.

Flory, P.J. **1953**. Molecular size and chemical reactivity; Principle of condensation polymerization, *Principles of polymer chemistry*. George Banta Publishing Company, Ithaca, New York, pp. 69-105.

Fox, C.S., McDonald, A.G. **2010**. Chemical and thermal characterization of three industrial lignis and their corresponding lignin esters. *BioResources*, 5, 990-1009.

Gandini, A., Belgacem, M.N. **2008**. Lignins as Components of Macromolecular Materials. *Monomers, polymers and composites from renewable resources*, 243-271.

- Gargulak, J.D., Lebo, S.E. **2000**. Commercial use of lignin-based materials, in: Glasser, W.G., Northy, R.A., Schultz, T.P. (Eds.), *Lignin: Historical, Biological, and Materials Perspectives*. American Chemical Society, Washington DC, p. 304.
- Gellerstedt, G. **1976**. Reactions of Lignin during Sulfite Pulping. *Svensk Papperstidning-Nordisk Cellulosa*, 79, 537-543.
- Gellerstedt, G. **2009**. Chemistry of chemical pulping, in: Ek, M., Gellerstedt, G., Henriksson, G. (Eds.), *Pulp and Paper Chemistry and Technology Volume 2 Pulping Chemistry and Technology*, pp. 91-120.
- Glasser, W.G. **2000**. Classification of lignin according to chemical and molecular structure, in: Glasser, W.G., Northy, R.A., Schultz, T.P. (Eds.), *Lignin: Historical, Biological, and Materials Perspectives*. American Chemical Society, Washington DC, pp. 216-238.
- Glasser, W.G., Barnett, C.A., Muller, P.C., Sarkanen, K.V. **1983**. The Chemistry of Several Novel Bioconversion Lignins. *Journal of Agricultural and Food Chemistry*, 31, 921-930.
- Glasser, W.G., Barnett, C.A., Rials, T.G., Saraf, V.P. **1984**. Engineering plastics from lignin. II. Characterization of hydroxyalkyl lignin derivatives. *Journal of Applied Polymer Science*, 29, 1815-1830.
- Glasser, W.G., Jain, R.K. **1993**. Lignin Derivatives .1. Alkanoates. *Holzforschung*, 47, 225-233.
- Goring, D.A.I. **1971**. Polymer properties of lignin and lignin derivatives, in: Sarkanen, K.V., Ludwig, C.H. (Eds.), *Lignins: occurrence, formation, structure and reactions*. Wiley-interscience, New York, pp. 695-768.
- Grabber, J.H., Ralph, J., Lapierre, C., Barriere, Y. **2004**. Genetic and molecular basis of grass cell-wall degradability. I. Lignin-cell wall matrix interactions. *C R Biol*, 327, 455-465.
- Guo, Z.X., Gandini, A. **1991**. Polyesters from Lignin .2. The Copolyesterification of Kraft Lignin and Polyethylene Glycols with Dicarboxylic-Acid Chlorides. *European Polymer Journal*, 27, 1177-1180.
- Guo, Z.X., Gandini, A., Pla, F. **1992**. Polyesters from Lignin .1. The Reaction of Kraft Lignin with Dicarboxylic-Acid Chlorides. *Polymer International*, 27, 17-22.

- Hatakeyama, H., Hatakeyama, T. **2010**. Lignin Structure, Properties, and Applications. *Biopolymers: Lignin, Proteins, Bioactive Nanocomposites*, 232, 1-63.
- Henriksson, G. **2009**. Lignin, in: Ek, M., Gellerstedt, G., Henriksson, G. (Eds.), *Pulp and Paper Chemistry and Technology*. Walter de Gruyter GmbH & Co. KG, Berlin, pp. 121-145.
- Holladay, J.E., Bozell, J.J., White, J.F., Johnson, D. **2007**. Top value-added chemicals from biomass, Volume II: Results of screening for potential candidates from biorefinery lignin. Pacific Northwest National Laboratory, Richland, WA.
- Kang, Y., Chen, Z., Wang, B., Yang, Y. **2014**. Synthesis and mechanical properties of thermoplastic films from lignin, sebacic acid and poly(ethylene glycol). *Industrial Crops and Products*, 56, 105-112.
- Kelley, S.S., Glasser, W.G., Ward, T.C. **1988**. Engineering plastics from lignin XV. Polyurethane Films from Chain-Extended Hydroxypropyl Lignin. *Journal of Applied Polymer Science*, 36.
- Kim, D.E., Pan, X.J. **2010**. Preliminary Study on Converting Hybrid Poplar to High-Value Chemicals and Lignin Using Organosolv Ethanol Process. *Industrial & Engineering Chemistry Research*, 49, 12156-12163.
- Klemm, D., Heublein, B., Fink, H.P., Bohn, A. **2005**. Cellulose: Fascinating biopolymer and sustainable raw material. *Angewandte Chemie-International Edition*, 44, 3358-3393.
- Kumar, P., Barrett, D.M., Delwiche, M.J., Stroeve, P. **2009**. Methods for Pretreatment of Lignocellulosic Biomass for Efficient Hydrolysis and Biofuel Production. *Industrial & Engineering Chemistry Research*, 48, 3713-3729.
- Laurichesse, S., Avérous, L. **2013**. Chemical modification of lignins: Towards biobased polymers. *Progress in Polymer Science*.
- Lendlein, A., Kelch, S. **2002**. Shape-memory polymers. *Angewandte Chemie International Edition*, 41, 2034-2057.
- Lendlein, A., Langer, R. **2002**. Biodegradable, elastic shape-memory polymers for potential biomedical applications. *Science*, 296, 1673-1676.

- Lewis, N.G. **1987**. Lignin in Adhesives - Introduction and Historical-Perspective. Abstracts of Papers of the American Chemical Society, 194, 10-Cell.
- Lewis, N.G., Lantzy, T.R. **1989**. Lignin in adhesive introduction and historical perspective, in: Hemingway, R.W., Conner, A.H., Branham, S.J. (Eds.), Adhesive from renewable resources. ACS Symposium Series, New Orleans, pp. 13-26.
- Li, Y., Ragauskas, A.J. **2012a**. Ethanol organosolv lignin-based rigid polyurethane foam reinforced with cellulose nanowhiskers. RSC Advances, 2, 3347.
- Li, Y., Ragauskas, A.J. **2012b**. Kraft lignin based rigid polyurethane foam. Journal of Wood Chemistry and Technology, 32, 210-224.
- Li, Y., Sarkanen, S. **2000**. Thermoplastics with very high lignin contents, in: Glasser, W.G., Northey, R.A., Schultz, T.P. (Eds.), Lignin: Historical, Biological, and Materials Perspectives. American Chemistry Society, Washington D.C., pp. 351-366.
- Li, Y., Sarkanen, S. **2002**. Alkylated kraft lignin-based thermoplastic blends with aliphatic polyesters Macromolecules, 35, 9707-9715.
- Li, Y., Sarkanen, S. **2005**. Miscible blends of kraft lignin derivatives with low-T-g polymers. Macromolecules, 38, 2296-2306.
- Liu, C., Qin, H., Mather, P.T. **2007**. Review of progress in shape-memory polymers. Journal of Materials Chemistry, 17, 1543-1558.
- Lora, J. **2008**. Industrial commercial lignins: sources, properties and applications, Monomers, polymers and composites from renewable resources. Elsevier, Amsterdam; Boston, pp. 225-241.
- Lora, J.H. **2002**. Characteristics, industrial sources, and utilization of lignins from non-wood plants, in: Hu, T.Q. (Ed.), Chemical Modification, Properties, and Usage of Lignin. Kluwer Academic/Plenum publishers, New York, pp. 267-282.
- Lora, J.H., Glasser, W.G. **2002**. Recent Industrial Applications of Lignin: A Sustainable Alternative to Nonrenewable Materials. Journal of Polymers and the Environment, 10, 39-48.

- Marton, J. **1971**. Reactions in alkaline pulping, in: Sarkanen, K.V., Lugwid, C.H. (Eds.), Lignins: occurrence, formation, structure and reactions. Wiley-interscience, New York, pp. 639-694.
- Martone, P.T., Estevez, J.M., Lu, F., Ruel, K., Denny, M.W., Somerville, C., Ralph, J. **2009**. Discovery of lignin in seaweed reveals convergent evolution of cell-wall architecture. *Current Biology*, 19, 169-175.
- Matsushita, Y., Inomata, T., Takagi, Y., Hasegawa, T., Fukushima, K. **2011**. Conversion of sulfuric acid lignin generated during bioethanol production from lignocellulosic materials into polyesters with  $\epsilon$ -caprolactone. *Journal of Wood Science*, 57, 214-218.
- McDonald, A.G., Ma, L. **2012**. Plastic moldable lignin, in: Paterson, R.J. (Ed.), Lignin: Properties and applications in biotechnology and bioenergy. Nova Science Publisher, Inc., pp. 489-498.
- Meister, J.J. **2002**. Modification of lignin. *Journal of Macromolecular Science-Polymer Reviews*, C42, 235-289.
- Miller, S.A. **2013**. Sustainable Polymers: Opportunities for the Next Decade. *ACS Macro Letters*, 2, 550-554.
- Mohan, D., Pittman, C.U., Steele, P.H. **2006**. Pyrolysis of wood/biomass for bio-oil: A critical review. *Energy & Fuels*, 20, 848-889.
- Nimz, H.H. **1983**. Lignin based wood adhesives, in: Pizzi, A. (Ed.), Wood adhesives-chemistry and technology. Marcel Dekker, New York, pp. 257-288.
- Olivares, M., Guzman, J.A., Natho, A., Saavedra, A. **1988**. Kraft Lignin Utilization in Adhesives. *Wood Science and Technology*, 22, 157-165.
- Pan, X., Kadla, J.F., Ehara, K., Gilkes, N., Saddler, J.N. **2006**. Organosolv ethanol lignin from hybrid poplar as a radical scavenger: relationship between lignin structure, extraction conditions, and antioxidant activity. *Journal of Agricultural and Food Chemistry*, 54, 5806-5813.

- Pan, X., Xie, D., Kang, K.Y., Yoon, S.L., Saddler, J.N. **2007**. Effect of organosolv ethanol pretreatment variables on physical characteristics of hybrid poplar substrates. *Applied Biochemistry and Biotechnology*, 137, 367-377.
- Peacock, A., Calhoun, A. **2006**. *Polymer chemistry: Properties and applications*. Carl Hanser Verlag, Munich.
- Pearl, I.A. **1967**. *The chemistry of lignin*. Marcel Dekker, INC., New York, pp. 1-6.
- Piccolo, R.S.J., Santos, F., Frollini, E. **1997**. Sugar cane bagasse lignin in resol-type resin: Alternative application for lignin-phenol-formaldehyde resins. *Journal of Macromolecular Science-Pure and Applied Chemistry*, A34, 153-164.
- Pizzi, A., Cameron, F.A., Klashorst, G.H. **1989**. Soda bagasse lignin adhesives for particleboard—preliminary results, in: Hemingway, R.W., Conner, A.H., Branham, S.J. (Eds.), *Adhesive from renewable resources*. ACS Symposium Series, New Orleans, pp. 82-95.
- Plomion, C., Leprovost, G., Stokes, A. **2001**. Wood formation in trees. *Plant Physiology*, 127, 1513-1523.
- Pohjanlehto, H., Setälä, H.M., Kiely, D.E., McDonald, A.G. **2014**. Lignin-Xylaric Acid-Polyurethane-Based Polymer Network Systems: Preparation and Characterization. *Journal of Applied Polymer Science*, 131, 39714-39720.
- Qin, W., Kadla, J.F. **2012**. Carbon fibers based on pyrolytic lignin. *Journal of Applied Polymer Science*, 126, E203-E212.
- Quirino, R.L., Garrison, T.F., Kessler, M.R. **2014**. Matrices from vegetable oils, cashew nut shell liquid, and other relevant systems for biocomposite applications. *Green Chemistry*, 16, 1700-1715.
- Ralph, J. **1999**. Lignin structure: recent developments, *Proceedings of the 6th Brazilian Symposium Chemistry of Lignins and Other Wood Components*, Guaratingueta, Brazil, pp. 97-112.
- Ralph, J. **2010**. Hydroxycinnamates in lignification. *Phytochemistry Reviews*, 9, 65-83.
- Ralph, J., Brunow, G., Boerjan, W. **2007**. *Lignins*.

- Ralph, J., Lundquist, K., Brunow, G., Lu, F., kim, H., Schatz, P.F., Marita, J., Hatfield, R.D., Ralph, S.A., Christensen, J.H., Boerjan, W. **2004**. Lignins: Natural polymers from oxidative coupling of 4-hydroxyphenylpropanoids. *Phytochemistry Reviews*, 3, 29-60.
- Ralph, J., Peng, J.P., Lu, F.C., Hatfield, R.D., Helm, R.F. **1999**. Are lignins optically active? *Journal of Agricultural and Food Chemistry*, 47, 2991-2996.
- Rials, T.G., Glasser, W.G. **1984a**. Engineering plastics from lignin IV. Effect of Crosslinking density on polyurethane film properties-variation in NCO:OH ratio.pdf>. *Holzforschung*, 38, 191-199.
- Rials, T.G., Glasser, W.G. **1984b**. Engineering plastics from lignin V. Effect of crosslinking density on polyurethane film properties-variation in polyol hydroxy content.pdf>. *Holzforschung*, 38, 263-269.
- Rials, T.G., Glasser, W.G. **1986**. Engineering plastics from lignin XIII. Effect of lignin Structure on Polyurethane Network Formation. *Holzforschung*, 40, 353-360.
- Rodriguez, F., Cohen, C., Ober, C.K., Archer, L.A. **2003**. Principles of polymer systems. CRC Press, Boca Raton
- Roffael, E., Dix, B. **1991**. Lignin and Ligninsulfonate in Nonconventional Bonding - an Overview. *Holz Als Roh-Und Werkstoff*, 49, 199-205.
- Saha, B.C. **2003**. Hemicellulose bioconversion. *Journal of Industrial Microbiology and Biotechnology*, 30, 279-291.
- Sahaf, A., Laborie, M.-P.G., Englund, K., Garcia-Perez, M., McDonald, A.G. **2013**. Rheological Properties and Tunable Thermoplasticity of Phenolic Rich Fraction of Pyrolysis Bio-Oil. *Biomacromolecules*, 14, 1132-1139.
- Saito, T., Brown, R.H., Hunt, M.A., Pickel, D.L., Pickel, J.M., Messman, J.M., Baker, F.S., Keller, M., Naskar, A.K. **2012**. Turning renewable resources into value-added polymer: development of lignin-based thermoplastic. *Green Chemistry*, 14, 3295-3303.
- Saito, T., Perkins, J.H., Jackson, D.C., Trammel, N.E., Hunt, M.A., Naskar, A.K. **2013**. Development of lignin-based polyurethane thermoplastics. *RSC Advances*, 3, 21832-21840.

- Saka, S. **2000**. Chemical composition and distribution, in: Hon, D.N.-S., Shiraishi, N. (Eds.), *Wood and Cellulosic chemistry*, 2<sup>nd</sup> ed. Marcel Dekker Inc, New York, pp. 51-81.
- Sannigrahi, P., Ragauskas, A.J., Miller, S.J. **2010**. Lignin Structural Modifications Resulting from Ethanol Organosolv Treatment of Loblolly Pine. *Energy & Fuels*, 24, 683-689.
- Saraf, V.P., Glasser, W.G. **1984**. Hydroxyalkyl lignin derivative. III. Structure property relationships in solution cast polyurethane films. *Journal of Applied Polymer Science*, 29, 1831-1841.
- Saraf, V.P., Glasser, W.G., Wilkes, G.L. **1985a**. Engineering plastics from lignin VI. Structure-property relationship of PEG-containing polyurethane networks. *Journal of Applied Polymer Science*, 30, 2207-2224.
- Saraf, V.P., Glasser, W.G., Wilkes, G.L. **1985b**. Engineering plastics from lignin VII. Structure Property Relationships of Polybutadiene Glycol-Containing Polyurethane Networks. *Journal of Applied Polymer Science*, 30, 3809-3823.
- Sarkanen, K.V., Ludwig, C.H. **1971**. Definition and nomenclature, in: Sarkanen, K.V., Ludwig, C.H. (Eds.), *Lignins: occurrence, formation, structure and reactions*. Wiley-interscience, New York, pp. 1-18.
- Scholze, B., Hanser, C., Meier, D. **2001**. Characterization of the water-insoluble fraction from fast pyrolysis liquids (pyrolytic lignin) Part II. GPC, carbonyl groups, and C-13-NMR. *Journal of Analytical and Applied Pyrolysis*, 58, 387-400.
- Scholze, B., Meier, D. **2001**. Characterization of the water-insoluble fraction from pyrolysis oil (pyrolytic lignin). Part I. PY-GC/MS, FTIR, and functional groups. *Journal of Analytical and Applied Pyrolysis*, 60, 41-54.
- Sellers, T., McGinnis, G.D., Ruffin, T.M., Janiga, E.R. **2004**. Lignin-modified phenol-formaldehyde resin development for fiberboard. *Forest Products Journal*, 54, 45-51.
- Shiraishi, N. **1989**. Recent Progress in Wood Dissolution and Adhesives from Kraft Lignin. *ACS Symposium Series*, 397, 488-495.



- Simmons, B.A., Logue, D., Ralph, J. **2010**. Advances in modifying lignin for enhanced biofuel production. *Current Opinion in Plant Biology*, 13, 313-320.
- Sivasankarapillai, G., McDonald, A.G. **2011**. Synthesis and properties of lignin-highly branched poly (ester-amine) polymeric systems. *Biomass and Bioenergy*, 35, 919-931.
- Sivasankarapillai, G., McDonald, A.G., Li, H. **2012**. Lignin valorization by forming toughened lignin-co-polymers: Development of hyperbranched prepolymers for cross-linking. *Biomass and Bioenergy*, 47, 99-108.
- Sjostrom, E. **1993**. *Wood chemistry: Fundamentals and applications* (2<sup>nd</sup> edition). Academic Press, Inc, San Diego, CA.
- Stockburger, P. **1993**. An Overview of near-Commercial and Commercial Solvent-Based Pulping Processes. *Tappi Journal*, 76, 71-74.
- Teramoto, N. **2011**. Synthetic green polymers from renewable monomers, in: Sharma, S.K., Mudhoo, A. (Eds.), *A Handbook of Applied Biopolymer Technology: Synthesis, Degradation and Applications*. Royal Society of Chemistry, pp. 22-78.
- Thielemans, W., Wool, R.P. **2004**. Butyrate kraft lignin as compatibilizing agent for natural fiber reinforced thermoset composites. *Composites Part a-Applied Science and Manufacturing*, 35, 327-338.
- Thielemans, W., Wool, R.P. **2005**. Lignin esters for use in unsaturated thermosets: lignin modification and solubility modeling. *Biomacromolecules*, 6, 1895-1905.
- Umezawa, T. **2000**. Chemistry of extractives, in: Hon, D.N.-S., Shiraishi, N. (Eds.), *Wood and Cellulosic chemistry*, 2<sup>nd</sup> ed. Marcel Dekker Inc, New York, pp. 213-241.
- Uraki, Y., Sugiyama, Y., Koda, K., Kubo, S., Kishimoto, T., Kadla, J.F. **2012**. Thermal mobility of beta-O-4-type artificial lignin. *Biomacromolecules*, 13, 867-872.
- Vanholme, R., Demedts, B., Morreel, K., Ralph, J., Boerjan, W. **2010**. Lignin biosynthesis and structure. *Plant Physiology*, 153, 895-905.
- Vanholme, R., Morreel, K., Ralph, J., Boerjan, W. **2008**. Lignin engineering. *Current Opinion in Plant Biology*, 11, 278-285.

Vassilev, S.V., Baxter, D., Andersen, L.K., Vassileva, C.G. **2010**. An overview of the chemical composition of biomass. *Fuel*, 89, 913-933.

Voit, B.I., Lederer, A. **2009**. Hyperbranched and Highly Branched Polymer Architectures- Synthetic Strategies and Major Characterization Aspects. *Chemical Reviews*, 109, 5924-5973.

Wagermaier, W., Kratz, K., Heuchel, M., Lendlein, A. **2010**. Characterization Methods for Shape-Memory Polymers, in: Lendlein, A. (Ed.), *Shape-Memory Polymers*. Springer-Verlag Berlin, pp. 97-145.

Wagner, A., Donaldson, L., Ralph, J. **2012**. Lignification and Lignin Manipulations in Conifers. *Lignins: Biosynthesis, Biodegradation and Bioengineering*, 61, 37-76.

Wang, J.S., Manley, R.S., Feldman, D. **1992**. Synthetic-Polymer Lignin Copolymers and Blends. *Progress in Polymer Science*, 17, 611-646.

Weng, J.K., Chapple, C. **2010**. The origin and evolution of lignin biosynthesis. *New Phytol*, 187, 273-285.

Wu, L.C.F., Glasser, W.G. **1984**. Engineering plastics from lignin. I. Synthesis of hydroxypropyl lignin. *Journal of Applied Polymer Science*, 29, 1111-1123.

Xie, T. **2010**. Tunable polymer multi-shape memory effect. *Nature*, 464, 267-270.

Xie, T. **2011**. Recent advances in polymer shape memory. *Polymer*, 52, 4985-5000.

Yakacki, C.M. **2013**. Shape-Memory and Shape-Changing Polymers. *Polymer Reviews*, 53, 1-5.

Yao, K., Tang, C. **2013**. Controlled Polymerization of Next-Generation Renewable Monomers and Beyond. *Macromolecules*, 46, 1689-1712.

Yoshida, H., Morck, R., Kringstad, K.P. **1987**. Fractionation of Kraft lignin by successive extraction with organic solvents. *Holzforschung*, 41, 171-176.

Zakzeski, J., Bruijninx, P.C., Jongerius, A.L., Weckhuysen, B.M. **2010**. The catalytic valorization of lignin for the production of renewable chemicals. *Chemical Reviews*, 110, 3552-3599.

Zhou, S., Garcia-Perez, M., Pecha, B., Kersten, S.R.A., McDonald, A.G., Westerhof, R.J.M. **2013a.** Effect of the Fast Pyrolysis Temperature on the Primary and Secondary Products of Lignin. *Energy & Fuels*, 27, 5867-5877.

Zhou, S., Garcia-Perez, M., Pecha, B., McDonald, A.G., Kersten, S.R.A., Westerhof, R.J.M. **2013b.** Secondary Vapor Phase Reactions of Lignin-Derived Oligomers Obtained by Fast Pyrolysis of Pine Wood. *Energy & Fuels*, 27, 1428-1438.

Zhou, S., Osman, N.B., Li, H., McDonald, A.G., Mourant, D., Li, C.Z., Garcia-Perez, M. **2013c.** Effect of sulfuric acid addition on the yield and composition of lignin derived oligomers obtained by the auger and fast pyrolysis of Douglas-fir wood. *Fuel*, 103, 512-523.

## 2 Fractionation and Characterization of Industrial Lignin

### 2.1 Abstract

Three industrial lignins (Indulin AT Kraft softwood, Protobind 1000, and corn stover) were fractionated in methanol to obtain soluble and insoluble fractions. The original lignin and obtained lignin fractions were characterized chemically by a combination of FTIR spectroscopy, pyrolysis-gas chromatography-mass spectrum (py-GC-MS), and derivatization followed by reductive cleavage (DFRC). The methanol soluble lignin fractions contained fewer condensed structures than the original lignin and methanol insoluble fractions. The thermal (e.g. glass transition temperature ( $T_g$ ) and thermal stability) and rheological properties of the lignins were characterized by a combination of DSC, TMA, TGA and parallel plate rheology. TMA and modulated temperature DSC (MTDSC) proved to be sensitive techniques in determining  $T_g$ . The methanol soluble lignin fractions had the lowest  $T_g$  values relative to the original lignin and methanol insoluble fractions. The original lignin and methanol insoluble fractions had a higher thermal degradation temperature relative to the methanol soluble lignin. Solvent partitioning offers a practical approach to fractionate lignin into low weight average molar mass ( $M_w$ ) and  $T_g$  fractions which show promise as starting materials for making lignin-copolymers.

### 2.2 Introduction

Lignin is widely distributed throughout the plant kingdom where lignification is not confined to xylem (wood) and annual plants but also found in fruit, seeds, bark, roots, bast, pith and cork cells (Pearl, 1967). Recently, lignin has also been found in seaweed (Martone et al., 2009). Due to this extensive distribution, lignin is ranked second in content behind cellulose in terrestrial natural resources (Lewis and Lantzy, 1989) and being nature's most abundant aromatic polymer (Lora and Glasser, 2002). Lignin content varies depending on species and typically 20-30 % for hardwoods and 25-35% for softwoods (Dimmel, 2010). Although the vast quantities of lignin in nature, historically, lignin has had a negative role in pulp and paper industry as well as an emerging biorefinery industry, where efforts are made to

remove the polymer. Subsequently, large amounts of lignin are produced annually, for instance, the pulp and paper industry alone produced 45 million metric tons of extracted lignin in 2004 (Zakzeski et al., 2010). The application of value-added lignin, however, is limited to a low level with only approximately 2 % of the total availability of lignin from pulp and paper industry (Gosselink et al., 2004). The limited application of industrial lignin is largely due to its complex three-dimensional aromatic structure and heterogeneity based on feedstock type and extraction process. Industrial or extracted lignin is brittle, has a high glass transition temperature ( $T_g$ ), a complex chemical structure and low solubility in common solvent are contributing factors which limits its use as a polymer (Li et al., 1997). Lignin's brittleness is due to its 3-dimensional structure and inter-and intra-chain H-bonds (Aracri et al., 2014). Thermoplasticity can be introduced to lignin by substituting hydroxyl groups which will inhibit H-bonding (McDonald and Ma, 2012; Sivasankarapillai et al., 2012).

There have been considerable efforts to improve lignins properties by substitution, namely methylation (Li et al., 1997), esterification (Fox and McDonald, 2010) and benzylation (McDonald and Ma, 2012), to impart thermoplasticity. Substitution also resulted in lowering the glass  $T_g$  of lignin. Other strategies for lignin modification have involved its incorporation into polyurethane, polyester, polyolefin, polyethylene oxide, and vinyl polymers (Chung and Washburn, 2013; Gandini and Belgacem, 2008; Li and Sarkanen, 2000; Miller, 2013; Pohjanlehto et al., 2014; Wang et al., 1992).

To improve lignin's miscibility with other polymers, solvent partitioning, using methanol, have been employed to separate out a low and high molar mass fractions (Sivasankarapillai and McDonald, 2011; Sivasankarapillai et al., 2012). Early work by Yoshida et al. had fractionated kraft lignin and black liquor by successive extraction with solvents and had characterized the fraction's properties (Morck et al., 1986; Yoshida et al., 1987; Yuan et al., 2009). Kraft hardwood lignin was also fractionated in methanol for use in lignin based thermoplastics and lignin-polymer systems (Saito et al., 2012; Saito et al., 2013; Saito et al., 2014). Work by Argyropoulos' group had used an acetone soluble lignin fraction in poly(arylene-ether-sulfone) based copolymer systems (Argyropoulos et al., 2014). Arshanitsa

et al (2013) and Ponomarenko et al. (2014) sequentially applied organic solvents to fractionate industrial lignin to improve their role as antioxidants. Membrane based separation on industrial lignin has been applied for use in adhesives and carbon fibers (Brodin et al., 2009, 2010).

The aim of this study was to fractionate industrial lignin to obtain low molar mass lignin that could be used in lignin-copolymer systems. The original lignin and methanol soluble/insoluble fractions were characterized for chemical characteristics and thermal properties and their relationships.

### **2.3 Materials and methods**

Protobind 1000 (PB) lignin (agricultural fiber soda pulp) was supplied by ALM India Pvt. Ltd and used as received. Indulin AT (IN) lignin (softwood kraft) was provided by MeadWestvaco and used as received. Corn stover (CS) lignin (from cellulosic ethanol production) was obtained from the National Renewable Energy Laboratory and washed with hot water (60 °C) and vacuum dried.

#### **2.3.1 Lignin preparation and fractionation**

Lignin (250 g) was stirred in methanol (1.5 L) for 5 h at 60 °C. The methanol soluble (MS) and methanol insoluble (MI) fractions were recovered by filtration, vacuum dried and yields recorded. For example, the lignin sample PB was fractionated into PB-MS and PB-MI.

#### **2.3.2 Chemical analysis**

Klason lignin and acid soluble lignin analyses were performed according to ASTM D1106-96 (2013) and Tappi UM250 (1991), respectively.

The  $M_w$  of IN-MS, PB-MS and CS-MS were determined by electrospray ionization-MS (ESI-MS) on a LCQ-Deca (ThermoFinnigan) according to Osman et al (2012).

Lignin (1.00 g) was acetylated in a 1:1 (v/v) mixture of acetic anhydride/pyridine (6 mL) for 24 h at 20°C. The acetylated lignin product was precipitated in ice-water. The precipitate was further washed with water, freeze-dried and yield recorded.

FTIR spectra were collected by a ThermoNicolet Avatar 370 spectrometer operating in the attenuated total reflection (ATR) mode (SmartPerformer, ZnSe crystal). The spectra were ATR and baseline corrected. For the quantitative analysis, the spectra were normalized and curve-fitted using Igor Prof 6.03 software (WaveMetrics, Inc) (Wei et al., 2013) and the area of each fitted band was integrated. The aromatic/aliphatic OH ratio was calculated as the ratio of areas under the carbonyl (C=O) bands at 1760 to 1742 cm<sup>-1</sup> (Glasser and Jain, 1993). The syringyl/guaiacyl (S/G) ratio was calculated as the ratio of the areas for the S unit at 1327 cm<sup>-1</sup> to G unit at 1267 cm<sup>-1</sup> (Poursorkhabi et al., 2013). The condensation indices of lignin was determined from the FTIR spectra using Equation 2.1 (Faix, 1991b):

$$\text{Condensation Indices (CI)} = \frac{\sum \text{minima between } 1500 \text{ and } 1050 \text{ cm}^{-1}}{\sum \text{maxima between } 1600 \text{ and } 1030 \text{ cm}^{-1}} \quad (2.1)$$

Lignin DFRC analysis were performed as following (Lu and Ralph, 1997): (i) lignin (20 mg) was dissolved in acetic acid/acetyl bromide (4:1 v/v, 5 mL) and stirred for 1 h at 50°C and reagents removed under vacuum at 40°C; (ii) the residue was dissolved in dioxane/acetic acid/water (5:4:1 v/v, 5mL) to which zinc powder (50 mg) was added and the mixture stirred for 30 min at 20°C. Zinc was removed by filtration and an internal standard (10 mg tetracosane in CH<sub>2</sub>Cl<sub>2</sub>, 10 mL) was added to the filtrate, mixed, washed with saturated NH<sub>4</sub>Cl (10 mL), CH<sub>2</sub>Cl<sub>2</sub> layer recovered, dried and concentrated to dryness; (iii) The reduced material was acetylated with acetic anhydride/pyridine (1:1 v/v, 2 mL) for 80 min at 20°C, then ethanol added to quench the reaction and excess reagents were removed under vacuum. The residue was dissolved in CH<sub>2</sub>Cl<sub>2</sub> (1.5 mL) and analyzed by GC-MS (Polaris Q, Thermofinnigan). Separation was performed on a ZB-1 capillary column (30m × 0.25 mm i.d., Phenomenex) with a temperature program of 100°C (1 min) to 300°C at 5°C/min. *p*-Hydroxy phenyl (P), G, and S units were determined using response factors 1.76, 1.85, and 2.06, respectively.

Pyrolysis GC-MS analysis (Focus-ISQ, ThermoScientific) was performed on lignin (<0.1 mg) in a quartz capillary tube and pyrolyzed (Pyrojector II, SGE) at 500°C. Separation was achieved on a RTX-5ms capillary column (30 m × 0.25 mm i.d., Restek) with a temperature program of 50 to 250°C (10 min) at 5°C/min. Compounds were identified with known standards, NIST 2008 mass spectral library and literature (Meier and Faix, 1992). The S/G ratios were determined according to Nonier et al. (2006) and Nunes et al (2010).

### 2.3.3 Thermal analysis

DSC was performed on a TA instruments model Q 200 DSC equipped with refrigerated cooling on 5-7 mg of sample. Conventional DSC with annealing the sample was heated to 90°C and annealed for 10 min, then cooled to 0°C (3 min), then heated to 200°C at 10°C/min (second cycle). DSC without annealing was carried out from 40 to 200°C at 10°C/min. MTDSC was equilibrated at 0°C for 5 min, then heat modulated +/- 0.66°C every 50 s, and then ramped from 0 to 250°C. The inflection point of heat flow change from heating cycle was assigned as  $T_g$ . Kinetic studies were carried out using conventional DSC with annealing at 5°C/min, 10°C/min, and 15°C/min to determine activation energy of the  $T_g$  transition (Moynihan et al., 1974).

TMA was carried out with Perkin Elmer TMA 7 instrument using the penetration probe (static force 10 mN) from 30 to 300°C at 5°C/min. Lignin samples were pressed to a small disc (2 mm x 1 mm). The onset point of softening was assigned as  $T_g$ .

Parallel plate rheometry (25 mm dia serrated) was performed using a Bohlin CVO100 instrument with an extended temperature unit. Lignin samples were compression molded into 25 mm x 2 mm discs. Experiments were performed at 1 Hz from 180 to 40°C at -2°C/min with a normal force applied at 1 N, and strain of 0.05 % (within the linear viscoelastic range). Data was analyzed using the Bohlin software v 06.32 (Fox and McDonald, 2010).

TGA was carried out using a Perkin Elmer TGA 7 instrument from 30 to 900°C at 20°C/min under N<sub>2</sub> (30 mL/min). Kinetic study of thermal decomposition was carried out by TGA under 5°C/min, 10°C/min, and 15°C/min.



## 2.4 Results and Discussion

### 2.4.1 Chemical analysis

Partitioning lignin into low and high molar mass fractions based on partial methanol solubility (Hildebrand solubility parameter of  $14.3 \text{ (cal/mL)}^{1/2}$ ) was selected because of practical ease of separation (Argyropoulos et al., 2014; Saito et al., 2014; Sivasankarapillai and McDonald, 2011)(Schuerch, 1952). Three industrial lignin samples (PB, IN, CS) were fractionated and obtained methanol soluble yields of PB-MS (45% w/w), IN-MS (50% w/w), and CS-MS (12% w/w). The purity of the lignin samples was based on Klason and acid soluble lignin contents and the results are given in Table 2.1. Lignin analysis showed that the MS lignin fractions had the highest lignin content of 93-95%. Due to solubility issues only the MS lignin samples were analyzed by ESI-MS to determine their  $M_w$  which were 654 g/mol for IN-MS, 958 g/mol for PB-MS, and 741 g/mol for CS-MS.

Table 2.1 Lignin contents based on Klason lignin and acid soluble lignin

Lignin sample	Klason lignin (%)	Acid soluble (%)	Total (%)
IN	91.0±0.4	2.51±0.08	93.5
IN-MS	90.8±0.8	3.13±0.03	93.9
IN-MI	90.8±0.0	1.31±0.01	92.1
PB	86.4±0.6	3.87±0.15	90.3
PB-MS	90.5±0.1	2.83±0.01	93.3
PB-MI	84.7±0.1	2.86±0.06	87.6
CS	87.5±2.2	2.20±0.02	89.7
CS-MS	93.6±0.4	1.74±0.04	95.3
CS-MI	88.2±1.3	2.08±0.01	90.3

#### 2.4.1.1 FTIR results

FTIR spectroscopy was performed on the various lignin fractions and the spectra are shown in Figure 2.1 and band assignments are given in Table 2.2. Characteristic lignin bands for O-H stretching ( $3400 \text{ cm}^{-1}$ ), C-H stretching ( $2930$  and  $2850 \text{ cm}^{-1}$ ), aromatic skeletal vibrations

(1600 and 1510  $\text{cm}^{-1}$ ) were observed. IN showed a typical G bands at 1264  $\text{cm}^{-1}$  (G ring plus C=O stretch), 854  $\text{cm}^{-1}$  (C-H out-of-plane in positions 2 and 5) and 813  $\text{cm}^{-1}$  (C-H out-of-plane in position 6 of G). PB and CS lignin samples were of the HGS type with strong bands at 1327  $\text{cm}^{-1}$ , 1257  $\text{cm}^{-1}$ , 832  $\text{cm}^{-1}$  (C-H out-of-plane in positions 2 and 6 of S units, and in all position of H units), and 1160  $\text{cm}^{-1}$  (typical for HGS) which matches the results from other results (Fox and McDonald, 2005; Sahoo et al., 2011). HGS characteristics of PB and CS were confirmed by their high S/G ratios (Table 2.6).

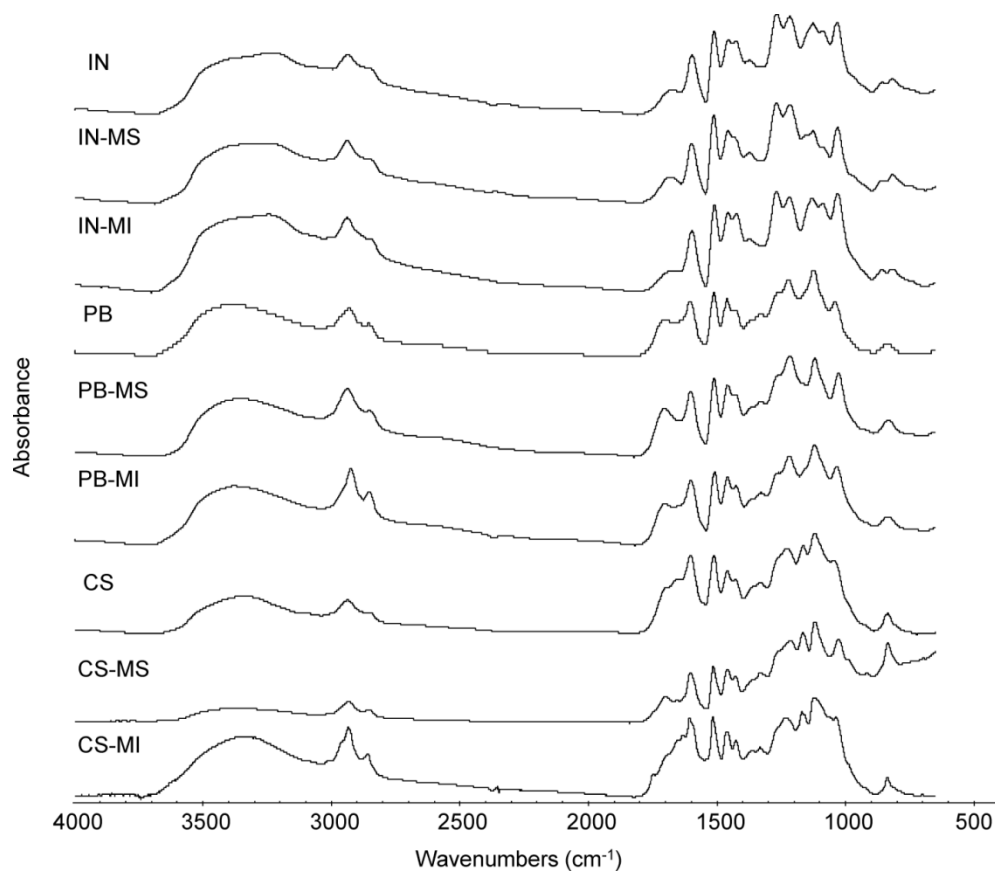


Figure 2.1 FTIR spectra of all the lignin samples.

Table 2.2 Assignments of FTIR bands of lignin (Faix, 1991a)

No.	IN	PB	CS	Assignments
	Band (cm <sup>-1</sup> )	Band (cm <sup>-1</sup> )	Band (cm <sup>-1</sup> )	
1	3411	3403	3355	OH stretching
2	2932	2927	2932	CH asymmetric stretching
3	2847	2852	2847	CH symmetric stretching
4	-	1700	1702	C=O stretching
5	1669	-	1640	C=O stretching, in conjugated
6	1593	1600	1598	Aromatic skeletal vibrations
7	1507	1508	1508	Aromatic skeletal vibrations
8	1454	1457	1456	Asymmetric bending deformation of methyl and methylene groups
9	1422	1424	1425	C-H in-plane deformation with aromatic ring stretching
10	1370	1368	1367	Symmetric bending deformation of methyl group
11	-	1326	1327	C-O of syringyl ring
12	1264	1259	1262	C-O of guaiacyl ring
13	1214	1218	1223	C-C plus C-O stretch
14		1160	1162	Typical for HGS lignin, conjugated C=O in ester groups
15	1123	1120	1116	C-O deformation in ester bond
16	1085			C-O deformation in secondary alcohols and aliphatic ethers
17	1029	1036	1042	Aromatic C-H in-plane deformation (G > S) plus C-O deformation in primary alcohols
18	854			C-H out-of-plane in position 2,5 and 6 of G units
19		832	832	C-H out-of-plane in position 2 and 6 of S, and in all position of H units
20	813			C-H out-of-plane in position 2,5 and 6 of G units

The level of condensed structures, as CI, in the lignin samples was determined by FTIR using equation 2.1 (Table 2.3) (Faix, 1991b). PB-MS, IN-MS and CS-MS were shown to have the lowest CI values followed by original lignin and then the MI fractions. For example, the CI for PB-MS was 0.53 while for PB-MI was 0.57. These findings suggest that the least condensed

structures were more soluble in methanol. Among the three lignin samples, IN had the highest CI (0.62) compared to PB (0.55) and CS (0.55), which is consistent with previous work using the permanganate oxidation protocol (Fox and McDonald, 2010). Furthermore, the CI results were comparable to those reported in the literature (Schorr et al., 2014).

Table 2.3 Lignin aromatic/aliphatic OH group ratios on acetylated samples and lignin condensation indices (CI) determined by FTIR spectroscopy

	IN	IN-MS	IN-MI	PB	PB-MS	PB-MI	CS	CS-MS	CS-MI
aromatic/aliphatic OH ratio	0.88	1.05	0.87	0.87	0.93	0.82	0.90	1.07	0.88
CI	0.62	0.59	0.63	0.55	0.53	0.57	0.55	0.49	0.55

Hydroxyl groups were quantitatively determined on acetylated lignin samples (Table 2.3), based on the intensity of 1742 and 1760  $\text{cm}^{-1}$  bands which were assigned as aliphatic and aromatic C=O stretching, respectively (Faix et al., 1994; Glasser and Jain, 1993). The MS lignin fractions were shown to have the highest aromatic/aliphatic OH ratio (0.93-1.07) as compared to their original (0.87- 0.90) and MI (0.82-0.88) fractions. This result was consistent with previous reports that higher content of aromatic hydroxyl groups found in solvent soluble fractions (such as methanol) (Morck et al., 1986; Saito et al., 2014).

#### 2.4.1.2 Py-GC-MS results

Analytical py-GC-MS was performed to obtain H/G/S ratios for the various lignin fractions and the results are given in Table 2.4. The H/G/S ratios for IN, PB, and CS were 4/91/5, 20/52/28, and 44/30/26, respectively, indicating the G type for IN lignin and HGS type for PB and CS lignin. The MS lignin fractions showed highest S content for all three lignins. The higher abundance of S units in lignin is accompanied by the lower condensed structure (Li et al., 2012).

Table 2.4 Compound identification and intensities of the various lignins by py-GC-MS

Peak No.	Ret. Time (mins)	Compound	M <sup>+</sup> (m/z)	Monomer type	IN	IN-MS	IN-MI	PB	PB-MS	PB-MI	CS	CS-MS	CS-MI
1	1.17	carbon dioxide	44		7.9	7.9	11.8	10.9	9.7	10.4	14.0	6.6	15.9
2	1.78	acetic acid	60		0.5	0.6	0.6	0.7	0.7	0.9	2.8	2.1	3.0
3	7.84	phenol	94	H	0.6	0.7	0.8	1.9	2.1	1.6	2.6	3.3	2.3
4	9.83	2-methyl-phenol,	108	H	0.4	0.5	0.6	0.6	0.6	0.5	0.4	0.6	0.3
5	10.45	4-methyl-Phenol,	108	H	0.8	0.7	1.1	1.3	1.4	1.0	1.9	2.8	1.8
6	10.80	guaiacol	124	G	7.4	9.1	6.5	4.2	4.4	4.2	2.6	3.1	2.1
7	12.45	Dimethyl-phenol	122	H	0.4	0.4	0.8	0.5	0.5	0.3	0.4	0.6	0.0
8	13.04	4-ethyl-phenol	122	H		0.3	0.6	2.0	1.8	1.0	2.7	3.7	2.3
9	13.27	methyl-guaiacol,	138	G	0.4	0.5	0.5	0.4	0.7	0.3	0.2	0.3	0.1
10	13.71	4-methyl-guaiacol	138	G	7.7	6.2	8.5	2.9	3.1	3.2	1.6	2.5	1.5
11	14.15	Catechol	110	G	2.7	2.8	4.4	2.3	2.3	1.6	0.7	2.1	0.6
12	14.61	4-vinyl-phenol	120	H	0.4	0.4	0.4	5.3	6.3	5.0	14.5	10.8	15.8
13	14.98	4-ethyl-3-methyl-phenol	136	H		0.3	0.5	0.5	0.4	0.3	0.3	0.3	0.3
14	15.53	4-propyl-phenol	136	H							1.6	0.4	0.2
15	15.68	3-methoxy-catechol	140	G	1.6	1.4	2.4	3.4	3.1	3.3	0.6	2.7	1.8
16	16.07	4-ethyl-guaiacol	152	G	1.7	1.8	2.1	2.1	2.2	1.3	0.8	1.4	0.7
17	16.42	3-methyl-catechol	124	G	1.5	1.8	3.2	1.6	1.4	0.9	0.8	0.3	0.6
18	16.57	methyl-catechol	124	G								1.1	0.0
19	16.77	4-propenyl-phenol	134	H				0.4	0.5	0.3	0.1	0.3	0.3
20	17.07	4-vinyl-guaiacol	150	G	6.3	5.7	6.5	7.2	8.3	7.8	5.0	3.7	4.9
21	17.28	3-methoxy-5-methyl-phenol	138	G				0.4	0.5	0.5	0.4	0.4	0.4
22	17.82	4-(2-propenyl)-phenol	134	H				0.4	0.4	0.3	0.7	1.0	0.7
23	18.09	syringol	154	S	0.8	1.6	0.9	4.1	4.9	3.6	2.7	4.2	2.1

24	18.14	eugenol	164	G	1.1	1.0	1.1				0.3	0.5	0.3
25	18.27	3,4-dimethoxy-phenol	154	S				1.1	1.0	0.6	0.5	0.9	0.4
26	18.38	4-propyl-guaiacol	166	G	1.0	0.4	1.6	0.7	0.6	0.4	0.6	0.2	0.1
27	18.54	4-hydroxy-benzaldehyde	122	H								0.6	0.6
28	18.96	4-ethyl-catechol	138	G	0.2	0.6	1.2	1.1	0.8	0.3	0.1	0.6	0.1
29	19.31	vanillin	152	G	5.4	5.0	2.2	1.1	1.4	0.8	1.1	1.2	1.2
30	19.43	isoeugenol (cis)	164	G	0.7	0.7	0.9	0.3	0.3	0.3	0.2	0.3	0.2
31	19.55	3,4-dimethoxy-toluene	152	S				0.2	0.2	0.2	0.1	0.2	0.1
32	20.44	isoeugenol (trans)	164	G	3.4	3.1	3.7						
33	20.48	4-methyl-syringol	168	S				4.2	4.5	4.2	2.9	3.5	2.7
34	21.45	acetoguaiacone	168	G	3.8	2.1	1.9	1.3	0.9	1.4	1.1	0.6	1.1
35	22.35	4-ethyl-syringol	182	S		1.1		0.7	0.9	0.5	0.2	0.7	0.2
36	22.48	guaiacyl acetone	180	G	1.3	1.3	1.5	0.6	0.9	0.8	0.4	0.5	0.4
37	23.29	4-vinyl-syringol	180	S	1.1		0.9	2.5	3.1	3.3	1.9	1.4	1.8
38	23.68	propio-guaiacone	180	G	1.3	1.3	1.3	0.6	0.6	0.5	0.6	0.9	0.3
39	24.13	cis-4-propenyl-syringol	194	S				0.3	0.4	0.4	0.5	0.7	0.5
40	24.26	homosyringaldehyde	196	S				0.2	0.3	0.1	0.1	0.3	0.1
41	25.12	dihydroconiferyl alcohol	182	G	2.8	4.1	2.3						
42	25.23	trans-4-propenyl-syringol	194	S				0.5	0.8	0.3	0.6	1.5	0.6
43	25.54	syringaldehyde	182	S	0.5	0.5	0.2	0.8	0.9	0.6	0.8	1.6	0.8
44	25.64	coniferyl alcohol (cis)	180	G	0.3	0.4	0.3	0.1	0.1				
45	26.35	4-allyl-syringol	194	S		0.1		1.1	1.3	1.5	1.8	1.8	1.8
46	27.06	coniferyl alcohol (trans)	180	G	1.9	3.5	1.9	1.8	2.3	2.4			
47	27.12	acetosyringone	196	S							1.6	1.9	1.7
48	27.87	syringyl acetone	210	S	0.3			0.7	0.9	0.7	0.5	0.8	0.5
49	28.96	propiosyringone	210	S	0.1			0.3	0.4	0.2	0.4	0.7	0.4
50	29.14	sinapaldehyde	208	S				0.4	0.5	0.4	0.4	0.5	0.4
	H/G/S				4/9	6/89/	8/89/	20/	21/50	18/52	44/3	36/33/	45/30
					0/5	5	3	52/	/29	/30	0/26	31	/25
								28					

### 2.4.1.3 DFRC results

The levels of uncondensed arylglycerol- $\beta$ -aryl ( $\beta$ -O-4) ether linkages in the lignin fractions were determined by DFRC (Table 2.5). Due to limited solubility no data was obtained for CS and CS-MI samples. Low ether linkage levels (G+S) were obtained for all lignin samples (<200  $\mu\text{mol/g}$ ), as expected since these were highly processed lignin. Tohmura and Argyropoulos also obtained low values (21  $\mu\text{mol/g}$ ) for residual kraft lignin which clearly shows a high level of  $\beta$ -O-4 degradation (Tohmura and Argyropoulos, 2001). For unprocessed wood samples DFRC values of around 1000  $\mu\text{mol/g}$  were reported (902  $\mu\text{mol/g}$  for hybrid poplar cellulosic enzyme lignin (Osman, 2010), aspen 696  $\mu\text{mol/g}$  (Lu and Ralph, 1998)). Total released uncondensed monomer yields of MS fractions from IN and PB (132 and 190  $\mu\text{mol/g}$ ) were the highest followed by original and MI fractions (Table 2.4). These results were indicative of the MS lignin having the lowest condensed structures as supported by FTIR data.

Table 2.5 DFRC results of aryl ether linkage levels for the various lignin samples

Lignin sample	G unit ( $\mu\text{mol/g}$ )	S unit ( $\mu\text{mol/g}$ )	Total yield ( $\mu\text{mol/g}$ )
IN	115	nd	115
IN-MS	132	nd	132
IN-MI	38	nd	38
PB	59	85	144
PB-MS	72	118	190
PB-MI	42	79	121
CS	ns <sup>b</sup>	ns	ns
CS-MS	48	27	75
CS-MI	ns	ns	ns

<sup>a</sup> nd means not detected

<sup>b</sup> ns means lignin sample failed to dissolve in solvent.

### 2.4.1.4 S/G determination by FTIR, py-GC-MS and DFRC

S/G ratios were determined by 3 different methods (FTIR, py-GC-MS, and DFRC) and compared (Table 2.6). The IN lignin samples had no detectable S units by DFRC and FTIR

methods and therefore only PB and CS lignin samples were analyzed. The MS lignin fractions gave higher S/G ratios than the original lignin and MI fractions, as determined by FTIR and py-GCMS. The DFRC method gave different S/G values than FTIR and py-GCMS. The DFRC method relies on the release of the uncondensed monomers and this could give a biased result, while FTIR examines the complete sample. It was difficult to interpret these results due to the variability in the S/G values between methods. Nunes et al. (2010) also found S/G discrepancies in hardwood lignin comparing py-GC-MS to alkaline nitrobenzene oxidation.

Table 2.6 Syringyl to guaiacyl ratios (S/G) of the various lignin samples by FTIR, py-GC-MS and DFRC

Lignin samples	S/G ratio		
	FTIR	Py-GC-MS	DFRC
PB	1.05	0.53	1.44
PB-MS	1.82	0.59	1.63
PBMI	1.54	0.56	1.86
CS	0.69	0.89	nd <sup>a</sup>
CS-MS	0.73	0.92	0.56
CS-MI	0.63	0.85	nd

<sup>a</sup> nd - not detected.

## 2.4.2 Thermal analysis

### 2.4.2.1 T<sub>g</sub> determination

Lignin's T<sub>g</sub> is an important property when it comes to polymer applications of industrial lignin and have been reported to be between 90 and 180°C (Glasser and Jain, 1993; Lora, 2008; Lora and Glasser, 2002; Tejado et al., 2007). With the purpose of determining T<sub>g</sub> of different industrial lignins and their fractions, we applied and compared different techniques (conventional DSC with and without annealing, MTDSC, TMA and dynamic rheology) to establish the most suitable method(s). The DSC thermogram, without annealing, showed a broad endothermic peak contributed to enthalpy relaxation phenomenon which prevented



accurate determination of  $T_g$  (Figure 2.2a) (Cui et al., 2013; Rials and Glasser, 1984). Therefore, sub- $T_g$  annealing was required to eliminate this phenomenon. However, lignin is susceptible to thermal reactions at around 120 °C and therefore annealing at 90 °C was employed (Poursorkhabi et al., 2013). A clear  $T_g$  transition for annealed lignin was shown by DSC in Figure 2.2b. Values of  $T_g$  obtained from DSC are given in Table 2.7. The  $T_g$  were shown to sequentially increase from the MS fraction to the original lignin then to the MI fraction. For example, the  $T_g$ s of IN-MS, IN and IN-MI were respectively, 117, 147, and 200°C.

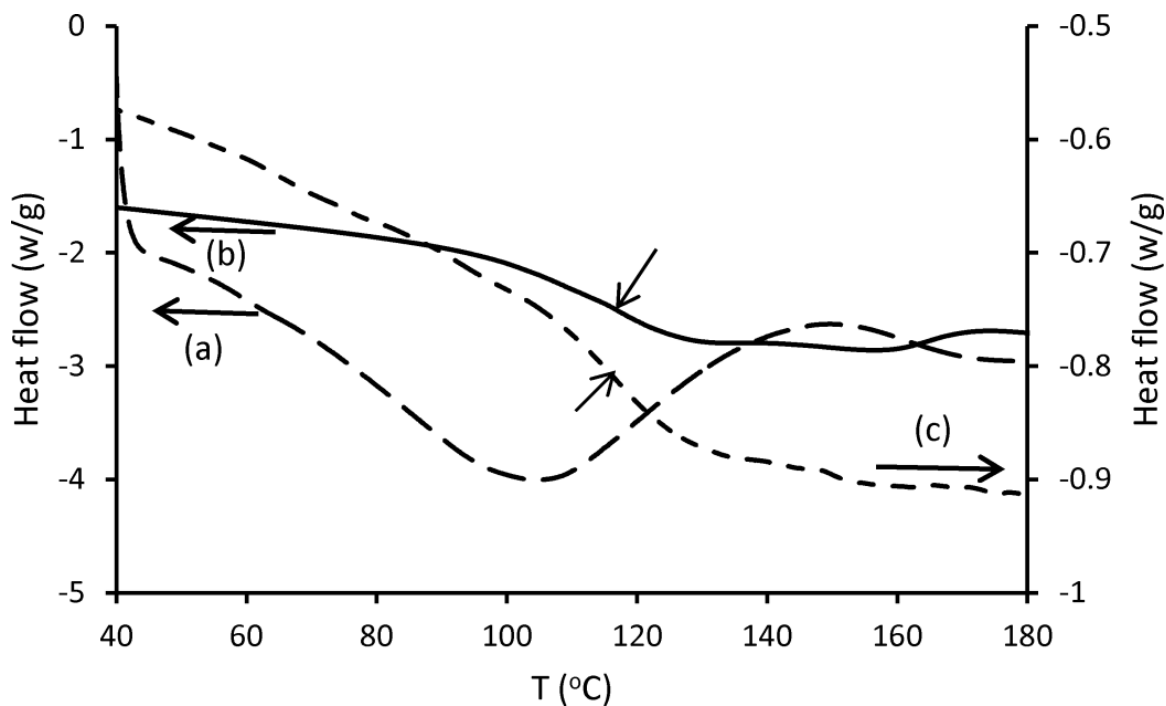


Figure 2.2 DSC thermograms of IN-MS lignin: (a) conventional DSC without annealing, (b), conventional DSC with annealing, (c) reversible heat flow from MTDSC. Note: arrows pointed to  $T_g$

Table 2.7 Comparison of  $T_g$ s of the various lignin samples determined by DSC, MTDSC, TMA and rheometry.

Lignin samples	Conventional DSC with annealing			TMDSC ( $^{\circ}\text{C}$ )	TMA ( $^{\circ}\text{C}$ )	Rheology ( $^{\circ}\text{C}$ )
	$T_g$ ( $^{\circ}\text{C}$ )	$\Delta T^a$ ( $^{\circ}\text{C}$ )	$\Delta C_p$ ( $\text{Jg}^{-1}\text{K}^{-1}$ )			
IN	147	13	0.35	143	157	180
IN-MS	117	14	0.56	118	123	143
IN-MI	200	18	0.21	202	203	nd
PB	162	14	0.39	163	164	179
PB-MS	132	13	0.54	138	143	161
PB-MI	186	20	0.22	210	205	nd
CS	nd <sup>b</sup>	nd	nd	199	218	nd
CS-MS	131	8	0.51	133	137	160
CS-MI	nd	nd	nd	200	219	nd

<sup>a</sup>  $\Delta T = T_{\text{end}} - T_{\text{onset}}$  in the  $T_g$  region

<sup>b</sup> nd - not detected

A kinetic study of annealed IN, IN-MS and IN-MI lignin samples  $T_g$  by DSC was performed to determine  $E_a$  according to equation 2.2:

$$\ln|\beta| = -\frac{E}{RT} \quad (2.2) \text{ (Moynihan et al., 1974)}$$

where  $\beta$  is heating rate (K/min),  $R$  is gas constant (8.314 J/K/mol),  $T$  is temperature (K),  $E$  is activation energy (J/mol). Glass transition  $E_a$ s of IN, IN-MS and IN-MI were 323, 278, and 413 kJ/mol, respectively (Song et al., 2014). These results were comparable to  $E_a$  of 265 kJ/mol for Alcell lignin (Guigo et al., 2009) obtained by MTDSC and 252-274 kJ/mol for in situ lignin (Laborie et al., 2004) obtained by DMA. The  $E_a$  was in the range of values for an  $\alpha$ -transition ( $T_g$ ) of a rigid polymer, such as polystyrene (Kovacs, 1958).

Temperature difference ( $\Delta T$ ) and heat capacity difference between glassy and rubbery states ( $\Delta C_p$ ) were determined on the lignin samples by DSC with annealing. The IN-MI (18 °C) and PB-MI (20 °C) demonstrated the highest  $\Delta T$  as compared to IN, IN-MS, PB and PB-MS samples, indicating higher relaxation times of molecular motion (Yoshida et al., 1987). The lower  $T_g$  lignin samples (IN-MS, PB-MS and CS-MS) had the highest  $\Delta C_p$  (0.51-0.56 Jg<sup>-1</sup>K<sup>-1</sup>) while the IN-MI and PB-MI fractions had the lowest  $\Delta C_p$  (0.21-0.22 Jg<sup>-1</sup>K<sup>-1</sup>) and are in agreement with Alcell lignin (Guigo et al., 2009) (Table 2.7). The high  $\Delta C_p$  was correlated with a low  $T_g$  and the index of molecular mobility (Hatakeyama et al., 2010; Hatakeyama and Hatakeyama, 1995), revealing that MS lignin fractions have highest molecular mobility which manifest as a low  $T_g$ .

Reversible heat flow of MTDSC was successfully applied to determine the  $T_g$  of all the lignin samples with the merits of high sensitivity and without the necessity to anneal the sample (Figure 2.2c, Table 2.7) (Guigo et al., 2009). The  $T_g$ s of the lignin samples by MTDSC were comparable to those obtained by DSC. For example, PB had a  $T_g$  of 162 °C by DSC as compared to 163 °C by MTDSC. Differences in  $T_g$  values can be attributed to the different heating rates between DSC and MTDSC methods (Moynihan et al., 1974). Cui, et al. (2013) and Argyropoulos et al (2014). obtained a  $T_g$  of 153 °C on softwood kraft lignin with heating rate of 5 °C/min. Sjöholm and coworkers (2013) carried out a round robin of lignin thermal properties and obtained different  $T_g$ s from different laboratories. As for DSC, MTDSC showed a sequential increase in  $T_g$ s for IN-MS (118 °C), IN (143 °C) and IN-MI (202 °C), also seen in the PB and CS lignin series, and has also been reported on fractionated lignin (Lora and Glasser, 2002; Saito et al., 2014).

$T_g$  (or softening temperature,  $T_s$ ) of all the lignin samples was also determined by TMA due to its increased sensitivity and ease of use than DSC (Table 2.7 and Figure 2.3). Based on DSC analysis of  $E_a$  of lignin  $T_g$  it was comfortable to assume that  $T_s$  was  $T_g$  by TMA. The TMA derived  $T_g$ s were slightly higher by a few °C than those obtained by DSC and MTDSC. For example, IN has a  $T_g$  of 157, 143 and 147 °C as determined by TMA, MTDSC and DSC, respectively. The  $T_g$  value for IN was 13 °C lower than that obtained by Kubo (1996) for kraft

lignin by TMA. Again, the  $T_g$ s were shown to sequentially increase from the MS fraction to the original lignin then to the MI fraction.

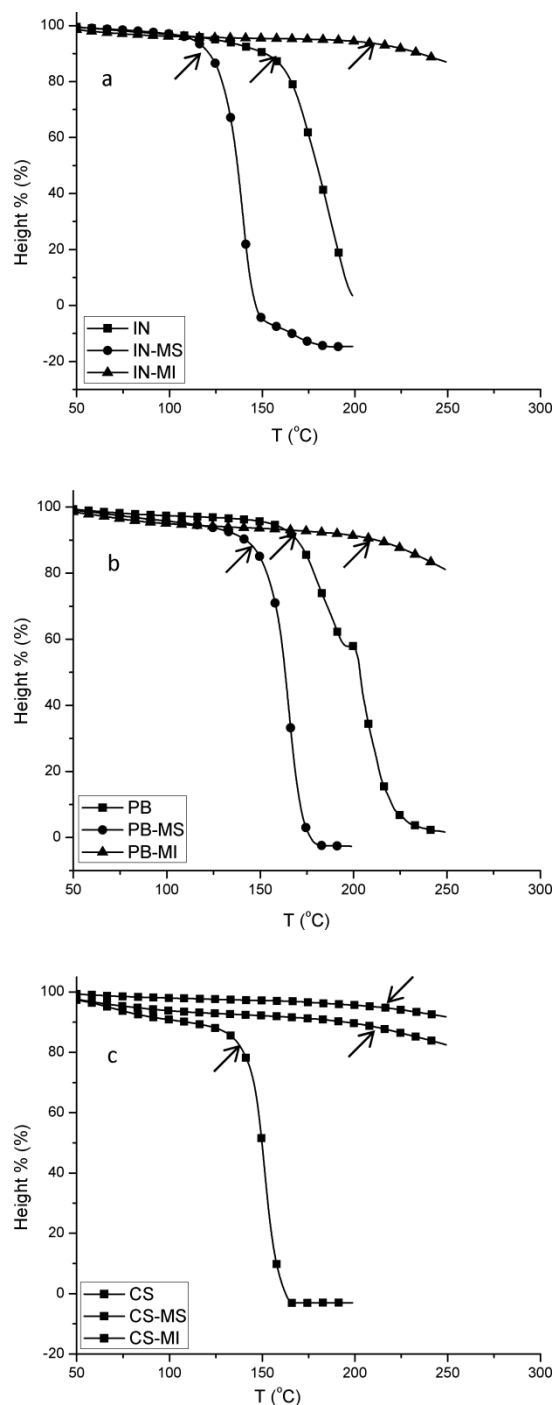


Figure 2.3 TMA thermograms of lignin samples: (a) IN, IN-MS, and IN-MI; (b) PB, PB-MS and PB-MI; and (c) CS, CS-MS and CS-MI. Note: arrows pointed to  $T_g$

Finally, lignin  $T_g$  was determined from the  $G''$  maxima by dynamic rheometry since it examines the deformation and flow of viscoelastic materials (Table 2.7 and Figure 2.4) (Rodriguez et al., 2003). Rheological data could be obtained but only from half of the lignin samples due to plate slippage. It was noticed that the IN-MS and PB-MS gave a lower  $G''$  peak maxima and temperature as compared to IN and PB (Figure 2.4).

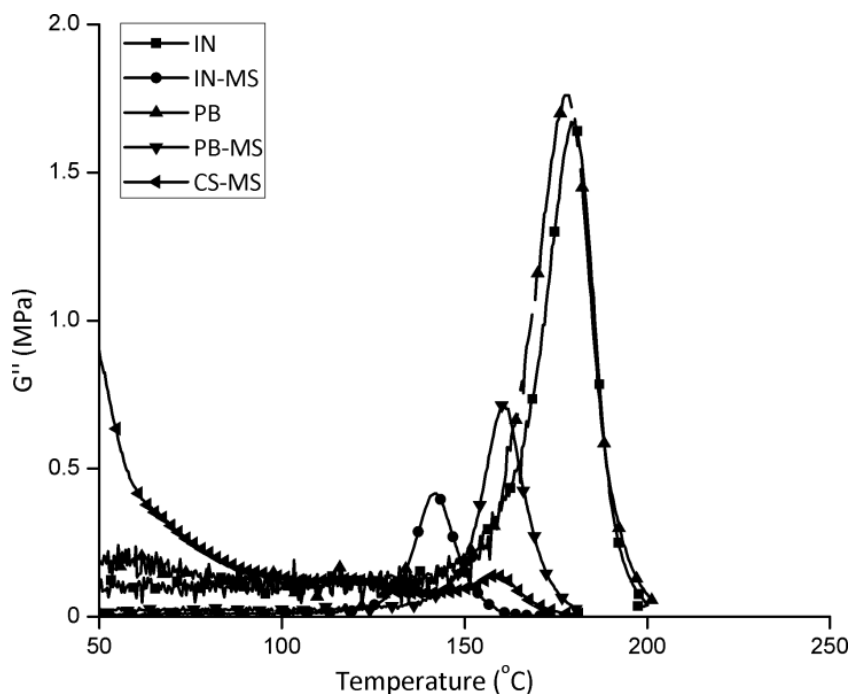


Figure 2.4 Dynamic rheological thermograms of various lignin samples.

Comparison of the different methods to determine  $T_g$  of lignin clearly showed that MTDSC and TMA were the only methods to obtain values for all samples. TMA values were a few  $^{\circ}\text{C}$  higher than those obtained by MTDSC which could be a result of the different detection techniques and different heating rates (e.g. thermal lag) (Uraki et al., 2012). Another possible explanation is that TMA in penetration mode likely measures  $T_s$  which is generally close to  $T_g$  for amorphous polymers (Bair et al., 2009). The large differences in  $T_g$  between rheology and DSC has also been observed (Fox and McDonald, 2010; Menard, 1999).

#### 2.4.2.2 Thermal Degradation

TGA was used to determine the thermal stability of the lignin samples (Figure 2.5). The thermograms show two stages of lignin decomposition based on the differential TGA (DTG)

plots. The first stage is centered about 275°C and second stage is centered about 350-410°C. Lignin degradation is in consistent with Stamm's results (1956). The onset temperature of degradation ( $T_{\text{onset}}$ ) for the 1<sup>st</sup> stage, temperature at the maximum rate of decomposition ( $T_{\text{Max}}$ ) for the 2<sup>nd</sup> stage, completion temperature for the 2<sup>nd</sup> stage ( $T_{\text{comp}}$ ), and mass remaining at 500°C for the various lignin samples are listed in Table 2.8.

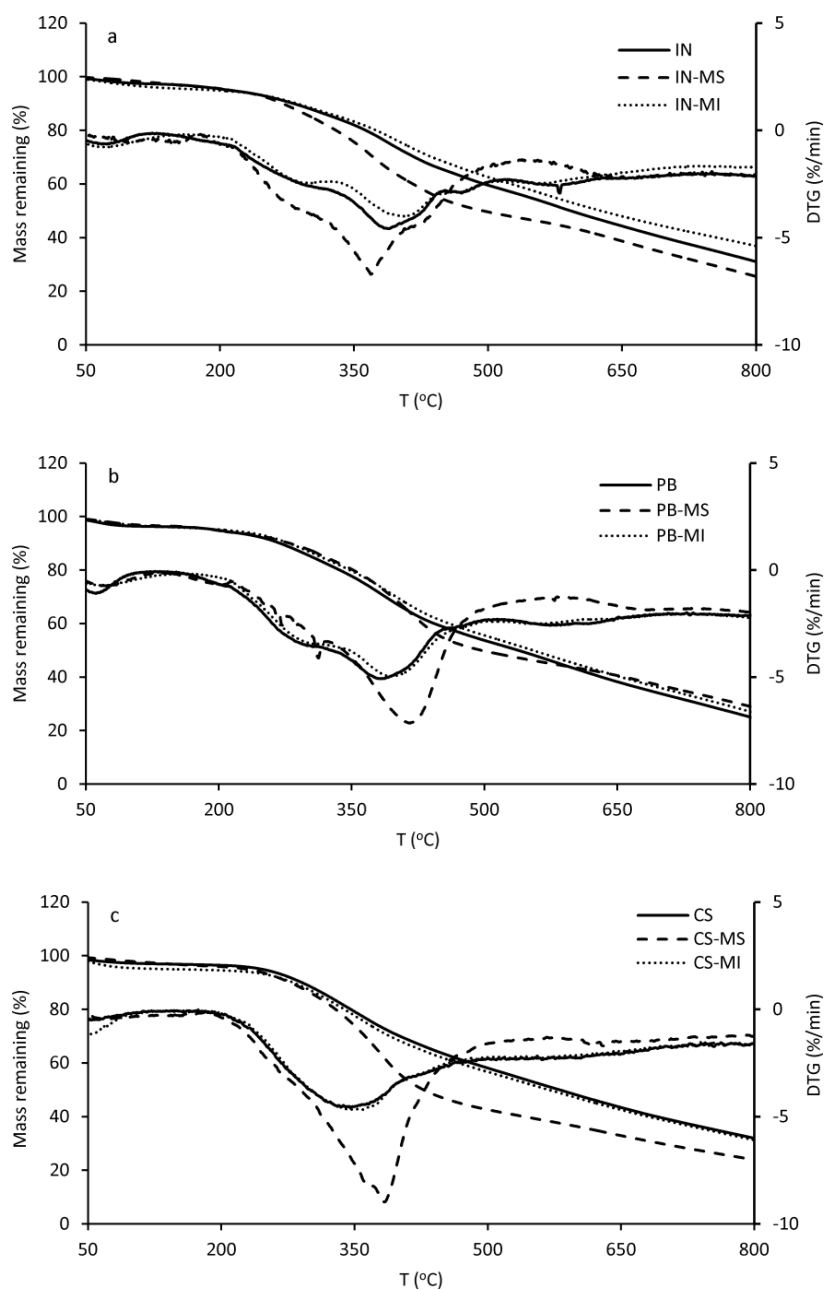


Figure 2.5 TGA thermograms of the various lignin samples: (a), IN, IN-MS and IN-MI; (b), PB, PB-MS and PB-MI; and (c), CS, CS-MS and CS-MI.

Table 2.8 Thermogravimetric analysis results of the various lignin samples

Lignin	T <sub>onset</sub> 1 <sup>st</sup> stage (°C)	T <sub>Max</sub> 2 <sup>nd</sup> stage (°C)	T <sub>comp</sub> 2 <sup>nd</sup> stage (°C)	Mass remaining @ 500°C (%)
IN	231	384	426	59.5
IN-MS	192	369	457	49.6
IN-MI	250	404	<sup>a</sup>	62.6
PB	202	380	430	53.7
PB-MS	175	415	452	49.7
PBMI	254	393	461	55.5
CS	265	331	<sup>a</sup>	58.1
CS-MS	244	383	412	42.6
CS-MI	259	343	<sup>a</sup>	56.7

<sup>a</sup> no obvious end to the second stage transition was found in IN-MI, CS, and CS-MI samples.

The onset of initial degradation is an important parameter for thermal material properties which can limit its application in plastics (Prime et al., 2009). The T<sub>onset</sub> was shown to sequentially increase from the MS fraction to the original lignin to the MI fraction. For example, the T<sub>onset</sub> of IN-MS, IN and IN-MI were respectively, 192, 231, and 250°C. The MI lignin samples were shown to have the highest thermal stability and most likely due to their high level of condensed structures.

The thermal decomposition activation energy (E<sub>a</sub>) for the IN lignin series were determined by TGA under conversion rates (α) of 40 to 80% using the following equations:

$$\ln \frac{\beta}{T^2} = \ln \frac{AR}{E} + 0.6075 - \frac{E}{RT} \quad (2.3) \text{ (Miura and Maki, 1998)}$$

$$\ln \beta = \ln A - \frac{E}{RT} \quad (2.4) \text{ (Karger-Kocsis et al., 2014)}$$

where β is heating rate (K/min), R is gas constant (8.314 J/K/mol), T is temperature (K), E is activation energy (J/mol), A is pre-exponential factor and the results are given in Table 2.9. Different E<sub>a</sub> values were obtained at different α values indicating that complex reactions occur during pyrolysis of lignin (Chrissafis et al., 2009). E<sub>a</sub>s of IN, IN-MS and IN-MI obtained

from Eq 3 for  $\alpha$  between 40 and 80% were 131-276, 171-235, and 137-161 kJ/mol, respectively. These results compare well with literature ( $E_a$  of 129-361kJ/mol for Alcell lignin and 80-158 kJ/mol for kraft lignin) over a similar temperature range (Ferdous et al., 2002).

Table 2.9 Thermal decomposition activation energies ( $E_a$ ) determined by TGA for IN, IN-MS and IN-MI samples.

$\alpha^a$ (%)	IN (kJ mol <sup>-1</sup> )		IN-MS (kJ mol <sup>-1</sup> )		IN-MI (kJ mol <sup>-1</sup> )	
	E(3) <sup>b</sup>	E(4) <sup>c</sup>	E(3)	E(4)	E(3)	E(4)
40	131	142	235	247	140	151
50	154	166	174	187	161	172
60	236	248	171	184	142	154
70	276	234	174	187	137	149
80	222	288	179	192	137	149
Average	204	216	187	199	143	155

<sup>a</sup> conversion rate

<sup>b</sup>  $E_a$  from Equation 2.3

<sup>c</sup>  $E_a$  from Equation 2.4

### 2.4.3 Correlations of lignin chemical structure and thermal properties

The high  $T_g$  of lignin is attributed to the rigid aromatic backbone of the macromolecules and abundant amount of hydrogen bonding by hydroxyl groups especially phenolic hydroxyl groups (Yoshida et al., 1987). Therefore, we examined relationships between lignin chemical properties ( $M_w$ , CI and aromatic/aliphatic OH ratio) and  $T_g$  (determined either by TMA and MTDSC).

A correlation ( $R^2=0.59$ ) between  $T_g$  and aromatic/aliphatic OH ratio was obtained for all the lignin samples (Figure 2.6a). Improved correlations were observed for lignin samples belonging to the same series (e.g. IN, PB and CS). A similar trend was observed by Osman in lignin from hot-pressed poplar (Osman, 2010). An increase of high aromatic/aliphatic OH implies that more  $\beta$ -O-4 ether linkages were cleaved exposing more end groups,



consequently of lower  $M_w$  and a lower  $T_g$  (Nielsen, 1974). From a limited data set of 3 samples (IN-MS, PB-MS and CS-MS) a relationship was also observed between lignin  $M_w$  and  $T_g$  (Figure 2.6b) and attributable to the decrease of polymer free volume. Osman also observed this relationship in lignin from hot-pressed poplar (Osman, 2010).

For a particular lignin series (e.g. PB, PB-MS and PB-MI) a good correlation ( $R^2=0.96$ ) between  $T_g$  (determined by TMA) and CI, was observed (Figure 2.6c). For the different lignin series, their plots were shown to have similar slopes, but were offset slightly. This phenomenon (level of lignin condensed structures) was observed by Baumberger et al. in lignin isolated from genetically manipulated poplars (Baumberger et al., 2002) and by Osman (2010) in in-situ lignin from hot-pressed poplar. A high lignin CI would hinder molecular segmental movement due to increased C-C cross-links which would result in a high  $T_g$ .

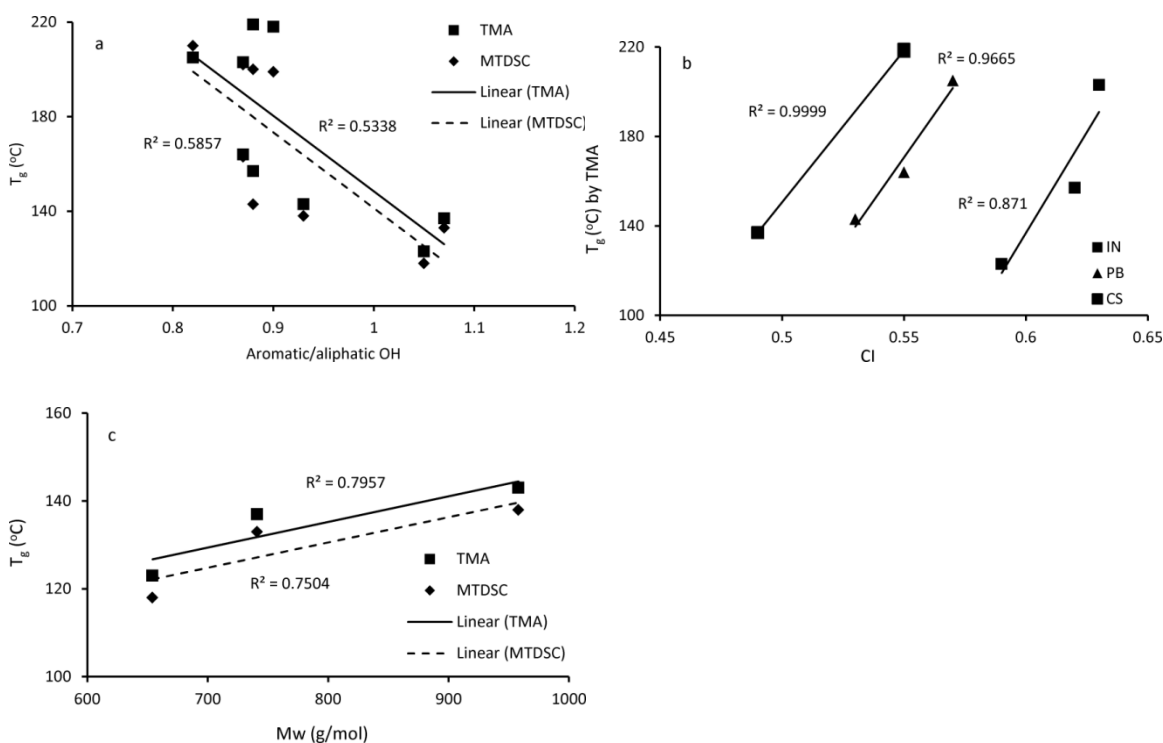


Figure 2.6 Correlations between lignin  $T_g$  (by MTDSC and TMA) with (a), aromatic/aliphatic OH; (b), condensation index (CI); and (c),  $M_w$

## 2.5 Conclusions

Industrial lignin was successively fractionated to methanol soluble and insoluble fractions. The MS lignin fractions were shown to contain fewer condensed structures, lower aromatic/aliphatic OH ratio, higher  $\beta$ -O-4 linkages, lower  $M_w$  and  $T_g$ , and lower thermal degradation properties than the original lignin and MI lignin fractions. TMA and MTDSC were established to be sensitive and reliable techniques to determine lignin  $T_g$ s, even on difficult samples such as corn-stover lignin. Correlations between lignin chemistry and thermal properties ( $T_g$ ) were observed. This strategy for lignin selection based on source and fractionation offers a practical option for obtaining lignin starting or building block materials with different properties (e.g.  $T_g$ ) for incorporation into copolymers.

## 2.6 References

Aracri, E., Díaz Blanco, C., Tzanov, T. **2014**. An enzymatic approach to develop a lignin-based adhesive for wool floor coverings. *Green Chemistry*, 2597-2603.

Argyropoulos, D.S., Sadeghifar, H., Cui, C., Sen, S. **2014**. Synthesis and characterization of poly(arylene ether sulfone) Kraft lignin heat stable copolymers. *ACS Sustainable Chemistry & Engineering*, 2, 264-271.

Arshanitsa, A., Ponomarenko, J., Dizhbite, T., Andersone, A., Gosselink, R.J.A., van der Putten, J., Lauberts, M., Telysheva, G. **2013**. Fractionation of technical lignins as a tool for improvement of their antioxidant properties. *Journal of Analytical and Applied Pyrolysis*, 103, 78-85.

ASTMD1106-96 **2013**. Standard Test Method for Acid-Insoluble Lignin in Wood, ASTM International Vol. 04.10 Wood

Bair, H.E., Akinay, A.E., Menczel, J.D., Prime, B.R., Jaffe, M. **2009**. Thermomechanical Analysis (TMA) and Thermogravimetry (TD), in: Menczel, J.D., Prime, B.R. (Eds.), *Thermal Analysis of Polymers, Fundamentals and Applications*. John Wiley, New Jersey, pp. 319-385.

Baumberger, S., Dole, P., Lapierre, C. **2002**. Using transgenic poplars to elucidate the relationship between the structure and the thermal properties of lignins. *Journal of Agricultural and Food Chemistry*, 50, 2450-2453.

Brodin, I., Sjöholm, E., Gellerstedt, G. **2009**. Kraft lignin as feedstock for chemical products: The effects of membrane filtration. *Holzforschung*, 63, 290-297.

Brodin, I., Sjöholm, E., Gellerstedt, G. **2010**. The behavior of kraft lignin during thermal treatment. *Journal of Analytical and Applied Pyrolysis*, 87, 70-77.

Chrissafis, K., Paraskevopoulos, K.M., Pavlidou, E., Bikiaris, D. **2009**. Thermal degradation mechanism of HDPE nanocomposites containing fumed silica nanoparticles. *Thermochimica Acta*, 485, 65-71.

Chung, H., Washburn, N.R. **2013**. Chemistry of lignin-based materials. *Green Materials*, 1, 137-160.

Cui, C., Sadeghifar, H., Sen, S., Argyropoulos, D.S. **2013**. Toward thermoplastic lignin polymers; part II: Thermal & polymer characteristics of Kraft lignin & derivatives. *BioResources*, 8, 864-886.

Dimmel, D. **2010**. Overview, in: Heitner, C., Dimmel, D. (Eds.), *Lignin and lignans: Advances in chemistry*. CRC press, Boca Raton, FL, pp. 1-10.

Faix, O. **1991a**. Classification of lignins from different botanical origins by FT-IR spectroscopy. *Holzforschung*, 45, 21-27.

Faix, O. **1991b**. Condensation Indexes of Lignins Determined by Ftir-Spectroscopy. *Holz Als Roh-Und Werkstoff*, 49, 356-356.

Faix, O., Argyropoulos, D.S., Robert, D., Neirinck, V. **1994**. Determination of Hydroxyl-Groups in Lignins Evaluation of H-1-Nmr, C-13-Nmr, P-31-Nmr, Ftir and Wet Chemical Methods. *Holzforschung*, 48, 387-394.

- Fox, C.S., McDonald, A.G. **2005**. The esterification of different industrial lignins to form lignin bioplastics, Materials and processing technologies for revolutionary applications Fall Technical Conference (37th ISTC), Seattle, WA, pp. 74-81.
- Fox, C.S., McDonald, A.G. **2010**. Chemical and thermal characterization of three industrial lignins and their corresponding lignin esters. *BioResources*, 5, 990-1009.
- Ferdous, D., Dalai, A.K., Bej, S.K., Thring, R.W. **2002**. Pyrolysis of lignins: Experimental and kinetics studies. *Energy & Fuels*, 16, 1405-1412.
- Fox, C.S., McDonald, A.G. **2010**. Chemical and thermal characterization of three industrial lignins and their corresponding lignin esters. *BioResources*, 5, 990-1009.
- Gandini, A., Belgacem, M.N. **2008**. Lignins as Components of Macromolecular Materials. Monomers, polymers and composites from renewable resources, 243-271.
- Glasser, W.G., Jain, R.K. **1993**. Lignin Derivatives .1. Alkanoates. *Holzforschung*, 47, 225-233.
- Gosselink, R.J.A., de Jong, E., Guran, B., Abächerli, A. **2004**. Co-ordination network for lignin—standardisation, production and applications adapted to market requirements (EUROLIGNIN). *Industrial Crops and Products*, 20, 121-129.
- Guigo, N., Mija, A., Vincent, L., Sbirrazzuoli, N. **2009**. Molecular mobility and relaxation process of isolated lignin studied by multifrequency calorimetric experiments. *Physical Chemistry Chemical Physics*, 11, 1227-1236.
- Hatakeyama, H., Tsujimoto, Y., Zarubin, M.J., Krutov, S.M., Hatakeyama, T. **2010**. Thermal decomposition and glass transition of industrial hydrolysis lignin. *Journal of Thermal Analysis and Calorimetry*, 101, 289-295.
- Hatakeyama, T., Hatakeyama, H. **1995**. Effect of chemical structure of amorphous polymers on heat capacity difference at glass transition temperature. *Thermochimica Acta*, 267, 249-257.

- Karger-Kocsis, J., Grishchuk, S., Soroachynska, L., Rong, M.Z. **2014**. Curing, Gelling, Thermomechanical, and Thermal Decomposition Behaviors of Anhydride-Cured Epoxy (DGEBA)/Epoxidized Soybean Oil Compositions. *Polymer Engineering and Science*, 54, 747-755.
- Kovacs, A.J. **1958**. La Contraction Isotherme Du Volume Des Polymeres Amorphes. *Journal of Polymer Science*, 30, 131-147.
- Kubo, S., Uraki, Y., Sano, Y. **1996**. Thermomechanical analysis of isolated lignins. *Holzforschung*, 50, 144-150.
- Laborie, M.P.G., Salmen, L., Frazier, C.E. **2004**. Cooperativity analysis of the in situ lignin glass transition. *Holzforschung*, 58, 129-133.
- Lewis, N.G., Lantzy, T.R. **1989**. Lignin in adhesive introduction and historical perspective, in: Hemingway, R.W., Conner, A.H., Branham, S.J. (Eds.), *Adhesive from renewable resources*. ACS Symposium Series, New Orleans, pp. 13-26.
- Li, M., Foster, C., Kelkar, S., Pu, Y., Holmes, D., Ragauskas, A., Saffron, C.M., Hodge, D.B. **2012**. Structural characterization of alkaline hydrogen peroxide pretreated grasses exhibiting diverse lignin phenotypes. *Biotechnology for Biofuels*, 5, 38.
- Li, Y., Mlynar, J., Sarkanen, S. **1997**. The First 85% Kraft Lignin-Based Thermoplastics. *Journal of polymer science Part B: Polymer physics*, 35, 1899-1910.
- Li, Y., Sarkanen, S. **2000**. Thermoplastics with very high lignin contents, in: Glasser, W.G., Northey, R.A., Schultz, T.P. (Eds.), *Lignin: Historical, Biological, and Materials Perspectives*. American Chemistry Society, Washington D.C., pp. 351-366.
- Lora, J. **2008**. Industrial commercial lignins: sources, properties and applications, *Monomers, polymers and composites from renewable resources*. Elsevier, Amsterdam; Boston, pp. 225-241.

Lora, J.H., Glasser, W.G. **2002**. Recent Industrial Applications of Lignin: A Sustainable Alternative to Nonrenewable Materials. *Journal of Polymers and the Environment*, 10, 39-48.

Lu, F., Ralph, J. **1998**. The DFRC method for lignin analysis. 2. Monoers from isolated lignins. *Journal of Agricultural and Food Chemistry*, 46, 547-552.

Lu, F., Ralph, J. **1997**. DFRC method for lignin analysis 1 New method for beta-aryl ether cleavage--lignin model studies. *Journal of Agricultural and Food Chemistry*, 45, 4655-4660.

Martone, P.T., Estevez, J.M., Lu, F.C., Ruel, K., Denny, M.W., Somerville, C., Ralph, J. **2009**. Discovery of Lignin in Seaweed Reveals Convergent Evolution of Cell-Wall Architecture. *Current Biology*, 19, 169-175.

McDonald, A.G., Ma, L. **2012**. Plastic moldable lignin, in: Paterson, R.J. (Ed.), *Lignin: Properties and applications in biotechnology and bioenergy*. Nova Science Publisher, Inc., pp. 489-498.

Meier, D., Faix, O. **1992**. Pyrolysis-Gas Chromatography-Mass Spectrometry, in: Lin, S.Y., Dence, C.W. (Eds.), *Methods in Lignin Chemistry*. Springer-Verlag, Berlin, pp. 177-199.

Menard, K.P. **1999**. *Dynamic mechanical analysis: A practical introduction*. CRC Press, Boca Raton, FL.

Miller, S.A. **2013**. *Sustainable Polymers: Opportunities for the Next Decade*. ACS Macro Letters, 2, 550-554.

Miura, K., Maki, T. **1998**. A simple method for estimating  $f(E)$  and  $k(0)(E)$  in the distributed activation energy model. *Energy & Fuels*, 12, 864-869.

Morck, R., Yoshida, H., Kringstad, K.P. **1986**. Fractionation of Kraft lignin by successive extraction with organic solvents. *Holzforschung*, 40, 51-60.

Moynihan, C.T., Easteal, A.J., Wilder, J., Tucker, J. **1974**. Dependence of Glass-Transition Temperature on Heating and Cooling Rate. *Journal of Physical Chemistry*, 78, 2673-2677.

Nielsen, L.E. **1974**. Mechanical properties of polymers and composites. Marcel Dekker Inc., New York, p. 23.

Nonier, M.F., Vivas, N., de Gaulejac, N., Absalon, C., Soulie, P., Fouquet, E. **2006**. Pyrolysis-gas chromatography/mass spectrometry of Quercus sp wood application to structural elucidation of macromolecules and aromatic profiles of different species. *Journal of Analytical and Applied Pyrolysis*, 75, 181-193.

Nunes, C.A., Lima, C.F., Barbosa, L.C., Colodette, J.L., Gouveia, A.F., Silverio, F.O. **2010**. Determination of Eucalyptus spp lignin S/G ratio: a comparison between methods. *Bioresour Technol*, 101, 4056-4061.

Osman, N.B. **2010**. Ph.D. dissertation: Chemistry of hot-pressing hybrid poplar wood, Natural Resources. University of Idaho, Moscow.

Osman, N.B., McDonald, A.G., Laborie, M.P.G. **2012**. Analysis of DCM extractable components from hot-pressed hybrid poplar. *Holzforschung*, 66, 927-934.

Pearl, I.A. **1967**. The chemistry of lignin. Marcel Dekker, INC., New York, pp. 1-6.

Pohjanlehto, H., Setälä, H.M., Kiely, D.E., McDonald, A.G. **2014**. Lignin-Xylaric Acid-Polyurethane-Based Polymer Network Systems: Preparation and Characterization. *Journal of Applied Polymer Science*, 131, 39714-39720.

Ponomarenko, J., Dizhbite, T., Lauberts, M., Viksna, A., Dobeles, G., Bikovens, O., Telysheva, G. **2014**. Characterization of softwood and hardwood LignoBoost kraft lignins with emphasis on their antioxidant activity. *BioResources*, 9, 2051-2068.

Poursorkhabi, V., Misra, M., Mohanty, A.K. **2013**. Extraction of lignin from a coproduct of the cellulosic ethanol industry and its thermal characterization *BioResources*, 8, 5083-5101.

Prime, B.R., Bair, H.E., Vyazovkin, S., Gallagher, P.K., Riga, A. **2009**. Thermogravimetric analysis (TGA), in: Menczel, J.D., Prime, B.R. (Eds.), *Thermal Analysis of Polymers, Fundamentals and Applications*. John Wiley, New Jersey, pp. 241-317.

Rials, T.G., Glasser, W.G. **1984**. Engineering plastics from lignin X. Enthalpy relaxation of prepolymers. *Journal of Wood Chemistry and Technology*, 4, 331-345.

Rodriguez, F., Cohen, C., Christopher, O., Archer, L.A. **2003**. *Principles of polymer systems* CRC press, New York.

Sahoo, S., Seydibeyoğlu, M.Ö., Mohanty, A.K., Misra, M. **2011**. Characterization of industrial lignins for their utilization in future value added applications. *Biomass and Bioenergy*, 35, 4230-4237.

Saito, T., Brown, R.H., Hunt, M.A., Pickel, D.L., Pickel, J.M., Messman, J.M., Baker, F.S., Keller, M., Naskar, A.K. **2012**. Turning renewable resources into value-added polymer: development of lignin-based thermoplastic. *Green Chemistry*, 14, 3295-3303.

Saito, T., Perkins, J.H., Jackson, D.C., Trammel, N.E., Hunt, M.A., Naskar, A.K. **2013**. Development of lignin-based polyurethane thermoplastics. *RSC Advances*, 3, 21832-21840.

Saito, T., Perkins, J.H., Vautard, F., Meyer, H.M., Messman, J.M., Tolnai, B., Naskar, A.K. **2014**. Methanol Fractionation of Softwood Kraft Lignin: Impact on the Lignin Properties. *ChemSusChem*, 7, 221-228.

Schuerch, C. **1952**. The solvent properties of liquids and their relation to the solubility, swelling, isolation, and fractionation of lignin. *Journal of American Chemical Society*, 74, 5061-5067.

Sivasankarapillai, G., McDonald, A.G. **2011**. Synthesis and properties of lignin-highly branched poly (ester-amine) polymeric systems. *Biomass and Bioenergy*, 35, 919-931.



Sivasankarapillai, G., McDonald, A.G., Li, H. **2012**. Lignin valorization by forming toughened lignin-co-polymers: Development of hyperbranched prepolymers for cross-linking. *Biomass and Bioenergy*, 47, 99-108.

Sjoholm, E., Aldaeus, F., Nordstrom, Y., Reimann, A. **2013**. Cost Action FP0901: Round robins of lignin samples Part 2: Thermal analysis

Song, K.L., Yin, Y.F., Salmen, L., Xiao, F.M., Jiang, X.M. **2014**. Changes in the properties of wood cell walls during the transformation from sapwood to heartwood. *Journal of Materials Science*, 49, 1734-1742.

Stamm, A.J. **1956**. Thermal degradation of wood and cellulose. *Industrial & Engineering Chemistry*, 48, 413-417. Schorr, D., Diouf, P.N., Stevanovic, T. **2014**. Evaluation of industrial lignins for biocomposites production. *Industrial Crops and Products*, 52, 65-73.

Tappi UM250 **1991**. Acid-soluble lignin in wood and pulp.

Tejado, A., Pena, C., Labidi, J., Echeverria, J.M., Mondragon, I. **2007**. Physico-chemical characterization of lignins from different sources for use in phenol-formaldehyde resin synthesis. *Bioresource Technology*, 98, 1655-1663.

Tohmura, S.-i., Argyropoulos, D.S. **2001**. Determination of Arylglycerol- $\beta$ -aryl Ethers and Other Linkages in Lignins Using DFRC/ $^{31}\text{P}$  NMR *Journal of Agricultural and Food Chemistry*, 49, 536-542.

Uraki, Y., Sugiyama, Y., Koda, K., Kubo, S., Kishimoto, T., Kadla, J.F. **2012**. Thermal Mobility of  $\beta$ -O-4-Type Artificial Lignin. *Biomacromolecules*, 13, 867-872.

Wang, J., John Manley, R.S., D., F. **1992**. Synthetic polymer-lignin copolymers and blends. *Progress in Polymer Science*, 17, 611-646.

Wei, L.Q., McDonald, A.G., Freitag, C., Morrell, J.J. **2013**. Effects of wood fiber esterification on properties, weatherability and biodurability of wood plastic composites. *Polymer Degradation and Stability*, 98, 1348-1361.

Yoshida, H., Morck, R., Kringstad, K.P. **1987**. Fractionation of Kraft lignin by successive extraction with organic solvents. *Holzforschung*, 41, 171-176.

Yuan, T.-Q., He, J., Xu, F., Sun, R.-C. **2009**. Fractionation and physico-chemical analysis of degraded lignins from the black liquor of *Eucalyptus pellita* KP-AQ pulping. *Polymer Degradation and Stability*, 94, 1142-1150.

Zakzeski, J., Bruijninx, P.C.A., Jongerius, A.L., Weckhuysen, B.M. **2010**. The Catalytic Valorization of Lignin for the Production of Renewable Chemicals. *Chemical Reviews*, 110, 3552-3599.

### 3 Lignin Valorization by Forming Toughened Thermally-stimulated Shape Memory Copolymeric Elastomers: Evaluation of Different Industrial Lignins

#### 3.1 Abstract

Lignin-based thermal responsive dual shape memory copolymeric elastomers were prepared with a hyper branched prepolymer (HBP, A<sub>2</sub>B<sub>3</sub> type) via a simple one-pot bulk polycondensation reaction. The effect of fractionated lignin type on copolymer properties was investigated. The thermal and mechanical properties of the copolymers were characterized by DMA, DSC, and TGA. Tensile properties were dominated by HBP <45% lignin content while lignin dominated >45% content. The copolymers glass transition temperature (T<sub>g</sub>) increased with lignin content and lignin type did not play a significant role. Thermally-stimulated dual shape memory effects (SME) of the copolymers were quantified by cyclic thermomechanical tests. All copolymers had shape fixity rate >95% and >90% shape recovery for all compositions. The copolymer shape memory transition temperature (T<sub>trans</sub>) increased with lignin content and T<sub>trans</sub> was 20 °C higher than T<sub>g</sub>. Lignin, a renewable resource, can be used as a netpoint segment in polymer systems with SME behavior.

#### 3.2 Introduction

Petroleum-based polymers are important materials and used extensively in modern society. The United States alone produced  $4.7 \times 10^{10}$  kg of all polymers during 2010 (Chung and Washburn, 2013). However, these are derived from non-renewable resources and have a large carbon foot print (Teramoto, 2011). Alternatively, the utilization of bio-resources to produce sustainable bio-based materials can overcome the finite petroleum resource and offset CO<sub>2</sub> emissions. Currently, considerable efforts have been made in the development of commercial biopolymers fabricated from refined natural resources (e.g. glucose) including poly(lactic acid)(Drumright et al., 2000; Kawashima, 2003; Kawashima et al., 2005; Proikakis et al., 2002), cellulose derivatives (Beheshti et al., 2006; El Idrissi et al., 2013). polyhydroxyalkanoate (poly(hydroxybutyrate), poly(2-hydroxybutyrate-co-hydroxyvalerate)) (Hu et al., 2013; Wei et al., 2014), thermoplastic starch (Boonprasith et al., 2013; Pang et al.,

2013) and vegetable-oil-based polymers (Miao et al., 2012; Quirino et al., 2014; Valverde et al., 2011). However, there is potential to produce biopolymers from industrial byproduct streams, such as lignin from cellulosic ethanol or pulping operations.

Lignin is an underdeveloped feedstock for producing polymers. Lignin is distributed widely throughout the plant kingdom and its abundance is behind that of cellulose and hemicellulose (15-30% by weight) (Lewis and Lantzy, 1989; Perlack et al., 2005). However, lignin is historically treated as byproduct of pulp and paper industry which produced substantial amounts of industrial lignin, for example,  $4.5 \times 10^{10}$  kg in 2004 (Zakzeski et al., 2010). Merely 2% of industrial lignin is commercialized into low-value products such as dispersing or binding agents with remainder burned as compensating fuel (Gosselink et al., 2004). Possible reasons for its low utilization is its brittleness and high glass transition temperature ( $T_g$ ) due to lignin's rigid aromatic backbone and inter/intra-molecular H-bonding structures (Li et al., 1997). Furthermore, the chemical structural variations due to species and extraction techniques can result in large heterogeneity within lignin. Therefore, modification of lignin mainly focused on reducing the H-bonding by substitution resulting in lowering the  $T_g$  and improving its toughness and flexibility. Chemical modification approaches employed to alleviate the situation are alkylation (similar to polystyrene in terms of tensile properties) (Li and Sarkanen, 2002), benzylation (tunable  $T_g$  as degree of substitution varied from 183 °C to 60 °C) (McDonald and Ma, 2012), oxypropylation (obtained polyols with decreased  $T_g$  and decreased  $T_g$  and polyols for polyurethane fabrications) (Cui et al., 2013; Li and Ragauskas, 2012; Sadeghifar et al., 2012; Wu and Glasser, 1984), and esterification (Fox and McDonald, 2010; Glasser and Jain, 1993). Esterification is probably the most feasible pathway to carry out in terms of the reaction parameters and reactants. Other lignin based polymers products incorporate polyester, epoxy resins, xylic acid-polyurethane and elastomeric materials (Pohjanlehto et al., 2014; Sailaja and Deepthi, 2010; Saito et al., 2012; Sivasankarapillai and McDonald, 2011; Sivasankarapillai et al., 2012). A comprehensive review on lignin chemical modification could be found in a recent report by Laurichesse and Averous (Laurichesse and Avérous, 2013). Furthermore, lignin based

thermoresponsive materials were obtained which transitioned from hydrophilic to hydrophobic nature above 32 °C in aqueous solution (Kim and Kadla, 2010).

Polymers that have the ability to memorize different shapes and can be recovered in a predefined way upon exertion of suitable stimulus such as heat, magnetism, electricity, moisture, or light, are designated as shape memory polymers (SMPs) (Behl and Lendlein, 2007; Behl and Lendlein, 2010; Beloshenko et al., 2005; Lendlein and Kelch, 2002; Lendlein and Langer, 2002; Liu et al., 2007; Xie, 2010, 2011; Yakacki, 2013). Temperature caused shape change is named thermally stimulated shape memory effect (Ts-SME) (Lendlein and Kelch, 2002). Since SMPs were first introduced in 1984 in Japan (Dietsch and Tong, 2007), they have attracted increasing attention both in academic and industrial fields and been used in smart fabrics, heat shrinkable tubes for electronics, films for packaging, self-deployable sun sails in spacecraft, self-disassembling mobile phones, intelligent medical devices, and implants for minimally invasive surgery (Behl and Lendlein, 2007). In principle, a SMP is first heated to a deformation temperature ( $T_d$ ), which leads to the material softening (storage modulus ( $E'$ ) drop). A deformation force is subsequently applied (i.e. loading, strain controlled or stress controlled (Wagermaier et al., 2010)). The SMP is then cooled down to lower temperature still under load. The deformed shape is then fixed before removal of load. The programming is the procedure of the shape fixing. When the deformed SMP under temporary shape is re-heated to a higher temperature without stress exertion, the permanent shape is recovered. Typically both deformation temperature and so-called recovery temperature are above the reversible thermal transition temperature ( $T_g$  or melting point  $T_m$ ) of the SMP, which is thus called shape memory transition ( $T_{trans}$ ) (Xie, 2011). Ts-SME could not be simply obtained via single polymers, but a combination of polymer structures or polymer morphologies with in turn distinct  $T_g$ s, where two segments are responsible for the Ts-SME, netpoints segment (controlling permanent shape, sometimes also called hard segment) and switching segment (controlling temporary shape, also called soft segment). Liu, et al. (2007) comprehensively reviewed four classes of SMPs based on molecular architectures, that is, chemically cross-linked glassy thermosets; chemically cross-

linked semi-crystalline rubbers; physically cross-linked thermoplastics; and physically cross-linked block copolymers.

This current investigation belongs to the chemically cross-linked glassy thermoset mechanism, where  $T_{\text{trans}}$  is controlled by  $T_g$ . Our previous research developed protocols for the synthesis and characterization of lignin based elastomeric copolymers with HBP (Sivasankarapillai and McDonald, 2011; Sivasankarapillai et al., 2012). Lignin was the rigid “netpoint” segment with high  $T_g$  while the HBP was the soft highly flexible segment with appreciably low  $T_g$ . Therefore, we hypothesize that the copolymer of lignin and HBP would possess  $T_g$ -SME. Based on the hypothesis, copolymers from lignin and HBP were synthesized and investigated with respects to determining their SME properties. Furthermore, different industrial lignins and content were evaluated in order to tailor their thermal, mechanical, and SME properties.

### **3.3 Materials and methods**

#### **3.3.1 Materials**

Indulin AT softwood kraft lignin (MeadWestvaco), Protobind 1000 soda lignin (ALM India Pvt. Ltd.), and corn stover lignin (CS, National Renewable Energy Laboratory) were used. CS lignin was washed with hot water and freeze dried. Each lignin (250 g) type was fractionated by stirring in methanol (1500 mL) for 5 h at 50 °C and the methanol soluble fraction was filtered, concentrated to dryness and yields recorded (Li and McDonald, 2014). The methanol soluble lignin yields for protobind, indulin and corn stover were 50%, 45% and 12%, respectively. These methanol soluble lignins (respectively coded PB, IN and CS) were used for copolymer synthesis. 1,1,1-triethanolamine (TEA, B<sub>3</sub>), adipic acid (AA, A<sub>2</sub>), methanol and tetrahydrofuran (THF) were obtained from Acros Organics and used as received.

### 3.3.2 Methods

#### 3.3.2.1 Synthesis of HB prepoly(ester-amine) (E1)

The synthetic method was described in our previous publication (Sivasankarapillai and McDonald, 2011). The mixture of TEA (0.04 mol) and AA (0.08 mol) with mole ratio 1:2 was prepared in a beaker (50 mm dia), then the beaker was placed in a preheated vacuum oven. The polycondensation reaction was controlled to below 650 mm Hg at 100 °C. The reaction was monitored every 2 h to check the reaction viscosity and solubility in methanol.

Yield: 94%; IR (ATR,  $\text{cm}^{-1}$ ):  $\nu = 3500\text{-}3200$  (vb;  $\nu(\text{OH stretching})$ ), 2945 (s;  $\nu_{\text{as}}(\text{CH}_2)$ ), 2870 (s;  $\nu_{\text{s}}(\text{CH}_2)$ ), 2500 (vb; (OH of COOH)), 1723 (vs; (C=O from ester)), 1558 (m; (COO<sup>-</sup>)), 1455 (w, (CH<sub>2</sub>)), 1391 (w; (OH)), 1169 and 1140  $\text{cm}^{-1}$  (vs; (COO in ester)); <sup>1</sup>H NMR (500 MHz, DMSO-*d*<sub>6</sub>,  $\delta$ ): 4.00-4.06 (m, N-CH<sub>2</sub>-CH<sub>2</sub>-O), 3.39-3.46 (m, N-CH<sub>2</sub>-CH<sub>2</sub>-OH), 2.72-2.79 (m, N-CH<sub>2</sub>-CH<sub>2</sub>-O), 2.56-2.63 (m, N-CH<sub>2</sub>-CH<sub>2</sub>-OH), 2.50 (p, DMSO-*d*<sub>6</sub>), 2.25-2.31 (m, -OOC-CH<sub>2</sub>-CH<sub>2</sub>-), 2.17-2.23 (m, HOOC-CH<sub>2</sub>-CH<sub>2</sub>-), 1.45-1.57 (m, -OOC-CH<sub>2</sub>-CH<sub>2</sub>-CH<sub>2</sub>-CH<sub>2</sub>-COO-); <sup>13</sup>C NMR (125.76 MHz, DMSO-*d*<sub>6</sub>,  $\delta$ ): 174.24 and 174.19 (COOH), 172.61 (COO<sup>-</sup>), 62.16 and 62.11 (N-CH<sub>2</sub>-CH<sub>2</sub>-O), 59.37, 59.29 and 58.91 (N-CH<sub>2</sub>-CH<sub>2</sub>-OH), 57.00, 56.96, and 56.72 (N-CH<sub>2</sub>-CH<sub>2</sub>-OH), 53.02, 52.87 and 52.64 (N-CH<sub>2</sub>-CH<sub>2</sub>-O), 33.36 and 33.27 (HOOC-CH<sub>2</sub>-CH<sub>2</sub>-), 33.18 and 33.09 (-OOC-CH<sub>2</sub>-CH<sub>2</sub>-), 24.00, 23.90, 23.80 (-OOC-CH<sub>2</sub>-CH<sub>2</sub>-CH<sub>2</sub>-COO-).

#### 3.3.2.2 Synthesis of lignin-copoly(ester-amine)

Lignin samples (IN, PB, and CS) were dispersed in the minimum amount of THF and mixed with HBP E1 proportionally to synthesize lignin-copoly(ester-amine). THF was then removed under a stream of N<sub>2</sub> at 80 °C. The highly viscous mixture was then transferred to a prepared aluminum pan (15 x 15 cm<sup>2</sup>) and was placed into vacuum oven at 80 °C and 750 mm Hg to remove residual solvent and moisture (about 30 min). Then the reaction temperature was increased to 120 °C at 650 mm Hg, and the reaction proceeded for 20hrs. The final lignin-copoly(ester-amine) displayed a highly bright and glossy surface and was insoluble in common organic solvents. Copolymers were prepared from the three lignin types at varying lignin contents. The synthesis approach is shown in Figure 3.1.

IR (ATR,  $\text{cm}^{-1}$ ):  $\nu = 3500\text{-}3200$  (vb;  $\nu(\text{OH stretching})$ ),  $2945$  (s;  $\nu_{\text{as}}(\text{CH}_2)$ ),  $2870$  (s;  $\nu_{\text{s}}(\text{CH}_2)$ ),  $1726$  (vs;  $(\text{C}=\text{O}$  from ester)),  $1600$  (m; aromatic skeletal vibration),  $1512$  (m; aromatic skeletal vibration),  $1455$  (w,  $(\text{CH}_2)$ ),  $1419$  (w, CH in-plane deformation),  $1378$  (w,  $\text{CH}_3$ ),  $1169$  and  $1140$   $\text{cm}^{-1}$  (vs;  $(\text{COO}$  in ester)).

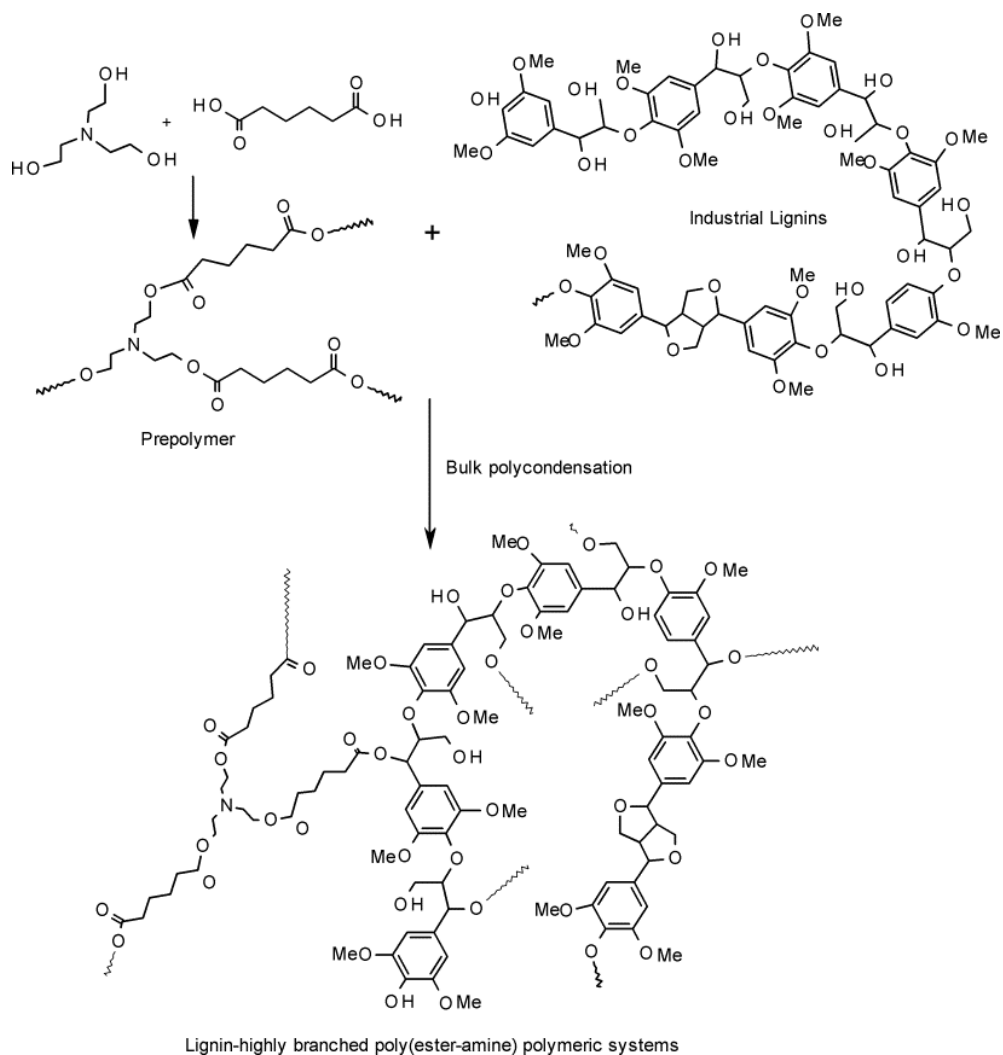


Figure 3.1 Synthetic route for lignin-copoly(ester-amine) elastomer

### 3.3.3 Characterization techniques

#### 3.3.3.1 FTIR and NMR

All Fourier transform infrared (FTIR) spectra were carried out with a ThermoNicolet Avatar 370 spectrometer operating in the attenuated total reflection (ATR) mode (Smart



performance, ZnSe crystal).  $^1\text{H}$  and  $^{13}\text{C}$  nuclear magnetic resonance (NMR) spectra were obtained on prepolymer and acetylated lignin (Capanema et al., 2004) samples on a Bruker Avance 500 spectrometer. Chemical shifts were referenced to DMSO-d<sub>6</sub> at 39.5 for  $^{13}\text{C}$  and 2.50 for  $^1\text{H}$  spectra at 30 °C.

### 3.3.3.2 Electrospray Ionization – MS

Molar mass of the lignin and E1 HBP samples were determined by positive ion ESI-MS on a LCQ-Deca instrument (Thermo Finnigan). Lignin samples were dissolved in methanol (1 mg/mL) containing 1% acetic acid and introduced into the ESI source at a flow rate of 10  $\mu\text{L}/\text{min}$  (Osman et al., 2012). The ion source and capillary voltages were 4.48 kV and 47V, respectively at a temperature of 275°C. The MS were scanned between  $m/z$  (mass to charge ratio) 150 and 2000. The number average molar mass ( $M_n$ ) was calculated as  $M_n = \sum M_i N_i / \sum N_i$  and weight average molar mass ( $M_w$ ) as  $M_w = \sum M_i^2 N_i / \sum M_i N_i$ , where  $M_i$  and  $N_i$  are the  $m/z$  and intensity of the ions, respectively (Parees et al., 1998).

### 3.3.3.3 Thermal and Mechanical analysis

Differential scanning calorimetric (DSC) was performed on a TA instruments model Q200 DSC equipped with a refrigeration cooling unit to monitor the thermal behavior of materials. The polymers (5-7 mg) were analyzed from -70 °C to 50 °C at a heating rate of 3 °C /min and held isothermally for 5 min. All the data were collected from the second heating cycle (typically from -70 to 50 °C). Lignin samples were annealed at 90 °C for 10 min, then cooled to 0 °C (3 min), then heated to 200°C at 10 °C/min (second cycle). Thermogravimetric analysis (TGA) was performed on a TGA-7 (Perkin Elmer) instrument from 50 to 900 °C at a heating rate of 20 °C /min in  $\text{N}_2$ . Dynamic mechanical analysis (DMA) experiments were performed using a TA Instruments model Q800 DMA, both under isothermal and non-isothermal conditions in  $\text{N}_2$  atmosphere in the tensile mode (12 mm  $\times$  4 mm  $\times$  0.2 mm). The heating scans were carried out at 1 Hz and at a heating rate of 3 °C/min. The tensile properties of the polymeric materials (triplicate per sample) were measured using DMA at room temperature with ramp 3 N/min. Specifically, energy at break was determined as the area of the stress-strain curve.

The SME of lignin based copolymers were determined in the tensile mode using a DMA. A stress-controlled cycle thermomechanical test was applied. Four programming steps were proceeded, in which (i) the copolymers were heated to a temperature of  $T_g (E'' \text{ maxima}) + 20$  °C (designated as  $T_{\text{high}}$ ) with ramp of 5 °C/min, then set load to 2 N static force with ramp of 0.2 N/min, the copolymers were stretched to temporary shapes; (ii) cooled to  $T_g - 20$  °C (ramp 5 °C/min) (designated as  $T_{\text{low}}$ ); and (iii) release the static force while keeping at  $T_{\text{low}}$ , the copolymers kept the temporary shapes; (iv) heated up to  $T_{\text{high}}$  again and kept isothermal for 15 mins, the permanent shape was achieved again. The same programming procedure was repeated for 3 times (cycle 1 to 3).

### 3.4 Results and Discussion

#### 3.4.1 Preparation and analyses of lignin and HBP samples

The thermal and chemical properties of starting materials (lignin and HBP) were partially characterized in our previous research (Li and McDonald, 2014; Sivasankarapillai and McDonald, 2011). Starting material properties would play an important role in subsequent polymerization. For lignin, the ease of solubility, abundance of hydroxyl groups, molecular mass and  $T_g$ , while for the HBP, the amount of available carboxylic acid groups, chemical branching structure and  $T_g$  are of significance.

The commercial lignin samples were separated into a low molar mass fraction by solubilization in hot methanol. The fractionated lignin samples were measured for lignin content by the Klason lignin plus acid soluble lignin procedures at IN (94.0 %), PB (93.3 %), and CS (95.4 %). Aromatic and aliphatic hydroxyl group contents in lignin, as their acetate, were quantitatively determined by FTIR ( $1762 \text{ cm}^{-1}$  (aromatic ester) and  $1743 \text{ cm}^{-1}$  (aliphatic ester)) (Figure 2bT) and  $^1\text{H}$  NMR (2.28 ppm (aromatic ester) and 2.01 ppm (aliphatic ester)) techniques (Table 3.1). The two techniques gave similar results, except for IN.  $M_w$  of lignin samples were determined by ESI-MS (Table 3.2). The PB had the highest  $M_w$  at 958 g/mol and the results are consistent with fractionated commercial lignin (Teng et al., 2013).

Table 3.1 Hydroxyl group determination from acetylated lignin by FTIR and  $^1\text{H}$  NMR

Lignin	Aromatic/Aliphatic OH	
	FTIR	$^1\text{H}$ NMR
IN	1.05	1.01
PB	0.93	0.93
CS	1.07	1.07

Table 3.2 Molar mass determination of different fractionated industrial lignins and E1 prepolymer

sample	IN	PB	CS	E1
$M_n$ (g/mol)	355	658	446	987
$M_w$ (g/mol)	654	958	741	1206
PDI	1.84	1.46	1.66	1.22

The HBP E1 ( $\text{A}_2\text{B}_3$ ) was prepared according to our previous procedure (Sivasankarapillai and McDonald, 2011) with slight modification. In the HBP synthesis, the reaction conditions were controlled to make sure that only partial conversion of functional groups from monomers occurred to prevent the formation of cross-linked or excessively high molar mass polymers. The resulting polymers were slightly yellow in color and were highly viscous in nature. Ester formation was confirmed by FTIR ( $1723\text{ cm}^{-1}$ ) and  $^{13}\text{C}$  NMR (172.6 ppm). The carboxylic acid group (174 ppm) in E1 and hydroxyl group ( $\sim 3500\text{ cm}^{-1}$ ) in lignin were also monitored for their depletion during esterification. Furthermore, acid ( $\text{CH}_2\text{COOH}$  2.20 ppm) conversion to ester ( $\text{CH}_2\text{COO-ester}$  2.30 ppm) could be determined by  $^1\text{H}$  NMR and 56 % acid groups were available for the subsequent polycondensation (Stumbe and Bruchmann, 2004). The degree of branching (DB) for a E1 HBP was determined by  $^{13}\text{C}$  NMR and chemical shifts at 53.02, 52.87 and 52.60 ppm were assigned to terminal (T), linear (L) and dendritic (D) structures, respectively as shown in Figure 3.2 (Holter et al., 1997; Sivasankarapillai et al., 2012). From these assignments and peak intensity the DB could be calculated as 0.711, where  $\text{DB} = (\text{T}+\text{D}) / (\text{T}+\text{L}+\text{D})$  (Hawker et al., 1991). The calculated value revealed an appreciably high cross-link

occurrence during prepolymerization.  $M_w$  (1206 g/mol) and polydispersity index (1.22) of E1 were determined by ESI-MS (Figure 3.3 and Table 3.2).

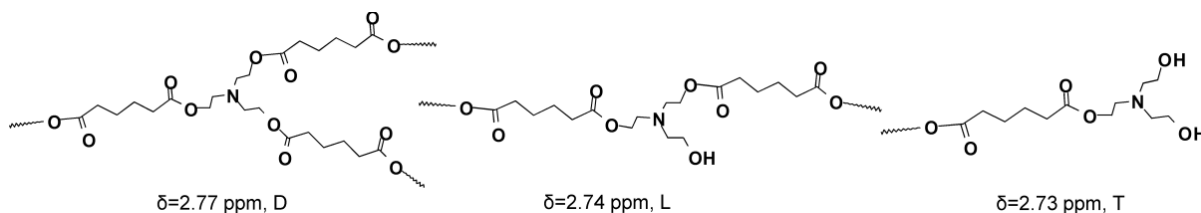


Figure 3.2 Branching structures in E1 prepolymer; Dendritic (D), linear (L) and terminal (T)

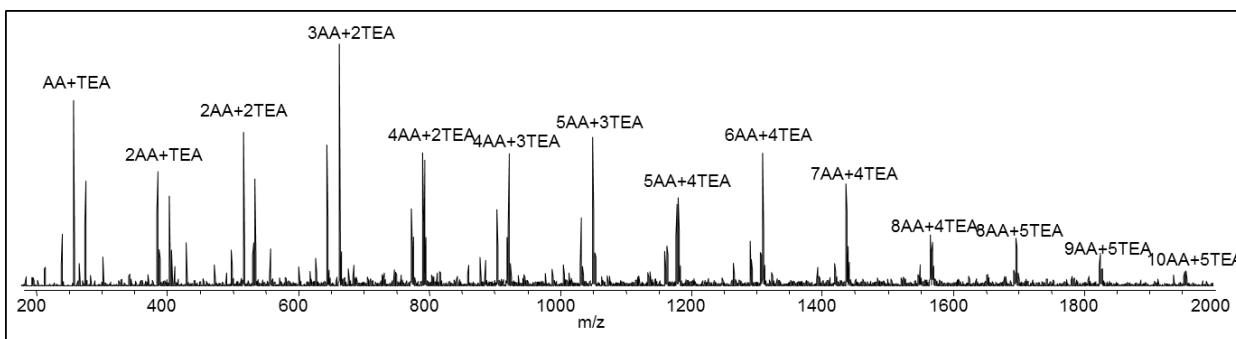


Figure 3.3 Positive ion distribution of E1 prepolymer from ESI-MS

Detailed oligomeric composition and sequences based on molecular adduct ions  $[AA_x+TEA_y-H_2O_z+H]^+$  ( $z=x+y-1$ ) are given in Figure 3.3 and Table 3.3. Furthermore, detailed analysis of the ESI-MS ions suggests that both acyclic and cyclic structures (Li et al., 2006) were present in E1 under the reaction conditions employed. Generally, cyclization could be formed through intramolecular and intermolecular reactions (Holter et al., 1997). However, based on ESI-MS, it was exclusively managed to designate the intramolecular reactions (due to side reactions such as intramolecular esterification or etherification reactions) (Kricheldorf, 2007; Li et al., 2006; Voit and Lederer, 2009). The representative structures of dimer, trimer and tetramer cyclic structures are illustrated in Figure 3.4.

Table 3.3 ESI-MS ion assignments of E1 oligomeric structures

m/z	Ion percentage (%)	Composition	m/z	Ion percentage (%)	Composition
260	1.4	[AA+TEA-2H <sub>2</sub> O+H] <sup>+</sup>	1052	6.6	[5AA+3TEA-7H <sub>2</sub> O+H] <sup>+</sup>
278	5.1	[AA+TEA-H <sub>2</sub> O+H] <sup>+</sup>	1165	2.0	[5AA+4TEA-9H <sub>2</sub> O+H] <sup>+</sup>
388	5.3	[2AA+TEA-3H <sub>2</sub> O+H] <sup>+</sup>	1183	4.5	[5AA+4TEA-8H <sub>2</sub> O+H] <sup>+</sup>
406	3.4	[2AA+TEA-2H <sub>2</sub> O+H] <sup>+</sup>	1293	2.0	[6AA+4TEA-10H <sub>2</sub> O+H] <sup>+</sup>
519	5.1	[2AA+2TEA-4H <sub>2</sub> O+H] <sup>+</sup>	1311	8.0	[6AA+4TEA-9H <sub>2</sub> O+H] <sup>+</sup>
537	3.8	[2AA+2TEA-3H <sub>2</sub> O+H] <sup>+</sup>	1421	1.4	[7AA+4TEA-11H <sub>2</sub> O+H] <sup>+</sup>
647	4.0	[3AA+2TEA-5H <sub>2</sub> O+H] <sup>+</sup>	1439	6.9	[7AA+4TEA-10H <sub>2</sub> O+H] <sup>+</sup>
665	6.8	[3AA+2TEA-4H <sub>2</sub> O+H] <sup>+</sup>	1567	3.6	[8AA+4TEA-11H <sub>2</sub> O+H] <sup>+</sup>
775	2.9	[4AA+2TEA-6H <sub>2</sub> O+H] <sup>+</sup>	1681	0.9	[8AA+5TEA-13H <sub>2</sub> O+H] <sup>+</sup>
793	6.1	[4AA+2TEA-5H <sub>2</sub> O+H] <sup>+</sup>	1698	2.8	[8AA+5TEA-12H <sub>2</sub> O+H] <sup>+</sup>
906	4.5	[4AA+3TEA-7H <sub>2</sub> O+H] <sup>+</sup>	1826	1.8	[9AA+5TEA-13H <sub>2</sub> O+H] <sup>+</sup>
924	6.4	[4AA+3TEA-6H <sub>2</sub> O+H] <sup>+</sup>	1958	0.8	[10AA+5TEA-14H <sub>2</sub> O+H] <sup>+</sup>
1034	3.8	[5AA+3TEA-8H <sub>2</sub> O+H] <sup>+</sup>			
General formula		[AA <sub>x</sub> +TEA <sub>y</sub> -H <sub>2</sub> O <sub>z</sub> +H] <sup>+</sup> (z=x+y): cyclic [AA <sub>x</sub> +TEA <sub>y</sub> -H <sub>2</sub> O <sub>a</sub> +H] <sup>+</sup> (a=x+y-1): acyclic			

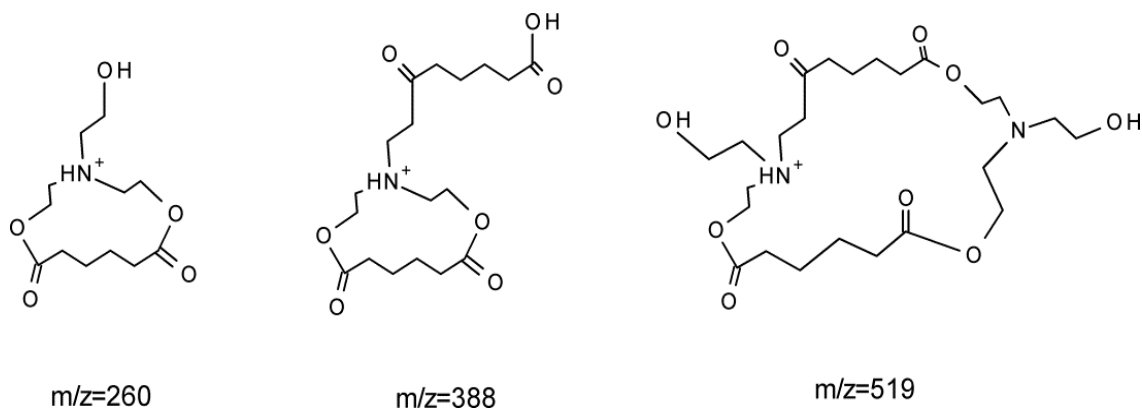


Figure 3.4 Possible cyclic structures in E1 prepolymer

### 3.4.2 Synthesis of lignin-copoly(ester-amine) elastomers

The synthesis route of lignin-copolymer was carried out with a two-step one-pot bulk polymerization (melt condensation) process (Figure 3.1) (Scholl et al., 2007). The lignin copolymer formulation was adjusted by using different industrial lignins and lignin content in

order to modify lignin-copolymer properties. In the preliminary work, PB lignin with content ranging from 20 to 80%, were used and the final material showed that < 30% the lignin-copolymer was too soft to sustain mechanical exertion, while >50% the lignin-copolymer was brittle and showed phase separation. Therefore, for the IN and CS lignin samples, lignin contents evaluated were controlled at 30%, 35%, 40% and 45%. Samples were coded for lignin type (IN, PB and CS), the HBP E1 and lignin content (20-80%) (e.g. INE1-30) and the control sample without lignin was coded E1-0.

The PBE1-0 to 80 copolymers were analyzed by FTIR spectroscopy (Figure 3.5) together with the original PB lignin, acetylated PB lignin, E1-0 control and PBE1-40 copolymer. Ester formation between lignin and HBP was supported by the reduction of the OH band (3600-3100  $\text{cm}^{-1}$ ) and increase in the ester carbonyl band (1800-1650  $\text{cm}^{-1}$ ). Furthermore, no band at 1762  $\text{cm}^{-1}$  (characteristic of an aromatic carbonyl ester) was observed (Figure 3.5d). An aliphatic ester band at 1723  $\text{cm}^{-1}$  was observed in the copolymer, relative to acetylated lignin (at 1743  $\text{cm}^{-1}$ ), suggesting that aliphatic hydroxyl groups in lignin shows the presence of H-bonding in lignin copolymer (Kadla and Kubo, 2003). The effect of lignin content on the lignin-E1 copolymer were examined by FTIR (Figure 3.6) and showed that the band broadened indicating increased H-bonding with lignin content and this phenomenon has been documented in the literature (Kadla and Kubo, 2003; Sivasankarapillai and McDonald, 2011).

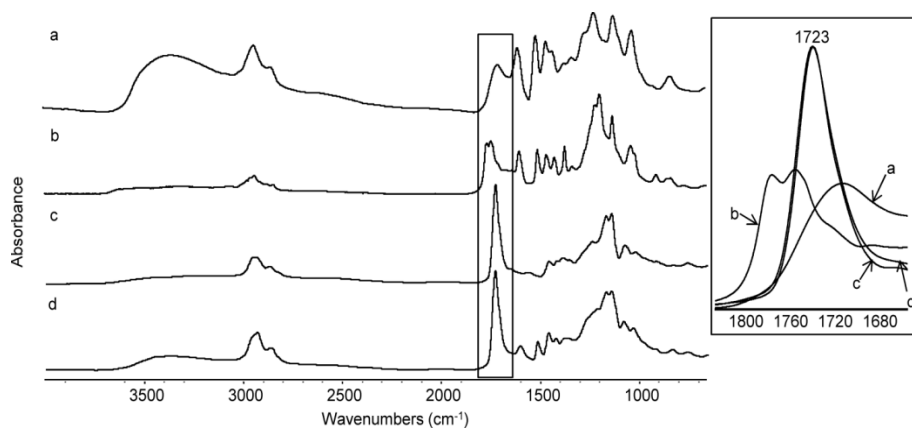


Figure 3.5 FTIR spectra of (a), PB; (b), acetylated PB; (c), E1-0 polymer; and (d), PBE1-40 copolymer

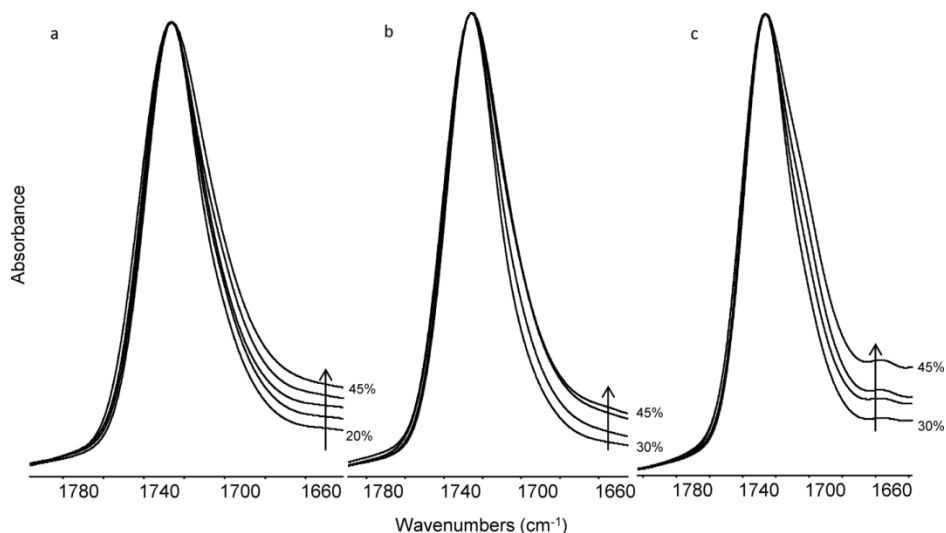


Figure 3.6 FTIR spectra of the carbonyl region of (a), PBE1-20 to 45 copolymer; (b), INE1-30 to 45 copolymer; and (c), CSE1-30 to 45 copolymer. Note: arrows mean increase in lignin content

### 3.4.3 Mechanical properties

The tensile properties of lignin-copolymers produced are given in Table 3.4. Stress-strain curves for copolymers INE1-45, PBE1-45 and CSE1-45 are shown in Figure 3.7. The tensile properties were shown to increase with lignin content to a maximum of 45% lignin content. The control (E1-0) polymer had a tensile strength of 0.4 MPa and increased to 1.2 MPa at 20% lignin (PBE1-20) and finally to 16.2 MPa at 50% lignin (PBE1-50). The tensile modulus also increased from 0.1 MPa (E1-0 control) to 194 MPa (PBE1-50) as lignin content was increased with a concomitant decrease in strain at break with lignin. The CSE1-30 to 45 and INE1-30 to 45 based copolymers also show similar tensile property trends. There were differences in the tensile properties between the copolymers made with different lignin especially at 45% lignin content. The INE1-45 (20.8 MPa) was shown to have the highest tensile strength followed by PBE1-45 (15.7 MPa) then CSE1-45 (12.6 MPa). A similar trend was observed for the tensile moduli. At high lignin contents the copolymer tensile properties were dominated by lignin and probably due to intramolecular and intermolecular H-bonding. In contrast, at low lignin contents the copolymer tensile properties were dominated by HBP properties and attributable to covalent bonds between HBP and lignin. The toughness of the copolymer was assessed by its energy at break (EAB) and maximum values were obtained at

lignin contents of 45%. The EAB of INE1-45, PBE1-45 and CSE1-45 were respectively at 1300, 1020 and 1080 MPa. The data for the lignin-copolymers show that lignin influences the mechanical properties of copolymers.

Table 3.4 Tensile properties of different industrial lignin based copolymers at room temperature

Sample	Tensile strength (MPa)	Young's modulus (MPa)	Strain at break (%)	Energy at break (MPa)
E1-0	0.40	0.10	259	37
PBE1-20	1.2	2.6	60	40
PBE1-30	2.2	5.4	89	113
PBE1-35	4.9	25.4	77	223
PBE1-40	5.0	12.4	97	282
PBE1-45	15.7	160	89	1020
PBE1-50	16.2	194	58	769
INE1-30	4.2	11.7	70	165
INE1-35	5.7	14.1	114	357
INE1-40	4.2	15.6	107	216
INE1-45	20.8	297	84	1300
CSE1-30	4.2	8.3	86	187
CSE1-35	6.0	7.2	214	634
CSE1-40	3.6	8.4	154	280
CSE1-45	12.6	109	122	1080



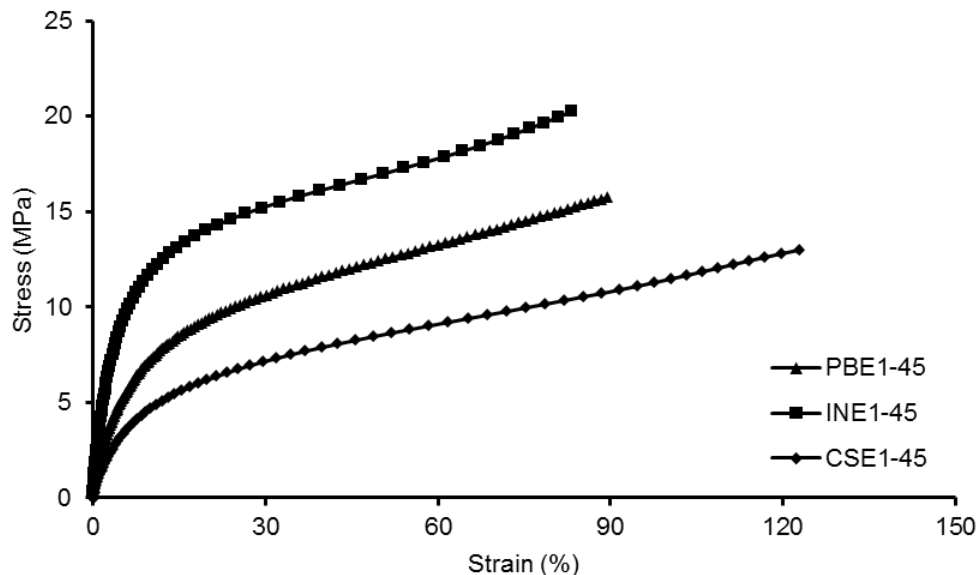


Figure 3.7 Tensile stress-strain curves of PBE1-45, INE1-45 and CSE1-45 copolymers

#### 3.4.4 Thermal properties

$T_g$  is a second-order phase transition of an amorphous polymeric which confines its threshold in engineering applications (Overley et al., 2000). The determination of  $T_g$  of the lignin copolymers was determined by DMA from the maxima of the loss modulus ( $E''$ ) peak (Figures 3.8b and 3.9a). In addition,  $T_g$  of the various lignin copolymers were obtained by DSC (Figures 3.8a and 3.9b). The  $T_g$  was shown to increase with copolymer lignin content. The increasing  $T_g$  of the copolymer could be explained by high  $T_g$  of lignin which introduces an aromatic backbone and H-bonding to the polymer network and as content increases further restricts the free movement of side-chains and reduces the polymer free volume. An interesting point to mention is that the  $T_g$  of IN lignin ( $117^\circ\text{C}$ ) was lower than those of PB ( $132^\circ\text{C}$ ) and CS ( $131^\circ\text{C}$ ), probably due to differences in  $M_w$ , however, the INE1 copolymers showed comparable  $T_g$ s with the other two lignin-copolymers (at a given lignin content). This finding revealed that the E1 HBP plays a determining role in terms of thermal properties and implies that lignin is evenly dispersed in the prepolymer matrix. The miscibility of the two polymers (lignin and E1) was examined by the DSC and DMA. All the DSC thermograms showed one  $T_g$  and the DMA thermograms showed only a single  $E''$  peak for all copolymer

samples and this revealed excellent miscibility between the two polymers (Figure 3.10) (Kadla and Kubo, 2003; Sivasankarapillai and McDonald, 2011). Miscibility was dependent on the covalent reaction between lignin and E1 and the occurrence of exothermic interactions, such as H-bonding (Kadla and Kubo, 2003; Sivasankarapillai and McDonald, 2011). Figure 3.10 shows that as lignin content increases the  $E''$  peak broadens and lowers in intensity which indicates that increased cross-linking which will result in the reduction of the polymer system volume and thus will require more energy to dissipate the polymer system (del Río et al., 2011).

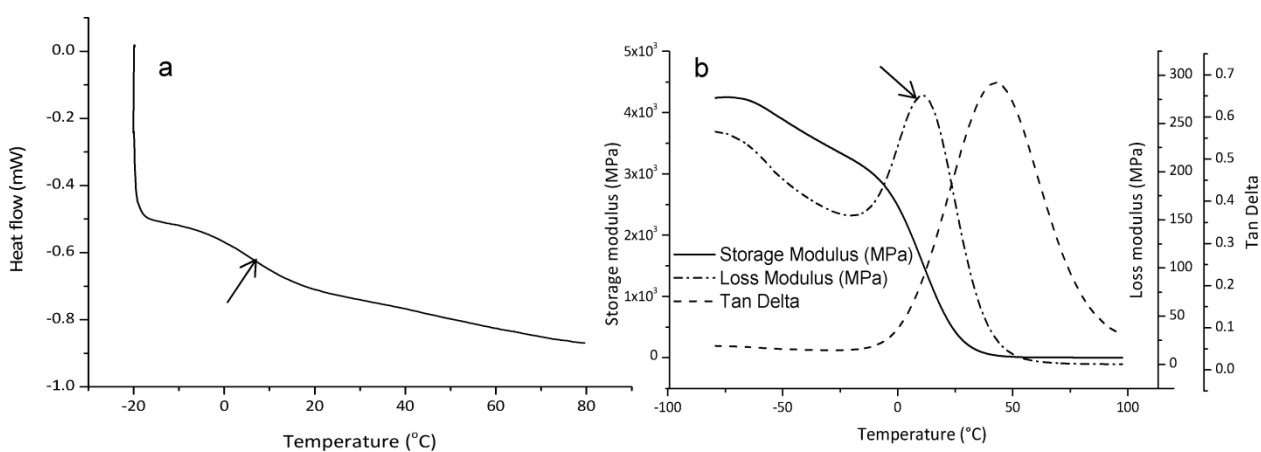


Figure 3.8 DSC (a) and DMA (b) thermograms of PBE1-40 copolymer

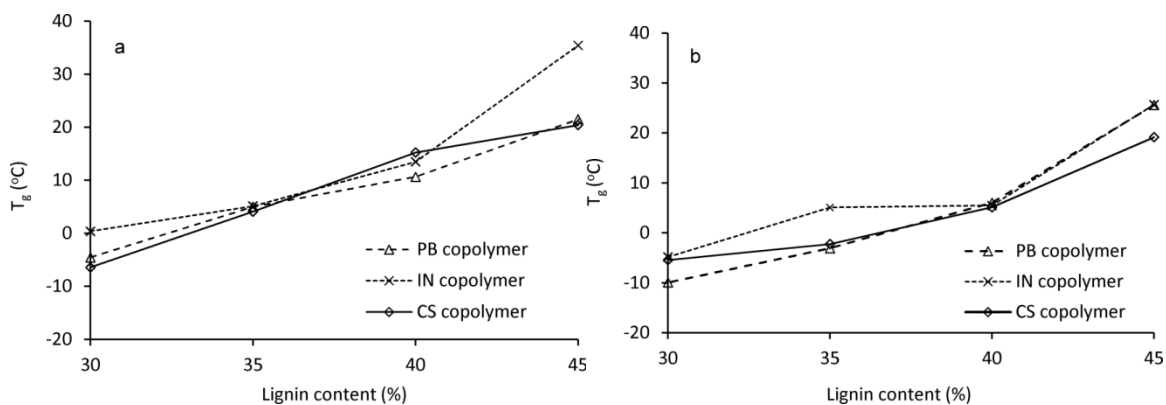


Figure 3.9 T<sub>g</sub> of IN, PB and CS lignin-copolymers as a function of lignin content: a, obtained from DMA  $E''$ ; and b, from DSC

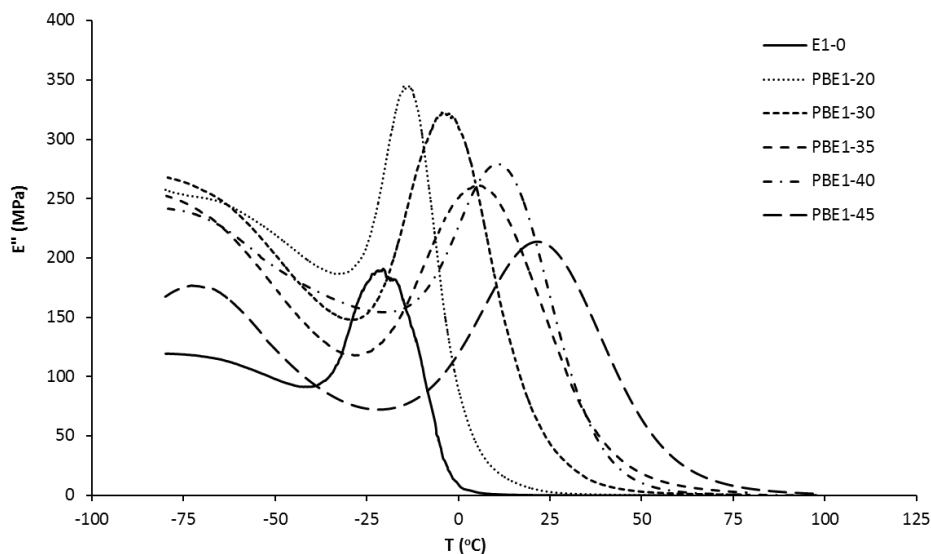


Figure 3.10 Thermograms showing tensile loss moduli ( $E''$ ) for all PBE1-20 to 45 copolymers and E1-0 polymer

### 3.4.5 Thermal stability of the lignin-copoly(ester-amine)s

The thermal stability of the lignin-copoly(ester-amine)s was studied by TGA. For all copolymers regardless of lignin type, three stages of decomposition were observed by TGA (Table 3.5 and Figure 3.11). To observe the transitions differential TGA (DTG) was also performed (Figure 3.11). The first stage was between 220 and 350 °C. The second stage was between 350 and 425 °C. The third stage was between 500 and 650 °C. It was reasonable to identify the initial decomposition from E1 and later with from lignin as verified as shown in Figure 3.11d, because E1 is constituted with highly branched aliphatic chains and ester groups were considerably labile to thermal decomposition (Pramanik et al., 2014; Pramanik et al., 2013). Whereas lignin, comprised of highly cross-linked aromatic backbones and various aliphatic side chains, gradually degraded and resisted thermal decomposition to form appreciable amount of char (Nassar and MacKay, 1984). Lignin content was not shown to affect the first degradation stage of the copolymers. However, lignin content in the copolymers influenced the second and third stage decompositions (Figure 3.11a, b and c). When comparing between copolymers of different lignin type, it appears that IN based copolymers had a higher relative thermal stability than those made with PB and CS lignin which could be attributed to its more condensed structure (Table 3.5 and Figure 3.11) (Fox

and McDonald, 2010). The residual content for the INE1-45, PBE1-45, and CSE1-45 copolymers at 650 °C were respectively, 47%, 44% and 41%. The variation is contributed by the difference of lignins structure in the higher temperature region (Li and McDonald, 2014).

Table 3.5 Thermal decomposition of different lignin based copolymers from TGA data

Sample #	1st stage		2nd stage		3rd stage		Max peak
	T (°C)	Remaining mass (%)	T (°C)	Remaining mass (%)	T (°C)	Remaining mass (%)	
PBE1-20	373	78.8	421	28.4	581	16.5	400
PBE1-30	373	77.5	413	35.9	582	22.6	394
PBE1-35	372	80.0	413	40.6	583	25.1	388
PBE1-40	350	84.8	419	35.5	584	25.2	392
PBE1-45	370	81.6	424	43.6	583	29.4	391
PBE1-50	365	82.6	428	43.8	580	30.8	379
INE1-30	375	77.6	418	36.9	566	25.0	391
INE1-35	367	82.7	426	36.3	588	24.2	388
INE1-40	347	86.5	427	36.7	577	26.8	388
INE1-45	374	78.1	424	46.8	557	34.4	387
CSE1-30	377	75.0	417	37.8	554	25.1	394
CSE1-35	357	85.3	418	34.4	566	23.2	395
CSE1-40	359	82.0	413	37.6	564	23.8	389
CSE1-45	364	81.0	421	40.8	564	28.4	388

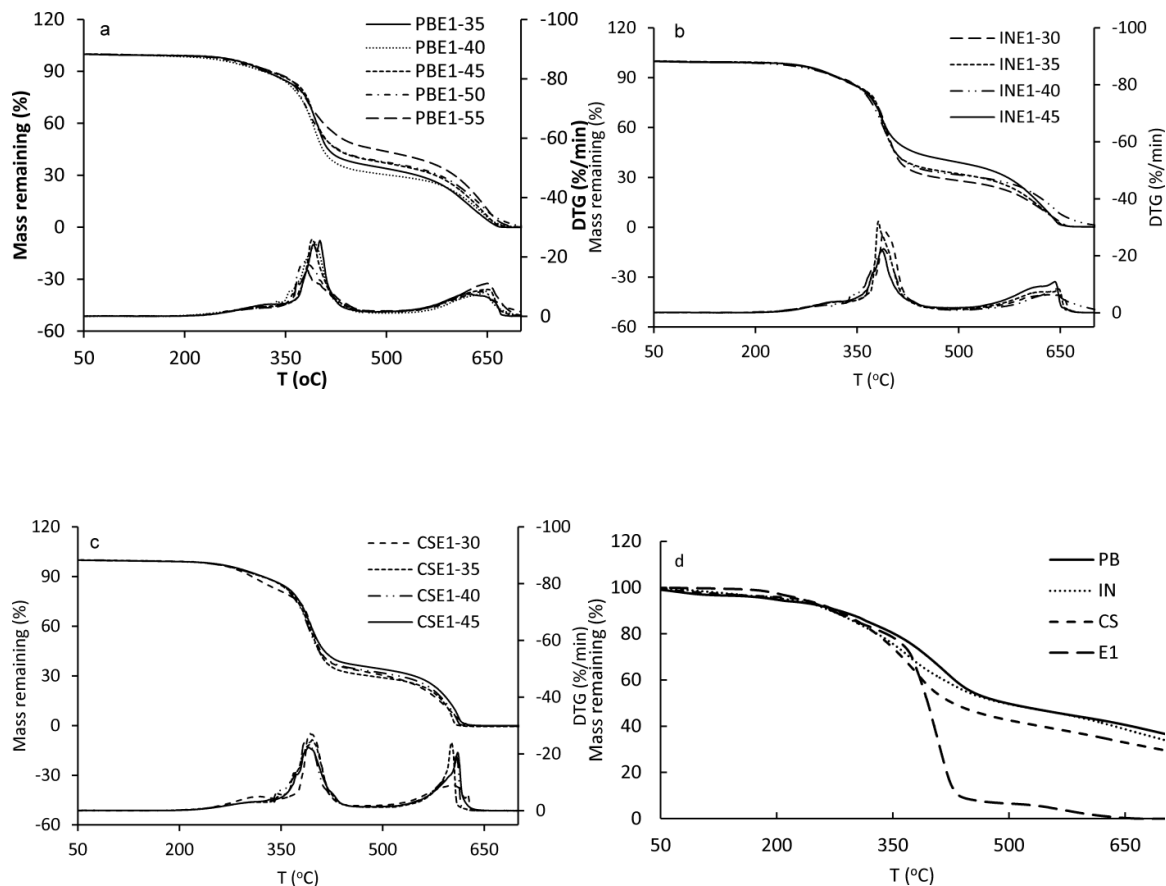


Figure 3.11 TGA thermograms of lignin based copolymers: (a), PB based copolymer; (b), IN based copolymer; (c), CS based copolymer; and d, starting materials PB, IN, CS, and E1.

### 3.4.6 Thermally-stimulated dual shape memory effect ( $T_s$ -SME)

$T_s$ -SME could be obtained in a polymer system which contains two kinds of segments, i.e., soft segment controlling temporary shape and netpoint segment determining permanent shape (Figure 3.12) (Lendlein and Kelch, 2002). Therefore, this could be applied to the HBP with a flexible aliphatic backbone and side chains having an appreciably low  $T_g$  and functions as a soft segment. Whereas, lignin is a rigid and compact aromatic structure with a high  $T_g$  and functions as netpoint segment. The SME properties of lignin based copolymers were quantified by tensile stress-controlled thermomechanical cyclic testing. Figure 3.13 shows the results of cyclic thermomechanical testing of PBE1-20 copolymer. The shape memory recovery ratio ( $R_r$ ) and fixity ratio ( $R_f$ ) were calculated according to the following equations (Lendlein and Kelch, 2002):

$$R_r(N) = \frac{\varepsilon_1(N) - \varepsilon_p(N)}{\varepsilon_1(N) - \varepsilon_p(N-1)} \times 100\% \quad (3.1)$$

$$R_f(N) = \frac{\varepsilon_u(N)}{\varepsilon_1(N)} \times 100\% \quad (3.2)$$

Where  $R_r(N)$  is the shape recovery ratio at  $N^{\text{th}}$  cycle,  $R_f(N)$  is the shape fixity ratio at  $N^{\text{th}}$  cycle,  $N$  is cycle number from 1 to 3,  $\varepsilon_1(N)$  is the maximum strain with load,  $\varepsilon_u(N)$  is the tensile strain after unloading at  $T_{\text{low}}$ ,  $\varepsilon_p(N-1)$  and  $\varepsilon_p(N)$  are the recovered strain in two successive cycles in the stress-free state before exertion of yield stress at  $T_{\text{high}}$ . Reporting values were based on the average of three cycles. Second and third cycles were highly superimposable and overlapped compared to the first cycle and an appreciable improvement of  $R_f$  and  $R_r$  observed. This small training effect was contributed by the occurrence of some chain relaxation during the first mechanical cycle, leading to a deviation in the later cycles, which was a characteristic phenomenon of SMPs according to Gautrot and Zhu (Gautrot and Zhu, 2006, 2009).  $R_f$  describes the ability to fix the mechanical deformation under  $T_{\text{low}}$ , while  $R_r$  quantifies how well the shape recovers in the  $N^{\text{th}}$  cycle (for  $N > 1$ ) in terms of the recovered shape of the previous  $(N-1)^{\text{th}}$  cycle (Sauter et al., 2013). The results of  $R_r$  and  $R_f$  of all the lignin copoly(ester-amine)s as a function of lignin content are shown in Figure 3.14a and b, respectively. All the copolymers were shown to have high  $R_f$  with more than 95% fixity rate. The PB based copolymers were shown to have an excellent  $R_r > 85\%$  at lignin contents  $< 40\%$ . However, at lignin content greater than 40%, the  $R_r$  values decreased to 73% for PBE1-45 and 76% for PBE1-50. A 90% shape recovery was obtained for all the CS and IN based copolymers.  $T_{\text{trans}}$  is another important parameter of Ts-SME polymers and was determined at which the polymer can be switched back to its original shape upon removal of external stimuli measured as first derivative peak of the strain versus temperature plot. The  $T_{\text{trans}}$  of various lignin-copolymers as a function of lignin content is shown in Figure 3.14c. It was observed that the  $T_{\text{trans}}$  increased for the lignin-copoly(ester-amine)s with lignin content implying that this parameter could be tailored to meet specific temperature requirements.  $T_{\text{trans}}$  was approximately 20 °C higher than the  $T_g$  of the copolymers (determined from  $E''$ ). The  $T_{\text{trans}}$ s of the different lignin based copolymers were comparable at the same lignin

content, which indicated that the  $T_{\text{trans}}$  of the copolymers was dominated by the soft segment.

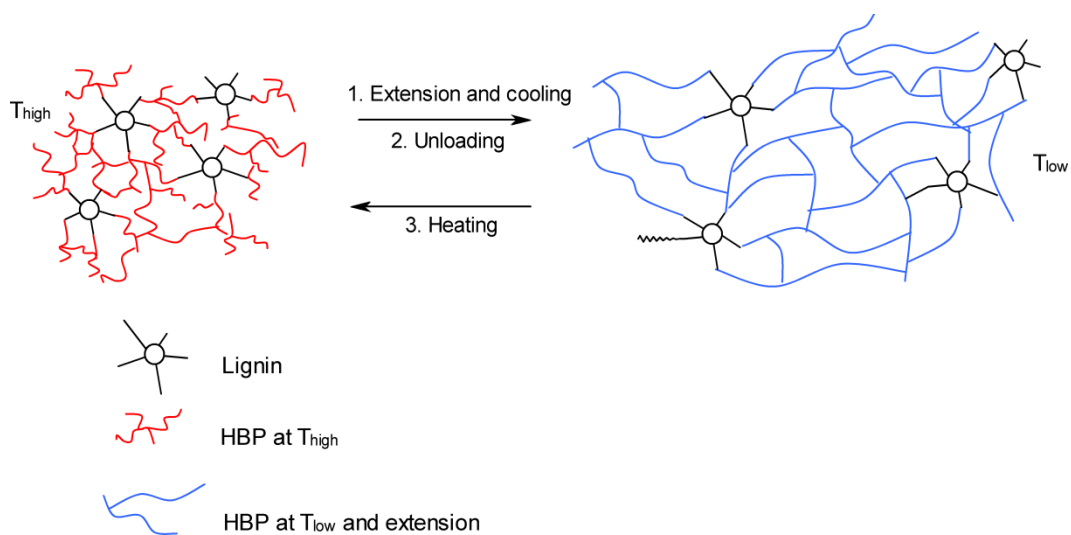


Figure 3.12 Molecular mechanism of Ts-SME of lignin-co-poly(ester-amine) elastomer.

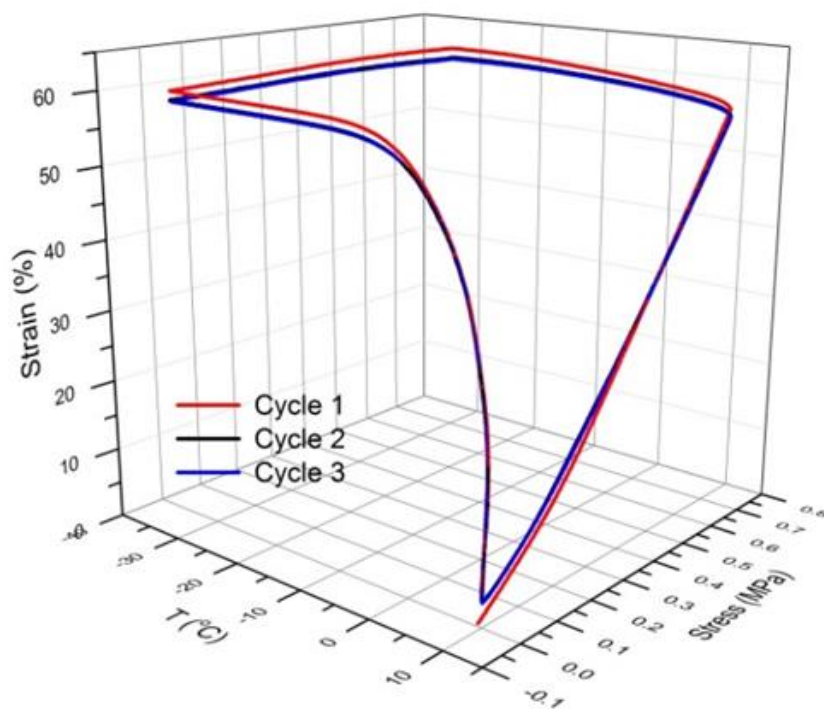


Figure 3.13 Tensile stress-temperature-strain ( $\sigma$ - $T$ - $\epsilon$ ) curve of PBE1-20 copolymer.

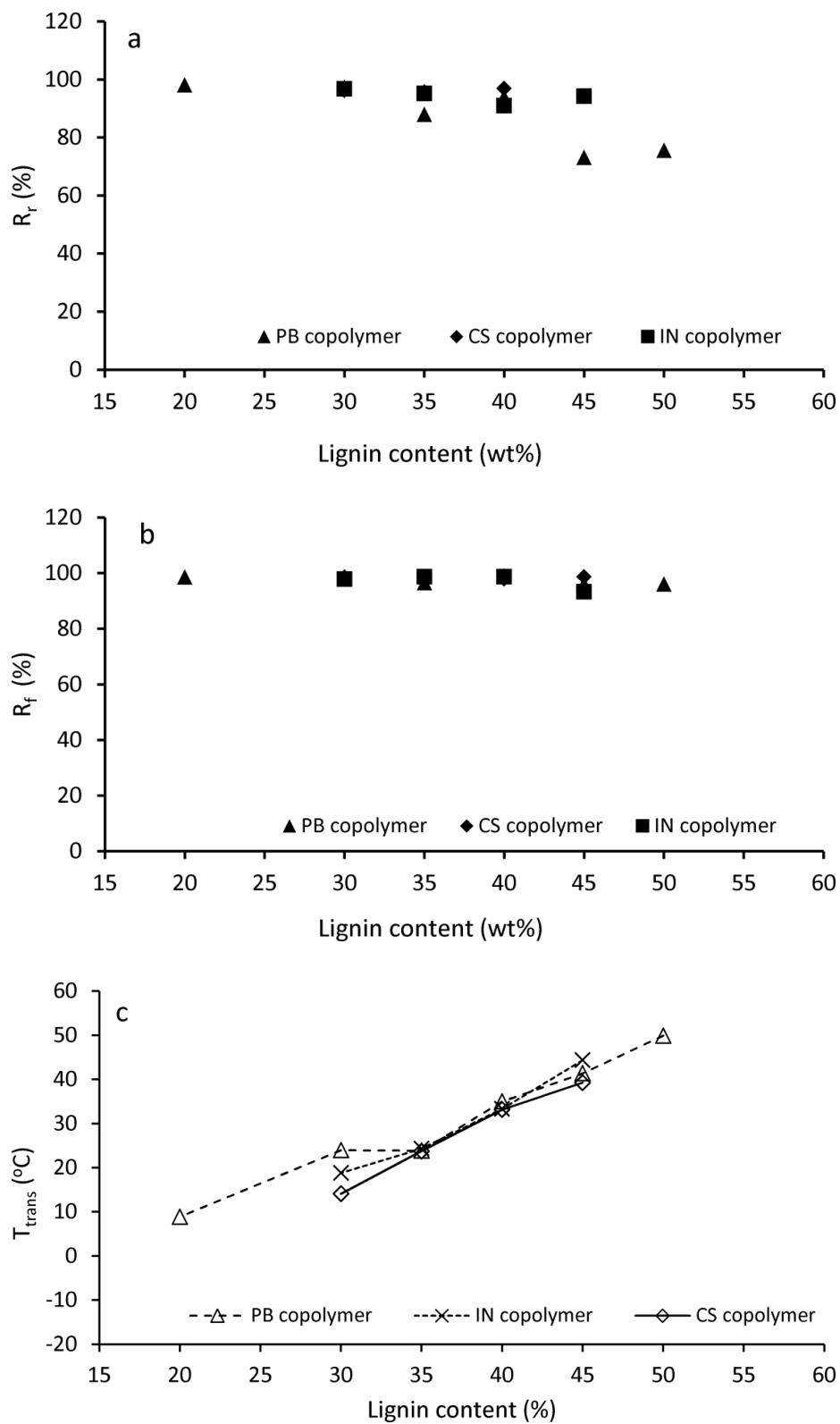


Figure 3.14 (a),  $R_r$ ; (b),  $R_f$ ; and (c),  $T_{trans}$  results of IN, PB and CS lignin-copoly(ester-amine)s as a function of lignin content



### 3.5 Conclusions

Lignin-based Ts-SME dual shape memory copolymers were successfully synthesized using a variety of industrial lignins and HBP via a one-pot two step bulk polycondensation reaction. Lignin content and lignin type (IN, PB and CS) were shown to influence copolymer properties. At high lignin levels (>40%) the copolymer mechanical properties were dominated by lignin while  $\leq 40\%$  lignin the properties were dominated by HBP. The copolymers were shown to have > 95% fixity rate and >90 shape recovery. The  $T_{\text{trans}}$  was shown to increase with copolymer lignin content and this demonstrates that the properties can be tuned by lignin content. This study clearly demonstrates that lignin, a renewable resource and byproduct, can be used as a netpoint segment in polymer systems with SME behavior.

### 3.6 References

- Beheshti, N., Nguyen, G.T.M., Kjoniksen, A.L., Knudsen, K.D., Nystrom, B. **2006**. Structure and dynamics of aqueous mixtures of an anionic cellulose derivative and anionic or cationic surfactants. *Colloids and Surfaces a*, 279, 40-49.
- Behl, M., Lendlein, A. **2007**. Shape-memory polymers. *Materials Today*, 10, 20-28.
- Behl, M., Lendlein, A. **2010**. Overview of shape memory polymers, in: Leng, J.S., Du, S.Y. (Eds.), *Shape-memory polymers and multifunctional composites*. CRC Press/Taylor & Francis, Boca Raton, pp. 1-20.
- Beloshenko, V.A., Beigel'zimer, Y.E., Varyukhin, V.N., Voznyak, Y.V. **2005**. Shape memory and electric resistance of an epoxy polymer-expanded graphite composition. *Polymer Science Series A*, 47, 723-729.
- Boonprasith, P., Wootthikanokkhan, J., Nimitsiriwat, N. **2013**. Mechanical, thermal, and barrier properties of nanocomposites based on poly(butylene succinate)/thermoplastic starch blends containing different types of clay. *Journal of Applied Polymer Science*, 130, 1114-1123.

- Capanema, E.A., Balakshin, M.Y., Kadla, J.F. **2004**. A comprehensive approach for quantitative lignin characterization by NMR spectroscopy. *Journal of Agricultural and Food Chemistry*, 52, 1850-1860.
- Chung, H., Washburn, N.R. **2013**. Chemistry of lignin-based materials. *Green Materials*, 1, 137-160.
- Cui, C.Z., Sadeghifar, H., Sen, S., Argyropoulos, D.S. **2013**. Toward Thermoplastic Lignin Polymers; Part II: Thermal & Polymer Characteristics of Kraft Lignin & Derivatives. *BioResources*, 8, 864-886.
- del Río, E., Lligadas, G., Ronda, J.C., Galià, M., Cádiz, V., Meier, M.A.R. **2011**. Shape Memory Polyurethanes from Renewable Polyols Obtained by ATMET Polymerization of Glyceryl Triundec-10-enoate and 10-Undecenol. *Macromolecular Chemistry and Physics*, 212, 1392-1399.
- Dietsch, B., Tong, T. **2007**. A review - Features and benefits of shape memory polymers. *Journal of Advanced Materials*, 39, 3-12.
- Drumright, R.E., Gruber, P.R., Henton, D.E. **2000**. Polylactic acid technology. *Advanced Materials*, 12, 1841-1846.
- El Idrissi, A., El Barkany, S., Amhamdi, H., Maaroufi, A.K. **2013**. Synthesis and characterization of the new cellulose derivative films based on the hydroxyethyl cellulose prepared from esparto "stipa tenacissima" cellulose of Eastern Morocco. II. Esterification with acyl chlorides in a homogeneous medium. *Journal of Applied Polymer Science*, 127, 3633-3644.
- Fox, C.S., McDonald, A.G. **2010**. Chemical and thermal characterization of three industrial lignins and their corresponding lignin esters. *BioResources*, 5, 990-1009.
- Gautrot, J.E., Zhu, X.X. **2006**. Main-chain bile acid based degradable elastomers synthesized by entropy-driven ring-opening metathesis polymerization. *Angewandte Chemie International Edition*, 45, 6872-6874.

- Gautrot, J.E., Zhu, X.X. **2009**. Shape Memory Polymers Based on Naturally-Occurring Bile Acids. *Macromolecules*, 42, 7324-7331.
- Glasser, W.G., Jain, R.K. **1993**. Lignin Derivatives .1. Alkanoates. *Holzforschung*, 47, 225-233.
- Gosselink, R.J.A., de Jong, E., Guran, B., Abächerli, A. **2004**. Co-ordination network for lignin—standardisation, production and applications adapted to market requirements (EUROLIGNIN). *Industrial Crops and Products*, 20, 121-129.
- Hawker, C.J., Lee, R., Frechet, J.M.J. **1991**. One-Step Synthesis of Hyperbranched Dendritic Polyesters. *Journal of the American Chemical Society*, 113, 4583-4588.
- Holter, D., Burgath, A., Frey, H. **1997**. Degree of branching in hyperbranched polymers. *Acta Polymerica*, 48, 30-35.
- Hu, S.J., McDonald, A.G., Coats, E.R. **2013**. Characterization of polyhydroxybutyrate biosynthesized from crude glycerol waste using mixed microbial consortia. *Journal of Applied Polymer Science*, 129, 1314-1321.
- Kadla, J.F., Kubo, S. **2003**. Miscibility and hydrogen bonding in blends of poly(ethylene oxide) and kraft lignin. *Macromolecules*, 36, 7803-7811.
- Kawashima, N. **2003**. A development of polylactic acid as bio-based polymers. *Journal of Synthetic Organic Chemistry, Japan* 61, 496-505.
- Kawashima, N., Matsuo, M., Sugi, M. **2005**. Role of bio-based polymers toward building a sustainable society - Through a business development of polylactic acid, LACEA((R)). *Kobunshi Ronbunshu*, 62, 233-241.
- Kim, Y.S., Kadla, J.F. **2010**. Preparation of a thermoresponsive lignin-based biomaterial through atom transfer radical polymerization. *Biomacromolecules*, 11, 981-988.
- Kricheldorf, H.R. **2007**. Polycondensation of 'a-b(n)' or 'a(2)+b(n)' Monomers - A comparison. *Macromolecular Rapid Communications*, 28, 1839-1870.

Laurichesse, S., Avérous, L. **2013**. Chemical modification of lignins: Towards biobased polymers. *Progress in Polymer Science*.

Lendlein, A., Kelch, S. **2002**. Shape-memory polymers. *Angewandte Chemie International Edition*, 41, 2034-2057.

Lendlein, A., Langer, R. **2002**. Biodegradable, elastic shape-memory polymers for potential biomedical applications. *Science*, 296, 1673-1676.

Lewis, N.G., Lantzy, T.R. **1989**. Lignin in adhesive introduction and historical perspective, in: Hemingway, R.W., Conner, A.H., Branham, S.J. (Eds.), *Adhesive from renewable resources*. ACS Symposium Series, New Orleans, pp. 13-26.

Li, H., McDonald, A.G. **2014**. *Fractionation and Characterization of Industrial Lignin*. University of Idaho, Moscow, Idaho.

Li, X., Lu, X., Lin, Y., Zhan, J., Li, Y., Liu, Z., Chen, X., Liu, S. **2006**. Synthesis and characterization of hyperbranched poly(ester-amide)s from commercially available dicarboxylic acids and multihydroxyl primary amines. *Macromolecules*, 39, 7889-7899.

Li, Y., Mlynar, J., Sarkanen, S. **1997**. The First 85% Kraft Lignin-Based Thermoplastics. *Journal of polymer science Part B: Polymer physics*, 35, 1899-1910.

Li, Y., Ragauskas, A.J. **2012**. Kraft lignin based rigid polyurethane foam. *Journal of Wood Chemistry and Technology*, 32, 210-224.

Li, Y., Sarkanen, S. **2002**. Alkylated kraft lignin-based thermoplastic blends with aliphatic polyesters *Macromolecules*, 35, 9707-9715.

Liu, C., Qin, H., Mather, P.T. **2007**. Review of progress in shape-memory polymers. *Journal of Materials Chemistry*, 17, 1543-1558.

McDonald, A.G., Ma, L. **2012**. Plastic moldable lignin, in: Paterson, R.J. (Ed.), *Lignin: Properties and applications in biotechnology and bioenergy*. Nova Science Publisher, Inc., pp. 489-498.

Miao, S.D., Wang, P., Su, Z.G., Liu, Y.Y., Zhang, S.P. **2012**. Soybean oil-based shape-memory polyurethanes: Synthesis and characterization. *European Journal of Lipid Science and Technology*, 114, 1345-1351.

Nassar, M.M., MacKay, G.D.M. **1984**. Mechanism of thermal decomposition of lignin. *Wood and Fiber Science*, 16, 441-453.

Osman, N.B., McDonald, A.G., Laborie, M.P.G. **2012**. Analysis of DCM extractable components from hot-pressed hybrid poplar. *Holzforschung*, 66, 927-934.

Overley, R.M., Buenviaje, C., Luginuni, R., Dinelli, F. **2000**. Glass and structural transitions measured at polymer surfaces on the nanoscale. *Journal of Thermal Analysis and Calorimetry*, 59, 205-225.

Pang, M.M., Pun, M.Y., Ishak, Z.A.M. **2013**. Natural weathering studies of biobased thermoplastic starch from agricultural waste/polypropylene blends. *Journal of Applied Polymer Science*, 129, 3237-3246.

Parees, D.M., Hanton, S.D., Clark, P.A.C., Willcox, D.A. **1998**. Comparison of mass spectrometric techniques for generating molecular weight information on a class of ethoxylated oligomers. *Journal of the American Society for Mass Spectrometry*, 9, 282-291.

Perlack, R.D., Wright, L.L., Turhollow, A., Graham, R.L., Stokes, B.J., Erbach, D.C. **2005**. U.S. Department of Energy, Biomass as feedstock for a bioenergy and bioproducts industry---- the technical feasibility of a billion-ton annual supply.

Pohjanlehto, H., Setälä, H.M., Kiely, D.E., McDonald, A.G. **2014**. Lignin-Xylaric Acid-Polyurethane-Based Polymer Network Systems: Preparation and Characterization. *Journal of Applied Polymer Science*, 131, 39714-39720.

- Pramanik, S., Konwarh, R., Barua, N., Buragohain, A.K., Karak, N. **2014**. Bio-based hyperbranched poly(ester amide)-MWCNT nanocomposites: multimodalities at the biointerface. *Biomaterials Science*, 2, 192-202.
- Pramanik, S., Konwarh, R., Sagar, K., Konwar, B.K., Karak, N. **2013**. Bio-degradable vegetable oil based hyperbranched poly(ester amide) as an advanced surface coating material. *Progress in Organic Coatings*, 76, 689-697.
- Proikakis, C.S., Tarantili, P.A., Andreopoulos, A.G. **2002**. Synthesis and characterization of low molecular weight polylactic acid. *Journal of Elastomers and Plastics*, 34, 49-63.
- Quirino, R.L., Garrison, T.F., Kessler, M.R. **2014**. Matrices from vegetable oils, cashew nut shell liquid, and other relevant systems for biocomposite applications. *Green Chemistry*, 16, 1700-1715.
- Sadeghifar, H., Cui, C., Argyropoulos, D.S. **2012**. Toward Thermoplastic Lignin Polymers. Part 1. Selective Masking of Phenolic Hydroxyl Groups in Kraft Lignins via Methylation and Oxypropylation Chemistries. *Industrial and Engineering Chemistry Research*, 51, 16713-16720.
- Sailaja, R.R.N., Deepthi, M.V. **2010**. Mechanical and thermal properties of compatibilized composites of polyethylene and esterified lignin. *Material design*, 331, 4360-4379.
- Saito, T., Brown, R.H., Hunt, M.A., Pickel, D.L., Pickel, J.M., Messman, J.M., Baker, F.S., Keller, M., Naskar, A.K. **2012**. Turning renewable resources into value-added polymer: development of lignin-based thermoplastic. *Green Chemistry*, 14, 3295-3303.
- Sauter, T., Heuchel, M., Kratz, K., Lendlein, A. **2013**. Quantifying the Shape-Memory Effect of Polymers by Cyclic Thermomechanical Tests. *Polymer Reviews*, 53, 6-40.
- Scholl, M., Nguyen, T.Q., Bruchmann, B., Klok, H.A. **2007**. Controlling polymer architecture in the thermal hyperbranched polymerization of L-Lysine. *Macromolecules*, 40, 5726-5734.

Sivasankarapillai, G., McDonald, A.G. **2011**. Synthesis and properties of lignin-highly branched poly (ester-amine) polymeric systems. *Biomass and Bioenergy*, 35, 919-931.

Sivasankarapillai, G., McDonald, A.G., Li, H. **2012**. Lignin valorization by forming toughened lignin-co-polymers: Development of hyperbranched prepolymers for cross-linking. *Biomass and Bioenergy*, 47, 99-108.

Stumbe, J.F., Bruchmann, B. **2004**. Hyperbranched polyesters based on adipic acid and glycerol. *Macromolecular Rapid Communications*, 25, 921-924.

Teng, N.-Y., Dallmeyer, I., Kadla, J.F. **2013**. Effect of Softwood Kraft Lignin Fractionation on the Dispersion of Multiwalled Carbon Nanotubes. *Industrial and Engineering Chemistry Research*, 52, 6311-6317.

Teramoto, N. **2011**. Synthetic green polymers from renewable monomers, in: Sharma, S.K., Mudhoo, A. (Eds.), *A Handbook of Applied Biopolymer Technology: Synthesis, Degradation and Applications*. Royal Society of Chemistry, pp. 22-78.

Valverde, M., Yoon, S., Bhuyan, S., Larock, R.C., Kessler, M.R., Sundararajan, S. **2011**. Rubbers Based on Conjugated Soybean Oil: Synthesis and Characterization. *Macromolecular Materials and Engineering*, 296, 444-454.

Voit, B.I., Lederer, A. **2009**. Hyperbranched and Highly Branched Polymer Architectures- Synthetic Strategies and Major Characterization Aspects. *Chemical Reviews*, 109, 5924-5973.

Wagermaier, W., Kratz, K., Heuchel, M., Lendlein, A. **2010**. Characterization Methods for Shape-Memory Polymers, in: Lendlein, A. (Ed.), *Shape-Memory Polymers*. Springer-Verlag Berlin, pp. 97-145.

Wei, L., Guho, N.M., Coats, E.R., McDonald, A.G. **2014**. Characterization of Poly(3-hydroxybutyrate-co-3-hydroxyvalerate) Biosynthesized by Mixed Microbial Consortia Fed Fermented Dairy Manure. *Journal of Applied Polymer Science*, 131, 40333-40344.

Wu, L.C.F., Glasser, W.G. **1984**. Engineering plastics from lignin. I. Synthesis of hydroxypropyl lignin. *Journal of Applied Polymer Science*, 29, 1111-1123.

Xie, T. **2010**. Tunable polymer multi-shape memory effect. *Nature*, 464, 267-270.

Xie, T. **2011**. Recent advances in polymer shape memory. *Polymer*, 52, 4985-5000.

Yakacki, C.M. **2013**. Shape-Memory and Shape-Changing Polymers. *Polymer Reviews*, 53, 1-5.

Zakzeski, J., Bruijninx, P.C.A., Jongerius, A.L., Weckhuysen, B.M. **2010**. The Catalytic Valorization of Lignin for the Production of Renewable Chemicals. *Chemical Reviews*, 110, 3552-3599.



## 4 Lignin Valorization by Forming Thermally-stimulated Shape Memory Copolymeric Elastomers - Partially Crystalline Hyperbranched Polymer as Crosslinks

### 4.1 Abstract

Lignin based thermal-responsive elastomers were produced by a melt polycondensation reaction with a long alkyl chain hyperbranched poly(ester-amine-amide) ( $B_3-A_2-CB_3^1$ ). The effect of lignin content on elastomers properties was investigated. The thermal and mechanical properties of the copolymers were characterized by DMA, DSC, and TGA. The morphology of the copolymer was examined by SEM. Tensile properties were dominated by HBP <25% lignin content while lignin dominated >25% content. The copolymers glass transition temperature ( $T_g$ ) increased with lignin content. The elastomer with 30% lignin content demonstrated optimal mechanical properties (tensile strength 5.3 MPa, Young's modulus 8.9 MPa, strain at break 301%, and toughness 1.03 GPa). Thermally-stimulated dual shape memory effects (SME) of the copolymers were quantified by cyclic thermomechanical tests. The transition temperature ( $T_{trans}$ ) of the polymer was able to be controlled (room to body temperature) by varying the amount of lignin added which broadens the range to medical applications.

### 4.2 Introduction

Lignin is an underutilized biopolymer byproduct from both the pulping (about  $5 \times 10^{10}$  kg produced in 2004) and cellulosic ethanol industries and shows potential as a substrate for producing bioplastic materials (Zakzeski et al., 2010). Lignin's utilization is hampered by its high glass transition temperature ( $T_g$ ) and brittleness due to its high intra/inter H-bonding. Applications for lignin has been to incorporate it as a filler, extender or as a reinforcing pigment in rubber (Wang et al., 1992) and in thermoset resins (Feldman, 2002). Another approach to alter lignin properties, such as thermoplasticity, has been chemically modified such as alkylation (Li and Sarkanen, 2002), benzylation (McDonald and Ma, 2012), and oxypropylation (Cui et al., 2013; Li and Ragauskas, 2012; Sadeghifar et al., 2012; Wu and

Glasser, 1984), which inhibits intramolecular H-bonding and thus lower's its  $T_g$ . More recent work has been using lignin as a hard segment in the preparation of highly and hyper branched elastomeric copolymers with tunable properties (Li et al., 2014; Sivasankarapillai and McDonald, 2011; Sivasankarapillai et al., 2012). The properties were easily tuned by changing the copolymer structure and lignin content.

Hyperbranched polymers (HBP) are an attractive type of dendritic polymer due to its high branching density and structure (Voit and Lederer, 2009). HBP based on polyesters are attractive due to the availability of monomers (e.g. symmetric diacid ( $A_2$ ) and trihydroxy ( $B_3$ )) and ease of preparation by polycondensation. To increase the structural diversity of the HBP combinations of various branched structures are required such as  $A_2$ ,  $B_3$  and trihydroxy-monoamino ( $CB_3^1$ ) monomer units. The key of this approach is the employment of multifunctional monomers with suitable unequal reactivity, where both B and C can react with an A group, as a result, hyperbranched polyesters with amine cores and amide linkages can be formed (Li et al., 2006; Li et al., 2005; Li et al., 2004; Sivasankarapillai et al., 2012). A series of lignin HBP-copolymer have been formed by melt condensation using the monomers: adipic acid ( $A_2$ ), triethanolamine (TEA,  $B_3$ ) and tris(hydroxymethyl)aminomethane (THAM,  $CB_3^1$ ). The advantage of this system was that TEA acted as the reaction solvent and catalyst, and THAM introduced the amide linkage and increased the complexity of the structure. Furthermore, these lignin HBP copolymers showed interesting thermal properties and elasticity (Sivasankarapillai and McDonald, 2011; Sivasankarapillai et al., 2012).

Dodecanedioic acid (DDDA) is a  $C_{12}$  diacid which has been extensively applied to polymer synthesis with superior thermal and mechanical properties. Furthermore, DDDA was also involved medical polymer synthesis because of its solubility in water, low acidity and being biocompatible (Guo and Huang, 2004; Wu et al., 2008). Barbiroli et al. (2003) synthesized a series polyethylene-like polymers with DDDA and different alkyl chain diols and were shown to have melting and crystalline behavior. Nagata (2001) produced polyesteramines based on TEA and different alkyl-chain length diacids including DDDA. The polyesteramines made with DDDA showed a  $T_g$  at  $-34^\circ\text{C}$  and melting temperature ( $T_m$ ) at  $13^\circ\text{C}$ . Melting peaks were also

found in HBP based on diacid-TEA which demonstrated a crystalline surface and amorphous interior (Sivasankarapillai and McDonald, 2011; Sivasankarapillai et al., 2012).

Based on previous research (Sivasankarapillai et al., 2012), we hypothesize that the hyperbranched prepolymers (based on using the diacid DDDA) when copolymerized with lignin (as the rigid netpoint segment) will have a good elasticity and shape memory properties. This current study will investigate the elastomers from copolymerization of DDDA-based hyperbranched prepolymer with lignin. The effect of lignin content on thermal, mechanical, and SME properties of elastomers were studied.

### 4.3 Materials and Methods

#### 4.3.1 Materials

Protobind 1000 soda lignin was supplied by ALM India Pvt. Ltd. The methanol soluble fraction of the soda lignin was used for copolymer synthesis (lignin content = 93.3%,  $M_w = 958$  g/mol (ESI-MS), aromatic/aliphatic hydroxyl group ratio = 0.93,  $T_g = 138$  °C (MTDSC)) (Li and McDonald, 2014; Li et al., 2014). TEA, THAM, DDDA, methanol and tetrahydrofuran (THF) were obtained from Acros Organics and used as received.

#### 4.3.2 Methods

##### 4.3.2.1 Synthesis of hyperbranched prepoly(ester-amine-amide) (D1)

The synthetic method was described in our previous work (Li et al., 2014). The mixture of TEA (2.98 g, 0.02 mol), THAM (2.42 g, 0.02 mol), and DDDA (9.21g, 0.04 mol) with mole ratio 1:1:2 was prepared in a beaker (50 mm dia), then the beaker was placed in a preheated vacuum oven. The polycondensation reaction was controlled to below 650 mm Hg at 100 °C for 13 h. The D1 prepolymer was a yellow-pale solid at room temperature.

Yield: 95%; IR (ATR,  $\text{cm}^{-1}$ ):  $\nu = 3500\text{-}3200$  (vb;  $\nu(\text{OH stretching})$ ), 2923 (vs;  $\nu_{\text{as}}(\text{CH}_2)$ ), 2853 (vs;  $\nu_{\text{s}}(\text{CH}_2)$ ), 2500 (vb; (OH of COOH)), 1730 (vs; (C=O from ester)), 1651 (vs; (C=O from amide)), 1555 (b; (N-H and  $\text{COO}^-$ )), 1455 (w, (CH<sub>2</sub>)), 1391 (w; (OH)), 1169 and 1140  $\text{cm}^{-1}$  (vs; (COO in ester));  $^1\text{H NMR}$  (500 MHz,  $\text{DMSO-}d_6$ ,  $\delta$ ): 7.44, 7.24, and 7.11 (s,  $\text{NHCOO}$ ), 4.00-4.06 (m,

NCH<sub>2</sub>CH<sub>2</sub>O), 3.49-3.62 (m, C(CH<sub>2</sub>)<sub>3</sub>O), 3.39-3.46 (m, NCH<sub>2</sub>CH<sub>2</sub>OH), 2.72-2.79 (m, NCH<sub>2</sub>CH<sub>2</sub>O), 2.56-2.63 (m, NCH<sub>2</sub>CH<sub>2</sub>OH), 2.50 (p, DMSO-d<sub>6</sub>), 2.25-2.31 (m, OOCCH<sub>2</sub>CH<sub>2</sub>), 2.17-2.23 (m, HOOCCH<sub>2</sub>CH<sub>2</sub>), 1.45-1.57 (m, OOCCH<sub>2</sub>(CH<sub>2</sub>)<sub>8</sub>CH<sub>2</sub>COO); <sup>13</sup>C NMR (125.76 MHz, DMSO-d<sub>6</sub>, δ): 174.79 (C=O), 173.86, 173.38 (NHCO), 172.83, 172.61, 166.44 (CH<sub>2</sub>OCO), 76.09, 74.19, 71.87, 62.19, 60.28 (C(CH<sub>2</sub>OCO)<sub>n</sub>(CH<sub>2</sub>OH)<sub>3-n</sub>), 70.40, 70.18, 65.86, 64.08, 61.91, 61.69, 60.88, 60.47, 59.85(C(CH<sub>2</sub>OCO)<sub>n</sub>(CH<sub>2</sub>OH)<sub>3-n</sub>), 62.16 (NCH<sub>2</sub>CH<sub>2</sub>O), 59.38, 59.33 and 59.17 (NCH<sub>2</sub>CH<sub>2</sub>OH), 57.14, 56.96, and 56.74 (NCH<sub>2</sub>CH<sub>2</sub>OH), 53.04, 52.96 and 52.78 (N-CH<sub>2</sub>-CH<sub>2</sub>-O), 35.86 (OCOCH<sub>2</sub>(CH<sub>2</sub>)<sub>8</sub>CONH), 34.07 (HOOC-CH<sub>2</sub>-CH<sub>2</sub>-), 33.51 (OOCCH<sub>2</sub>CH<sub>2</sub>), 28.84, 28.71, 28.59, 28.44, 24.66, 24.39, (OCOCH<sub>2</sub> (CH<sub>2</sub>)<sub>8</sub>CH<sub>2</sub>COO).

#### 4.3.2.2 Synthesis of lignin-copoly(ester-amine-amide) (lignin-D1-copolymer)

Lignin was dispersed in the minimum amount of THF and mixed with prepolymer D1 proportionally to synthesize the lignin-copoly(ester-amineamide) (lignin-D1-copolymer). THF was then removed under a stream of N<sub>2</sub> at 80°C. The highly viscous mixture was then transferred to a prepared aluminum pan (15 x 15 cm<sup>2</sup>) and was placed into vacuum oven at 80°C and 750 mm Hg to remove residual solvent and moisture (about 30 min). Then the reaction temperature was increased to 120°C at 650 mm Hg, and the reaction proceeded for 40 h. The final lignin-D1-copolymer displayed a highly bright and glossy surface and was insoluble in organic solvents. The D1 prepolymer was fully polymerized as described above as a control sample (D1 polymer). The synthesis approach is shown in Figure 4.1.

IR (ATR, cm<sup>-1</sup>): ν = 3500-3200 (vb; ν(OH stretching)), 2945 (vs; ν<sub>as</sub>(CH<sub>2</sub>)), 2870 (vs; ν<sub>s</sub>(CH<sub>2</sub>)), 1729 (vs; (C=O from ester)), 1651 (s; (C=O from amide)), 1600 (m; aromatic skeletal vibration), 1549 (w; N-H bending), 1511 (m; aromatic skeletal vibration), 1457 (w, (CH<sub>2</sub>)), 1419 (w, CH in-plane deformation), 1378 (w, CH<sub>3</sub>), 1169 and 1140 cm<sup>-1</sup> (vs; (COO in ester)).

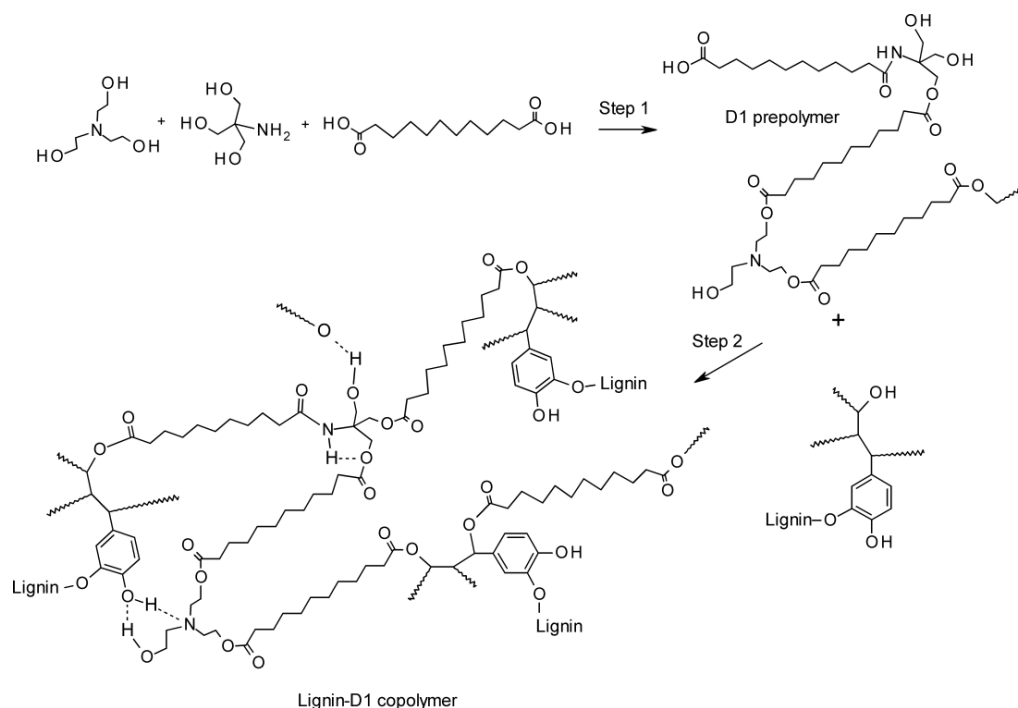


Figure 4.1 Synthesis approach for producing the lignin-D1-copolymer

### 4.3.3 Characterization techniques

#### 4.3.3.1 FTIR and NMR

All Fourier transform infrared (FTIR) spectra were carried out with a ThermoNicolet Avatar 370 spectrometer operating in the attenuated total reflection (ATR) mode (Smart performance, ZnSe crystal). <sup>1</sup>H and <sup>13</sup>C nuclear magnetic resonance (NMR) spectra were obtained on prepolymer D1 and acetylated lignin (Capanema et al., 2004) on a Bruker Avance 500 spectrometer. Chemical shifts were referenced to DMSO-d<sub>6</sub> at 39.5 for <sup>13</sup>C and 2.50 for <sup>1</sup>H spectra at 30°C.

#### 4.3.3.2 Electrospray Ionization – MS

Molar mass of the lignin and D1 prepolymer samples were determined by positive ion ESI-MS on a LCQ-Deca instrument (Thermo Finnigan). Samples were dissolved in methanol (1 mg/mL) containing 1% acetic acid and introduced into the ESI source at a flow rate of 10 μL/min (Osman et al., 2012). The ion source and capillary voltages were 4.48 kV and 47V, respectively, at a temperature of 275°C. The MS were scanned between m/z (mass to charge

ratio) 100 and 2000. The number average molar mass ( $M_n$ ) was calculated as  $M_n = \sum M_i N_i / \sum N_i$  and weight average molar mass ( $M_w$ ) as  $M_w = \sum M_i^2 N_i / \sum M_i N_i$ , where  $M_i$  and  $N_i$  are the  $m/z$  and intensity of the ions, respectively (Parees et al., 1998).

#### 4.3.3.3 Thermal and Mechanical analysis

Differential scanning calorimetry (DSC) was performed on a TA instruments model Q200 DSC equipped with a refrigeration cooling unit to monitor the thermal behavior of materials. Modulated temperature DSC (MTDSC) mode was applied. The lignin and polymers (5-7 mg) were equilibrated at  $-50^\circ\text{C}$  for 5 min, then heated by modulated heating  $\pm 0.66^\circ\text{C}$  every 50 s, and then ramped from  $-50$  to  $180^\circ\text{C}$  at  $5^\circ\text{C}/\text{min}$ . The inflection point of heat flow change from reversible heat flow curve was assigned as  $T_g$ . Thermogravimetric analysis (TGA) was performed on a TGA-7 (Perkin Elmer) instrument from  $50$  to  $900^\circ\text{C}$  at a heating rate of  $20^\circ\text{C}/\text{min}$  in  $\text{N}_2$ . Dynamic mechanical analysis (DMA) experiments were performed using a TA Instruments model Q800 DMA, both under isothermal and non-isothermal conditions in  $\text{N}_2$  atmosphere in the tensile mode ( $12 \text{ mm} \times 4 \text{ mm} \times 0.2 \text{ mm}$ ). The heating scans were carried out at 1 Hz and at a heating rate of  $3^\circ\text{C}/\text{min}$ . The tensile properties of the lignin based elastomers (in triplicate) were measured using DMA at room temperature with ramp  $3 \text{ N}/\text{min}$ . Specifically, energy at break was determined as the area of the stress-strain curve.

The SME of lignin based copolymers were determined in the tensile mode using a DMA. A stress-controlled cycle thermomechanical test was applied. Four programming steps were proceeded, in which the copolymers were: (1) heated to a temperature of  $T_g + 20^\circ\text{C}$  (designated as  $T_{\text{high}}$ ) with ramp of  $5^\circ\text{C}/\text{min}$ , then set load to 2 N static force with ramp of  $0.2 \text{ N}/\text{min}$ , the copolymers were stretched to temporary shapes; (2) in the next step, cooled to  $T_g - 20^\circ\text{C}$  (ramp  $5^\circ\text{C}/\text{min}$ ) (designated as  $T_{\text{low}}$ ); and (3) release the static force while keeping at  $T_{\text{low}}$ , the copolymers kept the temporary shapes; (4) heated up to  $T_{\text{high}}$  again and kept isothermal for 15 min, the permanent shape recovered again. The same procedure was repeated for 3 times (cycle 1 to 3). The recovery elasticity of lignin based elastomers also applied the stress-controlled cycle mechanical test at  $30^\circ\text{C}$ . In detail, elastomers were stretched to approximate 100 % strain which was achieved by controlling the force

determined by measuring stress at 100% strain from tensile test results, then multiplying the cross sectional area of the sample. Then release the loaded force and hold for 15 min to recover back to the original length and the procedure repeated for 4 further times.

The crosslink density ( $\eta$ ) and molar mass between crosslinks ( $M_c$ ) was determined by equation (4.1) referring to the theory of rubber elasticity (Tran et al., 2010):

$$\eta = \frac{E_0}{3RT} = \frac{\rho}{M_c} \quad (4.1)$$

Where  $\eta$  is the number of active network chain segments per unit volume ( $\text{mol/m}^3$ );  $M_c$  is the molar mass between crosslinks ( $\text{g/mol}$ );  $E_0$  is Young's modulus from tensile strength ( $\text{Pa}$ );  $R$  is the universal gas constant ( $8.314 \text{ J/mol/K}$ );  $T$  is the absolute temperature ( $\text{K}$ ); and  $\rho$  is polymer density ( $\text{g/m}^3$ ) as measured from punched disc samples (3 mm diameter and 2mm thickness) ( $n=5$ ).

#### 4.3.3.4 Morphological analysis

Field emission scanning electron microscopy (SEM) was performed on a FEI Quanta 200F instrument at 10 kV. The cut cross-sections were dried and sputter coated with gold prior to examination.

### 4.4 Results and Discussion

#### 4.4.1 Preparation of D1 prepolymer and lignin-D1-copolymers

The prepolymer D1 ( $\text{B}_3+\text{A}_2+\text{CB}_3^1$ ) was prepared according to our previous procedure (Figure 4.1) The diacid, DDDA, was used because of its long alkyl chain length and this can partially crystallize with other DDDA units in the HBP. This will provide additional structural features to the lignin-D1-copolymer and possessed a  $T_g$  above room temperature (Nagata et al., 2001; Sivasankarapillai et al., 2012). The amine core with amide linkage endowed a complex structure and strengthened properties. The resulting polymers were slightly yellowish in color and were highly viscous at elevated temperature and solid at room temperature. Ester and secondary amide formation were confirmed by FTIR ( $1730$ ,  $1651$ , and  $1555 \text{ cm}^{-1}$ ) and  $^{13}\text{C}$  NMR ( $173.86$ ,  $173.38$ ,  $172.83$ ,  $172.61$ ,  $166.44 \text{ ppm}$ ). The carboxylic acid group ( $174 \text{ ppm}$ ) in

the D1 prepolymer and the hydroxyl group ( $3500\text{ cm}^{-1}$ ) in lignin were monitored for their depletion during esterification. Furthermore, acid ( $\text{CH}_2\text{COOH}$  2.20 ppm) conversion to ester ( $\text{CH}_2\text{COO}$ -ester 2.30 ppm and  $\text{CH}_2\text{CONH}$ - amide 2.17 ppm) could be determined by  $^1\text{H}$  NMR and 61 % acid groups were available for the subsequent polycondensation, where acid group remaining =  $I_{2.20}/(I_{2.20}+I_{2.30}+I_{2.17})$  (Stumbe and Bruchmann, 2004). The degree of branching (DB) for the D1 prepolymer was determined by  $^1\text{H}$  NMR and chemical shifts at 7.44, 7.24, and 7.11 ppm were assigned to semi-dendritic (sD), linear (L) and terminal (T) structures without dendritic structure, respectively (Sivasankarapillai et al., 2012). From these assignments and peak intensity the DB was calculated at 0.256, where  $\text{DB} = 2\text{D} / (\text{L}+2\text{D})$  (Hawker et al., 1991). The calculated value revealed a low cross-link occurrence during prepolymerization. The  $M_w$  (831 g/mol) and polydispersity index (1.74) of D1 were determined by ESI-MS. The low  $M_w$  obtained was consistent with a low DB.

The synthesis route for the lignin-D1-copolymer was carried out with a two-step one-pot bulk polymerization (melt polycondensation) process (Figure 4.1) (Scholl et al., 2007). The lignin based elastomer formulation was adjusted by varying lignin content in order to properties. In some preliminary work, lignin content >35% in the copolymer was shown to be brittle and tensile properties could not be determined successfully. Therefore, lignin-D1-copolymers with lignin contents from 0 to 35% were chosen for full evaluation.

The lignin-D1-copolymers, D1 polymer and original lignin were analyzed by FTIR spectroscopy (Figure 4.2). Ester formation between lignin and D1 prepolymer was supported by the reduction of the OH band ( $3600\text{-}3100\text{ cm}^{-1}$ ) and an increase in the ester carbonyl band ( $1729\text{ cm}^{-1}$ ). The ester band at  $1729\text{ cm}^{-1}$  (Normally at  $1740\text{ cm}^{-1}$ ) was affected by H-bonding between lignin and prepolymer as proposed in Figure 4.1. As lignin content increased, four functional groups changed dramatically, which involved a reduction of the amide I ( $1651\text{ cm}^{-1}$ ) and amide II ( $1549\text{ cm}^{-1}$ ) bands, as well as an increase of lignin aromatic skeletal vibration bands at  $1600$  and  $1511\text{ cm}^{-1}$ . The reduction of amide bands with an increase in lignin content supports that amide formation was essentially complete during prepolymerization and not participate with linkage to lignin (Bayer, 1947). Furthermore, no



band at  $1762\text{ cm}^{-1}$  (characteristic of an aromatic carbonyl ester) was observed suggesting that the prepolymer was ester linked with aliphatic hydroxyl groups of lignin (Figure 4.2).

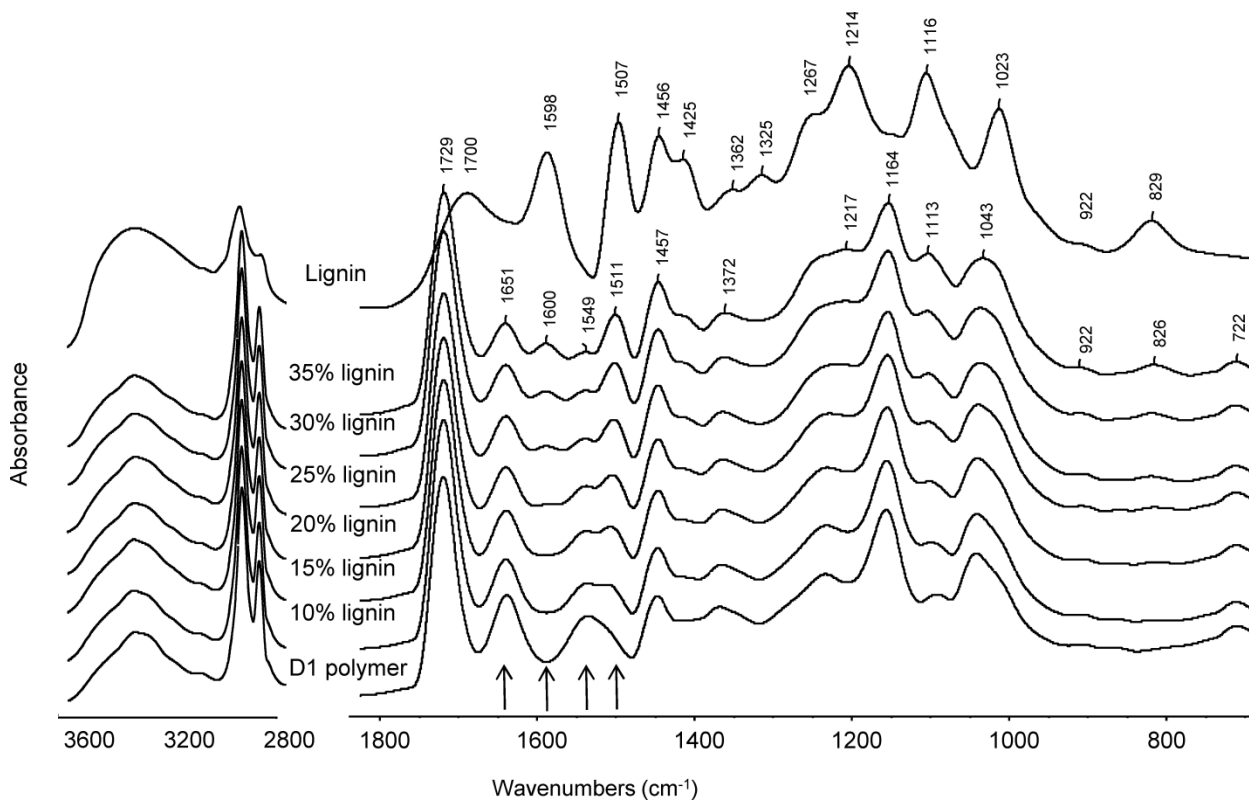


Figure 4.2 FTIR spectra of lignin, D1 polymer and lignin-D1-copolymers

#### 4.4.2 Mechanical properties

The tensile properties of lignin copolymers are shown in Figure 4.3. Generally, the tensile strength and Young's moduli of the lignin copolymers were shown to increase with lignin content. For example, the tensile strength increased from 0.7 to 2.7 MPa when lignin content increased from 0 to 25% then dramatically increased to 7.0 MPa at 35% lignin content. A similar trend was observed for the Young's modulus. The observed phenomena might be explained since lignin is acting as a reinforcing agent thus improving the mechanical properties of the copolymer due to high levels of crosslinking between the rigid lignin structure and prepolymer. The strain at break and toughness (as assessed by the energy at break (EAB)) of the copolymers are shown in Figure 4.3b. All the lignin copolymers showed excellent strain at break values due to the presence of the long chains of DDDA in the

prepolymer. The copolymer strain at break and EAB reached values of 301% and 1.03 GPa, respectively at a lignin content of 30%. However, at 35% lignin content both the strain at break and EAB decreased indicating that the lignin was contributing to its brittleness. Therefore, the optimal lignin content in the copolymers for good elastomeric properties was 30%.

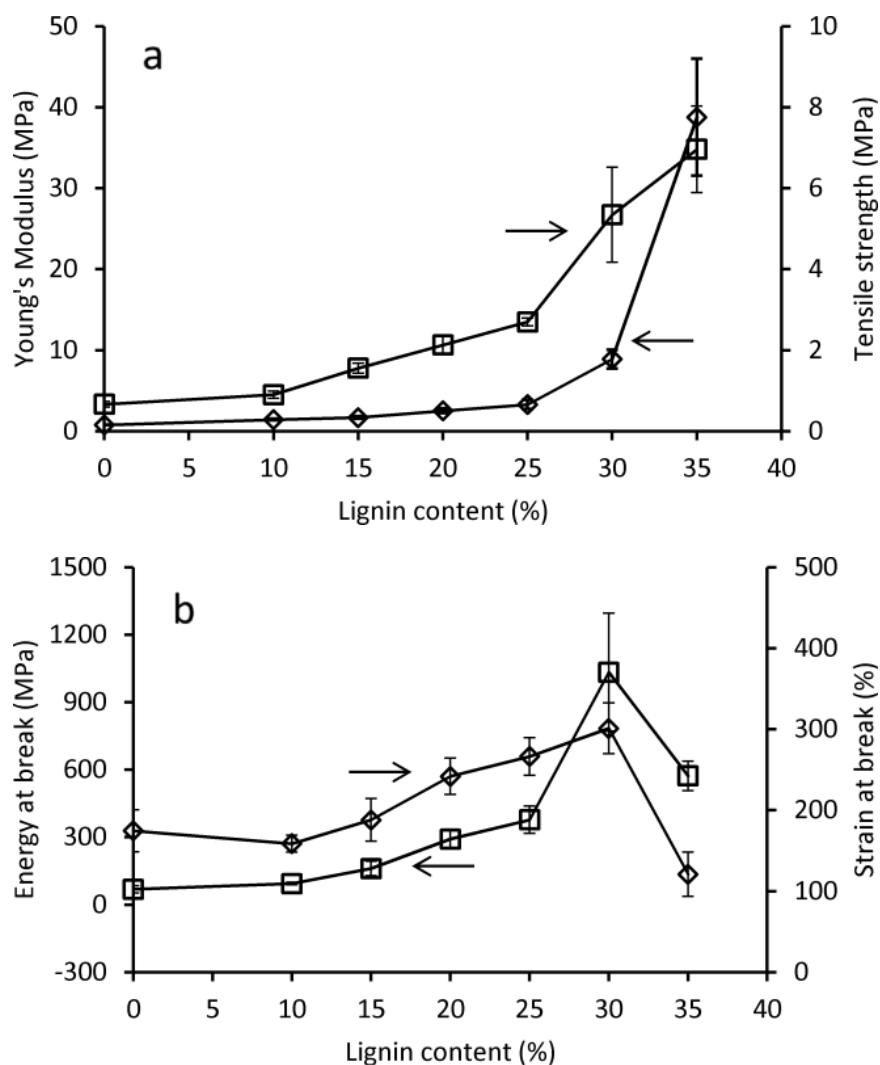


Figure 4.3 Tensile properties of lignin-D1-copolymers

#### 4.4.3 Thermal properties

Thermal properties of the lignin copolymers were characterized by MTDSC and DMA (Figure 4.4). The D1 polymer has a  $T_g$  of 4.4°C and a sharp melting peak at 18.5°C which had been observed in previous reports (Nagata et al., 2001; Sivasankarapillai and McDonald, 2011;

Sivasankarapillai et al., 2012). A sharp endothermic melting peak was due to the crystallization of the methylene units in long diacid chains (Nagata et al., 2001). The melting peak decreased considerably as lignin content increased and disappeared above 20% lignin content. This result can be explained since the amorphous nature of lignin is intertwined with the D1 matrix and interrupted the long chain crystalline state. The  $T_g$  is a second-order phase transition of an amorphous polymer which not only confines its threshold in engineering applications and determine the shape memory effect of smart polymers (Lendlein and Kelch, 2002; Overley et al., 2000). The determination of  $T_g$  of the lignin copolymers was quantified by reversible heat flow of MTDSC and DMA from the maxima of the loss modulus ( $E''$ ) peak (Figure 4.4b). All the lignin copolymers demonstrated an appreciably low and single  $T_g$  although lignin itself has a high  $T_g$  (138 °C). These results indicate the dominating effect of the D1 structure and the excellent miscibility between lignin and D1 over the lignin content range studied. Little  $T_g$  variations were found (5.3 to 7.7 °C) below 30% lignin content by DMA. However, above 30% lignin the  $T_g$  increased to a maximum of 16.8 °C at 35%. The MTDSC results of the lignin copolymers also showed similar trend but displayed relative lower  $T_g$  values than those from DMA (Fox and McDonald, 2010; Pohjanlehto et al., 2014).

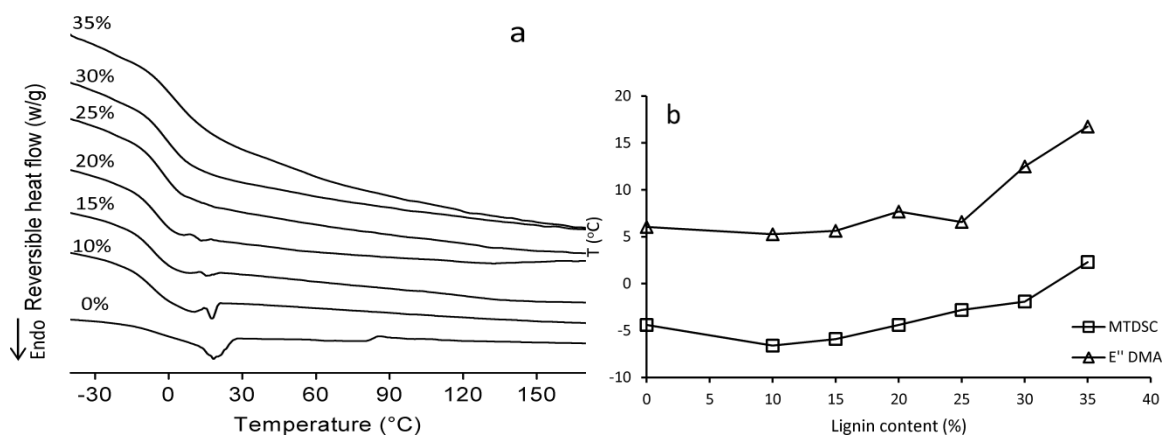


Figure 4.4 (a), MTDSC thermograms of lignin-D1 copolymers showing the reversible heat flow; and (b),  $T_g$  values of lignin-D1-copolymers from  $E''$  of DMA and MTDSC.

#### 4.4.4 Cross-link properties

The condensation reaction between the HBP D1 and lignin at different ratios will influence cross-link density ( $\eta$ , active network chain segments per unit volume) and therefore polymer properties. Thus varying degree of cross-linking shows promise to tailor polymer properties. The  $T_g$  of polymers can be increased by increasing cross-link density (Xin et al., 2014). Density ( $\rho$ ),  $\eta$ , and molar mass between crosslinks ( $M_c$ ) were determined according to eqn 4.1 and results are shown in Figure 4.5. The  $\rho$  of lignin copolymers was shown to range from 1.13 to 1.25 g/cm<sup>3</sup> which are in the region of commercial elastomers (Meier, 1996). The  $\eta$  for the lignin copolymers showed a dramatic increase from 104 mol/m<sup>3</sup> for the control D1 polymer to 5,182 mol/m<sup>3</sup> for the lignin-D1-copolymer at 35% lignin content. In contrast, the polymer  $M_c$  was shown to decrease from 10,800 g/mol for the D1 polymer to 226 g/mol for the lignin-D1-copolymer at 35% lignin. The results indicate that reacting lignin with the D1 prepolymer matrix led to cross-linked copolymers. High correlation between  $\eta$  and  $T_g$  from  $E''$  were achieved as shown in Figure 4.5c indicating positive relations between the two parameters. Furthermore, reacting lignin with the D1 prepolymer matrix forms a tightly packed network structure and improved tensile and thermal properties as discussed above.

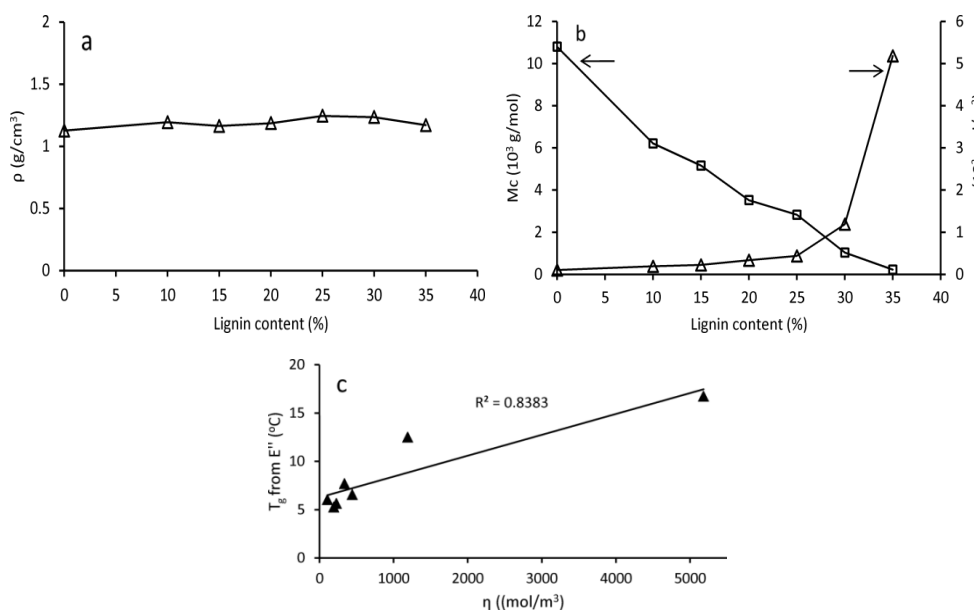


Figure 4.5 Bulk density ( $\rho$ ) (a), cross-link density ( $\eta$ ) and molecular weight between crosslinks ( $M_c$ ); and (b), correlation between  $\eta$  and  $T_g$  (c) of lignin-D1-copolymers

#### 4.4.5 Thermal stability

The thermal stability of the lignin copolymers was studied by TGA. Three stages of decomposition were observed by TGA for all lignin copolymers (Table 4.1 and Figure 4.6). To observe decomposition transitions differential TGA (DTG) was also performed (Figure 3.6). The first stage was between 170 and 380°C. The second stage was between 380 and 500°C. The third stage was between 500 and 650°C. The first and second stages are most likely assigned to the D1 component of the copolymer since these are constituted with highly branched aliphatic chains with labile ester linkages (Pramanik et al., 2014; Pramanik et al., 2013), although side chain of lignin also participated the decomposition (Figure 4.6). The long DDDA chains in D1 likely forms crystalline zones in the copolymer and will decompose at temperature range from 420 to 480°C (2<sup>nd</sup> stage herein) (Prime et al., 2009). The 3<sup>rd</sup> stage of decomposition is most likely due to the lignin component of the copolymer because of its highly cross-linked aromatic structure to form appreciable amount of char (Nassar and MacKay, 1984). Lignin content affected the 3<sup>rd</sup> stage decomposition residual mass such as 23.5% mass remaining at 580°C with a copolymer lignin content of 35%. Two DTG peaks (490 and 615°C) were observed in copolymers and assigned to D1 and lignin components, respectively.

Table 4.1 Thermal decomposition of lignin based long chain elastomers

Lignin content (%)	1st stage		2nd stage		3rd stage		Max peaks (°C)
	T (°C)	Remaining mass (%)	T (°C)	Remaining mass (%)	T (°C)	Remaining mass (%)	
0	422	82.0	496	11.2	565	7.2	480
10	408	81.2	489	16.8	575	11.1	480, 600
15	409	80.9	499	17.5	576	12.8	491, 613
20	366	90.0	498	21.2	580	16.2	490, 612
25	360	88.5	500	25.0	583	19.1	492, 616
30	379	87.5	487	29.3	572	21.8	477, 615
35	359	90.1	491	30.3	581	23.5	479, 616

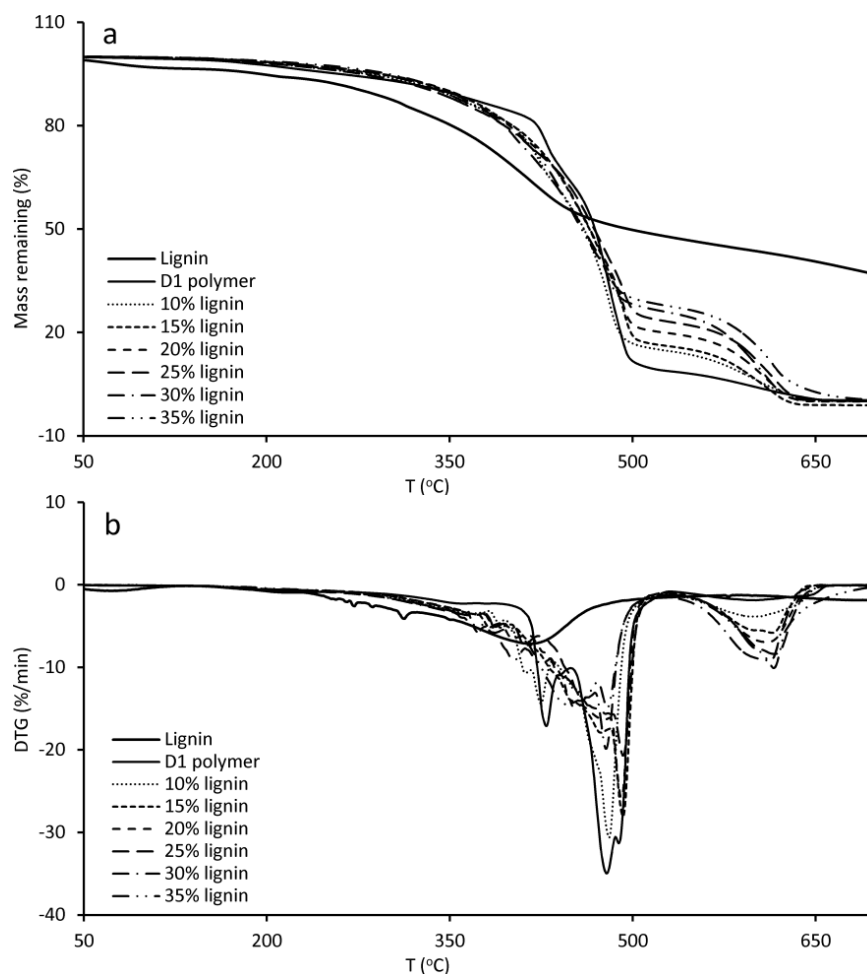


Figure 4.6 TGA (a) and DTG (b) thermograms of lignin, D1 polymer and lignin-D1 copolymers

#### 4.4.6 Thermal-stimulated shape memory effect ( $T_s$ -SME)

Thermally stimulated shape memory effect ( $T_s$ -SME) can be obtained in a polymer system which contains two kinds of segments, i.e., soft segment controlling temporary shape and netpoint segment determining permanent shape. Our previous research has shown the development of a series of lignin- copolymers with  $T_s$ -SME properties, where a short chain diacid highly branched polyesteramine prepolymer functioned as the soft segment and lignin as the netpoints segment (Li et al., 2014). Following this concept, we further modified the soft segment to be semi-crystalline by using a long chain diacid (DDDA) in the hyperbranched prepolymer. The shape memory properties of the lignin-D1-copolymers (with 15, 25 and 35%

lignin contents) were quantified by stress-controlled cyclic thermomechanical testing. Figure 4.8a shows the result of cyclic thermomechanical testing of lignin-D1-copolymer with 15% lignin content. The shape memory recovery ratio ( $R_r$ ) and fixity ratio ( $R_f$ ) were calculated from the test data according to the following equations (Lendlein and Kelch, 2002):

$$R_r(N) = \frac{\varepsilon_1(N) - \varepsilon_p(N)}{\varepsilon_1(N) - \varepsilon_p(N-1)} \times 100\% \quad (4.2)$$

$$R_f(N) = \frac{\varepsilon_u(N)}{\varepsilon_1(N)} \times 100\% \quad (4.3)$$

Where  $R_r(N)$  is the shape recovery ratio at  $N^{\text{th}}$  cycle,  $R_f(N)$  is the shape fixity ratio at  $N^{\text{th}}$  cycle,  $N$  is cycle number from 1 to 3,  $\varepsilon_1(N)$  is the maximum strain with load,  $\varepsilon_u(N)$  is the tensile strain after unloading at  $T_{\text{low}}$ ,  $\varepsilon_p(N-1)$  and  $\varepsilon_p(N)$  are the recovered strain in two successive cycles in the stress-free state before exertion of yield stress at  $T_{\text{high}}$ . The results were an average of three cycles. The same training effect was observed and attributed to the occurrence of some chain relaxation during the first mechanical cycle, leading to a deviation in the later cycles (Gautrot and Zhu, 2006, 2009; Li et al., 2014).  $R_f$  describes the ability to fix the mechanical deformation under  $T_{\text{low}}$ , while  $R_r$  quantifies how well the shape recovers in the  $N^{\text{th}}$  cycle (for  $N > 1$ ) in terms of the recovered shape of the previous  $(N-1)^{\text{th}}$  cycle (Sauter et al., 2013). The results of  $R_r$  and  $R_f$  of lignin-D1 copolymers are shown in Figure 4.7a. All measured copolymers demonstrated relative low  $R_f$  from 81 to 88%. Decreasing  $R_r$  values were observed from 98 to 83% as lignin content increased.  $R_f$  and  $R_r$  values for the lignin copolymer (at a lignin content of 35%) were  $> 95\%$  and was comparable to other lignin based elastomers (Li et al., 2014).  $T_{\text{trans}}$  is another important parameter of Ts-SME polymers and was determined since this is the temperature at which the polymer can be switched back to its original shape upon removal of external stimuli and measured as first derivative peak of the strain versus temperature plot. The  $T_{\text{trans}}$  of lignin copolymers as a function of lignin content is shown in Figure 4.7.  $T_{\text{trans}}$  was shown to increase from 24 to 36°C by increasing lignin content from 15 to 35%. These results show that  $T_{\text{trans}}$  can be tuned by varying lignin content. An interesting point to mention is that  $T_{\text{trans}}$  of 36°C is close to mammalian body temperature and these polymers have the potential to be used in medical applications and/or consumer products (Lendlein, 2002).

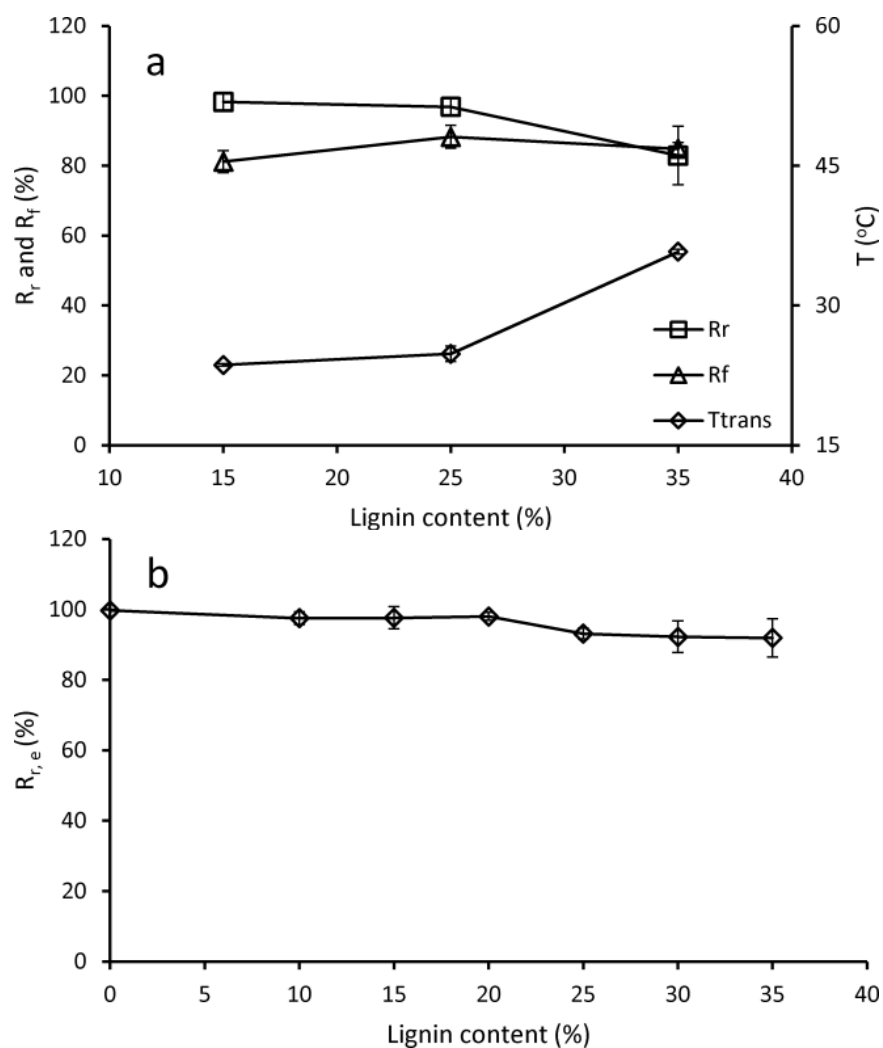


Figure 4.7 (a), Shape recovery ( $R_r$ ), shape fixity ( $R_f$ ) and  $T_{trans}$  of Ts-SME lignin-D1-copolymers determined by cyclic thermomechanical testing; and (b), Elasticity recovery ( $R_{r,e}$ ) determined at 30 °C



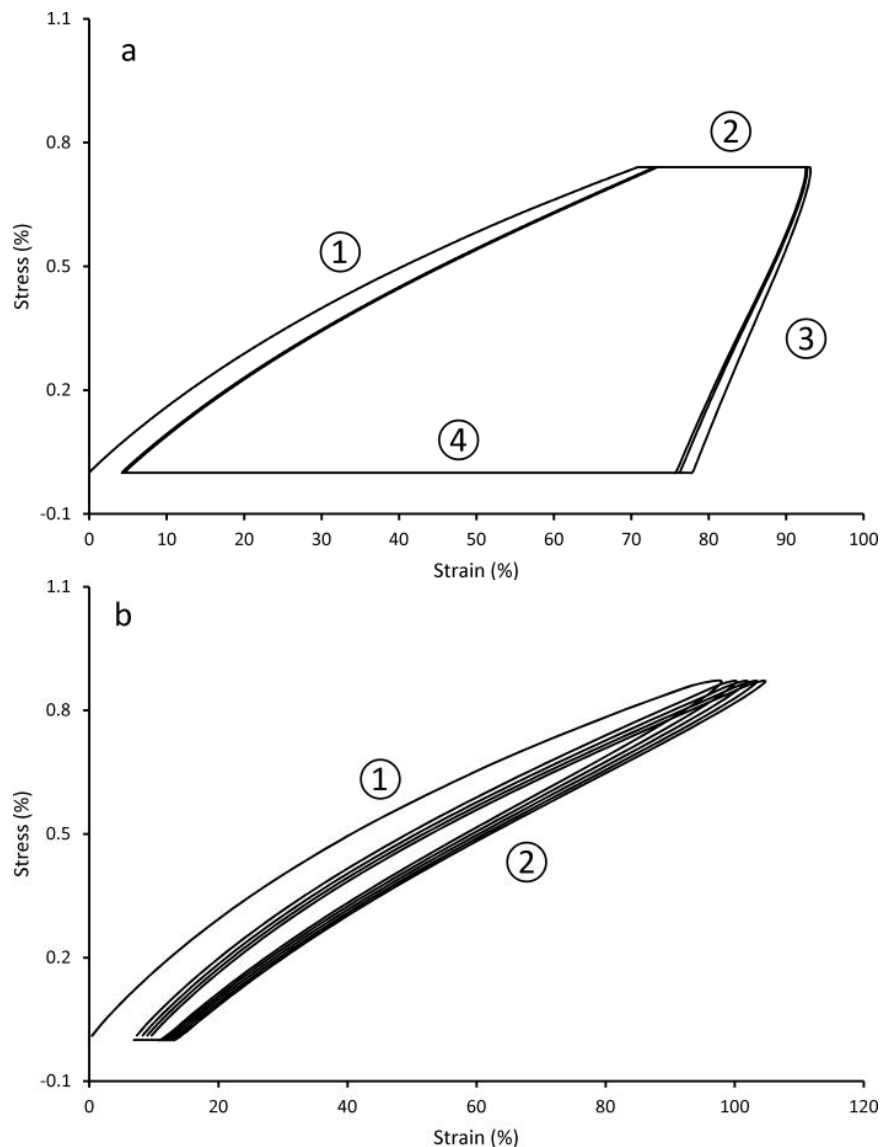


Figure 4.8 Cyclic thermomechanical testing of lignin-D1-copolymer (15% lignin content) showing (a), Ts-SME behavior (Four steps: 1, Stretching at  $T_{high}$ , 2, keep load at  $T_{low}$ , 3, unload at  $T_{low}$ , and 4, recovery at  $T_{high}$ ); and (b), elasticity recovery behavior at 30 °C (Two steps: 1, stretching at 30 °C, and 2, unload and recovery at 30 °C)

To further measure the elasticity of the lignin copolymers, cyclic tests ( $n=4$ ) were carried out to determine the recovery rate  $R_{r,e}$  (Figure 4.8b) using eqn 4.3. The lignin copolymers all demonstrated excellent  $R_{r,e}$  (>90%) values (Figure 6b). Furthermore, the more lignin added in the copolymer system, the lower the  $R_{r,e}$  will be achieved (from 100% to 92%).

#### 4.4.7 Morphological properties

The lignin-D1-copolymer morphology of cross-cut sections was examined by SEM (Figure 4.9). Good miscibility between lignin and D1 polymer was observed for all copolymers which was consistent with the results of single  $T_g$  from DSC and single peak of  $E''$  from DMA. At lignin contents between 0 and 30% a smooth cut surface was observed in the lignin-copolymers. As the lignin content increased (>35%) in the lignin-D1-copolymers the level of surface crazing increased. These observations could explain that as lignin content increased, the copolymers became more rigid, therefore, more fracture crazing was observed in the samples. An extreme example can be observed in the copolymer with 45% lignin content, which was very brittle, where high amounts of fracture were found.

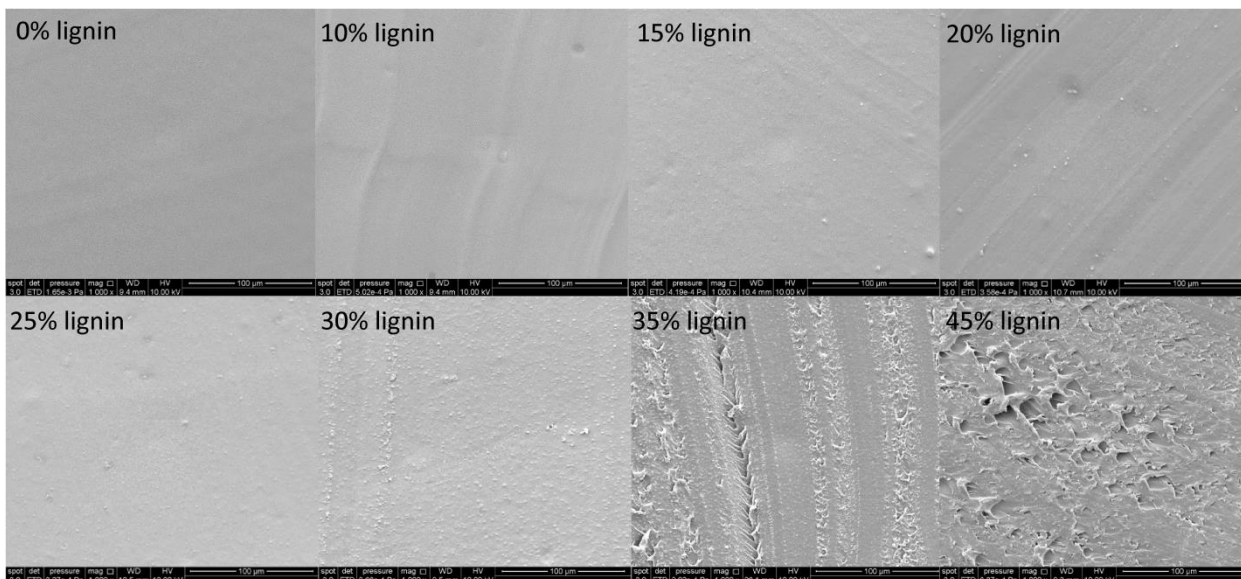


Figure 4.9 SEM micrographs of cut cross-sections of the lignin-D1-copolymers with increasing lignin content ( $\times 1000$ ).

#### 4.5 Conclusions

Lignin-copolymers with elastomeric properties were successfully developed using a long alkyl chain ( $C_{12}$ ) hyperbranched prepoly(ester-amine-amide) in a one-pot two-step bulk polycondensation reaction. Lignin-copolymer properties (tensile, thermal, and thermomechanical) were able to be tuned by variation of lignin content. The introduction of  $C_{12}$  diacid units in the hyperbranched prepolymer improved the polymer elasticity behavior

by increasing the bond length between branch points. At high lignin levels (>25%) the copolymer mechanical properties were dominated by the lignin segment while <25% lignin the properties were dominated by hyperbranched prepolymer segment. The lignin copolymer elastomers with 30% lignin content showed optimal mechanical properties and good SME behaviors. The  $T_{\text{trans}}$  of the lignin copolymers was tunable by lignin content to give a range of temperatures between room and body temperature. These developed polymer systems could be used in medical applications and consumer products where body temperature actuation of the material is required. Furthermore, this study clearly demonstrates that lignin, a renewable resource and industrial byproduct, can be used as a netpoint segment in polymer systems with SME behavior.

#### 4.6 References

Barbiroli, G., Lorenzetti, C., Berti, C., Fiorini, M., Manaresi, P. **2003**. Polyethylene like polymers. Aliphatic polyesters of dodecanedioic acid 1. Synthesis and properties. *European Polymer Journal*, 39, 655-661.

Bayer, O. **1947**. Das Di-Isocyanat-Polyadditionsverfahren (Polyurethane). *Angewandte Chemie*, 59, 257-272.

Capanema, E.A., Balakshin, M.Y., Kadla, J.F. **2004**. A comprehensive approach for quantitative lignin characterization by NMR spectroscopy. *Journal of Agricultural and Food Chemistry*, 52, 1850-1860.

Cui, C.Z., Sadeghifar, H., Sen, S., Argyropoulos, D.S. **2013**. Toward Thermoplastic Lignin Polymers; Part II: Thermal & Polymer Characteristics of Kraft Lignin & Derivatives. *BioResources*, 8, 864-886.

Feldman, D. **2002**. Lignin and its polyblends -- a review, in: Hu, T.Q. (Ed.), *Chemical modification, properties, and usage of lignin*. Kluwer Academic/Plenum, New York, pp. 81-99.

Fox, S.C., McDonald, A.G. **2010**. Chemical and Thermal Characterization of Three Industrial Lignins and Their Corresponding Lignin Esters. *BioResources*, 5, 990-1009.

Gautrot, J.E., Zhu, X.X. **2006**. Main-chain bile acid based degradable elastomers synthesized by entropy-driven ring-opening metathesis polymerization. *Angewandte Chemie International Edition*, 45, 6872-6874.

Gautrot, J.E., Zhu, X.X. **2009**. Shape Memory Polymers Based on Naturally-Occurring Bile Acids. *Macromolecules*, 42, 7324-7331.

Guo, W.X., Huang, K.X. **2004**. Preparation and properties of poly(dimer acid-dodecanedioic acid) copolymer and poly(dimer acid-tetradecanedioic acid) copolymer. *Polymer Degradation and Stability*, 84, 375-381.

Hawker, C.J., Lee, R., Frechet, J.M.J. **1991**. One-Step Synthesis of Hyperbranched Dendritic Polyesters. *Journal of the American Chemical Society*, 113, 4583-4588.

Lendlein, A. **2002**. Biodegradable, Elastic Shape-Memory Polymers for Potential Biomedical Applications. *Science*, 296, 1673-1676.

Lendlein, A., Kelch, S. **2002**. Shape-memory polymers. *Angewandte Chemie International Edition*, 41, 2034-2057.

Li, H., McDonald, A.G. **2014**. Fractionation and Characterization of Industrial Lignin. University of Idaho, Moscow, Idaho.

Li, H., Sivasankarapillai, G., McDonald, A.G. **2014**. Lignin valorization by forming toughened thermally-stimulated shape memory copolymeric elastomers: Evaluation of different industrial lignins.

Li, X., Lu, X., Lin, Y., Zhan, J., Li, Y., Liu, Z., Chen, X., Liu, S. **2006**. Synthesis and characterization of hyperbranched poly(ester-amide)s from commercially available dicarboxylic acids and multihydroxyl primary amines. *Macromolecules*, 39, 7889-7899.

Li, X.R., Su, Y.L., Chen, Q.Y., Lin, Y., Tong, Y.J., Li, Y.S. **2005**. Synthesis and characterization of biodegradable hyperbranched poly(ester-amide)s based on natural material.

*Biomacromolecules*, 6, 3181-3188.

Li, X.R., Zhan, J., Li, Y.S. **2004**. Facile syntheses and characterization of hyperbranched poly(ester-amide)s from commercially available aliphatic carboxylic anhydride and multihydroxyl primary amine. *Macromolecules*, 37, 7584-7594.

Li, Y., Ragauskas, A.J. **2012**. Kraft lignin based rigid polyurethane foam. *Journal of Wood Chemistry and Technology*, 32, 210-224.

Li, Y., Sarkanen, S. **2002**. Alkylated kraft lignin-based thermoplastic blends with aliphatic polyesters *Macromolecules*, 35, 9707-9715.

McDonald, A.G., Ma, L. **2012**. Plastic moldable lignin, in: Paterson, R.J. (Ed.), *Lignin: Properties and applications in biotechnology and bioenergy*. Nova Science Publisher, Inc., pp. 489-498.

Meier, J.F. **1996**. Fundamentals of plastics and elastomers, in: Harper, C.A. (Ed.), *Handbook of plastics, elastomers, and composites 3rd edition*. Technology Seminars, Inc., Lutherville, Maryland, pp. 1.78-71.19.

Nagata, M., Morooka, T., Sakai, W., Tsutsumi, N. **2001**. Synthesis, characterization, and biodegradability of novel regular-network polyester-amines based on 1,1,1-triethanolamine. *Journal of Polymer Science Part a-Polymer Chemistry*, 39, 2896-2903.

Nassar, M.M., MacKay, G.D.M. **1984**. Mechanism of thermal decomposition of lignin. *Wood and Fiber Science*, 16, 441-453.

Osman, N.B., McDonald, A.G., Laborie, M.P.G. **2012**. Analysis of DCM extractable components from hot-pressed hybrid poplar. *Holzforschung*, 66, 927-934.

Overley, R.M., Buenviaje, C., Luginuni, R., Dinelli, F. **2000**. Glass and structural transitions measured at polymer surfaces on the nanoscale. *Journal of Thermal Analysis and Calorimetry*, 59, 205-225.

Parees, D.M., Hanton, S.D., Clark, P.A.C., Willcox, D.A. **1998**. Comparison of mass spectrometric techniques for generating molecular weight information on a class of ethoxylated oligomers. *Journal of the American Society for Mass Spectrometry*, 9, 282-291.

Pohjanlehto, H., Setälä, H.M., Kiely, D.E., McDonald, A.G. **2014**. Lignin-Xylaric Acid-Polyurethane-Based Polymer Network Systems: Preparation and Characterization. *Journal of Applied Polymer Science*, 131, 39714-39720.

Pramanik, S., Konwarh, R., Barua, N., Buragohain, A.K., Karak, N. **2014**. Bio-based hyperbranched poly(ester amide)-MWCNT nanocomposites: multimodalities at the biointerface. *Biomaterials Science*, 2, 192-202.

Pramanik, S., Konwarh, R., Sagar, K., Konwar, B.K., Karak, N. **2013**. Bio-degradable vegetable oil based hyperbranched poly(ester amide) as an advanced surface coating material. *Progress in Organic Coatings*, 76, 689-697.

Prime, B.R., Bair, H.E., Vyazovkin, S., Gallagher, P.K., Riga, A. **2009**. Thermogravimetric analysis (TGA), in: Menczel, J.D., Prime, B.R. (Eds.), *Thermal Analysis of Polymers, Fundamentals and Applications*. John Wiley, New Jersey, pp. 241-317.

Sadeghifar, H., Cui, C., Argyropoulos, D.S. **2012**. Toward Thermoplastic Lignin Polymers. Part 1. Selective Masking of Phenolic Hydroxyl Groups in Kraft Lignins via Methylation and Oxypropylation Chemistries. *Industrial and Engineering Chemistry Research*, 51, 16713-16720.

Sauter, T., Heuchel, M., Kratz, K., Lendlein, A. **2013**. Quantifying the Shape-Memory Effect of Polymers by Cyclic Thermomechanical Tests. *Polymer Reviews*, 53, 6-40.

Scholl, M., Nguyen, T.Q., Bruchmann, B., Klok, H.A. **2007**. Controlling polymer architecture in the thermal hyperbranched polymerization of L-Lysine. *Macromolecules*, 40, 5726-5734.

Sivasankarapillai, G., McDonald, A.G. **2011**. Synthesis and properties of lignin-highly branched poly (ester-amine) polymeric systems. *Biomass and Bioenergy*, 35, 919-931.

Sivasankarapillai, G., McDonald, A.G., Li, H. **2012**. Lignin valorization by forming toughened lignin-co-polymers: Development of hyperbranched prepolymers for cross-linking. *Biomass and Bioenergy*, 47, 99-108.

Stumbe, J.F., Bruchmann, B. **2004**. Hyperbranched polyesters based on adipic acid and glycerol. *Macromolecular Rapid Communications*, 25, 921-924.

Tran, R.T., Thevenot, P., Gyawali, D., Chiao, J.C., Tang, L.P., Yang, J. **2010**. Synthesis and characterization of a biodegradable elastomer featuring a dual crosslinking mechanism. *Soft Matter*, 6, 2449-2461.

Voit, B.I., Lederer, A. **2009**. Hyperbranched and Highly Branched Polymer Architectures- Synthetic Strategies and Major Characterization Aspects. *Chemical Reviews*, 109, 5924-5973.

Wang, J., John Manley, R.S., D., F. **1992**. Synthetic polymer-lignin copolymers and blends. *Progress in Polymer Science*, 17, 611-646.

Wu, D.Q., Wang, T., Lu, B., Xu, X.D., Cheng, S.X., Jiang, X.J., Zhang, X.Z., Zhuo, R.X. **2008**. Fabrication of supramolecular hydrogels for drug delivery and stem cell encapsulation. *Langmuir*, 24, 10306-10312.

Wu, L.C.F., Glasser, W.G. **1984**. Engineering plastics from lignin. I. Synthesis of hydroxypropyl lignin. *Journal of Applied Polymer Science*, 29, 1111-1123.

Xin, J.N., Zhang, P., Huang, K., Zhang, J.W. **2014**. Study of green epoxy resins derived from renewable cinnamic acid and dipentene: synthesis, curing and properties. *RSC Advances*, 4, 8525-8532.

Zakzeski, J., Bruijninx, P.C.A., Jongerius, A.L., Weckhuysen, B.M. **2010**. The Catalytic Valorization of Lignin for the Production of Renewable Chemicals. *Chemical Reviews*, 110, 3552-3599.



## 5 Lignin Valorization by Forming Thermally-stimulated Shape Memory Copolymeric Elastomers: High Biobased Copolymer as Mixing Phase

### 5.1 Abstract

Copolymers containing as high levels of bio-derived components were obtained mainly from two industrial byproducts, glycerol and lignin. A series of hyperbranched prepolymers (HBP) prepared by glycerol (Gly, B<sup>2</sup>B<sup>3</sup><sub>2</sub>) and adipic acid (AA, A<sub>2</sub>) or with addition of commercially available diisopropanolamine (DIPA, DB<sup>4</sup><sub>2</sub>) or tris(hydroxymethyl)aminomethane (THAM, CB<sub>3</sub><sup>1</sup>) reacted with lignin to form thermally-stimulated shape memory copolymeric elastomers via one pot two step melt polycondensation reactions. The prepolymers were characterized chemically by FTIR, NMR, and ESI-MS. Thermal and rheological behaviors were analyzed by DSC, DMA, TGA and dynamic rheometry. The higher branching crosslinkers, DIPA and THAM, were shown to influence the chemical and thermal properties of the prepolymers. The hyperbranched biobased lignin-copolymers demonstrated good shape memory and elastic properties. The shape transition temperature ( $T_{\text{trans}}$ ) could be tuned by variations of Gly, DIPA and THAM proportions for applications under different temperature circumstances. This study demonstrates that more renewable glycerol based prepolymers could be incorporated into lignin based copolymeric systems with high biobased contents acting as soft segment to perform SME behavior.

### 5.2 Introduction

Lignin, an underutilized biopolymer byproduct from both the pulping (about  $5 \times 10^{10}$  kg produced in 2004) and cellulosic ethanol industries, shows potential as a substrate for producing bioplastic materials because of abundant functional groups (Zakzeski et al., 2010). Lignin's utilization is impaired by its high glass transition temperature ( $T_g$ ) and brittleness due to its rigid aromatic backbone, high intra/inter H-bonding, and heterogeneity (Yoshida et al., 1987). Applications for lignin has been to incorporate it as a filler (Mousavioun et al., 2013), extender or as a reinforcing pigment in rubber (Wang et al., 1992) and in thermoset resins (Feldman, 2002). Another alternative to endow thermoplasticity properties to lignin

has been conducted by various chemical modifications such as alkylation (Li and Sarkanen, 2002), benzylation (McDonald and Ma, 2012), and oxypropylation (Cui et al., 2013; Li and Ragauskas, 2012; Sadeghifar et al., 2012; Wu and Glasser, 1984), which inhibits H-bonding and thus lower's its  $T_g$  and more processable. More recent work has been using lignin as a hard segment in the preparation of highly and hyper branched smart elastomeric copolymers with tunable shape memory properties (Li et al., 2014a; Sivasankarapillai and McDonald, 2011; Sivasankarapillai et al., 2012). The properties were easily tailored by changing the prepolymer structure and lignin content.

Highly branched, or hyperbranched (HBP), polymers are attractive types of dendritic polymers due to their high branching structures, less tedious preparations, as well as affordable up-scale pathways (Gao and Yan, 2004; Hult et al., 1999; Muscat and van Benthem, 2001; Sivasankarapillai et al., 2012; Voit and Lederer, 2009). The term "hyperbranched polymers" was first introduced in 1988 to describe the structure of an imperfect dendrimer by preparation of polyphenylenes with  $AB_x$  type monomers (Kim and Webster, 1988). HBP based on polyesters were then become increasingly attractive due to incorporating commercial availability of monomers with more diverse functionalities (e.g. symmetric diacid ( $A_2$ ) and trihydroxy ( $B_3$ )) and ease of preparation by standard melt polycondensation methodology (Muscat and van Benthem, 2001). Combinations of various branched structures were involved such as  $A_2$ ,  $B_3$  and trihydroxy-monoamino ( $CB_3^1$ ) monomer units to increase the structural diversity from branched to HB (Sivasankarapillai et al., 2012). The key of this approach is the employment of multifunctional monomers with suitable unequal reactivity, where both B and C can react with an A group, as a result, hyperbranched poly(ester-amide)s with amine cores and amide linkages can be formed (Li et al., 2006; Li et al., 2005; Li et al., 2004; Sivasankarapillai et al., 2012). Furthermore, a series of lignin HyBP-copolymer have been produced by melt condensation with lignin using the monomers: AA ( $A_2$ ), triethanolamine (TEA,  $B_3$ ) and THAM ( $CB_3^1$ ). The advantage of this system was that TEA acted as the reaction solvent and catalyst, and THAM introduced the amide linkage and increased the complexity of the structure. In addition, these lignin HBP

copolymers showed interesting thermal properties and elasticity (Sivasankarapillai and McDonald, 2011; Sivasankarapillai et al., 2012).

The global biodiesel production by 2016 is estimated as  $1.4 \times 10^{11}$  L according to the report, which leads to approximately  $1.5 \times 10^{10}$  L of crude Gly available for utilization into biobased products (Anand and Saxena, 2012; Yang et al., 2012). Gly with trihydroxy functionality, consequently, makes it a sustainable alternative crosslinker for synthesis of HyBPs. Other benefits of Gly are that it can act as a solvent and has a high boiling point. Gly based HyBPs have been synthesized as early as 1929 (Kienle and Hovey, 1929). Stumbe and Bruchamann (2004) first synthesized HBP with Gly and AA using a tin catalyst at  $150^{\circ}\text{C}$ . An alternative to tin based catalysts, Kulshrestha et al. (2005) produced glycerol copolyesters using a lipase catalyst to control branching and molar mass. Wyatt et al. (Wyatt et al., 2006a; Wyatt et al., 2006b; 2011) synthesized a series of Gly based highly branched oligomers for use in coatings. More complex polymers based on poly(oleic diacid-co-glycerol) have been synthesized by Yang et al. (2011). In polyurethanes, Gly is also utilized as a polyol cross-linker (Chun et al., 2007).

AA is a high volume ( $2.6 \times 10^9$  kg) commodity chemical traditionally produced from petrochemicals, primarily used in nylon 66, is now being produced via several bio-based routes (De Guzman, 2010). One commercial approach by Verdezyne has been to convert vegetable or coconut oil to AA (Beardslee and Picataggio, 2012). An alternate process by Rennova has been to oxidize glucose to gluconic acid, which is then hydrogenated to AA. These new technologies clearly show a need for biobased building blocks.

Therefore, the aim of this study was to develop a new series of HB prepolymers based on bio-derived Gly and AA by a simple approach with addition of different crosslinkers such as DIPA ( $\text{DB}_2^4$ ) or THAM ( $\text{CB}_3^1$ ) to evaluate their effect on properties. Corresponding high biobased-content lignin copolymers were synthesized based on these prepolymers. The effect of prepolymer composition on thermal, mechanical, and shape memory effect (SME) properties of the prepolymers and lignin copolymers were investigated.

## 5.3 Materials and Methods

### 5.3.1 Materials

Protobind 1000 soda lignin was supplied by ALM India Pvt. Ltd. The methanol soluble fraction of the soda lignin was used for copolymer synthesis (lignin content = 93.3%,  $M_w$  = 958 g/mol (ESI-MS), aromatic/aliphatic hydroxyl group ratio = 0.93,  $T_g$  = 132°C (DSC)) (Li and McDonald, 2014; Li et al., 2014a). Gly, THAM, DIPA, AA, methanol and tetrahydrofuran (THF) were obtained from Acros Organics and used as received.

### 5.3.2 Methods

#### 5.3.2.1 Synthesis of hyperbranched prepolyesters G1 and G2

A mixture of Gly (2.30 g, 24.98 mmol) and AA (6.00g, 41.06 mmol) with mole ratio of total OH to COOH 1:1.1 was prepared in a beaker (50 mm dia), then the beaker was placed in a preheated vacuum oven (100°C), and a vacuum of 495 mm Hg was applied to avoid monomer loss for 30 min. Then the temperature and vacuum were raised to 150°C and 120 mm Hg, respectively for 3.5 h to afford the prepolymer G1. The prepolymer G2 was prepared as described above with Gly (1.68 g, 18.24 mmol) and AA (6.00g, 41.06 mmol) with mole ratio of total OH to COOH of 1:1.5. The final G1 and G2 prepolymers were white highly viscous liquids at room temperature and soluble in common organic solvent such as methanol, acetone, and THF.

Yield: G1=86.6% and G2=86.5%; IR (ATR,  $\text{cm}^{-1}$ ):  $\nu$  = 3500-3100 ( $\nu_{\text{b}}$ ;  $\nu(\text{OH stretching})$ ), 2923 ( $\nu_{\text{as}}(\text{CH}_2)$ ), 2853 ( $\nu_{\text{s}}(\text{CH}_2)$ ), 2500 ( $\nu_{\text{b}}$ ; (OH of COOH)), 1730 ( $\nu_{\text{s}}$ ; (C=O from ester)), 1712 and 1696 (C=O of COOH), 1455 (w,  $(\text{CH}_2)$ ), 1393 (w; (OH)), 1169 and 1140  $\text{cm}^{-1}$  ( $\nu_{\text{s}}$ ; (COO in ester));  $^1\text{H NMR}$  (500 MHz,  $\text{DMSO-}d_6$ ,  $\delta$ ): 11.97 (s,  $\text{COOH}$ ), 5.18 (m,  $\text{CH}(\text{OCO})(\text{CH}_2\text{OCO})_2$ ), 4.94 (m,  $\text{CH}(\text{OCO})(\text{CH}_2\text{OCO})(\text{CH}_2\text{OH})$ ), 4.24 and 4.14 (dd,  $\text{CH}(\text{OCO})(\text{CH}_2\text{OCO})_2$ ), 4.24 and 4.12 (dd,  $\text{CH}(\text{OCO})(\text{CH}_2\text{OCO})(\text{CH}_2\text{OH})$ ), 3.98 (t,  $\text{CH}(\text{OH})(\text{CH}_2\text{OCO})_2$ ), 4.10 and 3.92 (dd,  $\text{CH}(\text{OH})(\text{CH}_2\text{OCO})(\text{CH}_2\text{OH})$ ), 3.86 (t,  $\text{CH}(\text{OH})(\text{CH}_2\text{OCO})_2$ ), 3.63 (m,  $\text{CH}(\text{OH})(\text{CH}_2\text{OCO})(\text{CH}_2\text{OH})$ ), 3.49 (dd,  $\text{CH}(\text{OCO})(\text{CH}_2\text{OCO})(\text{CH}_2\text{OH})$ ), 3.33 (m,  $\text{CH}(\text{OH})(\text{CH}_2\text{OCO})(\text{CH}_2\text{OH})$ ), 2.50 (p,  $\text{DMSO-}d_6$ ), 2.31 (m,  $\text{OOCCH}_2\text{CH}_2$ ), 2.20 (m,  $\text{HOOCCH}_2\text{CH}_2$ ), 1.50-1.53 (m,  $\text{OOCCH}_2(\text{CH}_2)_2\text{CH}_2\text{COO}$ );  $^{13}\text{C}$

NMR (125.76 MHz, DMSO- $d_6$ ,  $\delta$ ): 174.19-174.27 ( $\underline{\text{C}}\text{OOH}$ ), 172.03-172.60 ( $\underline{\text{C}}\text{OO}$ ), 71.94 ( $\underline{\text{C}}\text{H}(\text{OCO})(\text{CH}_2\text{OCO})(\text{CH}_2\text{OH})$ ), 69.29 ( $\underline{\text{C}}\text{H}(\text{OH})(\text{CH}_2\text{OCO})(\text{CH}_2\text{OH})$ ), 68.76 ( $\underline{\text{C}}\text{H}(\text{OCO})(\text{CH}_2\text{OCO})_2$ ), 66.16 ( $\underline{\text{C}}\text{H}(\text{OH})(\text{CH}_2\text{OCO})_2$ ), 65.54 ( $\text{CH}(\text{OH})(\underline{\text{C}}\text{H}_2\text{OCO})(\text{CH}_2\text{OH})$ ), 64.81 ( $\text{CH}(\text{OH})(\underline{\text{C}}\text{H}_2\text{OCO})_2$ ), 62.64 ( $\text{CH}(\text{OH})(\text{CH}_2\text{OCO})(\underline{\text{C}}\text{H}_2\text{OH})$ ), 62.30 ( $\text{CH}(\text{OCO})(\underline{\text{C}}\text{H}_2\text{OCO})(\text{CH}_2\text{OH})$ ), 61.81 ( $\text{CH}(\text{OCO})(\underline{\text{C}}\text{H}_2\text{OCO})_2$ ), 59.51 ( $\text{CH}(\text{OCO})(\text{CH}_2\text{OCO})(\underline{\text{C}}\text{H}_2\text{OH})$ ), 32.84-33.37 ( $\text{OOC}\underline{\text{C}}\text{H}_2\text{CH}_2$  and  $\text{HOOC}\underline{\text{C}}\text{H}_2\text{CH}_2$ ), 23.65-24.02 ( $\text{OOCCH}_2(\underline{\text{C}}\text{H}_2)_2\text{CH}_2\text{COO}$ ).

### 5.3.2.2 Synthesis of hyperbranched prepoly(ester-amide)s (D1-D4)

The prepolymer D1 was prepared from a mixture of Gly (3.00 g, 32.58 mmol), DIPA (1.08 g, 8.11 mmol) and AA (9.57 g, 65.49 mmol) with mole ratio of total OH and NH to COOH 1:1.1 in a beaker (50 mm dia), then the beaker was placed in a preheated vacuum oven (100°C), and a vacuum of 495 mm Hg was applied to avoid monomers loss for 30 min. Then the temperature and vacuum were raised to 150°C and 120 mm Hg, respectively for 3.5 h. The prepolymers D2 to D4 were prepared as described above with: D2 (Gly (2.00 g, 21.72 mmol), DIPA (1.45 g, 10.89 mmol) and AA (7.86g, 53.78 mmol); D3 (Gly (2.00 g, 21.72 mmol), DIPA (2.17 g, 16.29 mmol) and AA (9.16 g, 62.68 mmol)); and D4 (Gly (2.00 g, 21.72 mmol), DIPA (2.89 g, 21.72 mmol) and AA (9.16 g, 71.64 mmol)), with mole ratio of total OH to COOH of 1:1.1. The final D1-D4 prepolymers were yellowish highly viscous liquid at room temperature and soluble in methanol, acetone, and THF.

Yield: D1-D4= 91.4, 88.6, 89.6, and 90.5%, respectively; IR (ATR,  $\text{cm}^{-1}$ ):  $\nu = 3500\text{-}3200$  ( $\nu\text{b}$ ;  $\nu(\text{OH stretching})$ ), 2923 ( $\nu\text{s}$ ;  $\nu_{\text{as}}(\text{CH}_2)$ ), 2853 ( $\nu\text{s}$ ;  $\nu_{\text{s}}(\text{CH}_2)$ ), 2500 ( $\nu\text{b}$ ;  $\text{OH of COOH}$ ), 1730 ( $\nu\text{s}$ ;  $\text{C=O from ester}$ ), 1712 and 1696 ( $\text{C=O of COOH}$ ), 1620 ( $\nu\text{s}$ ;  $\text{C=O from tertiary amide}$ ), 1455 ( $\text{w}$ ,  $(\text{CH}_2)$ ), 1391 ( $\text{w}$ ;  $\text{OH}$ ), 1169 and 1140  $\text{cm}^{-1}$  ( $\nu\text{s}$ ;  $\text{COO in ester}$ );  $^1\text{H NMR}$  (500 MHz, DMSO- $d_6$ ,  $\delta$ ): 5.18 (m,  $\underline{\text{C}}\text{H}(\text{OCO})(\text{CH}_2\text{OCO})_2$ ), 5.05, 3.76-3.92 (m,  $\text{NCH}_2\underline{\text{C}}\text{H}(\text{O})(\text{CH}_3)$ ), 4.94 (m,  $\underline{\text{C}}\text{H}(\text{OCO})(\text{CH}_2\text{OCO})(\text{CH}_2\text{OH})$ ), 4.73 (m,  $\underline{\text{C}}\text{H}(\text{OCO})(\text{CH}_2\text{OH})_2$ ), 4.24 and 4.14 (dd,  $\text{CH}(\text{OCO})(\underline{\text{C}}\text{H}_2\text{OCO})_2$ ), 4.24 and 4.12 (dd,  $\text{CH}(\text{OCO})(\underline{\text{C}}\text{H}_2\text{OCO})(\text{CH}_2\text{OH})$ ), 3.98 (t,  $\text{CH}(\text{OH})(\underline{\text{C}}\text{H}_2\text{OCO})_2$ ), 4.10 and 3.92 (dd,  $\text{CH}(\text{OH})(\underline{\text{C}}\text{H}_2\text{OCO})(\text{CH}_2\text{OH})$ ), 3.86 (t,  $\underline{\text{C}}\text{H}(\text{OH})(\text{CH}_2\text{OCO})_2$ ), 3.63 (m,  $\underline{\text{C}}\text{H}(\text{OH})(\text{CH}_2\text{OCO})(\text{CH}_2\text{OH})$ ), 3.49 (dd,  $\text{CH}(\text{OCO})(\text{CH}_2\text{OCO})(\underline{\text{C}}\text{H}_2\text{OH})$ ), 3.33 (m,  $\text{CH}(\text{OH})(\text{CH}_2\text{OCO})(\underline{\text{C}}\text{H}_2\text{OH})$ ), 2.63-3.52 (m,  $\text{NCH}_2\text{CH}(\text{O})(\text{CH}_3)$ ), 2.50 (p, DMSO- $d_6$ ), 2.31 (m,

$\text{OOCCH}_2\text{CH}_2$ ), 2.26 ( $\text{NCOCH}_2$ ), 2.20 (m,  $\text{HOOCCH}_2\text{CH}_2$ ), 1.50-1.53 (m,  $\text{OOCCH}_2(\text{CH}_2)_2\text{CH}_2\text{COO}$ ), 0.96-1.17 (m,  $\text{NCH}_2\text{CH}(\text{O})(\text{CH}_3)$ );  $^{13}\text{C}$  NMR (125.76 MHz,  $\text{DMSO}-d_6$ ,  $\delta$ ): 174.19-174.27 ( $\text{COOH}$ ), 172.03-172.60 ( $\text{COO}$ ), 75.45 ( $\text{CH}(\text{OCO})(\text{CH}_2\text{OH})_2$ ), 71.94 ( $\text{CH}(\text{OCO})(\text{CH}_2\text{OCO})(\text{CH}_2\text{OH})$ ), 69.29 ( $\text{CH}(\text{OH})(\text{CH}_2\text{OCO})(\text{CH}_2\text{OH})$ ), 68.76 ( $\text{CH}(\text{OCO})(\text{CH}_2\text{OCO})_2$ ), 68.49, 68.00, 64.98, 64.65, and 62.86 ( $\text{NCH}_2\text{CH}(\text{O})(\text{CH}_3)$ ), 66.16 ( $\text{CH}(\text{OH})(\text{CH}_2\text{OCO})_2$ ), 65.54 ( $\text{CH}(\text{OH})(\text{CH}_2\text{OCO})(\text{CH}_2\text{OH})$ ), 64.81 ( $\text{CH}(\text{OH})(\text{CH}_2\text{OCO})_2$ ), 62.64 ( $\text{CH}(\text{OH})(\text{CH}_2\text{OCO})(\text{CH}_2\text{OH})$ ), 62.30 ( $\text{CH}(\text{OCO})(\text{CH}_2\text{OCO})(\text{CH}_2\text{OH})$ ), 61.81 ( $\text{CH}(\text{OCO})(\text{CH}_2\text{OCO})_2$ ), 59.84 ( $\text{CH}(\text{OCO})(\text{CH}_2\text{OH})_2$ ), 59.51 ( $\text{CH}(\text{OCO})(\text{CH}_2\text{OCO})(\text{CH}_2\text{OH})$ ), 49.67-55.37 ( $\text{NCH}_2\text{CH}(\text{O})(\text{CH}_3)$ ), 32.84-33.37 ( $\text{OOCCH}_2\text{CH}_2$ ,  $\text{NCOCH}_2$ , and  $\text{HOOCCH}_2\text{CH}_2$ ), 23.65-24.02 ( $\text{OOCCH}_2(\text{CH}_2)_2\text{CH}_2\text{COO}$ ), 17.32-21.17 ( $\text{NCH}_2\text{CH}(\text{O})(\text{CH}_3)$ ).

### 5.3.2.3 Synthesis of hyperbranched prepoly(ester-amide)s (T1 - T4)

The preparations of: T1 (Gly (3.00 g, 32.64 mmol), THAM (0.99 g, 8.16 mmol) and AA (10.47 g, 71.65 mmol)); T2 (Gly (2.00 g, 21.72 mmol), THAM (1.32 g, 10.90 mmol) and AA (8.73 g, 59.74 mmol)); T3 (Gly (2.00 g, 21.72 mmol), THAM (1.97 g, 16.26 mmol) and AA (10.47 g, 71.64 mmol)); and T4 (Gly (2.00 g, 21.72 mmol), THAM (2.63g, 21.72mmol) and AA (12.22g, 83.62 mmol)), prepolymers with mole ratio of total OH and  $\text{NH}_2$  to  $\text{COOH}$  1:1.1 were prepared the same as described above. The final T1-T4 prepolymers were white highly viscous liquids at room temperature and soluble in common organic solvent such as methanol, acetone, and THF.

Yield: T1-T4=92.9, 89.0, 90.1, and 90.0%, respectively; IR (ATR,  $\text{cm}^{-1}$ ):  $\nu = 3500\text{-}3200$  (vb;  $\nu(\text{OH stretching})$  and  $\nu(\text{NH stretching})$ ), 2923 (vs;  $\nu_{\text{as}}(\text{CH}_2)$ ), 2853 (vs;  $\nu_{\text{s}}(\text{CH}_2)$ ), 2500 (vb; (OH of  $\text{COOH}$ )), 1730 (vs; (C=O from ester)), 1712 and 1696 (C=O of  $\text{COOH}$ ), 1651 (vs; (C=O from amide)), 1555 (b; (N-H and C-N)), 1455 (w,  $(\text{CH}_2)$ ), 1391 (w; (OH)), 1169 and 1140  $\text{cm}^{-1}$  (vs; (COO in ester));  $^1\text{H}$  NMR (500 MHz,  $\text{DMSO}-d_6$ ,  $\delta$ ): 7.71, 7.41, 7.21, 7.09 (s,  $\text{NHCOO}$ ), 5.18 (m,  $\text{CH}(\text{OCO})(\text{CH}_2\text{OCO})_2$ ), 4.94 (m,  $\text{CH}(\text{OCO})(\text{CH}_2\text{OCO})(\text{CH}_2\text{OH})$ ), 4.73 (m,  $\text{CH}(\text{OCO})(\text{CH}_2\text{OH})_2$ ), 4.27, 4.23, 4.19, 3.60, 3.56, and 3.52 (s,  $\text{NC}(\text{CH}_2\text{O})_3$ ), 4.24 and 4.14 (dd,  $\text{CH}(\text{OCO})(\text{CH}_2\text{OCO})_2$ ), 4.24 and 4.12 (dd,  $\text{CH}(\text{OCO})(\text{CH}_2\text{OCO})(\text{CH}_2\text{OH})$ ), 3.98 (t,  $\text{CH}(\text{OH})(\text{CH}_2\text{OCO})_2$ ), 4.10 and 3.92 (dd,  $\text{CH}(\text{OH})(\text{CH}_2\text{OCO})(\text{CH}_2\text{OH})$ ), 3.86 (t,  $\text{CH}(\text{OH})(\text{CH}_2\text{OCO})_2$ ), 3.63 (m,  $\text{CH}(\text{OH})(\text{CH}_2\text{OCO})(\text{CH}_2\text{OH})$ ), 3.49 (dd,  $\text{CH}(\text{OCO})(\text{CH}_2\text{OCO})(\text{CH}_2\text{OH})$ ), 3.48 and 3.42 (m,  $\text{CH}(\text{OCO})(\text{CH}_2\text{OH})_2$ ), 3.33 (m,

CH(OH)(CH<sub>2</sub>OCO)(CH<sub>2</sub>OH)), 2.50 (p, DMSO-d<sub>6</sub>), 2.31 (m, OOCCH<sub>2</sub>CH<sub>2</sub>), 2.20 (m, HOOCCH<sub>2</sub>CH<sub>2</sub>), 2.08 (m, HNC<sub>2</sub>CH<sub>2</sub>CH<sub>2</sub>), 1.45-1.55 (m, OOCCH<sub>2</sub>(CH<sub>2</sub>)<sub>2</sub>CH<sub>2</sub>COO); <sup>13</sup>C NMR (125.76 MHz, DMSO-d<sub>6</sub>, δ): 174.19-174.27 (C=O), 172.03-172.80 (C=O), 75.45 (CH(OCO)(CH<sub>2</sub>OH)<sub>2</sub>), 74.13, 72.12, 60.31, 58.48, and 56.88 (NC(CH<sub>2</sub>O)<sub>3</sub>), 71.94 (CH(OCO)(CH<sub>2</sub>OCO)(CH<sub>2</sub>OH)), 70.40, 70.18, 65.90, 64.07, 61.91, 61.69, 60.88, 60.47, 59.85 (C(CH<sub>2</sub>OCO)<sub>n</sub>(CH<sub>2</sub>OH)<sub>3-n</sub>), 69.29 (CH(OH)(CH<sub>2</sub>OCO)(CH<sub>2</sub>OH)), 68.76 (CH(OCO)(CH<sub>2</sub>OCO)<sub>2</sub>), 66.16 (CH(OH)(CH<sub>2</sub>OCO)<sub>2</sub>), 65.54 (CH(OH)(CH<sub>2</sub>OCO)(CH<sub>2</sub>OH)), 64.81 (CH(OH)(CH<sub>2</sub>OCO)<sub>2</sub>), 62.64 (CH(OH)(CH<sub>2</sub>OCO)(CH<sub>2</sub>OH)), 62.30 (CH(OCO)(CH<sub>2</sub>OCO)(CH<sub>2</sub>OH)), 61.81 (CH(OCO)(CH<sub>2</sub>OCO)<sub>2</sub>), 59.84 (CH(OCO)(CH<sub>2</sub>OH)<sub>2</sub>), 59.51 (CH(OCO)(CH<sub>2</sub>OCO)(CH<sub>2</sub>OH)), 35.51-35.34 (HNC<sub>2</sub>CH<sub>2</sub>CH<sub>2</sub>), 32.84-33.37 (OOCCH<sub>2</sub>CH<sub>2</sub> and HOOCCH<sub>2</sub>CH<sub>2</sub>), 23.65-24.02 (OOCCH<sub>2</sub>(CH<sub>2</sub>)<sub>2</sub>CH<sub>2</sub>COO).

### 5.3.2.4 Synthesis of lignin-copolyesters and -copoly(ester-amide)s

Lignin (2.00 g, 30% loading) was dispersed in the minimum amount of THF and mixed with each of the prepolymers G1 to T4 (4.66 g, 70% loading), respectively, to synthesize a series of lignin-copolymers. THF was then removed under a stream of N<sub>2</sub> at 80°C. The highly viscous mixture was then transferred to a prepared aluminum pan (15 x 5 cm<sup>2</sup>) and was placed into vacuum oven at 80°C and 750 mm Hg to remove residual solvent and moisture (about 30 min). Then the reaction temperature was increased to 120°C at 650 mm Hg, and the reaction proceeded for 40 h. The final lignin-copolymers all displayed a highly bright and glossy surface and were insoluble in organic solvents. The lignin-copolymers were named based on the prepolymer name, such as LG1 from the G1 prepolymer. The synthesis approach is shown in Figure 5.1.

IR (ATR, cm<sup>-1</sup>): LG1-LG2: ν = 3500-3200 (vb; ν(OH stretching)), 2928 (s; ν<sub>as</sub>(CH<sub>2</sub>)), 2870 (m; ν<sub>s</sub>(CH<sub>2</sub>) and ν(CH)), 1729 (vs; (C=O from ester)), 1708 (w; COOH), 1604 (m; aromatic skeletal vibration), 1514 (m; aromatic skeletal vibration), 1456 (w; (CH<sub>2</sub>)), 1417 (w; CH in-plane deformation), 1378 (w; CH<sub>3</sub>), 1164 and 1133 cm<sup>-1</sup> (vs; (COO in ester)).

LG1-LG4: ν = 3500-3200 (vb; ν(OH stretching)), 2932 (s; ν<sub>as</sub>(CH<sub>2</sub>) and (CH<sub>3</sub>)), 2872 (m; ν<sub>s</sub>(CH<sub>2</sub>), (CH<sub>3</sub>) and ν(CH)), 1727 (vs; (C=O from ester)), 1635 (m; tertiary amide), 1607 (m; aromatic

skeletal vibration), 1513 (m; aromatic skeletal vibration), 1456 (w; (CH<sub>2</sub>)), 1417 (w; CH in-plane deformation), 1378 (w; CH<sub>3</sub>), 1169 and 1126 cm<sup>-1</sup> (vs; (COO in ester)).

LT1-LT4:  $\nu = 3500-3200$  (vb;  $\nu(\text{OH stretching})$ ), 2945 (s;  $\nu_{\text{as}}(\text{CH}_2)$ ), 2870 (m;  $\nu_{\text{s}}(\text{CH}_2)$  and  $\nu(\text{CH})$ ), 1729 (vs; (C=O from ester)), 1655 (s; (C=O from amide), 1600 (m; aromatic skeletal vibration), 1546 (w; N-H bending), 1511 (m; aromatic skeletal vibration), 1459 (w; (CH<sub>2</sub>)), 1417 (w; CH in-plane deformation), 1378 (w, CH<sub>3</sub>), 1166 and 1134 cm<sup>-1</sup> (vs; (COO in ester)).

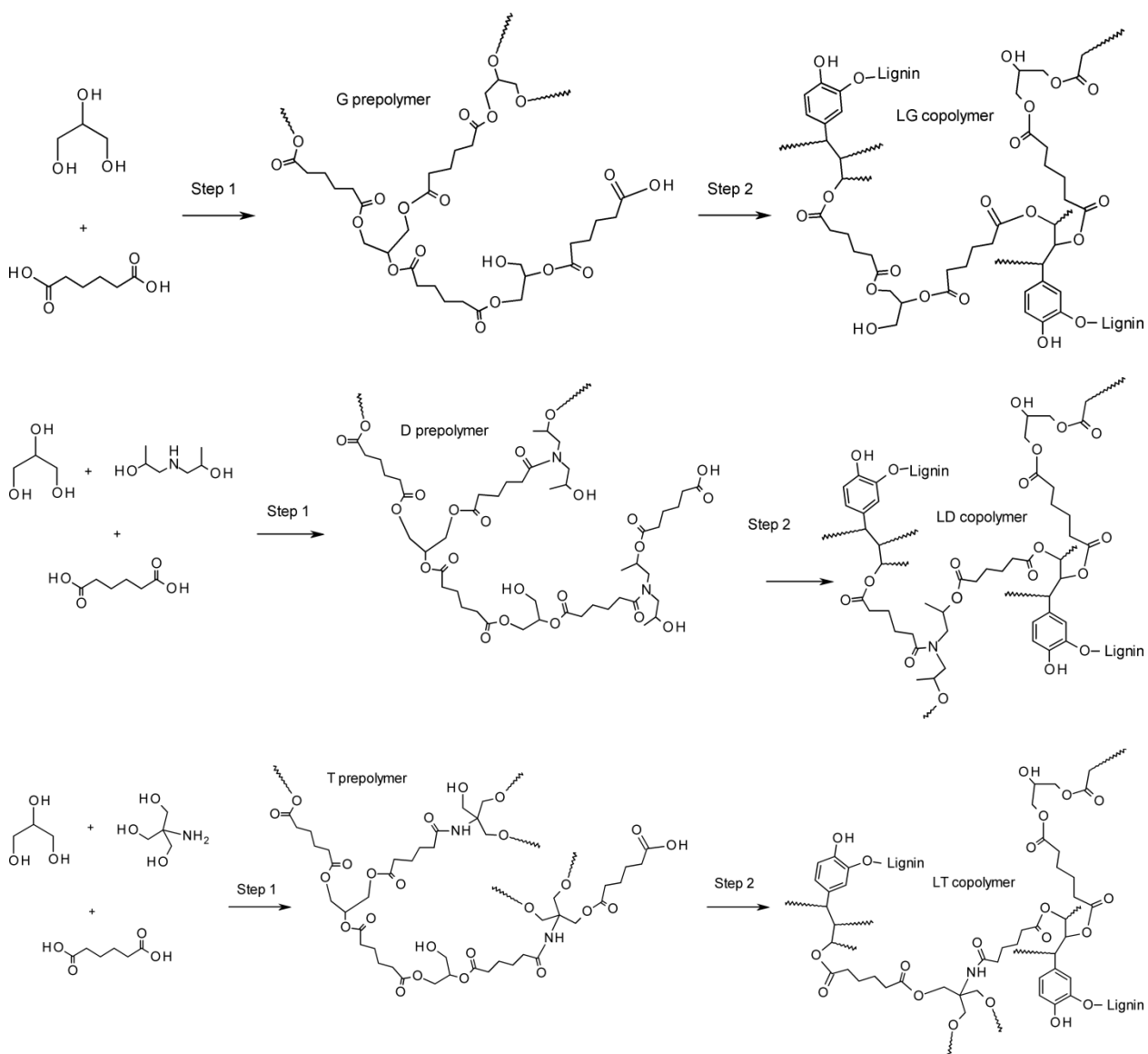


Figure 5.1 Synthesis of glycerol-based prepolymers and corresponding lignin based copolymers.



### 5.3.3 Characterization techniques

#### 5.3.3.1 FTIR and NMR

All Fourier transform infrared (FTIR) spectra were carried out with a ThermoNicolet Avatar 370 spectrometer operating in the attenuated total reflection (ATR) mode (Smart performance, ZnSe crystal).  $^1\text{H}$  and inverse-gated  $^{13}\text{C}$  NMR spectra were obtained on glycerol based prepolyesteramide on a Bruker Avance 500 spectrometer. Chemical shifts were referenced to DMSO- $d_6$  at 39.5 for  $^{13}\text{C}$  and 2.50 for  $^1\text{H}$  spectra at 30°C.  $^1\text{H}$ - $^1\text{H}$  COSY,  $^{13}\text{C}$ - $^1\text{H}$  HSQC NMR and  $^{13}\text{C}$  DEPT-135 spectra were recorded at ambient temperature and applying the standard Bruker pulse programs. G1, D4, and T4 prepolymers were presented.

#### 5.3.3.2 Electrospray Ionization – MS

Molar mass of the lignin and D1 prepolymer samples were determined by positive ion ESI-MS on a LCQ-Deca instrument (ThermoFinnigan). Samples were dissolved in methanol (1 mg/mL) containing 1% acetic acid and introduced into the ESI source at a flow rate of 10  $\mu\text{L}/\text{min}$  (Osman et al., 2012). The ion source and capillary voltages were 4.48 kV and 47V, respectively, at a temperature of 275°C. The MS were scanned between  $m/z$  (mass to charge ratio) 100 and 2000. The number average molar mass ( $M_n$ ) was calculated as  $M_n = \sum M_i N_i / \sum N_i$  and weight average molar mass ( $M_w$ ) as  $M_w = \sum M_i^2 N_i / \sum M_i N_i$ , where  $M_i$  and  $N_i$  are the  $m/z$  and intensity of the ions, respectively (Parees et al., 1998).

#### 5.3.3.3 Rheology analysis

Viscosity measurements were performed using a parallel-plate (25 mm dia) Bohlin CVO100 rheometer. Frequency sweep (0.05 to 10000  $\text{s}^{-1}$ ) measurements were performed at 30°C with a plate gap of 800  $\mu\text{m}$ .

#### 5.3.3.4 Thermal analysis

Differential scanning calorimetry (DSC) was performed on a TA instruments model Q200 DSC equipped with a refrigeration cooling unit to monitor the thermal behavior of materials. The polymers (5-7 mg) were analyzed from -70 to 80°C for Gly based prepolymers and from -70

to 150°C for lignin based copolymers at a heating rate of 3°C/min and held isothermally for 5 min. All the data were collected from the second heating cycle. The inflection point of heat flow change was assigned as  $T_g$ . Thermogravimetric analysis (TGA) was performed on a TGA-7 (Perkin Elmer) instrument from 50 to 900°C at a heating rate of 20°C/min in  $N_2$ . Dynamic mechanical analysis (DMA) experiments were performed using a TA Instruments model Q800 DMA, both under isothermal and non-isothermal conditions in  $N_2$  atmosphere in the tensile mode (12 mm × 4 mm × 0.2 mm). The heating scans were carried out at 1 Hz and at a heating rate of 3°C/min. The tensile properties of the lignin based elastomers (triplicate per sample) were measured using DMA at room temperature with ramp 3 N/min. Specifically, energy at break was determined as the area of the stress-strain curve.

The SME of lignin based copolymers were determined in the tensile mode by DMA. A stress-controlled cyclic thermomechanical test was applied. Four programming steps were proceeded, in which the copolymers were: (1) heated to a temperature of  $T_g+20^\circ\text{C}$  (designated as  $T_{\text{high}}$ ) with ramp of 5°C/min, then set load to 2 N static force with ramp of 0.2 N/min, the copolymers were stretched to temporary shapes; (2) in the next step, cooled to  $T_g-20^\circ\text{C}$  (ramp 5°C/min) (designated as  $T_{\text{low}}$ ); and (3) release the static force while keeping at  $T_{\text{low}}$ , the copolymers kept the temporary shapes; (4) heated up to  $T_{\text{high}}$  again and kept isothermal for 15 min, the permanent shape recovered again. The same procedure was repeated for 3 times (cycle 1 to 3). The recovery elasticity of lignin based elastomers also applied the stress-controlled cycle mechanical test at 30°C. In detail, the elastomers were stretched to approximate 100 % strain which was achieved by controlling the force determined by measuring stress at 100% strain from tensile test results, then multiplying the cross sectional area of the sample. Then release the loaded force and hold for 15 min to recover back to its original length and the procedure repeated a further 4 times. For sample LT3 this was evaluated at 70% strain due to having a lower than 100 % elongation at break.

## 5.4 Results and Discussion

### 5.4.1 Monomer selections

With the purpose of pursuing highly biobased polymers and value-added products from biobased starting materials (lignin, Gly, AA), lignin copolymeric elastomers were synthesized containing as high as 100% bio-derived materials (Table 5.1). In detail, HB prepolymers (G1 and G2) were first prepared by incorporating Gly to react with AA, and then lignin copolymers (LG1 and LG2) were synthesized. The advantage or starting point herein was that Gly, possessing trihydroxy functionalities, is a low cost renewable byproduct which replaced previous used non-renewable TEA monomer (Li et al., 2014a, b; Sivasankarapillai and McDonald, 2011; Sivasankarapillai et al., 2012). Besides, Gly also functioned as solvent for other reactants, introducing another important merit that no solvent needed during prepolymer syntheses. Moreover, AA is now being produced from biobased sources (Beardslee and Picataggio, 2012; De Guzman, 2010; Van de Vyver and Roman-Leshkov, 2013). Summation of all these merits we obtained between 81 and 100% biobased prepolymers. Furthermore, DIPA (D1-D4) and THAM (T1-T4) were added to G1 prepolymer proportionally to give rise to a different amide and core morphological structures in the prepolymers, although relative lower biobased materials were obtained (Table 5.1). Therefore, the resultant unique prepolymers including G prepolymers would possess diverse core structures derived from Gly, DIPA as well as THAM and possess different amide types, branching structure, and H-bonding. HyBP prepolymers were synthesized to determine the effect of the amounts of AA, DIPA, and THAM on properties. The monomer ratio was kept constant at 1:1.1 between total OH and NH<sub>2</sub> or NH to COOH to facilitate the final lignin copolymerization reactions except for G2 which was used to examine the effect of excess acid content (1:1.5).

Table 5.1 Analysis of bio-based components in Gly based prepolymers and lignin-copolymers

Sample #	Bio-based components in (%) <sup>a</sup>	
	Gly based prepolymers	Lignin-copolymers
LG1	100	100
LG2	100	100
LD1	92	94
LD2	87	91
LD3	84	89
LD4	81	87
LT1	93	95
LT2	89	92
LT3	86	90
LT4	84	89

<sup>a</sup> Calculation was based on mass percentage

#### 5.4.2 Preparation of Gly based prepolymers

We first adopted the reaction temperature of 100°C for G1 synthesis under vacuum which was consistent with our previous studies. However, it was found that no ester was formed according to FTIR even after 24 h. The phenomenon could be explained that Gly is less reactive toward AA than compared to TEA which acted as a catalyst for the esterification reaction due to high pH (10.6) and nucleophilic nature (Sivasankarapillai and McDonald, 2011). Therefore, a reaction temperature of 150°C was chosen to conduct the prepolymerization reaction according to Stumbe and Bruchmann (Stumbe and Bruchmann, 2004). A gel was formed after 5 h reaction. Thus, a final reaction condition of 150°C for 3.5 h was used as to achieve sufficient esterification/crosslinking but to have good solubility and dispersability with lignin for subsequent co-polymerization.

#### 5.4.3 Characterization of Gly-based prepolymers

Ester formation and structure elucidation of Gly based prepolymers were characterized by FTIR and NMR techniques. A band at 1733 cm<sup>-1</sup> verified ester formation for all the prepolymers. Moreover, a band at 1620 cm<sup>-1</sup> of prepolymers D1 to D4 was contributed by a tertiary amide. Furthermore, two bands at 1651 cm<sup>-1</sup> and 1555 cm<sup>-1</sup> in prepolymers T1 to T4 were respectively, assigned as amide I (C=O) and amide II (mixture of C-N and N-H bending).

All above assignments demonstrated that successful reactions between OH to COOH, NH to COOH as well as NH<sub>2</sub> to COOH occurred. Bands with high intensity from 3500-2500 were due to high amounts of OH and COOH. Furthermore, the bands at 1708 or 1695 cm<sup>-1</sup> were assigned to a free acid or an acid dimer (Figure 5.2) (Zagar and Grdadolnik, 2003). The unreacted free acid in the prepolymer will ensure the subsequent copolymerization with lignin.

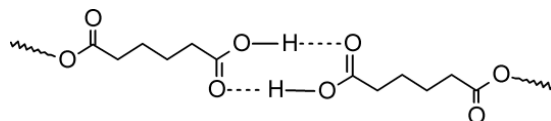


Figure 5.2 Carboxylic acid dimer

Detailed structural information based on NMR is shown in Figures 5.3 and 5.4. Most of Gly and THAM segments were managed to be elucidated based on 1D and 2D NMR, but it was difficult to exactly assign peaks for the DIPA series of prepolymers (D1-D4) because of overlapping peaks even with 2D NMR, as encountered previously (Gelade et al., 2001; van Benthem et al., 2001). The COOH remaining for subsequent reaction could be quantitatively determined by <sup>1</sup>H NMR which varied from 33 to 48% as listed in Table 5.2 (Stumbe and Bruchmann, 2004). The degree of branching (DB) for the Gly based prepolymers (G1, G2, D1-D4, and T1-T4) were determined by inverse gated <sup>13</sup>C NMR (elimination of nuclear Overhauser effect) (Kulshrestha et al., 2005) for the Gly segment and <sup>1</sup>H NMR for THAM segment (Table 5.2). The DB values of Gly segment ranged from 0.41 to 0.72, which is comparable with the result (48%) obtained under same temperature but with a tin catalyst (Stumbe and Bruchmann, 2004). Similarly, Kulshrestha et al. (2005) achieved the DB of 0.58 with 1:1 ratio of AA to Gly under 90°C with an enzyme as catalyst. A high acid content in prepolymer G2 gave the highest DB showing a higher level of reaction. The addition of DIPA and THAM into the prepolymer resulted in little variations of the DB. The DB derived from the THAM segment showed appreciably high values (0.76-0.81). Surprisingly, considerable amount of dendritic structure (D) was observed, while no observation on other reports due to steric hindrance with lower temperature (100°C) (Figure 5.4) (Li et al., 2004; Sivasankarapillai et al., 2012). This indicates high THAM crosslinking had occurred during

prepolymerization. Although DIPA also possesses different branching structures, it was difficult to determine the DB because of overlapping NMR signals. No  $T_{1,3}$  structures ( $^{13}\text{C}$  at 75.54 ppm) were found in the G1 and G2 prepolymers as reported in the literature (Kulshrestha et al., 2005). However,  $T_{1,3}$  structures were observed in all the D1-D4 and T1-T4 series prepolymers, indicating that DIPA and THAM improved the regioselectivity of coupling in the prepolymers. The  $M_w$  and polydispersity index (PDI) of Gly based prepolymers were determined by ESI-MS (Table 5.2). All the prepolymers had  $M_w$ s around 1,200 g/mol and PDI of 1.2.

Table 5.2 Reaction conditions for preparing Gly based prepolymers and properties

Prepolymer s	Monomers <sup>a</sup>	Monomer ratio <sup>b</sup>	COOH remaining <sup>c</sup> (%)	DB <sup>d</sup>		$M_w$ (g/mol) <sup>e</sup> : PDI	Viscosity at 30°C <sup>f</sup> (Pas)	$T_g^g$ (°C)	$T_d^h$ (°C)
				Gly segment	THAM segment				
G1	Gly, AA	1:1.64	33.2	0.48	-	1290 : 1.28	114	-42.4	422
G2	Gly, AA	1:2.25	44.1	0.72	-	1270 : 1.31	122	-41.6	421
D1	Gly, DIPA, AA	1:0.25:2.06	46.5	0.53	-	1260 : 1.27	157	-42.6	417
D2	Gly, DIPA, AA	1:0.5:2.48	41.1	0.47	-	1290 : 1.23	512	-29.9	418
D3	Gly, DIPA, AA	1:0.75:2.89	45.1	0.49	-	1290 : 1.23	805	-30.3	414
D4	Gly, DIPA, AA	1:1:3.3	48.0	0.47	-	1300 : 1.22	550	-26.4	412
T1	Gly, THAM, AA	1:0.25:2.20	41.0	0.51	0.81	1160 : 1.25	347	-31.6	419
T2	Gly, THAM, AA	1:0.5:2.75	42.0	0.53	0.80	1210 : 1.27	3140	-27.1	414
T3	Gly, THAM, AA	1:0.75:3.3	42.7	0.64	0.76	1190 : 1.27	1890	-28.5	416
T4	Gly, THAM, AA	1:1:3.85	41.0	0.41	0.78	1190 : 1.27	7190	-22.4	414

<sup>a</sup> Gly: glycerol, DIPA: diisopropanolamine, and THAM: tris(hydroxymethyl)aminomethane;

<sup>b</sup> monomer ratio was based on 1:1.1 of ratio between total OH and  $\text{NH}_2$  and COOH except for G2 (1:1.5);

<sup>c</sup> COOH remaining was calculated based on  $^1\text{H}$  NMR;

<sup>d</sup> Degree of branching was measured by NMR, Gly segment =  $(T_{1,2} + T_{1,3} + D) / (T_{1,2} + T_{1,3} + D + L_{1,2} + L_{1,3})$  from inverse gated  $^{13}\text{C}$  NMR, THAM segment =  $(T + sD + D) / (T + sD + D + L)$  from  $^1\text{H}$  NMR;

<sup>e</sup>  $M_w$  was determined by positive ion ESI-MS;

<sup>f</sup> Viscosity was taken at the zero-shear rate.

<sup>g</sup>  $T_g$  was measured by DSC;

<sup>h</sup>  $T_d$  was determined as the maxima of DTG thermograms.

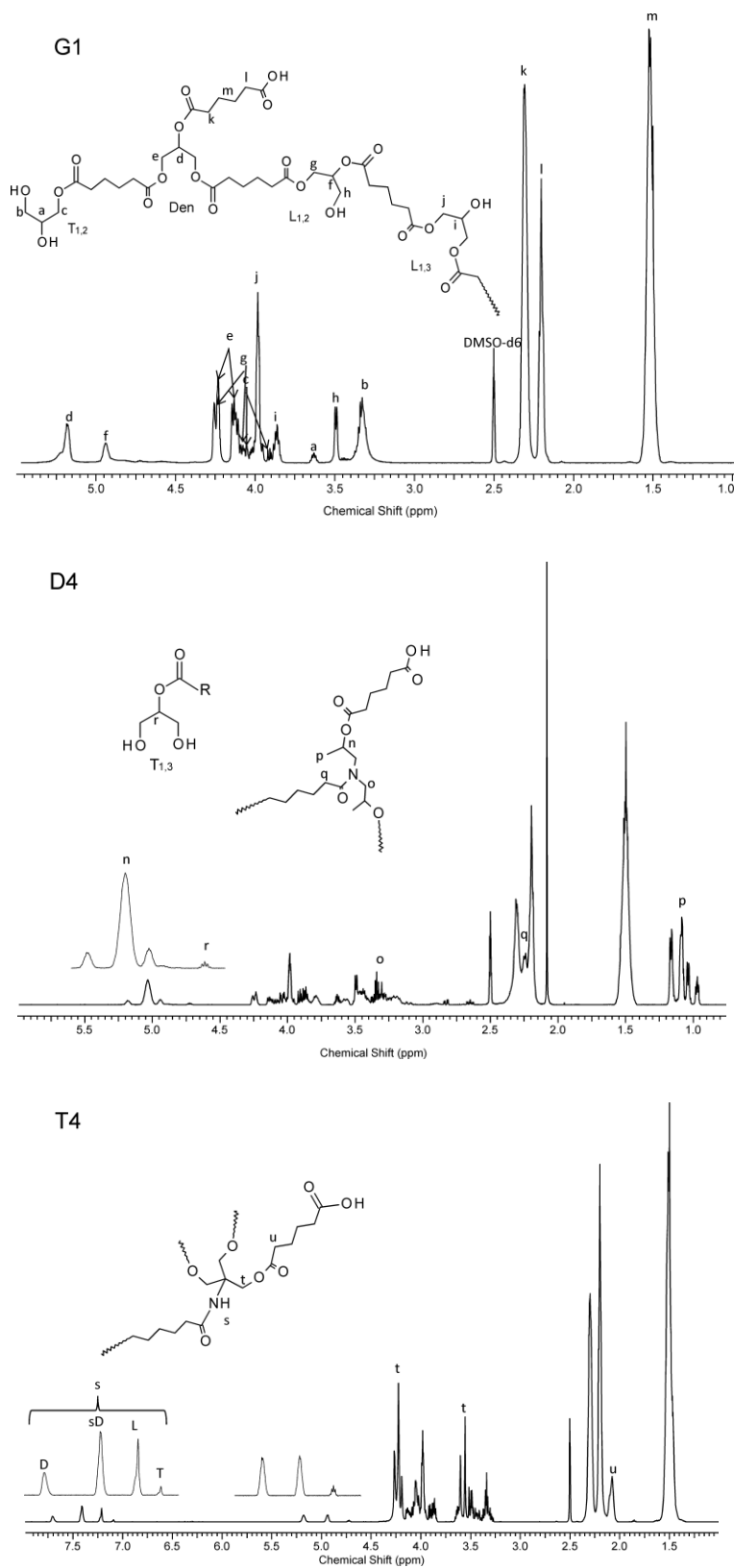


Figure 5.3  $^1\text{H}$  NMR spectra of G1, D4 and T4 Gly based prepolymers

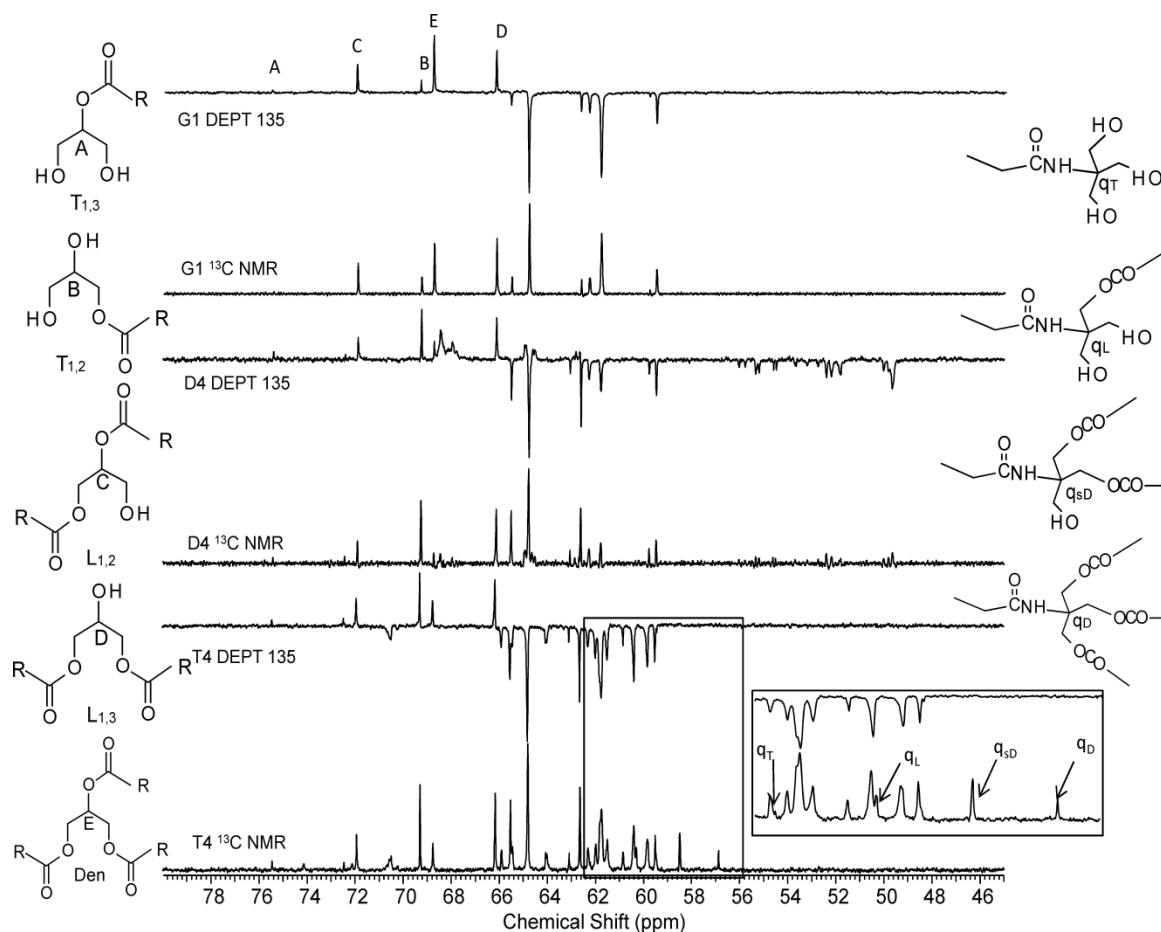


Figure 5.4  $^{13}\text{C}$  and DEPT 135 NMR spectra of G1, D4 and T4 Gly based prepolymers.

The apparent viscosity of the prepolymers was measured by parallel plate rheometry as a function of shear rate (Figure 5.5). All the prepolymers displayed shear thinning behavior which is common for HyBPs (Kadam et al., 2014; Soleimani et al., 2014). The viscosities at zero-shear rate for the prepolymers are given in Table 5.2. The G1 and G2 prepolymers were shown to have a low viscosity ( $\sim 120$  Pa.s) as compared to the D1-D4 and T1-T4 series prepolymers. The T series prepolymers all had significantly high viscosities (e.g. T4 at 7,185 Pa.s). The more rigid and crosslinked structures introduced by DIPA and THAM into the prepolymer could be responsible for their high viscosity. Furthermore, the prepolymer T series had a higher apparent viscosity than those of D series, which might be contributed by their highly crosslinked THAM core structures and high H-bonding comparing more linear structures by DIPA core (McKee et al., 2005).



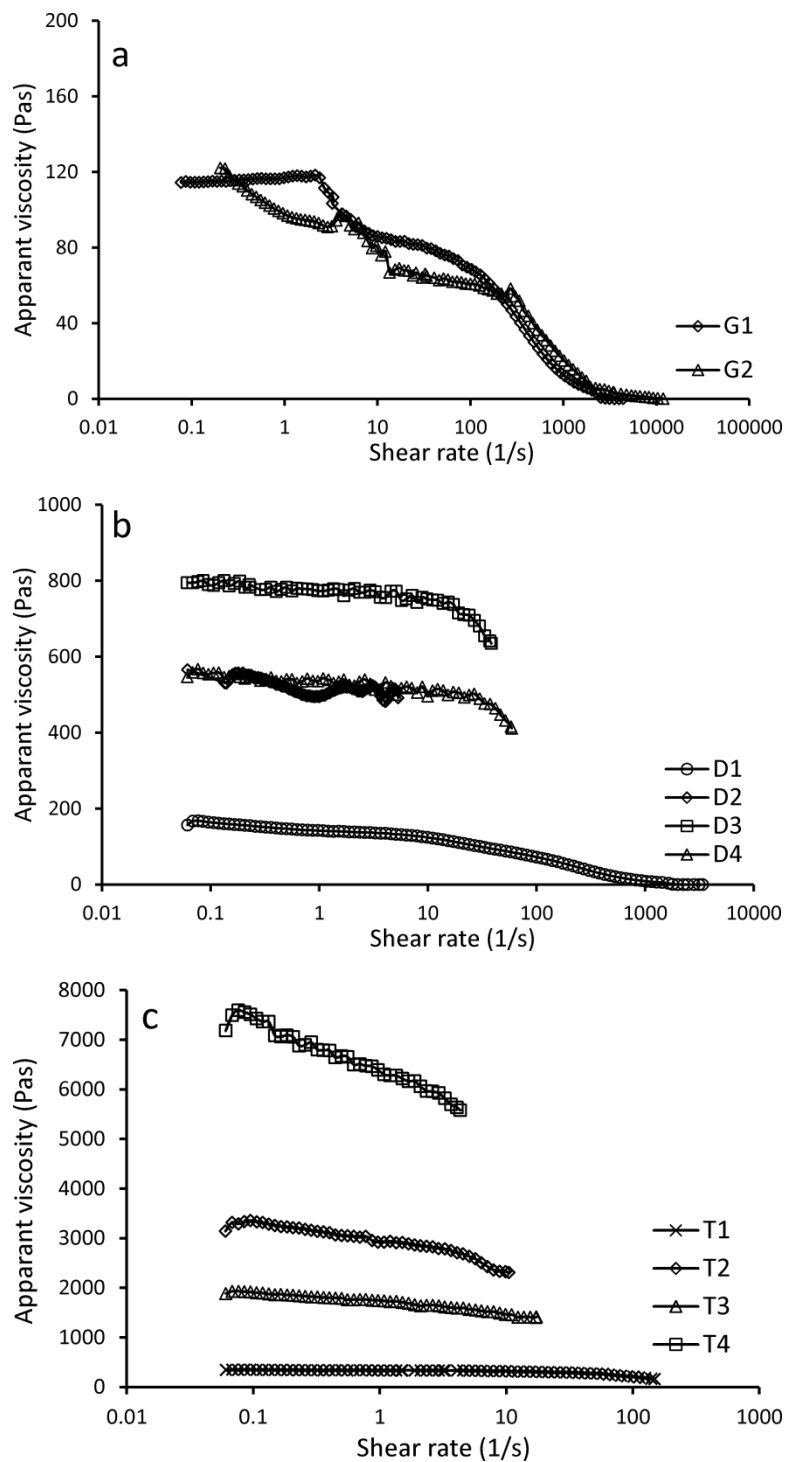


Figure 5.5 Apparent viscosity of Gly based prepolymers: (a), G1 and G2; (b), D1 to D4; and (c), T1 to T4.

All the Gly based prepolymers demonstrated considerably low  $T_g$ s as determined by DSC (Table 5.2) (Voit and Lederer, 2009). Variations of acid content did not affect  $T_g$  ( $-42.4^\circ\text{C}$  for

G1 and  $-41.6^{\circ}\text{C}$  for G2), but addition of DIPA and THAM dramatically increased the  $T_g$  ( $-42.6$  to  $-26.4^{\circ}\text{C}$  for D1 to D4 and  $-31.6$  to  $-22.4^{\circ}\text{C}$  for T1 to T4). Furthermore, the addition of THAM contributed to a greater increase in  $T_g$  than the addition of DIPA, at the same level, to the prepolymers. The increase in  $T_g$  by adding DIPA and/or THAM could be explained by the introduction of tertiary or secondary amides linkages. The lower  $T_g$  of the DIPA based prepolymers (D series) as compared to the THAM based prepolymers (T series) might be attributed to the methyl side group (more free volume) present in DIPA. Furthermore, H-bonding by the secondary amide (N-H bonding) of THAM will likely contribute to its higher  $T_g$  than DIPA. The thermal stability of the prepolymers was characterized by TGA. All the prepolymers gave a degradation temperature at  $420^{\circ}\text{C}$  based on the DTG maxima peak showing similar backbone degradations (Sivasankarapillai et al., 2012).

#### 5.4.4 Characterization of lignin-copolymers (LG1, LG2, LD1-LD4, and LT1-LT4)

##### 5.4.4.1 FTIR results

A series of lignin-copolymers with a biobased content ranging from 87 to 100% was successfully produced (Table 5.1). The lignin-copolymers were chemically analyzed by FTIR spectroscopy (Figure 5.6). Ester formation between lignin and Gly based prepolymers was supported by the reduction of the OH band ( $3600\text{-}3100\text{ cm}^{-1}$ ) and an increase in the ester carbonyl band ( $1800\text{-}1650\text{ cm}^{-1}$ ). More specifically, the ester band at  $1730\text{ cm}^{-1}$ , tertiary amide band at  $1635\text{ cm}^{-1}$  from the DIPA unit, and amide I and II bands at  $1655$  and  $1546\text{ cm}^{-1}$  from the THAM units in the prepolymers. The lignin aromatic skeletal vibration bands at  $1600$  and  $1511\text{ cm}^{-1}$  did not change because of a constant lignin content (30%) for all copolymers. The band region between  $1540\text{ cm}^{-1}$  to  $1800\text{ cm}^{-1}$  were expanded to obtain more information on linkages (Figure 5.7). The effects of DIPA and THAM on the copolymers were examined (Figure 5.7 b and c). As DIPA or THAM content increased, the tertiary band ( $1635\text{ cm}^{-1}$ ) of DIPA and Amide I ( $1655\text{ cm}^{-1}$ ) of THAM also increased. A trace carbonyl (COOH) shoulder was found at  $1708\text{ cm}^{-1}$  for all copolymers due to an excess of AA. A noticeable COOH band at  $1695\text{ cm}^{-1}$  was observed in LG2. The shift to lower band position was most likely contributed by the formation of an acid dimer which weakened the C=O bond (Figure

5.2) (Florio et al., 2003; Ren et al., 2004). Although the total molar ratio between OH+NH or NH<sub>2</sub> to COOH was all set to 1:1.1, differences in the COOH shoulder at 1708 cm<sup>-1</sup> were noticed as DIPA or THAM content increased. The intensity of the COOH shoulder band decreased as DIPA content increased (LD1-LD4), while the shoulder increased as THAM content increased (LT1-LT4) (Figure 5.7b and c). This could be explained by DIPA acting as a catalyst for esterification between the carboxylic acid and hydroxyl group. The underlying mechanism is shown in Figure 5.8. The formation of an oxazolinium-carboxylate ion pair facilitates both the polycondensation of tertiary amide to a HyBP polyesteramide and the esterification of the hydroxyalkyl amide end groups of this poly(ester-amide) with the carboxylic acid (Kelland, 2011; Stanssens et al., 1993; van Benthem et al., 2001). Furthermore, no band at 1760 cm<sup>-1</sup> (characteristic of an aromatic carbonyl ester) was observed suggesting that the prepolymer was ester linked through the aliphatic hydroxyl groups of lignin (Figure 5.6) (Gandini et al., 2002).

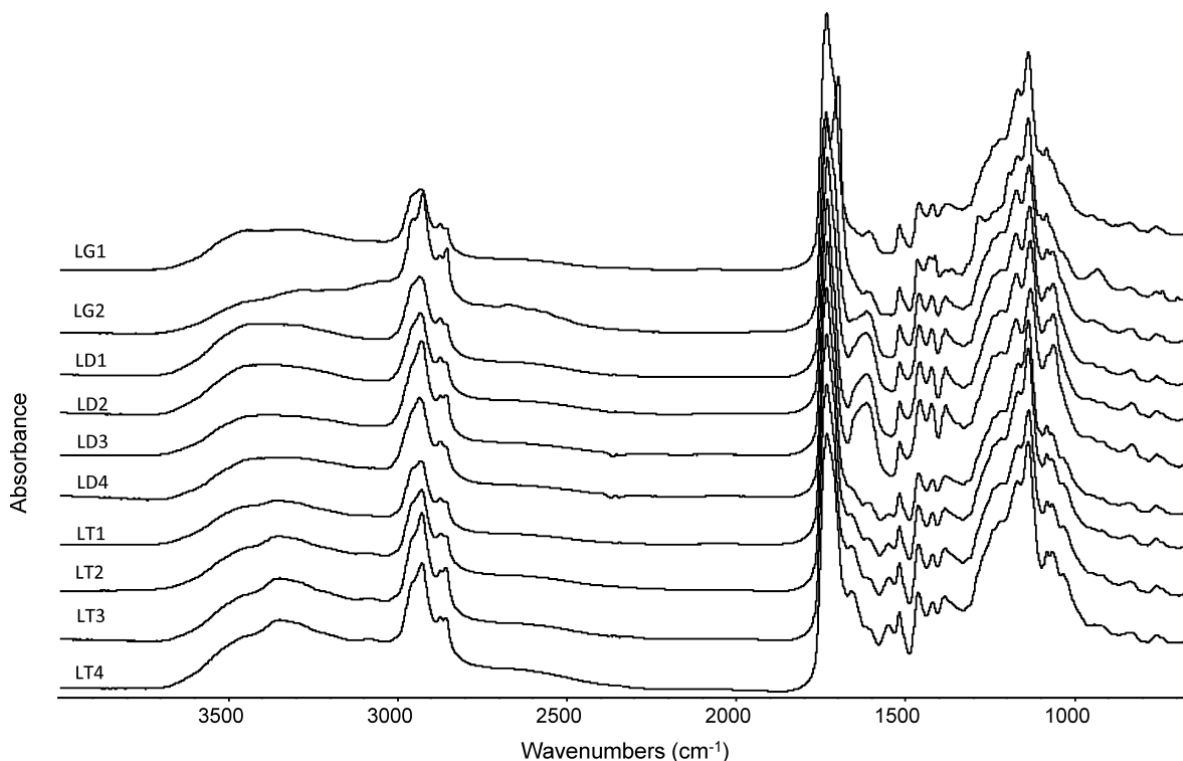


Figure 5.6 FTIR spectra of lignin-copolymers

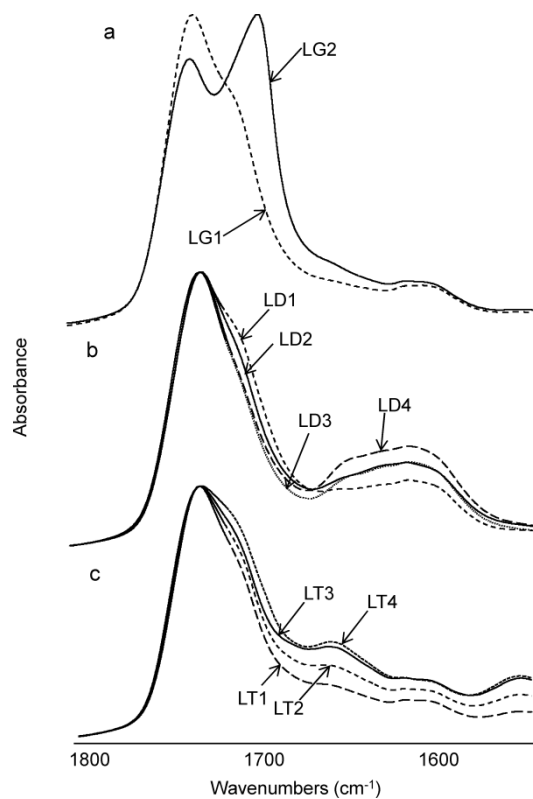


Figure 5.7 Expanded FTIR spectral region ( $1540\text{--}1800\text{ cm}^{-1}$ ) of lignin-copolymers: (a) LG1 and LG2, (b) LD1 to LD4, and (c) LT1 to LT4.

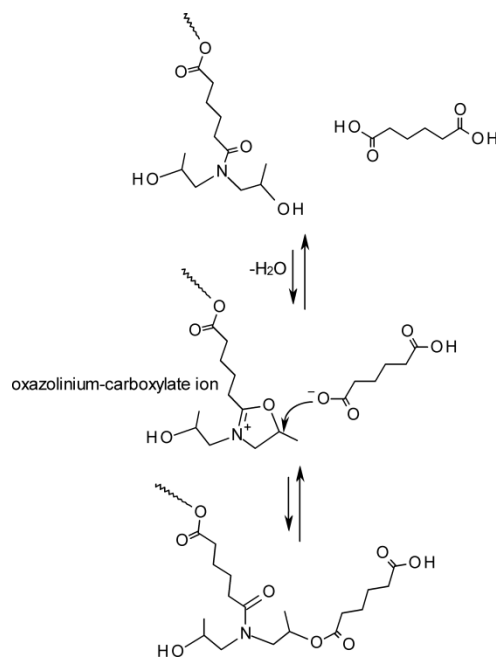


Figure 5.8 Oxazolinium-carboxylic ion formation in the D series prepolymer

#### 5.4.4.2 Mechanical properties

The tensile properties of all the lignin-copolymers are shown in Figure 5.9. The LG1 and LG2 copolymers showed relatively poor mechanical properties. However, the LG2, with more acid content, had the higher mechanical properties of this pair (tensile strength of 2.3 MPa and Young's modulus of 5.1 MPa). The additions of DIPA and THAM to the prepolymer improved the tensile properties of the lignin-copolymers (LD and LT series), except for LD1 (tensile strength of 1.2 MPa). The tensile strength and Young's modulus of the LD copolymers series showed an increase from LG1 to LG4, where LG3 had the highest tensile strength of 14.2 MPa and Young's modulus of 132 MPa and comparable to low density polyethylene (Rubin, 1990). The LT1-4 copolymer series all demonstrated good mechanical properties although a similar trend was observed that the more THAM content, the better the mechanical properties. The reason for the enhanced mechanical properties by the addition of DIPA and THAM was that amide linkages are more rigid than an ester linkage and introduce more H-bonding to the copolymers (Todros et al., 2013). Moreover, LT1-2 had higher mechanical properties than LD1-2 but lower for LT3-4, which could be explained that at lower DIPA or THAM content, the THAM rigid amide and core structures dominated, while at higher DIPA or THAM content, more oxazolinium-carboxylate ion catalyzed higher level of reactions. The strain at break and toughness (as assessed by the energy at break (EAB)) of the copolymers are shown in Figure 5.9b. The LD1-4 series copolymers showed better strain at break compared to LT1-4 series copolymers. Similar to tensile strength, the LD3 copolymer also demonstrated the highest strain at break and toughness of all lignin-copolymers. The conclusion drawn here was that more carboxylic acid groups available leads to improved mechanical properties and the addition of DIPA more so than THAM dramatically increased the mechanical properties.

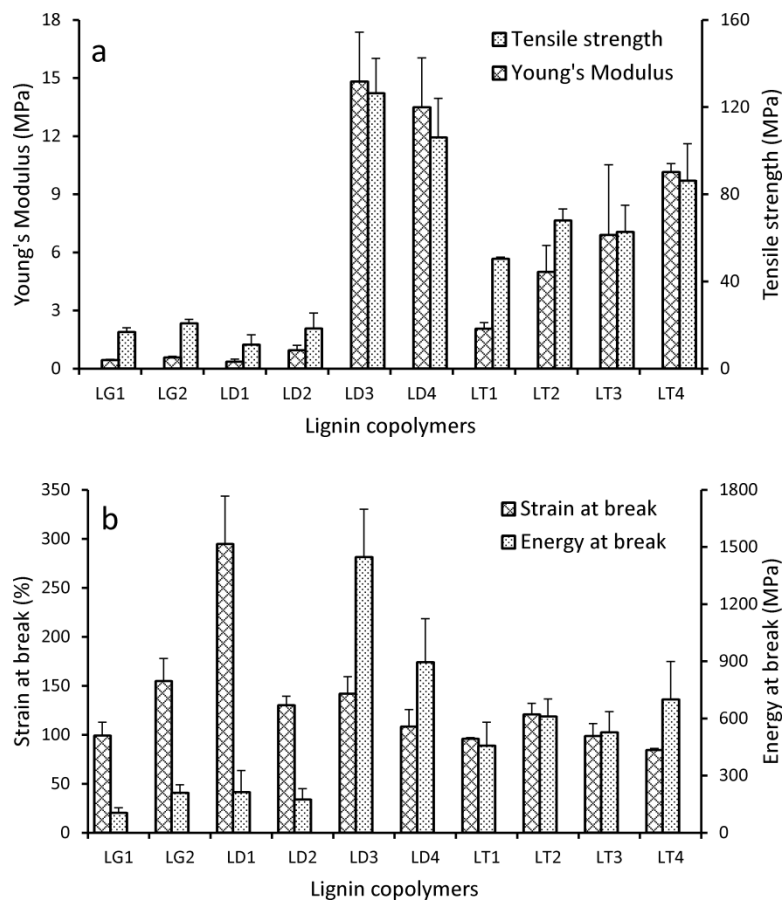


Figure 5.9 Tensile properties results of the lignin-copolymers.

#### 5.4.4.3 Thermal properties

The  $T_g$  of the lignin-copolymers were characterized by DSC and DMA (at loss modulus ( $E''$ ) maxima) (Figure 5.10). The  $T_g$  is a second-order phase transition of an amorphous polymer which not only confines its threshold in engineering applications and determine the SME of smart polymers (Lendlein and Kelch, 2002; Overlay et al., 2000). All the lignin-copolymers demonstrated a considerably low and single  $T_g$  although lignin's  $T_g$  was high at 132 °C, revealing the dominant role of the prepolymer and great miscibility between lignin and prepolymer matrix (Li and McDonald, 2014). The effect of varying the prepolymer structure (e.g DB) on  $T_g$  was also characterized. The Gly-AA based (LG1-2) copolymers showed the lowest  $T_g$  as compared to the DIPA (LD1-4) and THAM (LT1-4) based copolymers series. The LG2 copolymer had the lowest  $T_g$  relative to LG1 as obtained by DSC. The more DIPA or THAM added to the prepolymer composition, the higher the  $T_g$  of final lignin-copolymer

which is consistent with the results of the prepolymer properties. For example, the  $T_g$  increased from 4.4 to 25.6 °C, respectively for copolymers LD1 to LD4. A similar trend was observed for the THAM based copolymers LT1 ( $T_g$  9.8°C) to LT4 ( $T_g$  37.2°C). These results indicate that the rigid amide linkages in these prepolymers hindered the free thermal mobility of lignin-copolymers.  $T_g$  from DMA at  $E''$  maxima showed different values to those obtained from DSC (Figure 5.10) however demonstrated a similar trend as DSC. These values were also the basis for determining the SME properties from a material perspective.

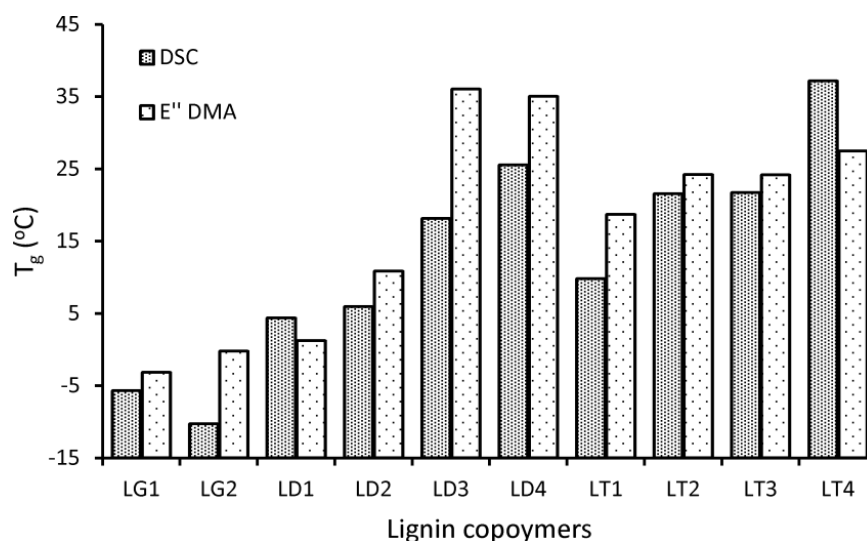


Figure 5.10  $T_g$  of lignin-copolymers from DSC and  $E''$  DMA.

The thermal stability of the lignin-copolymers was studied by TGA (Figure 5.11). Three stages of decomposition were observed by TGA for all the lignin-copolymers (Table 5.3 and Figure 5.11). The first stage was between 200 and 400°C. The second stage was between 400 and 440°C. The third stage was between 440 and 540°C. The first and second stages are most likely assigned to the Gly based polyester and poly(ester-amide) component of the copolymer since these are constituted with highly branched aliphatic chains with labile ester linkages (Pramanik et al., 2014; Pramanik et al., 2013), although the side chain/link of lignin also participated the decomposition (Figure 5.11). The major backbones of poly(ester-amide)s in the copolymer decomposed at temperature ranging from 400 to 440°C (2<sup>nd</sup> stage herein) (Prime et al., 2009). The 3<sup>rd</sup> stage of decomposition was most likely due to the lignin component of the copolymer because of its highly cross-linked aromatic structure to form

appreciable amount of char (Nassar and MacKay, 1984). The amount of carboxylic acid present in the DIPA and THAM prepolymers and copolymers mainly affected first region (200-400°C). The more carboxylic acid present resulted in less mass remaining (80% for LG1 to 73% for LG2) in the lignin-copolymer. Based on FTIR analysis, an appreciable amount of free carboxylic acid was observed in LG2 (1695 cm<sup>-1</sup>) which might be responsible for the high thermal decomposition in the first stage. Both LD1-4 and LT1-4 series copolymers showed a gradual decrease in first stage from 72% for LD1 to 57 for LD4 and from 83% for LT1 to 73% for LT4. Two DTG peaks (420 and 580°C) were observed in the lignin-copolymers and assigned to degradation of the major backbone of the prepolymers (same as T<sub>d</sub> of the prepolymers) and lignin components, respectively.

Table 5.3 Thermal decomposition of the lignin-copolymers

Sample #	1st stage		2nd stage		3rd stage		Max peaks (°C)
	T (°C)	Remaining mass (%)	T (°C)	Remaining mass (%)	T (°C)	Remaining mass (%)	
LG1	406	80.0	444	26.6	534	17.7	416, 562
LG2	403	72.8	443	25.6	544	17.1	437, 557
LD1	403	71.9	439	31.1	548	20.4	429, 578
LD2	404	65.8	441	29.3	548	20.8	423, 585
LD3	406	62.5	435	35.1	544	21.6	416, 574
LD4	410	57.4	437	34.2	546	21.8	418, 580
LT1	392	83.3	438	36.4	553	21.1	420, 574
LT2	394	79.7	439	36.4	555	21.8	427, 591
LT3	393	76.9	443	35.8	554	23.1	422, 597
LT4	393	73.4	442	35.5	557	24.4	426, 603



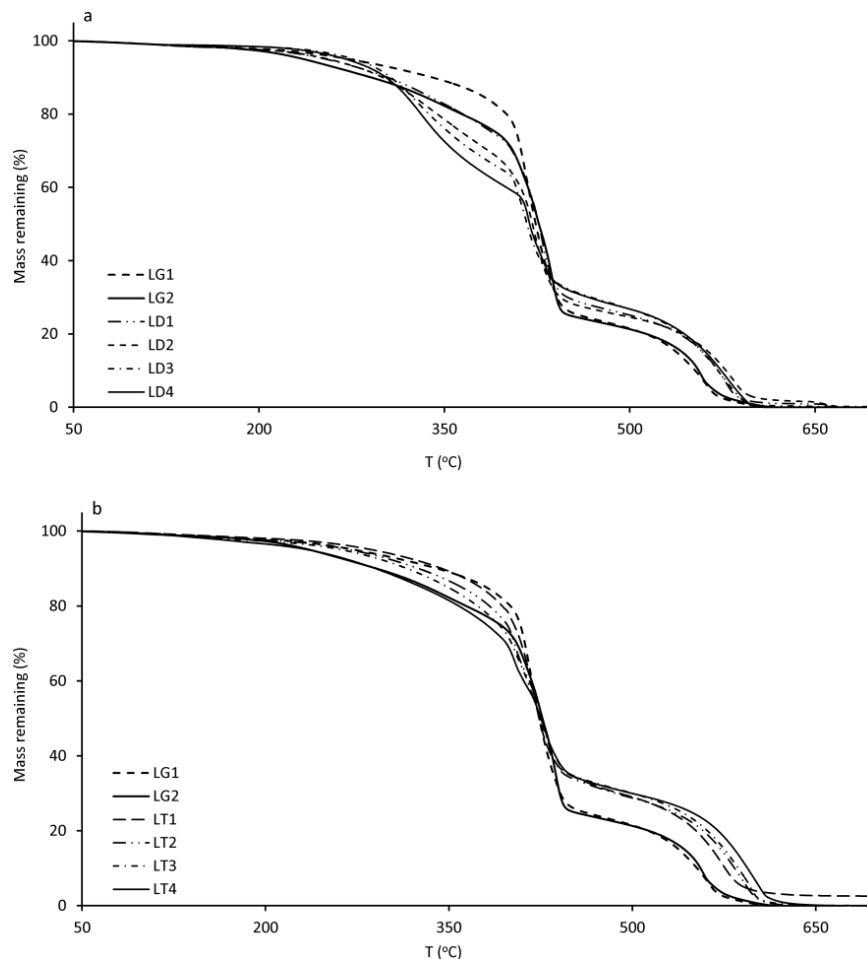


Figure 5.11 TGA results of lignin-copolymers

#### 5.4.4.4 Thermal-stimulated shape memory effect ( $T_s$ -SME)

Thermally stimulated shape memory effect ( $T_s$ -SME) can be obtained in a polymer system which contains two kinds of segments, i.e., soft segment controlling temporary shape and netpoint segment determining permanent shape. Our previous research has shown the development of a series of lignin-copolymers with  $T_s$ -SME properties, where a highly branched poly(ester-amine) prepolymer functioned as the soft segment and lignin as the netpoint segments (Li et al., 2014a). Following this concept, we further developed the soft segment using a series of Gly based polyester and poly(ester-amide)s. Figure 5.12 shows an example of SME of the LD1 copolymer by subjecting it to ice (0 °C) after curling the sheet at room temperature (25 °C). The curled shape was maintained in ice even after 180s, and then it was taken back to room temperature and gradually recovered the original shape in 150s.

The shape memory properties of the lignin-copolymers (LG1, LG2, LD1, LD3, LT1, and LT3) were quantified by stress-controlled cyclic thermomechanical testing (Table 5.4 and Figure 5.13). The shape memory recovery ratio ( $R_r$ ) and fixity ratio ( $R_f$ ) were calculated from the test data according to the following equations (Lendlein and Kelch, 2002):

$$R_r(N) = \frac{\varepsilon_l(N) - \varepsilon_p(N)}{\varepsilon_l(N) - \varepsilon_p(N-1)} \times 100\% \quad (5.1)$$

$$R_f(N) = \frac{\varepsilon_u(N)}{\varepsilon_l(N)} \times 100\% \quad (5.2)$$

Where  $R_r(N)$  is the shape recovery ratio at  $N^{\text{th}}$  cycle,  $R_f(N)$  is the shape fixity ratio at  $N^{\text{th}}$  cycle,  $N$  is cycle number from 1 to 3,  $\varepsilon_l(N)$  is the maximum strain with load,  $\varepsilon_u(N)$  is the tensile strain after unloading at  $T_{\text{low}}$ ,  $\varepsilon_p(N-1)$  and  $\varepsilon_p(N)$  are the recovered strain in two successive cycles in the stress-free state before exertion of yield stress at  $T_{\text{high}}$ . The results were an average of three cycles.  $R_f$  describes the ability to fix the mechanical deformation under  $T_{\text{low}}$ , while  $R_r$  quantifies how well the shape recovers in the  $N^{\text{th}}$  cycle (for  $N > 1$ ) in terms of the recovered shape of the previous  $(N-1)^{\text{th}}$  cycle (Sauter et al., 2013). The results of  $R_r$  and  $R_f$  of lignin based copolymers are shown in Table 4. All measured lignin-copolymers demonstrated relatively good  $R_r$  and  $R_f$ .  $T_{\text{trans}}$  is another important parameter of  $T_s$ -SME polymers and was determined since this is the temperature at which the polymer can be switched back to its original shape upon removal of external stimuli and measured as first derivative peak of the strain versus temperature plot. The  $T_{\text{trans}}$  of lignin copolymers as a function of different Gly based prepolymer structures were shown in Table 5.4.  $T_{\text{trans}}$  (20°C) of LD1 copolymer could explained why it could maintain the curling shape in ice while recovery at room temperature (Figure 5.12). Furthermore,  $T_{\text{trans}}$  was affected by carboxylic acid content as well as the addition of DIPA or THAM to the Gly based prepolymer formulations. The higher the carboxylic acid, DIPA or THAM contents in the prepolymer which concomitantly led to higher  $T_{\text{trans}}$  values. For example, the  $T_{\text{trans}}$  increased from 20.0 to 56.4°C respectively for the copolymers LD1 to LD3 series and 38.2 to 44.1°C for the copolymer LT1 to LT3 series. These results indicate that the  $T_{\text{trans}}$  could be tuned by changing the monomer ratios of the Gly based poly(ester-amide) formulations besides lignin content (Li et al., 2014a, b).

Table 5.4 Shape memory effect parameters ( $R_r$ ,  $R_f$ , and  $T_{trans}$ ) and elasticity recovery  $R_{r,e}$  of the lignin-copolymers

Sample #	$R_r$ (%)	$R_f$ (%)	$T_{trans}$ ( $^{\circ}\text{C}$ )	$R_{r,e}$
LG1	87.1 $\pm$ 18.1	97.7 $\pm$ 0.1	16.4 $\pm$ 0.4	98.7 $\pm$ 2.1
LG2	91.4 $\pm$ 11.7	97.6 $\pm$ 2.0	18.9 $\pm$ 0.1	95.2 $\pm$ 2.8
LD1	89.2 $\pm$ 9.3	99.1 $\pm$ 0.1	20.0 $\pm$ 0.4	92.1 $\pm$ 4.5
LD3	91.2 $\pm$ 8.5	86.6 $\pm$ 1.8	56.4 $\pm$ 0.1	98.6 $\pm$ 0.9
LT1	94.5 $\pm$ 5.2	89.8 $\pm$ 1.5	38.2 $\pm$ 0.1	88.0 $\pm$ 7.9
LT3	86.8 $\pm$ 12.2	94.5 $\pm$ 0.6	44.1 $\pm$ 0.2	77.7 $\pm$ 9.4

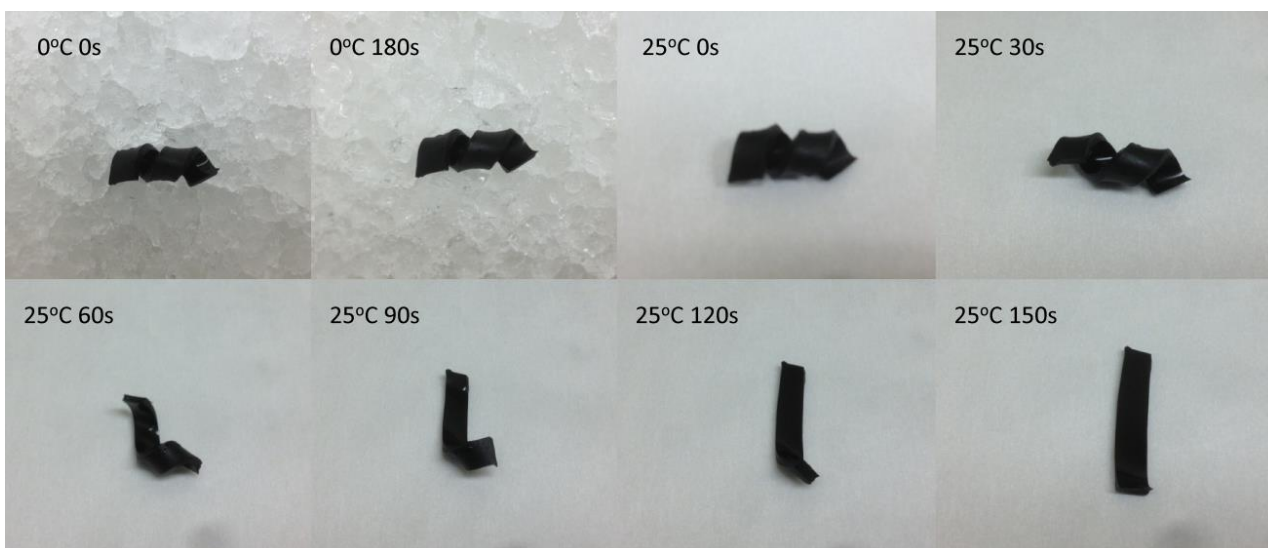


Figure 5.12 Photographs showing the SME of LD1 copolymer: (1) Curled at room temperature (25  $^{\circ}\text{C}$ ); (2) Subjected into ice (0  $^{\circ}\text{C}$ ), curled shape was maintained in ice even after 180 s; (3) taken back to room temperature; and (4) gradually recovered the original shape in 150 s

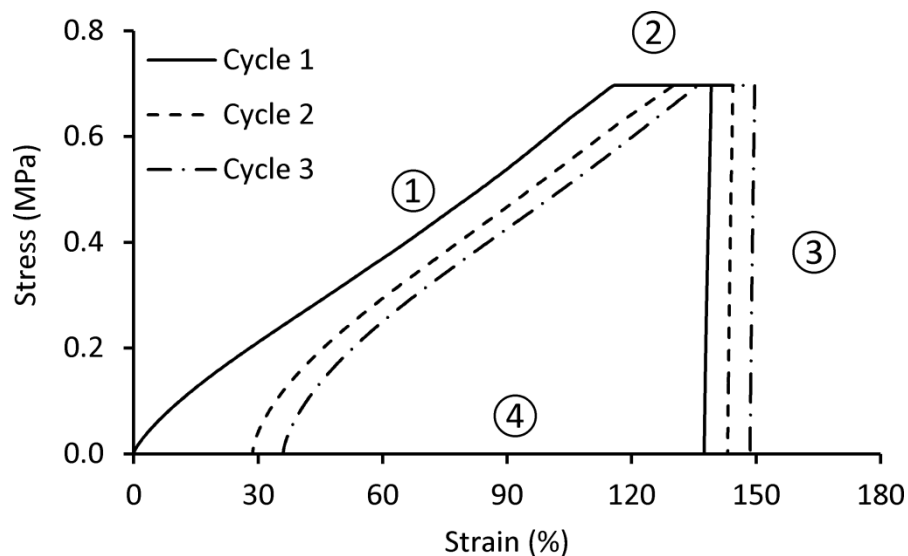


Figure 5.13 Cyclic thermomechanical testing of LD1 copolymer showing  $T_S$ -SME behavior (Four steps: (1) Stretching at  $T_{high}$  ( $21^{\circ}\text{C}$ ); (2) keep load at  $T_{low}$  ( $-19^{\circ}\text{C}$ ); (3) unload at  $T_{low}$  ( $-19^{\circ}\text{C}$ ); and (4) recovery at  $T_{high}$  ( $21^{\circ}\text{C}$ )) for 3 cycles

With the aim of further measuring the elasticity of the lignin copolymers, cyclic tests ( $n=4$ ) were carried out to determine the recovery rate,  $R_{r,e}$  (Table 5.4) using eqn 5.1. The lignin-copolymers all demonstrated excellent  $R_{r,e}$  ( $>90\%$ ) values except for the LT series copolymers. LG copolymers show superior  $R_{r,e}$  ( $>95\%$ ) because of a more flexible Gly core. The reason of low elasticity of LT copolymers might be that the secondary amide brought out a strong resonance structure ( $\text{O}=\text{C}=\text{N}^+\text{H}$ ) and H-bonding ( $\text{C}=\text{O}\cdots\text{H}-\text{N}$ ), restricting the free movement of molecular chains. After exerting the mechanical stretch, these structures were non-reversibly destructed, consequently low  $R_{r,e}$ .

## 5.5 Conclusions

A series highly to hyper branched Gly based prepoly(ester-amide)s with varying branching structures (ie.,  $\text{B}^2\text{B}^3_2\text{-A}_2$ ,  $\text{B}^2\text{B}^3_2\text{-DB}^4_2\text{-A}_2$ , and  $\text{B}^2\text{B}^3_2\text{-CB}^1_3\text{-A}_2$ ) were successfully synthesized via melt polycondensation reactions. Lignin-copolymers were synthesized via a bulk polycondensation reaction to afford materials with  $T_S$ -SME dual shape memory behavior with as high as 100% biobased materials. The lignin-copolymer properties (tensile, thermal, and thermomechanical) were able to be tuned by altering the composition and branching structure of the prepolymer (soft segment). The addition of monomer units DIPA and THAM

were shown to influence the thermal and chemical properties of prepolymers by the addition of more rigid amide linkages. The copolymers demonstrated good shape memory and mechanical properties. The  $T_{\text{trans}}$  was shown to increase with DIPA and THAM content, revealing that the  $T_{\text{trans}}$  could be tuned by variations of DIPA and THAM. This study demonstrates that more renewable Gly and AA based prepolymers could act as soft segment in lignin based copolymer systems owning SME behavior.

## 5.6 References

- Anand, P., Saxena, R.K. **2012**. A comparative study of solvent-assisted pretreatment of biodiesel derived crude glycerol on growth and 1,3-propanediol production from *Citrobacter freundii*. *New Biotechnology*, 29, 199-205.
- Beardslee, T., Picataggio, S. **2012**. Bio-based adipic acid from renewable oils. *Lipid Technology*, 24, 223-225.
- Chun, B.C., Chong, M.H., Chung, Y.C. **2007**. Effect of glycerol cross-linking and hard segment content on the shape memory property of polyurethane block copolymer. *Journal of Materials Science*, 42, 6524-6531.
- Cui, C.Z., Sadeghifar, H., Sen, S., Argyropoulos, D.S. **2013**. Toward Thermoplastic Lignin Polymers; Part II: Thermal & Polymer Characteristics of Kraft Lignin & Derivatives. *BioResources*, 8, 864-886.
- De Guzman, D. **2010**. Bio-adipic acid prepares for entry. *ICIS Chemical Business*, 22-23.
- Feldman, D. **2002**. Lignin and its polyblends -- a review, in: Hu, T.Q. (Ed.), *Chemical modification, properties, and usage of lignin*. Kluwer Academic/Plenum, New York, pp. 81-99.
- Florio, G.M., Zwier, T.S., Myshakin, E.M., Jordan, K.D., Sibert, E.L. **2003**. Theoretical modeling of the OH stretch infrared spectrum of carboxylic acid dimers based on first-principles anharmonic couplings. *Journal of Chemical Physics*, 118, 1735-1746.

- Gandini, A., Belgacem, M.N., Guo, Z., Montanari, S. **2002**. Lignins as macromolecules for polyesters and polyurethanes, in: Hu, T.Q. (Ed.), *Chemical Modification, Properties, and Usage of lignin*. Kluwer Academic/Plenum Publishers, New York, pp. 57-80.
- Gao, C., Yan, D. **2004**. Hyperbranched polymers: from synthesis to applications. *Progress in Polymer Science*, 29, 183-275.
- Gelade, E.T.F., Goderis, B., de Koster, C.G., Meijerink, N., van Benthem, R.A.T.M., Fokkens, R., Nibbering, N.M.M., Mortensen, K. **2001**. Molecular structure characterization of hyperbranched polyesteramides. *Macromolecules*, 34, 3552-3558.
- Hult, A., Johansson, M., Malmstrom, E. **1999**. Hyperbranched polymers. *Branched Polymers* li, 143, 1-34.
- Kadam, P.G., Vaidya, P., Mhaske, S.T. **2014**. Synthesis and Characterization of Polyesteramide Hot Melt Adhesive from Low Purity Dimer Acid, Ethylenediamine, and Ethanolamine. *Journal of Polymers*, 1-8.
- Kelland, M.A. **2011**. Tuning the Thermoresponsive Properties of Hyperbranched Poly(ester amide)s Based on Diisopropanolamine and Cyclic Dicarboxylic Anhydrides. *Journal of Applied Polymer Science*, 121, 2282-2290.
- Kienle, R.H., Hovey, A.G. **1929**. The polyhydric alcohol-polybasic acid reaction I Glycerol-phthalic anhydride. *Journal of the American Chemical Society*, 51, 509-519.
- Kim, Y.H., Webster, O.W. **1988**. Hyperbranched Polyphenylenes. *Abstracts of Papers of the American Chemical Society*, 196, 104-POLY.
- Kulshrestha, A.S., Gao, W., Gross, R.A. **2005**. Glycerol copolyesters: Control of branching and molecular weight using a lipase catalyst. *Macromolecules*, 38, 3193-3204.
- Lendlein, A., Kelch, S. **2002**. Shape-memory polymers. *Angewandte Chemie International Edition*, 41, 2034-2057.

Li, H., McDonald, A.G. **2014**. Fractionation and Characterization of Industrial Lignin. University of Idaho, Moscow, Idaho.

Li, H., Sivasankarapillai, G., McDonald, A.G. **2014a**. Lignin valorization by forming toughened thermally-stimulated shape memory copolymeric elastomers: Evaluation of different industrial lignins.

Li, H., Sivasankarapillai, G., McDonald, A.G. **2014b**. Lignin valorization by forming toughened thermally-stimulated shape memory copolymeric elastomers: partially crystalline hyperbranched polymer as crosslinks.

Li, X., Lu, X., Lin, Y., Zhan, J., Li, Y., Liu, Z., Chen, X., Liu, S. **2006**. Synthesis and characterization of hyperbranched poly(ester-amide)s from commercially available dicarboxylic acids and multihydroxyl primary amines. *Macromolecules*, 39, 7889-7899.

Li, X.R., Su, Y.L., Chen, Q.Y., Lin, Y., Tong, Y.J., Li, Y.S. **2005**. Synthesis and characterization of biodegradable hyperbranched poly(ester-amide)s based on natural material. *Biomacromolecules*, 6, 3181-3188.

Li, X.R., Zhan, J., Li, Y.S. **2004**. Facile syntheses and characterization of hyperbranched poly(ester-amide)s from commercially available aliphatic carboxylic anhydride and multihydroxyl primary amine. *Macromolecules*, 37, 7584-7594.

Li, Y., Ragauskas, A.J. **2012**. Kraft lignin based rigid polyurethane foam. *Journal of Wood Chemistry and Technology*, 32, 210-224.

Li, Y., Sarkanen, S. **2002**. Alkylated kraft lignin-based thermaoplastic blends with aliphatic polyesters *Macromolecules*, 35, 9707-9715.

McDonald, A.G., Ma, L. **2012**. Plastic moldable lignin, in: Paterson, R.J. (Ed.), *Lignin: Properties and applications in biotechnology and bioenergy*. Nova Science Publisher, Inc., pp. 489-498.

McKee, M.G., Elkins, C.L., Park, T., Long, T.E. **2005**. Influence of random branching on multiple hydrogen bonding in poly(alkyl methacrylate)s. *Macromolecules*, 38, 6015-6023.

Mousavioun, P., Halley, P.J., Doherty, W.O.S. **2013**. Thermophysical properties and rheology of PHB/lignin blends. *Industrial Crops and Products*, 50, 270-275.

Muscat, D., van Benthem, R.A.T.M. **2001**. Hyperbranched polyesteramides - New dendritic polymers. *Dendrimers iii: Design, Dimension, Function*, 212, 41-80.

Nassar, M.M., MacKay, G.D.M. **1984**. Mechanism of thermal decomposition of lignin. *Wood and Fiber Science*, 16, 441-453.

Osman, N.B., McDonald, A.G., Laborie, M.P.G. **2012**. Analysis of DCM extractable components from hot-pressed hybrid poplar. *Holzforschung*, 66, 927-934.

Overley, R.M., Buenviaje, C., Luginuni, R., Dinelli, F. **2000**. Glass and structural transitions measured at polymer surfaces on the nanoscale. *Journal of Thermal Analysis and Calorimetry*, 59, 205-225.

Parees, D.M., Hanton, S.D., Clark, P.A.C., Willcox, D.A. **1998**. Comparison of mass spectrometric techniques for generating molecular weight information on a class of ethoxylated oligomers. *Journal of the American Society for Mass Spectrometry*, 9, 282-291.

Pramanik, S., Konwarh, R., Barua, N., Buragohain, A.K., Karak, N. **2014**. Bio-based hyperbranched poly(ester amide)-MWCNT nanocomposites: multimodalities at the biointerface. *Biomaterials Science*, 2, 192-202.

Pramanik, S., Konwarh, R., Sagar, K., Konwar, B.K., Karak, N. **2013**. Bio-degradable vegetable oil based hyperbranched poly(ester amide) as an advanced surface coating material. *Progress in Organic Coatings*, 76, 689-697.



Prime, B.R., Bair, H.E., Vyazovkin, S., Gallagher, P.K., Riga, A. **2009**. Thermogravimetric analysis (TGA), in: Menczel, J.D., Prime, B.R. (Eds.), *Thermal Analysis of Polymers, Fundamentals and Applications*. John Wiley, New Jersey, pp. 241-317.

Ren, Z.Y., Wu, H.P., Ma, J.M., Ma, D.Z. **2004**. FTIR studies on the model polyurethane hard segments based on a new waterborne chain extender dimethylol butanoic acid (DMBA). *Chinese Journal of Polymer Science*, 22, 225-230.

Rubin, I.I. **1990**. *Handbook of plastic materials and technology*. Wiley, New York.

Sadeghifar, H., Cui, C., Argyropoulos, D.S. 2012. Toward Thermoplastic Lignin Polymers. Part 1. Selective Masking of Phenolic Hydroxyl Groups in Kraft Lignins via Methylation and Oxypropylation Chemistries. *Industrial and Engineering Chemistry Research*, 51, 16713-16720.

Sauter, T., Heuchel, M., Kratz, K., Lendlein, A. **2013**. Quantifying the Shape-Memory Effect of Polymers by Cyclic Thermomechanical Tests. *Polymer Reviews*, 53, 6-40.

Sivasankarapillai, G., McDonald, A.G. **2011**. Synthesis and properties of lignin-highly branched poly (ester-amine) polymeric systems. *Biomass and Bioenergy*, 35, 919-931.

Sivasankarapillai, G., McDonald, A.G., Li, H. **2012**. Lignin valorization by forming toughened lignin-co-polymers: Development of hyperbranched prepolymers for cross-linking. *Biomass and Bioenergy*, 47, 99-108.

Soleimani, A., Drappel, S., Carlini, R., Goredema, A., Gillies, E.R. **2014**. Structure–Property Relationships for a Series of Poly(ester amide)s Containing Amino Acids. *Industrial & Engineering Chemistry Research*, 53, 1452-1460.

Stanssens, D., Hermanns, R., Worries, H. **1993**. On the Mechanism of the Esterification of a Beta-Hydroxy Alkylamide with a Carboxylic-Acid. *Progress in Organic Coatings*, 22, 379-391.

Stumbe, J.F., Bruchmann, B. **2004**. Hyperbranched polyesters based on adipic acid and glycerol. *Macromolecular Rapid Communications*, 25, 921-924.

Todros, S., Natali, A.N., Pace, G., Di Noto, V. **2013**. Correlation Between Chemical and Mechanical Properties in Renewable Poly(ether-block-amide)s for Biomedical Applications. *Macromolecular Chemistry and Physics*, 214, 2061-2072.

van Benthem, R.A.T.M., Meijerink, N., Gelade, E., de Koster, C.G., Muscat, D., Froehling, P.E., Hendriks, P.H.M., Vermeulen, C.J.A.A., Zwartkruis, T.J.G. **2001**. Synthesis and characterization of bis(2-hydroxypropyl)amide-based hyperbranched polyesteramides. *Macromolecules*, 34, 3559-3566.

Van de Vyver, S., Roman-Leshkov, Y. **2013**. Emerging catalytic processes for the production of adipic acid. *Catalysis Science & Technology*, 3, 1465-1479.

Voit, B.I., Lederer, A. **2009**. Hyperbranched and Highly Branched Polymer Architectures- Synthetic Strategies and Major Characterization Aspects. *Chemical Reviews*, 109, 5924-5973.

Wang, J., John Manley, R.S., D., F. **1992**. Synthetic polymer-lignin copolymers and blends. *Progress in Polymer Science*, 17, 611-646.

Wu, L.C.F., Glasser, W.G. **1984**. Engineering plastics from lignin. I. Synthesis of hydroxypropyl lignin. *Journal of Applied Polymer Science*, 29, 1111-1123.

Wyatt, V.T., Nunez, A., Foglia, T.A., Marmer, W.N. **2006a**. Synthesis of hyperbranched poly(glycerol-diacid) oligomers. *Journal of the American Oil Chemists Society*, 83, 1033-1039.

Wyatt, V.T., Nunuz, A., Foglia, T.A., Marmer, W.N. **2006b**. Acid catalyzed synthesis of hyperbranched poly(glycerol-diacid) oligomers. *Abstracts of Papers of the American Chemical Society*, 231.

Wyatt, V.T., Strahan, G.D., Nunez, A., Haas, M.J. **2011**. Characterization of Thermal and Mechanical Properties of Hyperbranched Oligo(glycerol-glutaric acid)s. *Journal of Biobased Materials and Bioenergy*, 5, 92-101.

Yang, F.X., Hanna, M.A., Sun, R.C. **2012**. Value-added uses for crude glycerol-a byproduct of biodiesel production. *Biotechnology for Biofuels*, 5.

Yang, Y.X., Lu, W.H., Cai, J.L., Hou, Y., Ouyang, S.Y., Xie, W.C., Gross, R.A. **2011**. Poly(oleic diacid-co-glycerol): Comparison of Polymer Structure Resulting from Chemical and Lipase Catalysis. *Macromolecules*, 44, 1977-1985.

Yoshida, H., Morck, R., Kringstad, K.P. **1987**. Fractionation of Kraft lignin by successive extraction with organic solvents. *Holzforschung*, 41, 171-176.

Zagar, E., Grdadolnik, J. **2003**. An infrared spectroscopic study of H-bond network in hyperbranched polyester polyol. *Journal of Molecular Structure*, 658, 143-152.

Zakzeski, J., Bruijninx, P.C.A., Jongorius, A.L., Weckhuysen, B.M. **2010**. The Catalytic Valorization of Lignin for the Production of Renewable Chemicals. *Chemical Reviews*, 110, 3552-3599.

## 6 Summary and Future Work

### 6.1 Summary of dissertation

Industrial lignin is an underutilized biopolymer byproduct from both the pulping and cellulosic ethanol biorefinery industries, showing potential as a substrate for producing biobased polyester materials because of abundant hydroxyl groups. This dissertation aimed at generating lignin based polymer systems with shape memory properties based on the following objectives:

1. Can we fractionate lignin from different sources with different  $T_g$ s;
2. Can we produce hyperbranched polymers with different branching structures;
3. Can we produce lignin-copolymers with a range of properties.

This dissertation shows that we were able to fractionate industrial lignins by solubilizing low molar mass lignin in methanol. This methanol soluble lignin fraction was shown to be dispersible in the HB prepolymer and has suitable thermal properties to act as netpoint (hard) segments for use in producing SMP. We were also able to produce various HBP structures by selectively changing the ratio of di-functional diacids with tri- and tetra-functional alcohol/amine building blocks to alter its thermal and viscoelastic properties. Finally, coreacting lignin with HBP via melt polycondensation resulted in lignin-copolymers with elastomeric and thermally-stimulated shape memory effect ( $T_g$ -SME) properties (Figure 6.1). The separate conclusions were addressed as follows:

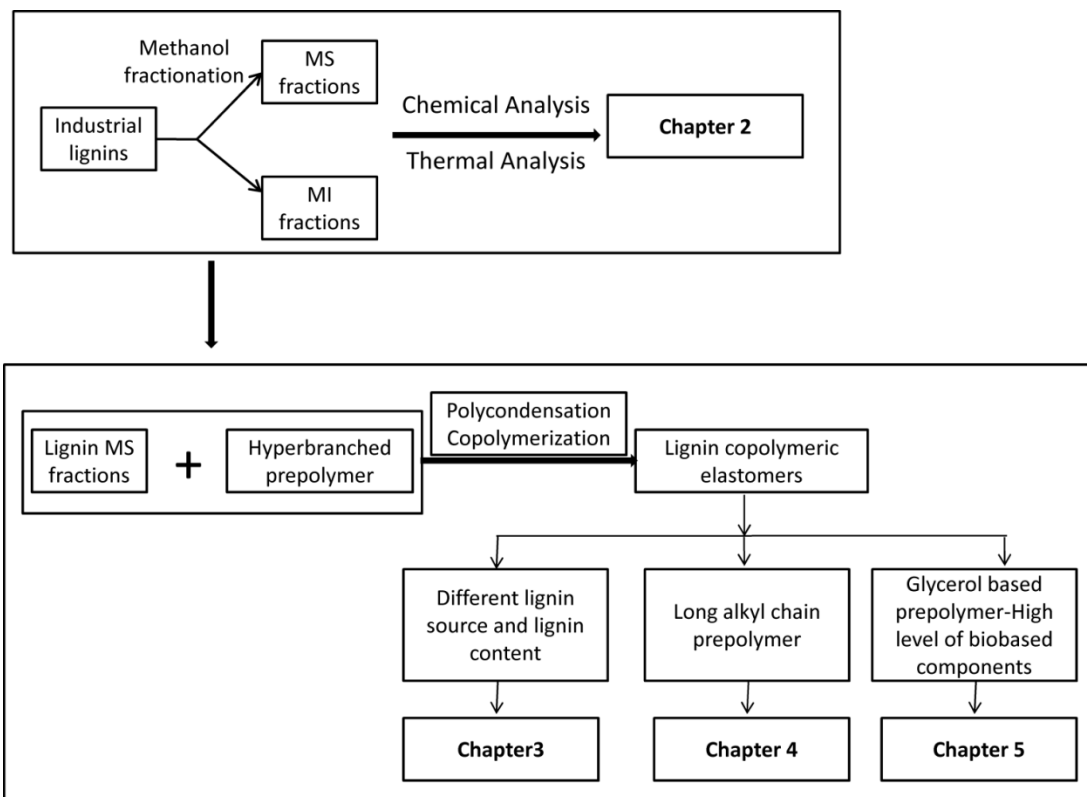


Figure 6.1 Summary of research conducted in the dissertation

It is well known that industrial lignin have limited solubility in common organic solvent and appreciable heterogeneity which hindered its application to a large extent. The first study (Chapter 2) was, therefore, about lignin preparation for copolymer synthesis. Three Industrial lignins (IN, PB and CS) were fractionated into methanol soluble (MS) and insoluble fractions (MI). The MS lignin fractions were shown to contain fewer condensed structures, lower aromatic/aliphatic OH ratio, higher  $\beta$ -O-4 linkages, lower  $M_w$  and  $T_g$ , and lower thermal degradation properties than the original lignin and MI lignin fractions. TMA and MTDSC were established to be sensitive and reliable techniques to determine lignin  $T_g$ s, even on difficult samples such as corn-stover lignin. Correlations between lignin chemistry and thermal properties ( $T_g$ ) were observed. This strategy for lignin selection based on source and fractionation offers a practical option for obtaining lignin starting or building block materials with different properties (e.g.  $T_g$ ) for incorporation into copolymers.

Synthesis and characterization of lignin based copolymers were carried out from chapter 3 to chapter 5 (Figure 6.2). Ts-SME was obtained for all lignin based copolymers, where

prepolymers were soft segment and lignins were netpoint segment. The obtained MS lignin fractions (IN, PB and CS) of first study were first applied to copolymerize in the second study (Chapter 3), with a HB prepoly(ester-amine) from TEA (trihydroxy) and AA to evaluate the effect of lignin source and lignin content on properties (thermal, mechanical as well as  $T_{5-SME}$ ). TEA played catalytic and solvent roles which, therefore, made the polycondensation reaction catalyst and solvent free during prepolymer synthesis. The results demonstrated that lignin content and type influenced copolymer properties. At high lignin levels (>40%) the copolymer mechanical properties were dominated by lignin while <40% lignin the properties were dominated by HBP. The copolymers were shown to have > 95% fixity rate and >90% shape recovery. The  $T_{trans}$  was shown to increase with copolymer lignin content and this demonstrates that the properties can be tuned by lignin content.

Then in the third study (Chapter 4), long alkyl chain prepolymer with partial crystalline structure was prepared to react with PB-MS lignin to obtain high elastic copolymers (Figure 6.2). Moreover, the prepolymer also possessed TEA (trifunctional) amine core and THAM (tetrafunctional) amide core with more cross-link variations and extent of branching. This long alkyl chain prepolymer gave lignin copolymers great elastomeric properties. The introduction of long diacid units in the hyperbranched prepolymer improved the polymer elasticity behavior by increasing the chain length between branch points. In addition, these long alkyl chains can co-crystallize and add other structural features to the polymer.

In the fourth study (Chapter 5), TEA was replaced with Gly (trihydroxy) to obtain highly biobased component prepolymers (as high as 100% biobased given that AA is now produced from biological sources). Different branch points were achieved, ie., Gly core, DIPA (trifunctional) core, as well as THAM (tetrafunctional) core (Figure 6.2). These cores and the extent of branching play key roles in terms of properties of prepolymer and final lignin copolymers. The copolymers demonstrated good shape memory and mechanical properties. The  $T_{trans}$  was shown to increase with DIPA and THAM content, revealing that the  $T_{trans}$  could be tuned by variations of DIPA and THAM. This study demonstrates that more renewable Gly

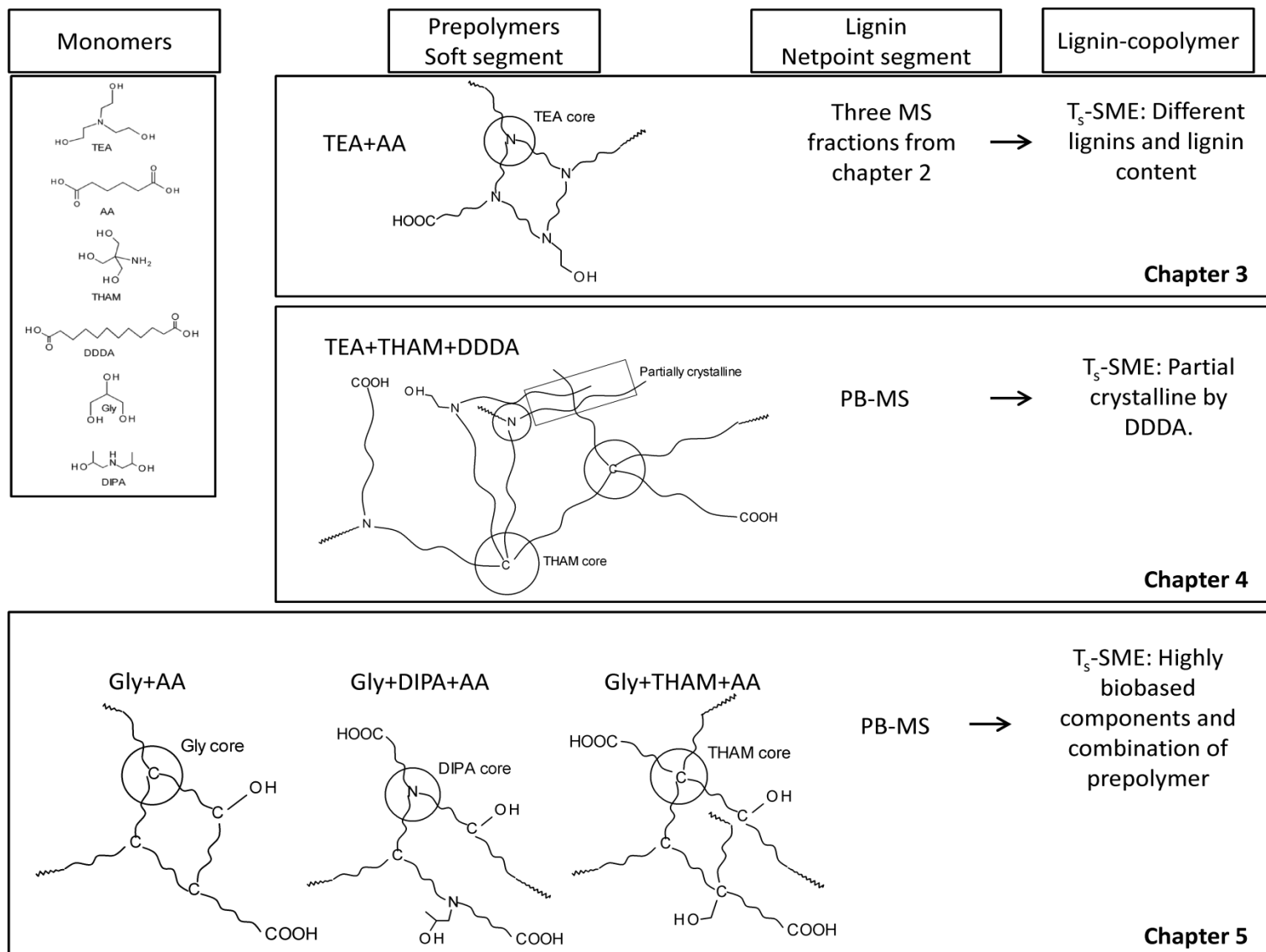


Figure 6.2 Summary of synthetic approaches of lignin based copolymers

and AA based prepolymers could act as soft segment in lignin based copolymer systems owning SME behavior.

## 6.2 Recommendation for the future work

- Throughout the dissertation, the lignin used was the MS fractions which left more than 50% MI lignin fraction. The value-added application of MI fractions also needs to be developed such as fast pyrolysis to thermochemically convert to smaller molecular fragments for biopolymer synthesis or biofuel upgrading. Pyrolytic lignin (PL) containing oligomeric lignin structures possess a low  $T_g$  and  $M_w$  and show promise as a netpoint segment for  $T_s$ -SME synthesis.
- As observed in all lignin copolymer synthesis, aromatic hydroxyl group barely participated into the polycondensation reaction because of its low reactivity toward esterification. Therefore, some minor modifications of lignin (such as mild oxypropylation or methylation of aromatic hydroxyl group) would endow more aliphatic hydroxyl group or mask the aromatic hydroxyl group to alleviate this situation and would improve the performance of final product, such as  $T_g$ , mechanical properties as well as elasticity.

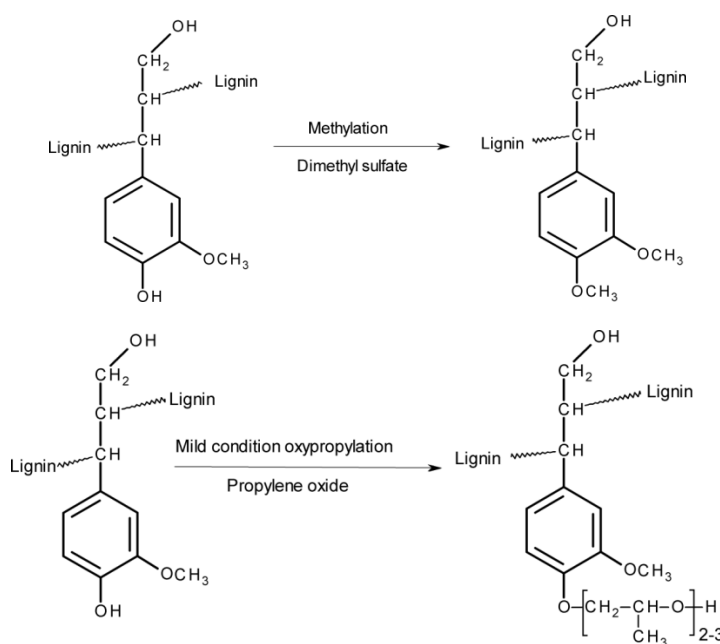


Figure 6.3 Recommended modifications (methylation and oxypropylation) of lignin



- More renewable prepolymer system could be developed, such as soybean oil with modification (epoxidized soybean oil) and derivatives which would also act as soft segment for the synthesis of lignin based  $T_5$ -SMP.
- Up-scale of new materials is always industrial preference, hence, the next step would be upscale the process to produce these lignin based copolymeric elastomers suitable for commercialization.